UNIVERSIDADE DE LISBOA
FACULDADE DE CIÊNCIAS

Ciências
ULisboa

Climate Change Impacts on Salt Marsh Vegetation Ecophysiology and Dynamics

Doutoramento em Biologia
Especialidade em Ecologia

Bernardo Afonso de Aranha Alhandra Duarte

Tese orientada por:
Prof. Doutora Maria Isabel Violante Caçador e Prof. Doutor João Carlos de Sousa Marques

Documento especialmente elaborado para a obtenção do grau de doutor

2016

UNIVERSIDADE DE LISBOA
FACULDADE DE CIÊNCIAS

Ciências
ULisboa

Climate Change Impacts on Salt Marsh Vegetation Ecophysiology and Dynamics

Doutoramento em Biologia
Especialidade em Ecologia

Bernardo Afonso de Aranha Alhandra Duarte

Tese orientada por:
Prof. Doutora Maria Isabel Violante Caçador e Prof. Doutor João Carlos de Sousa Marques

Júri:
Presidente:
- Professora Vanda Brotas

Vogais:
- Professora Janine Barbara Adams
- Professor Enrique Mateos-Naranjo
- Professora Anabela Silva
- Professor Manuel Graça
- Professor João Carlos Marques

Documento especialmente elaborado para a obtenção do grau de doutor

2016

Doctoral dissertation in Biology
(Specialization in Ecology)
Presented to the University of Lisbon

Dissertação apresentada à Universidade de Lisboa para obtenção do grau de Doutor em Biologia
(especialidade Ecologia)

Bernardo Afonso de Aranha Alhandra Duarte

2016

DECLARAÇÃO

Para efeitos do disposto n.° 2 do Art. 8° do Dec-Lei 388/70, o autor da dissertação declara que interveio na concepção do trabalho experimental, na interpretação dos resultados e na redacção dos manuscritos publicados e submetidos para publicação.

Bernardo Afonso de Aranha Alhandra Duarte
Janeiro de 2016

“Look deep into nature, and then you will understand everything better.”

Albert Einstein

TABLE OF CONTENTS

ACKNOWLEDGEMENTS

I hereby express my sincere gratitude to those who have contributed to the conclusion of this work.

To Professor Isabel Caçador, for her trust, supervision, friendship and encouragement and for believing and supporting my work, with her everyday councils making this thesis possible.

To Professor João Carlos Marques, for the support and advising with his essential commentaries during the redaction of the papers that compose this work and also for the opportunity to work with the wonderful IMAR team.

To all my co-authors that have contributed with their knowledge and different points of view to the works here presented making this thesis richer.

To all my colleagues of MARE – Centre of Marine and Environmental Sciences, for their support, advices, company, friendship and helpful brainstorms that improved much of this work.

To MARE – Centre of Marine and Environmental Sciences and its present Director, Professor Henrique Cabral, for making all this work possible by providing all the necessary conditions to its fulfilment.

To the Faculty of Sciences of the University of Lisbon, for accepting my PhD thesis proposal and for providing all the conditions to its realization.

To the "Fundação para a Ciência e Tecnologia (FCT)" for funding the research in the Marine and Environmental Sciences Centre (MARE) throughout the project UID/MAR/04292/2013 and by supporting my PhD workplan with a National PhD Grant (SFRH/BD/75951/2011) and throughout the ECOSAM project (PTDC/AAC-CLI/104085/2008).

To all my closest friends that were always with me during the good and bad moments of these last years, supporting me and cheering me up.

To my grandmother's memory, Maria Arlete Rosa Alhandra Duarte, to whom the achievement of this degree would be the final step to fulfil her life's dream.

To Pedro's memory, for growing up with me, for its unconditional friendship, support and brotherhood making me the person that I am today.

To my sister, for her endless support, confident listener in all the moments of my life and helpful corrections of the chapters that compose this thesis.

To my parents, for everything.

ABSTRACT

Ecosystems worldwide are experiencing the effects of climate change, and estuaries and salt marshes are no exceptions. Being highly productive, the plant community will be one of the most affected elements by these climatic shifts, both in terms of structure and dynamics, with undeniable effects on its productivity. This thesis aimed to study the effects of climate change on the marsh community dynamics, structure and productivity but also on its biogeochemical cycles and implications at the ecosystem level services. Although special attention was given to primary productivity and plant physiology, a multi-disciplinary approach was undertaken using both field assessments and mesocosmos trials were conducted. The results point out that these physically connected climatic changes are not only interconnected on a physical way, but also at an ecological level. Mediterranean marshes will be more severely affected on its foundations, putting the entire ecosystem at risk and prone to climate change side effects and/or to synergistic events. The majority of the evaluated climatic changes have its more negative impacts on the marsh pioneer species, affecting inevitably the marsh establishment and expansion. Although in a smaller extent, also the upper and middle marsh halophytes will suffer from these climate-driven negative impacts. Alongside the appearance of resistant non-indigenous species (NIS) will add an increased threat to the marsh. The reduction of the pioneer zone in a large extension together with a middle marsh fragilization will open new ecological niches for the colonization of resistant NIS, imposing serious shifts in the marsh structure, dynamics and services provided to the estuarine ecosystem. This is even more evident when a holistic approach is undertaken focusing not only plant physiology but also the marsh biogeochemistry and the estuarine hydrological features. All these evidences point out to the need to adopt new management efforts, highlighting the desired marsh attributes and ecosystem services in the face of human activities that threaten salt marsh ecosystems.

Keywords: climate change; halophyte ecophysiology; biogeochemistry; ecosystem services

RESUMO ALARGADO

A resiliência dos ecossistemas de sapal em cenários de impactos antropogénicos é amplamente reconhecida. Estes são de facto ecossistemas com elevado grau de resiliência. No entanto como todos os mecanismos de resiliência, estes implicam que a adaptação e recuperação dos ecossistemas acompanham a aplicação do fator de *stress*. Este é o caso das alterações climáticas que afetam os ecossistemas a nível global. A velocidade a que estas mudanças se têm dado e que atingirão no futuro, irá provavelmente ultrapassar a velocidade de adaptação e resiliência dos sapais, colocando estes valiosos ecossistemas em risco. Apesar de todas as pressões antropogénicas aplicadas aos sapais, a população humana continua a depender em larga escala destes ecossistemas, assim como todo ecossistema estuarino. Este facto levou a que os sapais fossem incluídos em diversas diretivas e convenções de proteção e gestão ambiental. O registo da perturbação antropogénica nestes ecossistemas pode ser reconstruído utilizando técnicas de datação rádio-isotópica e aponta para sistemas que já de si sofrem de perturbação antropogénica. É por isso admissível considerar que em sistemas cronicamente perturbados, qualquer fator de *stress* adicional pode ultrapassar a capacidade de resiliência das espécies. Para que melhor se posse compreender os limites desta capacidade, é necessário ter um maior conhecimento acerca dos mecanismos fisiológicos e biogeoquímicos nos quais se baseia a plasticidade e resistência do sapal e da sua comunidade.

Como em vários outros sapais, o fornecimento de sedimentos no período entre 1961 e 2001 permitiu que estes ecossistemas mantivessem a sua capacidade de sedimentação superior à velocidade de subida do nível do mar. No entanto as mais recentes previsões apontam para uma aceleração da taxa de subida do nível do mar, devido ao aumento da acumulação de energia radiativa nos oceanos e consequente expansão das massas de água. Assim é provável que até 2100 a taxa de subida do nível do mar ultrapassará a capacidade de acreção de alguns sapais de crescimento mais lento, como os que encontramos na margem sul do estuário do Tejo. Inevitavelmente este facto irá afetar os ritmos circadianos e a fisiologia das

comunidades de halófitos, que ficarão neste caso expostas a períodos de submersão mais prolongados. As zonas mais afetadas serão as zonas de sapal baixo, onde podemos encontrar as espécies halófitas pioneiras responsáveis pelo estabelecimento e crescimentos das comunidades de sapal. De acordo com os resultados apresentados na presente tese, a espécie *Spartina maritima* apesar da sua grande plasticidade fisiológica irá sofrer a curto prazo uma pequena redução da sua produção primária que numa perspetiva a longo prazo poderá levar a uma redução bastante significante da população deste importante halófito. No que diz respeito ao médio e alto sapal, a subida do nível médio do mar levará a um fator de *stress* acrescido: maior intrusão de água salgada e aumento da salinidade dos sedimentos. Inevitavelmente algumas espécies (por ex.: *Halimione portulacoides* e *Sarcocornia fruticosa*) irão sofrer períodos em que a salinidade do sedimento ultrapassará em larga escala o seu ótimo fisiológico, levando a quebras na sua produtividade primária e consequente decréscimo na sua área de colonização. Esta alteração na estrutura da comunidade tem como reflexo uma maior colonização de espécies exóticas (por ex.: *Spartina patens*) com maiores capacidades de tolerância a salinidades elevadas, expandindo as suas áreas de colonização e consequentemente alterando a dinâmica e serviços prestados pelo sapal. Estas alterações são marcadamente visíveis no que diz respeito à capacidade de sink do ecossistema e como ponto de reciclagem de matéria orgânica. Quer seja devido a maior alagamento dos sedimentos quer a um aumento de salinidade, algumas áreas de sapal irão ver os seus processos de senescência acelerados devido aos elevados níveis de *stress* a que os halófitos estarão sujeitos. Considerando as condições hidrodinâmicas que se verificam presentemente a maior parte dos detritos gerados pelos sapais retornam a sapais próximos onde podem ser reciclados e decompostos. Considerando as condições hidrodinâmicas previstas para um cenário de subida do nível médio do mar, uma grande parte destes detritos irá atingir o oceano adjacente ao estuário, levando com eles elevadas quantidades de nutrientes orgânicos e contaminantes, reduzindo a capacidade de *sink* do sapal bem como de fornecimento de nutrientes inorgânicos para os produtores primários estuarinos.

Todas as alterações climáticas apresentam como principal promotor, um aumento dos níveis de gases de efeito de estufa, como o CO_2. Os resultados aqui apresentados sugerem que a subida dos níveis de CO_2 atmosférico irá favorecer os halófitos que possuem metabolismos em C_3, enquanto os halófitos C_4 não serão afetados positivamente, apresentando até alguns sinais de *stress* em cenários de aumentos de CO_2 atmosférico. Mais uma vez, o baixo sapal será o mais prejudicado pelos efeitos das alterações climáticas devido à sua larga colonização por *S. maritima*, um halófito C_4. No entanto a expansão de halófitos C_3 poderá também estar ameaçada no caso de uma redução da colonização por parte de espécies pioneiras. Estas espécies são essenciais na modificação dos sedimentos para que outras espécies possam colonizar e elevar o sapal. Este aumento de CO_2 atmosférico far-se-à também sentir ao nível das concentrações de CO_2 dissolvido na coluna de água. Neste caso, o aumento da concentração de CO_2 dissolvido alivia o *stress* imposto pela submersão permitindo um aumento da produtividade primária dos halófitos em condições de submersão. Ao nível do ecossistema, este facto representa um aumento da oxigenação da coluna de água e uma eficiente tamponização da coluna de água através da captura fotossintética do excesso de CO_2 dissolvido e assim reduzindo os eventos de acidificação estuarina. Do ponto de vista biogeoquímico este aumento de CO_2 atmosférico terá também evidentes impactos nas funções dos sedimentos para o ecossistema. Mais uma vez o ecossistema apresenta uma capacidade tampão através da redução da reciclagem de compostos orgânicos ricos em carbono, reduzindo desta forma a emissão de CO_2 de volta para a atmosfera. No entanto esta alteração nas funções biogeoquímicas dos sapais leva inevitavelmente a um desequilíbrio dos ciclos biogeoquímicos estuarinos com impactos mais severos no que diz respeito à reciclagem de nutrientes.

Esta capacidade de auto-tamponização do ecossistema não representa uma resposta exclusiva ao aumento do CO_2 atmosférico. O mesmo pode ser verificado ao nível da resposta a um aumento de temperatura atmosférica. Seguindo as mais recentes previsões, é possível observar que o aumento de temperatura levará a uma redução dos fluxos respiratórios dos sedimentos, minimizando desta forma o efeito de estufa. Por outro lado, esta redução representa um aumento do *pool* de carbono

orgânico presente nos sedimentos o que mais uma vez leva a uma mudança das funções biogeoquímicas dos sapais. Enquanto uma subida gradual de temperatura terá os seus efeitos mais evidentes ao nível biogeoquímico, os eventos extremos de calor e de frio podem induzir danos severos nos halófitos. De acordo com as mais recentes previsões, a intensidade e frequência de eventos de calor extremos tende a aumentar nos próximos anos na zona Mediterrânica, havendo uma possível diminuição da frequência, mas não da intensidade das chamadas ondas de frio. A este nível os halófitos C_3 serão mais afetados por ondas de calor, sendo que os efeitos destes eventos extremos produzirão também efeitos nefastos na fisiologia dos halófitos C_4. Mais uma vez as fundações dos sapais serão severamente afetadas, através da redução da produção primária dos halófitos *Aster tripolium* e *S. maritima*. Todas estas alterações ao nível das fundações e do crescimento dos sapais levam a que estes se encontrem mais fragilizados em situações por exemplo de aumento do nível do mar. Como acima referido, este aumento da frequência de eventos extremos de calor e consequente redução da colonização das espécies do médio sapal abre portas à colonização de espécies exóticas altamente resistentes a estes eventos extremos, como seja a *S. patens*.

Torna-se desta forma bastante evidente que todas as alterações climáticas acima referidas, estão não só ligadas fisicamente, mas também ao nível ecológico. As fundações dos sapais mediterrânicos serão de longe as mais afetadas por todas estas alterações, levando a que todo o ecossistema fique vulnerável. O aumento da pressão antropogénica está a ultrapassar a capacidade de crescimento e resiliência dos sapais, impondo um novo desafio para estes ecossistemas e para as comunidades que deles dependem. Existe hoje uma maior necessidade de adotar novos esforços de gestão e conservação destes importantes ecossistemas, focando em particular a conservação e proteção das espécies halófitas e consequente manutenção dos serviços dos sapais.

Palavras-Chave: alterações climáticas; ecofisiologia de halófitos; biogeoquímica; serviços dos ecossistemas.

LIST OF PAPERS

This thesis is comprised by the papers listed below:

Duarte, B., Santos, D., Marques, J. C. and Caçador, I., 2013. Ecophysiological adaptations of two halophytes to salt stress: photosynthesis, PS II photochemistry and anti-oxidant feedback - Implications for resilience in climate change. Plant *Physiology and Biochemistry* 67, 178-188.

Duarte, B., Caçador, I., Marques, J.C. and Croudace, I., 2013. Tagus Estuary salt marshes feedback to sea level rise over a 40-year period: insights from the application of geochemical indices. *Ecological Indicators* 34, 268-276

Duarte, B., Santos, D., Marques, J.C. and Caçador, I., 2014. Biophysical probing of *Spartina maritima* Photo-system II changes during increased submersion periods: possible adaptation to sea level rise. *Plant Physiology and Biochemistry* 77, 122-132.

Duarte, B., Santos, D., Silva, H., Marques, J.C. and Caçador, I., 2014. Photochemical and Biophysical feedbacks of C_3 and C_4 Mediterranean halophytes to atmospheric CO_2 enrichment confirmed by their stable isotope signatures. Plant *Physiology ad Biochemistry* 80, 10-22

Duarte, B., Freitas, J., Valentim, J., Medeiros, J.P., Costa, J.L., Silva, H., Dias, J.M., Marques, J.C. and Caçador, I., 2014. Modelling abiotic control of salt marsh sediments respiratory CO_2 fluxes: new insights for climate change scenarios. *Ecological Indicators* 46, 110-118.

Duarte, B., Silva, H., Marques, J.C., Caçador, I. and Sleimi, N., 2014. Light-dark O_2 dynamics in submerged leaves of C_3 and C_4 halophytes under increased dissolved CO_2: Clues for saltmarsh response to climate change. *Annals of Botany Plants* 6, plu067.

Duarte, B., Santos, D., Marques, J.C. and Caçador, I., 2015. Ecophysiological constraints of two invasive plant species under a saline gradient: halophytes versus glycophytes. *Estuarine Coastal and Shelf Science* 167, 154-165.

Duarte, B., Marques, J.C. and Caçador, I., 2015. Impact of extreme heat and cold events on the energetic metabolism of the C_3 halophyte *Halimione portulacoides*. *Estuarine Coastal and Shelf Science* 167, 166-177.

Duarte, B., Marques, J.C. and Caçador, I. (*in press*) Ecophysiological responses of native and invasive *Spartina* species to extreme temperature events in Mediterranean marshes. *Biological Invasions* (doi: 10.1007/s10530-015-0958-4).

Duarte, B., Goessling, J., Marques, J.C. and Caçador, I., 2015. Ecophysiological constrains of *Aster tripolium* under extreme thermal events impacts: merging biophysical, biochemical and genetic insights. *Plant Physiology and Biochemistry* 97, 217-228.

Duarte, B., Vaz, N., Valentim, J.M., Dias, J.M., Silva, H., Marques, J.C. and Caçador, I. Revisiting the Outwelling Hypothesis: Modelling Salt Marsh Detrital Metal Exports under Extreme Climatic Events (submitted to Marine Chemistry).

This thesis is also comprised by the following book chapter listed below:

Caçador, I., **Duarte, B.**, Marques, J.C. and Sleimi, N., 2015. Carbon mitigation: a salt marsh ecosystem service in times of change. Halophytes for Food Security in Dry Lands. Muhammad Ajmal Khan, Munir Ozturk, Bliquees Gul and Muhammad Zaheer Ahmed (Eds.) Elsevier.

CHAPTER I

GENERAL INTRODUCTION

AIMS AND STRUCTURE OF THE THESIS

CHAPTER I

GENERAL INTRODUCTION

State of the Art

Our planet is undergoing an undeniable change in its climatic shift. On the basis of these shifts are continuous increases in the greenhouse gases (GHGs) emissions from anthropogenic sources. Since 2007, annual global GHGs emissions have continued to grow and reached 49.5 Gt of carbon dioxide equivalents (CO_2eq), in the year 2010, an unprecedented value (IPCC, 2014). In addition, pollutants such as carbon monoxide (CO), volatile organic compounds (VOC), nitrogen oxides (NO_x) and sulphur dioxide (SO_2), which by themselves are negligible GHGs, have an indirect effect on the greenhouse effect by altering the abundance of important gases such as methane (CH_4) and ozone (O_3), and/or by acting as precursors of secondary aerosols and the also amount of outgoing low wave radiation. These changes in the radiation emission have inevitable consequences on Earth's thermal budget. The radiative energy budget of the Earth is almost in balance, but the latest ocean heat content and satellite measurements indicate a small positive imbalance (Murphy *et al*., 2009; Trenberth *et al*., 2009; Hansen *et al*., 2011), consistent with the rapid changes in the atmospheric composition. These changes are in the genesis of all the climatic alterations our planet is facing. Global warming promoted by GHGs increase, leads to changes in atmospheric and ocean circulation, season succession, storm and precipitation patterns, drought periods and all the cascade of extreme thermal events observable in the last years with increasing frequency and severity (IPCC, 2012 and 2013).

Estuarine systems represent important ecosystems in the coastal landscape, providing essential ecosystems services such as water quality improvement, fisheries resources, habitat and food for migratory and resident animals, and recreational areas for human populations. In the past 40 years, estuarine conservation was

recognized as a priority at national and international levels through several acts as the Ramsar Convention, 1977 (Munari and Mistri, 2008), and Water Framework Directive, 2000. Despite all the conservation attempts on a worldwide-scale coastal, estuarine and transitional waters have been affected by man's activities. Historically, developing human civilizations have often been concentrated in coastal areas where access to water promoted trade and commerce. As a consequence, human alteration of natural ecosystems is profound in coastal areas. This is a central concern in terms of environmental management in order to develop policies to balance socio-economic growth and environmental protection (Borja and Dauer, 2008). Salt marshes are found fringing many of the world's coasts exposed to relatively low-energy hydrodynamic environments. They are characterized by a wide variety of herbaceous, succulent and woody vascular plants. Salt marshes have they upper limit occurrence approximately that of the highest astronomical tide (HAT) while the lower limit is rarely below mean high water neap (MHWN) tide level. These ecosystems appear mostly in estuarine ecosystem, but can also be found in barrier islands, spits, embayments and open shores exposed to low wave energy (Allen 2000), as well as fringing coastal lagoons. Salt marshes can be found within all tidal regime ranges, from microtidal to macrotidal, presenting a great plasticity to water-level fluctuations which can be seasonal, as in the Baltic or the estuaries of south-west Western Australia (Hodgkin and Hamilton 1998), or unpredictable, as in some lagoons where water level is determined by rainfall patterns and lagoon opening. Salt marshes have a great ecological value for the estuarine ecosystem, namely in terms of nutrient regeneration, primary production, wildlife habitat and as shoreline stabilizers. These ecosystems occupy the transition zone between terrestrial and marine biotopes and are characterized by a high productivity, which is considered essential in maintaining the detritus-based food chain of estuarine and coastal ecosystems (Marinucci, 1982). Salt marshes are key areas for the estuarine system, namely for primary production and nutrient regeneration (Caçador *et al*., 2009), becoming this way one of the most productive ecosystems in the planet (Lefeuvre *et al*., 2003). Estuarine wetlands, as salt marshes, constitute good carbon sinks having simultaneously reduced rates of GHGs emissions (Magenheimer *et al*., 1996), with a carbon sequestration capacity per unit area of about one order of magnitude higher

than other wetland systems (Bridgham *et al*., 2006). Salt marshes are usually located in estuarine systems and their primary production allows for a greater reduction of CO_2 in the atmosphere and incorporation on organic tissues through photosynthesis (Sousa *et al*. 2010). Wetlands represent the largest carbon pool with a capacity of 770 Gt of carbon, overweighing the total carbon storage of farms and rain forests (Han *et al*., 2005).

Being located in coastal systems, salt marshes are not only prone to the effects of altered atmospheric conditions (for e.g. increased CO_2 and altered thermal environment) but also to indirect effects driven from changes in the marine system itself (for e.g. sea level rise (SLR), altered dissolved carbon chemistry, salinity changes). Wetland systems are particularly vulnerable and susceptible to changes in quantity and quality of water supply. Aside from the evident atmospheric alterations, climate change may have its most pronounced effects on salt marshes through changes in hydrological regimes, specifically, the nature and variability of the hydroperiod and the number and severity of extreme events. However, other factors related to climate may play important roles, including increased temperature and altered evapotranspiration, changes in the estuarine biogeochemistry, altered sedimentation and erosion patterns, fire, oxidation of organic sediments and the physical effects of the wave environment (IPCC, 1998; Burkett and Kusler, 2000; USGCRP, 2000).

Climate change can affect salt marshes in a number of ways, including through SLR, particularly when sea walls and other anthropogenic structures squeeze marsh vegetation, preventing its movement upward and inland. However, some evidences indicate that SLR does not necessarily lead to the loss of marsh area, due to the ability of some marshes to accrete vertically, maintaining their elevation with respect to sea level. On the other hand, in organogenic marshes and in areas where sediment may be a limiting factor, these ecosystems may become prone to coastal squeeze, if some extreme predictions of accelerated rates of SLR are realized (Hughes, 2004). McKee *et al*. (2004) suggests that temperature increases and decreases in rainfall driven by climate change may dramatically affect tidal marshes. Increased temperature may interact with other stressors damaging coastal marshes. For example, during the spring to fall period of 2000 in the Mississippi delta, there

were large areas of salt marsh that were stressed and dying (Day *et al*. 2005). This resulted from a combination of effects driven from a strong La Niña event, resulting in prolonged low water levels, extreme drought, and high air temperatures. This combination of factors apparently raised soil salinities to stressful toxic levels. Another example points out to a replacement of the Gulf of Mexico salt marshes, by mangroves due to its migration northward, as result of the increasing temperatures these systems have been experiencing year after year. Chen and Twilley (1998) developed a model of mangrove response to freeze frequency. These authors found that when freezes occurred more often than once every 8 years, mangrove forests could not survive. At a freeze frequency of one every 12 years, mangroves replaced salt marsh. In other locations like along the Louisiana coast, freezes historically occurred about every 4 years. By 2004, however, a killing freeze had not occurred for 15 years and small mangroves started to appear over a large area near the coast. If this trend continues, mangroves will probably spread over much of the northern Gulf and part of the south Atlantic coast. In fact, mangroves are already establishing in a wider range due to warming (Day *et al*. 2005).

Climate-related changes to the carbon cycle are likely to alter the sequestration service provided by salt marshes, as well as affect long-term rates of salt marsh accretion and the ability of marshes to keep pace with SLR in ways that are still unclear. Anthropogenic increases in atmospheric CO_2, the major driver of climate change, will affect salt marsh plant species differentially. Due to metabolic differences, C_3 plants are expected to respond more positively to CO_2 increases than C_4 plants, a hypothesis that has been supported by field experiments that manipulate CO_2 concentrations (Ainsworth and Long, 2005). Some experiments conducted in a brackish tidal marsh in the Chesapeake Bay, showed that the experimental doubling of CO_2 concentrations elicited a sustained biomass increase in *Scirpus olneyi* (C_3 sedge) (Erickson *et al*., 2007). Salt marshes dominated by C_4 grasses, such as *Spartina* and *Phragmites spp*., may respond differently. In the same Chesapeake Bay study, C_4 grasses *Spartina patens* and *Distichlis spicata* did not grow more rapidly under elevated CO_2 conditions. The same trend was found in growth chamber studies using European C_4 salt marsh species exposed to elevated CO_2 conditions (Lenssen *et al*., 1993, Rozema *et al*., 1991). This evidence suggests that

the response of salt marshes to elevated CO_2 will be dependent on plant composition, with higher CO_2 concentrations favouring compositional shifts toward C_3 plants, as C_4 plants gradually reduce their area of colonization by competition.

Climate change could alter the geographical distribution of salt marshes, which currently span temperate and arctic latitudes (Chapman, 1977), or salt marsh plant species affecting inevitably the ecosystem productivity. Turner (1976) suggests that the productivity of salt marshes is tied to latitude and climate with greater productivity at lower latitudes. Since all gas exchanges (plant photosynthesis or sediment respiration) are physically dependent on the thermal environment, it becomes inevitable to consider the effects of an altered thermal regime in the marsh productivity and biogeochemistry, namely in terms of carbon stocks. Nowadays and with an increasing concern on the climatic changes undergoing on our planet, several studies aroused focusing the effects of global warming in respiration in several ecosystems (e.g. Florides and Christodoulides, 2009; Shakun *et al*., 2012). These studies point out to an important role of increasing temperatures while major contributors to enhance respiration and therefore the CO_2 fluxes to the atmosphere (Kirschbaum, 1995; Cox *et al*., 2000; Bond-Lamberty and Thomson, 2010).

With climate change, the intensity of hurricanes and extreme rain events are expected to increase (IPCC, 2007). As the first line of coastal defence, salt marshes are greatly affected by storms. In a long-term perspective, salt marshes are the ecosystems, which suffer less with the ecological disturbance caused by storms (Michener *et al*. 1997). In Cape Cod, for example, salt marshes were the only habitat with little reported damage from Hurricane Bob in 1991, mostly because unlike other upland habitats, salt marsh vegetation is highly adapted to salt stress and inundation (Valiela *et al*. 1998). Coastal storms do, however, have short-lived impacts in salt marsh communities. Storm surges push salt water up estuarine gradients, raising salinities in brackish and freshwater tidal marshes and temporarily shifting plant distributions. On the other hand, floodwaters can introduce large inputs of freshwater into salt marshes allowing the establishment of non-halophytic species in the salt marshes.

Historically, SLR has been interconnected with sediment delivery and geologic development of salt marshes. As the rates of SLR have increased, rates of salt marsh

accretion have also accelerated, sometimes exceeding SLR rates (Nixon, 1980; Roman *et al*., 1997). However, as SLR continues to accelerate, there is the concern that its rate will outpace the rate of accretion, drowning salt marshes. Sea level rise effects manifest in salt marshes in two different ways: 1) landward migration of salt marsh vegetation zones and submergence at lower elevations, and 2) interior ponding and marsh drowning. The landward migration of low-marsh and high-marsh vegetation zones has been attributed to SLR in New England. Donnelly and Bertness (2001) observed a rapid landward expansion of *Spartina alterniflora* over the past 200 years, coincident with the rate of SLR. Warren and Niering (1993) compared vegetation cover data and peat profiles from 1947 and 1987 and found an increase in pioneers and dwarfs *S. alterniflora* with a simultaneous decrease in *Spartina patens* and *Juncus gerardii* in the upper marsh. Since dwarf *S. alterniflora* and salt marsh pioneers generally occur in more waterlogged soil conditions, these results are also consistent with SLR. This rising phenomenon has also eroded the seaward edge of European salt marshes (e.g., Day *et al*., 1998). On the other side of the planet, SLR is contributing to the replacement of salt marsh by mangroves in Australia (Rogers *et al*., 2005). Rising water levels are of particular concern, since in several areas the response of plant communities is constrained by sharp shorelines and anthropogenic structures. Alongside, the high marsh may be particularly vulnerable to drowning. On the other hand, productivity of low marsh *S. alterniflora* increases with inundation (to a point). This lead Morris *et al.* (2002) to suggest that increases in accretion linked to plant productivity act as a stabilizing agent allowing these marshes to counteract SLR. However, in the high marsh, several plants are less productive under inundation with slower accretion rates. This combined feedback from the whole marsh community can quickly transform high marsh into open water. This was already observed in Chesapeake Bay and Mississippi River delta marshes (Barras *et al*., 2004; Kearney *et al*., 1988). Despite the uncertainty about many of the potential effects of climate change on salt marshes, it seems clear that SLR will profoundly alter salt marshes by causing migrations of plant species and their associated fauna as well as marsh drowning.

Alongside with these climatic changes, the altered marsh environment along with the changes in inter-specific relationships can provide conditions for the

establishment of NIS that will impose an additional stress factor to the native marsh community.

Objectives

Although these changes in salt marsh communities are well known, most of their physiological basis are not. Reductions in certain species productivity driven by the exposure to the abovementioned climatic changes have its source at the cellular level. This fact became the starting point of the present thesis. Knowledge is required to understand the physiological changes underlying the plant community responses to climate changes. This understanding is particular important in order to anticipate the changes that in the future may occur in salt marshes from the species level to an ecosystem approach. This is also true in which concerns the marsh biogeochemical services provided to the estuarine community, both in terms of sink and as a nutrient regenerator and provider to the primary and secondary production of the adjacent water bodies. Considering this the present thesis has as main objectives:

1. Evaluate the capacity of mesotidal marshes to accrete and survive SLR, while incorporating the impacts of prolonged inundation periods on the marsh species establishment, primary productivity and organic matter exports.
2. Understand the physiological effects of both atmospheric and dissolved increased CO_2 in the marsh productivity and organic matter decomposition.
3. Study the ecophysiological impacts of increased salinity regimes in the establishment of invasive and endemic species.
4. Assess the impacts of abnormal thermal environments on the vegetation primary production and in the biogeochemical carbon cycle.
5. Construct an overall picture of the future of Mediterranean marshes considering the predicted IPCC scenarios, in terms of vegetation dynamics and services provided to the estuarine community.

Thesis structure

For this the present thesis is divided in 6 chapters. In chapter II SLR impacts on Tagus salt marshes are studied from a geological, physiological and hydrodynamic point of view. In this chapter the ability of salt marshes to accrete during the last 40 years is discussed and compared to the SLR data for the Tagus estuary, using several geochemical markers as proxy of the erosion/accretion processes linking this to the heavy metal sink role well described for estuarine marshes. Alongside, this chapter also presents the physiological results obtained while exposing one of the most abundant pioneer specie in Mediterranean marshes (*Spartina maritima*) and its effects on its primary productivity and marsh establishment. As highly productive systems, these are also environments, are also producers of high amounts of senescent necromass, which fuel the primary and secondary production of the adjacent water bodies. Thus, in this chapter also became important to address the effects of altered hydrological regimes in the dispersion of these plant detritus and its imprisoned contaminants, throughout the estuarine system and nearby ocean shelf.

In chapter III, the effects of CO_2 rising in the salt marsh systems are the main focus. Again two different approaches are presented. By on side, it is discussed the effects of atmospheric and dissolved CO_2 in the marsh productivity focusing the differential response exhibited by C_3 and C_4 plants. Moreover, in which concerns the underwater photosynthesis processes, the role of these salt marshes as buffers of estuarine acidification, by withdrawing excessive dissolved CO_2, and as essential oxygen generators is discussed within several plausible scenarios. On the other side, CO_2 will also affect the marsh microbial community. Thus, this became another essential point of view to be discussed within this chapter, focusing some of the most important microbial extracellular enzymes known to be essential for organic matter recycling under scenarios of altered and normal atmospheric CO_2 environments.

Chapter IV deals with the ecophysiological feedback of native and NIS found in Mediterranean estuarine ecosystems. In the first section, *Halimione portulacoides* and *Sarcocornia fruticosa*, photobiology and ion accumulation is evaluated under

extreme salinity conditions, such as verified in the high marsh under prolonged high temperature periods, characterized by an intense red coloration oftenly found in large extensions in the upper marsh vegetation. On the other hand, changes in the salinity regime can also impose some constrains to NIS species colonization and expansion along the marsh spatio-temporal salinity gradient. For this two recently found NIS, *S. patens* and *Cyperus longus*, were evaluated along a salinity gradient which covers the range of salinities verified from the upper to the lower marsh from summer to winter, in order to understand how these NIS will have its spreading potential conditioned by salinity increases, like the ones promoted by e.g. an increased salt water intrusion driven from SLR or prolonged and exacerbated evapotranspiration periods.

In chapter V the effects of altered thermal environments are discussed both in terms of its influence on salt marsh sediments CO_2 effluxes but also focusing its effects in the halophyte physiology. In the first section a model is developed and tested in order to evaluate the role of air temperature in the carbon stocks and emissions during the present conditions and under the projected scenarios described by the IPCC storyline. In the second section of this chapter the effects of extreme thermal events like heat and cold waves are focused. Despite its punctual effects, the latest IPCC Special Report on Extreme Events (SREX; IPCC, 2012) points out to an increasing frequency of these events especially in the Mediterranean area. Thus, the effects of these punctual events are discussed in terms of its impacts on the halophyte primary production and physiology, but also in terms of interspecific competition between native and NIS, as discussed in chapter IV.

The last chapter of the present thesis intents to develop an integrative overview of all the findings presented in the previous chapters. The effects of the studied climatic changes are integrated in a holistic point of view, in order to make predictions on the future of the Mediterranean marshes, not only in terms of halophyte community structure and primary production, but also at a biogeochemical level and in terms of ecosystem services provided to the estuarine environment.

References

Ainsworth, E.A. and Long, S.P., 2005. What have we learned from 15 years of free-air CO_2 enrichment (FACE)? A meta-analytic review of the responses of photosynthesis, canopy properties and plant production to rising CO_2. *New Phytologist* 165, 351-372.

Allen, J.R.L., 2000. Morphodynamics of Holocene salt marshes: a review sketch from the Atlantic and Southern North Sea coasts of Europe. *Quaternary Science Reviews* 19, 1155–1231.

Barras, J., Beville, S., Britsch, D., Hartley, S., Hawes, S., Johnston, J., Kemp, P., Kinler, Q., Martucci, A., Porthouse, J., Reed, D., Roy, K., Sapkota, S. and Suhayda, J., 2004. Historical and projected coastal Louisiana land changes: 1978-2050. *USGS Open-File Report* 03-334, 39p.

Bond-Lamberty, B. and Thomson, A., 2010. Temperature-associated increases in the global soil respiration record. *Nature* 464, 579-583.

Borja, A. and Dauer, D.M., 2008. Assessing the environmental quality status in estuarine and coastal systems: Comparing methodologies and indices. *Ecological Indicators* 8, 331-337.

Bridgham, S.D., Megonigal, J.P., Keller, J.K., Bliss, N.B. and Trettin, C., 2006. The carbon balance of North American wetlands. *Wetlands* 26, 889-916.

Burkett, V. and Kusler, J., 2000. Climate change: potential impacts and interactions in wetlands of the United States. *Journal of the American Water Resources Association* 36, 313–320.

Caçador, I., Caetano, M., Duarte, B. and Vale, C., 2009. Stock and losses of trace metals from salt marsh plants. *Marine Environmental Research* 67, 75-82.

Chapman, V.J., 1977. Introduction. In *Wet Coastal Ecosystems*, ed. VJ Chapman, pp. 1-30. New York: Elsevier.

Chen, R.H. and Twilley, R.R., 1998. A gap dynamic model of mangrove forest development along gradients of soil salinity and nutrient resources. *Journal of Ecology* 86, 37–51.

Cox, P. M., Betts, R. A., Jones, C. D., Spall, S. A. and Totterdell, I. J., 2000. Acceleration of global warming due to carbon-cycle feedbacks in a coupled climate model. *Nature* 408, 184-187.

Day, J.W. Jr., Scarton, F., Rismondo, A. and Are, D., 1998. Rapid deterioration of a salt marsh in Venice Lagoon, Italy. *Journal of Coastal Research* 14, 583-590.

Day, J.W., Narras, J., Clairain, E., Johnston, J., Justic, D., Kemp, G.P., Ko, J.Y., Land, R., Mitsch, W.J., Steyer, G., Templet, P. and Yanez-Arancibia, A., 2005. Implications of global climatic change and energy cost and availability for the restoration of the Mississippi delta. *Ecological Engineering* 24, 253–265.

Donnelly, J.P. and Bertness, M.D., 2001. Rapid shoreward encroachment of salt marsh cordgrass in response to accelerated sea-level rise. *Proceedings of the National Academy of Sciences* 98, 14218-14223.

Erickson, J.E., Megonigal, J.P., Peresta, G. and Drake, B.G., 2007. Salinity and sea level mediate elevated CO_2 effects on C_3-C_4 plant interactions and tissue nitrogen in a Chesapeake Bay tidal wetland. *Global Change Biology* 13, 202-215.

Florides, G. A. and Christodoulides, P., 2009. Global warming and carbon dioxide through sciences. *Environmental International* 35, 390-401.

Han, B., Wang, X.K. and Ouyang, Z.Y., 2005. Saturation levels and carbon sequestration potentials of soil carbon pools in farmland ecosystems of China. *Rural Eco-Environment* 21, 6-11.

Hansen, J., Sato, M., Kharecha, P. and von Schuckmann, K., 2011. Earth's energy imbalance and implications. *Atmospheric Chemistry and Physics* 11, 13421–13449.

Hodgkin, E.P. and Hamilton, B., 1998. Changing estuarine wetlands: a long term perspective for management. In: *Wetlands for the Future*, ed. A.J. McComb and J.A. Davis. pp. 243–255. Adelaide, Australia: Gleneagles Publishing.

Hughes, R.G., 2004. Climate change and loss of saltmarshes: consequences for birds. *Ibis* 146(suppl 1), 21–28.

IPCC, 1998. The regional impacts of climate change: an assessment of vulnerability. In: Watson RT, Zinyowera MC, Moss RH (eds) *A special report of IPCC working group II*. Cambridge University Press, Cambridge.

IPCC, 2007. *Climate change 2007: the physical science basis.* Cambridge University Press, New York.

IPCC, 2012. *Managing the Risks of Extreme Events and Disasters to Advance Climate Change Adaptation. A Special Report of Working Groups I and II of the Intergovernmental Panel on Climate Change* [Field, C.B., V. Barros, T.F. Stocker, D. Qin, D.J. Dokken, K.L. Ebi, M.D. Mastrandrea, K.J. Mach, G.-K. Plattner, S.K. Allen, M. Tignor, and P.M. Midgley (eds.)]. Cambridge University Press, Cambridge, UK, and New York, NY, USA, 582 pp.

IPCC, 2013. *Climate Change 2013: The Physical Science Basis. Contribution of Working Group I to the Fifth Assessment Report of the Intergovernmental Panel on Climate Change* [Stocker, T.F., D. Qin, G.-K. Plattner, M. Tignor, S.K. Allen, J. Boschung, A. Nauels, Y. Xia, V. Bex and P.M. Midgley (eds.)]. Cambridge University Press, Cambridge, United Kingdom and New York, NY, USA, 1535 pp.

IPCC, 2014. *Climate Change 2014: Mitigation of Climate Change. Contribution of Working Group III to the Fifth Assessment Report of the Intergovernmental Panel on Climate Change* [Edenhofer, O., R. Pichs-Madruga, Y. Sokona, E. Farahani, S. Kadner, K. Seyboth, A. Adler, I. Baum, S. Brunner, P. Eickemeier, B. Kriemann, J. Savolainen, S. Schlömer, C. von Stechow, T. Zwickel and J.C. Minx (eds.)]. Cambridge University Press, Cambridge, United Kingdom and New York, NY, USA.

Kearney, M.S., Grace, R.E. and Stevenson, J.C., 1988. Marsh loss in Nanticoke Estuary, Chesapeake Bay. *Geographical Review* 78, 205-220.

Kirschbaum, M. U. F., 1995. The temperature dependence of soil organic matter decomposition, and the effect of global warming on soil organic C storage. *Soil Biology and Biochemistry* 27, 753-760.

Lefeuvre, J.C., Laffaille, P., Feunteun, E., Bouchard, V. and Radureau, A., 2003. Biodiversity in salt marshes: from patrimonial value to ecosystem functioning. The case study of the Mont-Saint-Michel bay. *Comptes Rendus Biologies* 326, 125-131.

Lenssen, G.M., Lamers, J., Stroetenga, M. and Rozema, J., 1993. Interactive effects of atmospheric CO_2 enrichment, salinity and flooding on growth of C_3 (*Elymus athericus*) and C_4 (*Spartina anglica*) salt marsh species. *Vegetatio* 104/105, 379-88.

Magenheimer, J.F., Moore, T.R., Chmura, G.L. and Daoust, R.J., 1996. Methane and carbon dioxide flux from a macrotidal salt marsh, Bay of Fundy, New Brunswick. *Estuaries* 19, 139-145.

Marinucci, A.C., 1982. Trophic importance of *Spartina alterniflora* production and decomposition to the marsh estuarine ecosystem. *Biological Conservation* 22, 35-58.

McKee, K., Mendelssohn, I.A. and Materne, M.D., 2004. Acute salt marsh dieback in the Mississippi River deltaic plain: a drought induced phenomenon? *Global Ecology and Biogeography* 13, 65–73.

Michener, W.K., Blood, E.R., Bildstein, K.L., Brinson, M.M. and Gardner, L.R., 1997. Climate change, hurricanes and tropical storms, and rising sea level in coastal wetlands. *Ecological Applications* 7, 770-801.

Morris, J.T., Sundareshwar, P.V., Nietch, C.T., Kjerfve, B. and Cahoon, D.R., 2002. Responses of coastal wetlands to rising sea level. *Ecology* 83, 2869-2877.

Munari, C. and Mistri, M., 2008. The performance of benthic indicators of ecological change in Adriatic coastal lagoons: throwing the baby with the water? *Marine Pollution Bulletin* 56, 95–105.

Murphy, D., Solomon, S., Portmann, R., Rosenlof, K., Forster, P. and Wong, T., 2009. An observationally based energy balance for the Earth since 1950. *Journal of Geophysical Research: Atmospheres* 114, D17107.

Nixon, S.W., 1980. Between coastal marshes and coastal waters--a review of twenty years of speculation and research on the role of salt marshes in estuarine productivity and water chemistry. In *Estuarine and Wetland Processes*, ed. Hamilton, P. and MacDonald, K., pp. 437- 523. New York: Plenum Publ. Corp.

Rogers, K., Saintilan, N. and Heijnis, H., 2005. Mangrove encroachment of salt marsh in Western Port Bay, Victoria: The role of sedimentation, subsidence and sea level rise. *Estuaries* 28, 551-559.

Roman, C.T., Peck, J.A., Allen, J.R., King, J.W. and Appleby, P.G., 1997. Accretion of a New England (U.S.A.) salt marsh in response to inlet migration, storms, and sea-level rise. *Estuarine Coastal and Shelf Science* 45, 717-727.

Rozema, J., Dorel, F., Janissen, R., Lenssen, G., Broekman R, Arp, W. and Drake, B.G., 1991. Effect of elevated atmospheric CO_2 on growth, photosynthesis and water relations of salt marsh grass species. *Aquatic Botany* 39, 45-55.

Shakun, J. D., Clark, P. U., He, F., Marcott, S. A., Mix, A. C., Liu, Z., Otto-Bliesner, B., Schmittner, A. and Bard, E., 2012. Global warming preceded by increasing carbon dioxide concentrations during the last deglaciation. *Nature* 484, 49-55.

Sousa, A. I., Lillebo, A. I., Pardal, M. A. and Caçador, I., 2010. The influence of *S. maritima* on carbon retention capacity in salt marshes from warm-temperate estuaries. *Marine Pollution Bulletin* 61, 215-223.

Trenberth, K.E., Fasullo, J.T. and Kiehl, J., 2009. Earth's global energy budget. *Bulletin of the American Meteorological Society* 90, 311–323.

Turner, R.E., 1976. Geographic variations in salt marsh macrophyte production: A review. *Contributions for Marine Science* 20, 47-68.

USGCRP, 2000. Climate change and America: overview document. *A report of the national assessment synthesis team*. US global change research program, Washington DC.

Valiela I, Peckol P, D'Avanzo C, Kremer J, Hersh D, Foreman, K., Lajtha, K., Seely, B., Geyer, W.R., Isaji, T. and Crawford, R., 1998. Ecological effects of major storms on coastal watersheds and coastal waters: Hurricane Bob on Cape Cod. *Journal of Coastal Research* 14, 218-38.

Warren, R.S. and Niering, W.A., 1993. Vegetation change on a northeast tidal marsh: interaction of sea-level rise and marsh accretion. *Ecology* 74, 96-103.

CHAPTER II

SEA LEVEL RISE IMPACTS ON ESTUARINE SALT MARSHES

CHAPTER II

2.1. SEA LEVEL RISE IMPACTS ON ESTUARINE SALT MARSHES

Introduction

The height of the ocean surface at a given location, or sea level, is measured either with respect to the surface of the solid Earth (relative sea level (RSL)) or a geocentric reference such as the reference ellipsoid (geocentric sea level). RSL is the more relevant quantity when considering the coastal impacts of sea level change, and it has been measured using tide gauges during the past few centuries and estimated from geological records. Changes in sea level occur over a broad range of temporal and spatial scales, with the many contributing factors, making it an integral measure of climate change (Milne *et al*., 2009; Church *et al*., 2010). The primary contributors to contemporary sea level change are the expansion of the ocean as it warms and the water transfer currently stored on land to the ocean, particularly from land ice (glaciers and ice sheets) (Church *et al*., 2011). Ocean thermal expansion and glacier melting have been the dominant contributors to 20th century global mean SLR. Records from warm periods during the last 3 million years indicate that global mean sea level has exceeded 5 m above the present level when global mean temperature was up to 2°C warmer than pre-industrial. According to the latest IPCC report it is very likely that the rate of global mean SLR during the 21st century will exceed the rate observed during 1971–2010, representing in a worst case scenario a rising rate of 8 to 16 mm yr^{-1} between 2081 and 2100. This increase will primarily be the result of an increase in mean sea level, with the frequency of a particular sea level extreme increasing by an order of magnitude or more in some regions by the end of the 21st century. Moreover, it is very likely that over about 95% of the world ocean, regional SLR will be positive, and most regions that will experience a sea level fall are located near current and former glaciers and ice sheets. About 70% of the global coastlines are projected to experience a relative sea level change within 20% of the global mean sea level change. Changes in ocean currents, ocean density and

sea level are all tightly coupled such that changes at one location impact sea level far from the location of the initial change, including changes in sea level at the coast in response to changes in open-ocean temperature (Landerer *et al*., 2007; Yin *et al*., 2010). Although both temperature and salinity changes can contribute significantly to regional sea level change (Church *et al*., 2010), only temperature change produces a significant contribution to global average ocean volume change due to thermal expansion or contraction (Gregory and Lowe, 2000). Along any coast, vertical motion of either the sea or land surface can cause changes in sea level relative to the land (known as relative sea level). For example, a local change can be caused by an increase in sea surface height, or by a decrease in land height. Over relatively short time periods (hours to years), the influence of tides, storms and climatic variability—such as El Niño—dominates sea level variations. Earthquakes and landslides can also have an effect by causing changes in land height and, sometimes, tsunamis. Over longer time periods (decades to centuries), the influence of climate change is the main contributor to sea level change in most regions. Over these longer time scales, various processes may also cause vertical motion of the land surface, which can also result in substantial changes in relative sea level. Since the late 20th century, satellite measurements of the height of the ocean surface relative to the centre of the Earth (known as geocentric sea level) show differing rates of geocentric sea level change around the world.

Vegetated coastal habitats are globally declining (Duarte *et al*., 2005), rendering shorelines more vulnerable to erosion due to increased SLR and increased wave action (e.g. Alongi, 2008) and leading to the loss of carbon stored in sediments. Together, the loss of coastal wetlands and seagrass meadows results in the release of 0.04 to 0.28 Pg C annually from organic deposits (Pendleton *et al*., 2012). The response of salt marshes to SLR involves landward migration of salt-marsh vegetation zones, submergence at lower elevations, and drowning of interior marshes. Ocean warming changing the range of vegetated coastal habitats. The poleward limit of mangrove forests is generally set by the 20 °C mean winter isotherm (Duke *et al*., 1998). Accordingly, migration of the isotherm with climate change (Burrows *et al*., 2011) should lead to a poleward expansion of mangrove forests, as observed in the Gulf of Mexico (Perry and Mendelssohn, 2009; Comeaux

et al., 2011; Raabe *et al*. 2012), and New Zealand (Stokes *et al*., 2010), leading to increased sediment accretion.

It is evident that SLR impacts need to be addressed on a regional scale, focusing the different ecosystem partners, but also in a multidisciplinary approach. The primary productivity of the coastal vegetation will be inevitably impacted, leading to consequences in the coastal accretion/erosion balance and in the adjacent water bodies biogeochemistry. Having these facts in mind, the present chapter intents to make a multidisciplinary approach of the SLR impacts on the Mediterranean marshes, focusing the primary productivity of the main colonizing species, its geological impacts and hydrodynamic and biogeochemical features, merging all these aspects on an ecosystem perspective.

References

Alongi, D.M., 2008. Mangrove forests: resilience, protection from tsunamis, and response to global climate change. *Estuarine, Coastal and Shelf Science* 76, 1-13.

Burrows, M.T., Schoeman, D.S., Buckley, L.B., Moore, P., Poloczanska, E.S., Brander, K.M., Brown, C., Bruno, J.F., Duarte, C.M., Halpern, B.S., Holding, J., Kappel, C.V., Kiessling, W., O'Connor, M.I., Pandolfi, J.M., Parmesan, C., Schwing, F.B., Sydeman, W.J. and Richardson, A.J., 2011. The pace of shifting climate in marine and terrestrial ecosystems. *Science* 334, 652-655.

Church, J.A., Gregory, J.M., White, N.J., Platten, S.M. and Mitrovica, J.X., 2011. Understanding and projecting sea level change. *Oceanography* 24, 130–143.

Church, J.A., Woodworth, P.L., Aarup, T. and Wilson, W.S. (eds.) 2010. Understanding Sea-Level Rise and Variability. Wiley-Blackwell, Hoboken, NJ, USA, 428 pp.

Comeaux, R.S., Allison, M.A. and Bianchi, T.S., 2011. Mangrove expansion in the Gulf of Mexico with climate change: implications for wetland health and resistance to rising sea levels. *Estuarine, Coastal and Shelf Science* 96, 81-95.

Duarte, C.M., Middelburg, J.J. and Caraco, N., 2005. Major role of marine vegetation on the oceanic carbon cycle. *Biogeosciences* 2, 1-8.

Duke, N.C., Ball, M.C. and Ellison, J.C., 1998. Factors influencing biodiversity and distributional gradients in mangroves. *Global Ecology and Biogeography Letters* 7, 27-47.

Gregory, J.M., and Lowe, J.A. 2000. Predictions of global and regional sea-level rise using AOGCMs with and without flux adjustment. *Geophysical Research Letters* 27, 3069–3072.

Landerer, F. W., J. H. Jungclaus, and J. Marotzke, 2007: Regional dynamic and steric sea level change in response to the IPCC-A1B scenario. *Journal of Physical Oceanography* 37, 296–312.

Milne, G.A., Gehrels, W.R., Hughes, C.W. and Tamisiea, M.E., 2009. Identifying the causes of sea-level change. *Nature Geosciences* 2, 471–478.

Pendleton, L., Donato, D.C., Murray, B.C., Crooks, S., Jenkins, W.A., Sifleet, S., Craft, C., Fourqurean, J.W., Kauffman, J.B., Marba, N., Megonigal, P., Pidgeon, E., Herr, D., Gordon, D. and Baldera, A., 2012. Estimating global "blue carbon" emissions from conversion and degradation of vegetated coastal ecosystems. *PLoS One* 7, e43542.

Perry, C.L. and Mendelssohn, I.A., 2009. Ecosystem effects of expanding populations of *Avicennia germinans* in a Louisiana salt marsh. *Wetlands* 29, 396-406.

Raabe, E.A., Roy, L.C. and McIvor, C.C., 2012: Tampa Bay coastal wetlands: nineteenth to twentieth century tidal marsh-to-mangrove conversion. *Estuaries and Coasts* 35, 1145-1162.

Stokes, D.J., Healy, T.R. and Cooke, P.J., 2010. Expansion dynamics of monospecific, temperate mangroves and sedimentation in two embayments of a barrier enclosed lagoon, Tauranga Harbour, New Zealand. *Journal of Coastal Research*, 26, 113-122.

Yin, J. J., Griffies, S.M. and Stouffer, R.J., 2010. Spatial variability of sea level rise in twenty-first century projections. *Journal of Climate* 23, 4585–4607.

2.2. HYDRODYNAMICAL CHANGES DRIVEN BY SEA LEVEL RISE AND ITS IMPACT ON MARSH PRODUCTIVITY AND BIOGEOCHEMICAL CYCLING[1]

Abstract

The Tagus estuary is a model mesotidal bay estuary located in the Western Portuguese coast, characterized by large areas of salt marshes (17.24 km2) and tidal flats distributed along the margins. Halophyte vegetation in this system concentrates heavy metals in their organs along the growing season and subsequently releases these metals to the ocean following senescence. Although there currently there are no metal discharges to the estuarine bay, this was not true in the past, and thus there are still large amounts of metals within the system. The results here presented show that in the case of Tagus estuary, a contaminated marsh can export about 162 Zn kg m^{-2} y^{-1}, 26 Cu kg m^{-2} y^{-1}, 28 Pb kg m^{-2} y^{-1} and 1 Cd kg m^{-2} y^{-1}. Mixing eddies are generated inside the estuary, during frequent flood events, enhancing erosion and transport of particles to the coastal ocean. During neap tide periods plant detritus is mostly retained in the inner estuary in the vicinity of the marsh source; during spring tides, however, export to the main channel and to the ocean is significantly increased. Sea level rise (SLR) and/or expected increase in the frequency of flood events will increase detrital movement within the estuary and discharges of metal contaminated particles to the ocean shelf. This research highlights the capacity of the present estuary to moderate metal fluxes to the ocean, but also call for efforts to reduce present contaminant inputs from the watershed to mitigate contaminant transport to the ocean in the future.

[1] This section under revision in: **Duarte, B.**, Vaz, N., Valentim, J.M., Dias, J.M., Silva, H., Marques, J.C. and Caçador, I. Revisiting the Outwelling Hypothesis: Modelling Salt Marsh Detrital Metal Exports under Extreme Climatic Events (submitted to Marine Chemistry).

Introduction

Heavy metals have always been a major concern when addressing urbanized estuaries and coastal areas (Brian, 1971; Kersten and Förstner, 1986; Caçador *et al*., 1996 and other hereafter from the same authors). The metal transport mechanisms from the river to the estuary and from this last one into the ocean, depends on the links established between metals and the organic ligands present in the dissolved phase and also on the nature and amount of mineral and organic particles in suspension (Viers *et al*., 2009). Since the industrial revolution large amounts of contaminants have been released to the atmosphere, soils and watercourses. Most of these emissions will be transferred in ultimate analysis into a water matrix, either by atmospheric deposition or by soil erosion, where they will stay dissolved or associated to sediment particles (Nriagu, 1988; Viers *et al*., 2009). This is a very dynamic mechanism greatly influenced by the river hydrological conditions.

Coastal waters nutrient regeneration and detrital consumers are mostly supported by particulate organic matter (POM) exported from the adjacent coastal systems. A large amount of this detritus is originated in wetlands due to the senescence of its plant community and has been considered an important functional role of wetlands giving strong arguments for its conservation (Snedaker, 1978; Macintosh, 1981; Caçador *et al*., 2009; Duarte *et al*., 2010). This process was initially described by Odum (1968) as “outwelling”. Some years later, its creator reviewed the hypothesis and concluded that detrital “outwelling” from estuarine wetlands is a widespread process, greatly dependent on the physical characteristics of the wetland (Odum, 1980). Through this process, estuarine and coastal ecosystems are interconnected, exchanging energy in several forms (nutrients, organic matter and organisms), being this highly modulated by their biotic and abiotic interactions (Bouchard, 2007). More recently, the concept of outwelling has been subsumed into the concept of “coupled ecosystems” that recognizes that material transport between marshes, estuaries, and coastal ecosystems and between riparian boundaries and rivers can be in both directions. (Bouchard, 2007). Junk *et al*. (1989) recognized that episodic changes in river flow may contribute significantly to material exchange between coupled ecosystems. Nevertheless, it is also widely accepted that the export of organic matter from upland (e.g., riparian zones and salt

marshes) to marine systems fuels secondary production (Deegan *et al*. 2000). The existence of this ecological connection between aquatic and their adjacent terrestrial environments is considered to be one of the most important factors in which relies the integrity of both ecosystems (Bouchard, 2007). Recently, reports on salt marsh dieback have appeared all over the world (Alber *et al*., 2008). Wetland dieback or deterioration from any cause can increased material transport to adjacent coastal waters (Dagg *et al*., 2007). Wetlands and in particular salt marshes are known to be highly productive, being among the most valuable ecosystems on the planet (Constanza *et al*., 1997), with a gross primary production that can reach the 3700 g m-2 y-1, on a biomass basis, according to Gallagher *et al*. (1980). Along with high productivity, salt marshes also generate proportionately large amounts of plant detritus as part of the phenological cycle (Duarte *et al*., 2012; Caçador *et al*., 2009; Duarte *et al*., 2010). Belowground necromass is normally incorporated into the sediments and subjected to mineralization processes (Duarte *et al*., 2008; 2010). On the other hand, aboveground detritus fall into the surface sediment and become prone to the tidal erosion and export (Caçador *et al*., 2009). Detritus generation and transport also varies from species to species. Due to the high floristic diversity European marshes generate not only large amounts of necromass but also a wide range of qualitatively different detritus during a large temporal window (Beeftink, 1977; Lefeuvre *et al*., 1994; Caçador *et al*., 2009).

Marsh detritus exportation is dependent on the primary production, on-line burial, decomposition and exports. Belowground biomass is more prone to burial and decomposition, being decomposed on-site with consequent impacts on the local contamination levels (Duarte *et al*., 2008), while for above ground detritus production, these two processes become out of the equation being highly exported to the water column (Caçador *et al*., 2009) Thus, there is a need to revisit the balance between primary production and flooding frequency incorporating this high diversity of halophytes in the European marshes and their differential primary productivity, N and C allocation, as well as differential contaminant uptake, like heavy metals. Although the quantification of detrital production is well known for several types and marsh locations (Snedaker, 1978; Macintosh, 1981; Bouchard and Lefeuvre, 2000; Bouchard, 2007; Caçador *et al*., 2009; Das *et al*., 2010), there is

almost no information on detritus trajectories and fate. Since detritus exports is highly dependent on the so-called 'flood pulse', the hydrodynamic evaluation of these mechanisms from the estuarine area to adjacent coastal waters bring new insights on the ecohydrology of these systems (Valentim *et al*., 2013). As predicted sea level rise is likely to flood and erode many coastal and estuarine wetland ecosystems (Valentim *et al*., 2013; Duarte *et al*., 2013; Duarte *et al*., 2014), the fate of marsh detritus needs to be better understood. Due to the large urbanization level of the estuarine margins, Tagus salt marshes have no room for upland migration under a SLR scenario, becoming prone to erosion.

In the present study, the authors determine the rate of detritus production at one marsh bordering the Tagus estuary and, using a hydrodynamic model of the estuary, determine the present fate of this detritus. This model is then used to determine the differences in detrital transport during high and low flows from the watershed and under anticipated conditions of sea level rise.

.

Material and Methods

Study area

The Tagus Estuary (Figure 2.2.1; also called Tejo in Portuguese and Tajo in Spanish) drains a watershed of 80,000 km^2 in Spain and Portugal, which includes the capitals cities of both countries (Madrid and Lisbon). The Estuary is mesotidal and has a surface area of about 320 km^2, an average depth of 10.6 m, and a mean volume of 1900 x 106 m^3. The estuary is from 2 to 15 km wide. The Estuary can be subdivided into two distinctly different topographic and hydrodynamic regions: The upper Estuary is characterized by narrow channels, small islands, and tidal flats (approximately 40% of the estuarine floor is exposed at low tide). The lower Estuary is characterized by a well-defined channel, deeper water, and its direct connection to the Ocean.

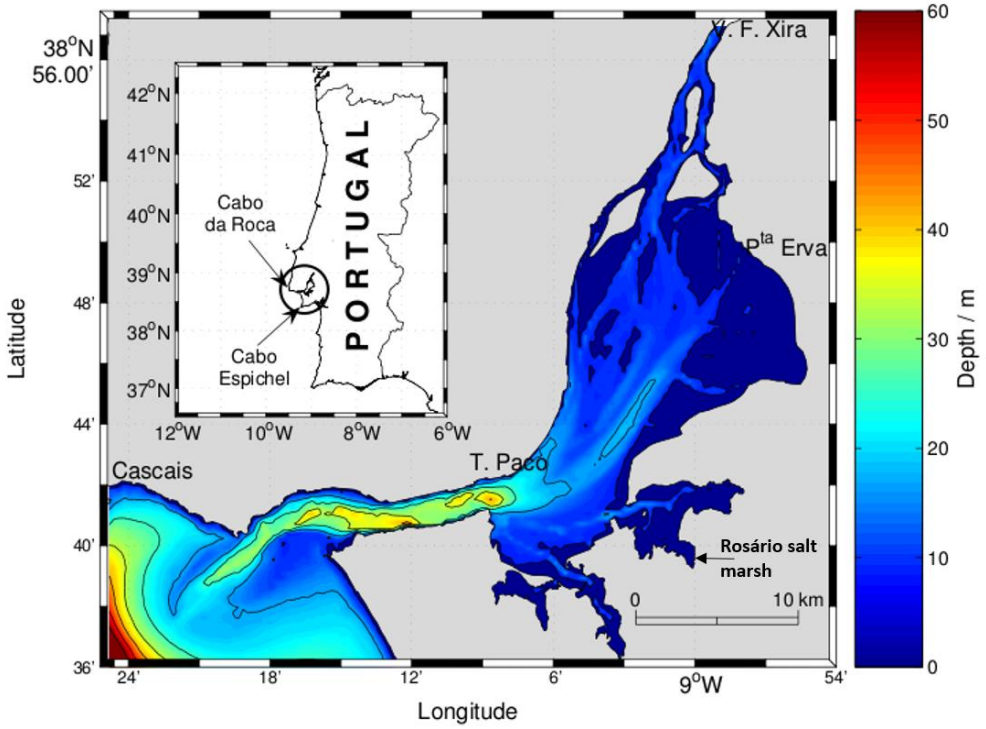

Figure 2.2.1. Tagus Estuary bathymetry and sampling site location (from Neves, 2010).

The Tagus River is the major freshwater source to the Estuary (mean annual discharge 4000 m^3 s^{-1}), but two minor tributaries, the Sorraia and Trancão Rivers, contribute 35 and 2.5 m^3 s^{-1}, respectively, discharge to the upper Estuary. The Tagus Estuary is ebb dominated, with flood flows typically 1 hour longer than ebb flows and ebb velocities larger than flood velocities. Tides propagate upstream for approximately 80 km and maximum tidal currents can reach 2.0 m^3 s^{-1}. The Tagus is ebb dominated, with floods typically 1 h longer than ebbs (stronger velocities during ebbs), and thus inducing a net export of sediments (Fortunato *et al*., 1999). The area affected by tides reaches 80 km landward of Lisbon and maximum tidal currents achieve about 2.0 m s^{-1} (Gameiro *et al*., 2007).

Sampling

Plant sampling was carried out in Rosário salt marsh adjacent to the Tagus estuary (Figure 1), This site is inundated by semidiurnal tides and is dominated by *Halimione portulacoides*, *Sarcocornia perennis*, *Sarcocornia fruticosa* and *Spartina maritima* (Caçador *et al*., 2013). Sampling was conducted during the growing season from March to December 2012. The above ground biomass of pure stands of each

species was sampled by clipping five squares, each of 0.25 m^2 in five permanent transects. The biomass was washed with deionized water to remove dust and sediment, stored in plastic bags, and returned to the laboratory for drying, homogenizing, weighing and the determination of metal content. As described before (Caçador *et al*., 1999) the selected period comprises the beginning and the end of the growing season, allowing to sample in the maximum and minimum biomass period for all the studied species. Previous works also shown that this approach was sufficient to have a representative sampling of both the plants biomass and metal pools (Caçador *et al*., 1996; Caçador *et al*., 2009; Duarte *et al*., 2010). The aboveground plant biomass collected was washed with Milli-Q water to remove dust and sediment, dried at 60°C and powdered in a grinding ball mill (Glen Creston MM2000) (Gross *et al*., 1991). Net Primary Production (NPP, Kg m^{-2}) was calculated as:

$$\mathrm{NPP} = \mathrm{Maximum\ biomass} - \mathrm{Minimum\ Biomass}$$

, where Maximum biomass is the biomass attained at the end of the growing season and before senescence and the Minimum biomass is the biomass of the plants at the beginning of the growing season.

Aboveground biomass losses (ABL, Kg m^{-2}) were calculated as:

$$\mathrm{ABL} = \mathrm{Maximum\ biomass} - \mathrm{Lowest\ following\ biomass}$$

, where the Lowest following biomass is the biomass at the end of the senescence period.

Each transect was considered a replicate with all four species present a used to calculate the NPP and ABL over the time period considered individually. For global export calculations an average value of each species in all transects was used.

Plant tissues heavy metal concentration

Plant samples (approximately 100 mg) were digested with 10 mL of $HNO_3/HClO_4$ (7:1 v/v) at 110°C. This procedure was repeated twice, as described by Otte (1991). Metal concentrations (Cu, Co, Zn, Pb and Cd) of the most abundant

elements known to be present in the Tagus system (Caçador *et al*., 1996; 2009; Duarte *et al*., 2010; Duarte *et al*., 2014), were determined by flame atomic absorption spectrometry (FAAS) with a mobile phase of air-acetylene. International certified reference material BCR 62 was used to ensure accuracy and precision was determined by analysing replicate samples. Trace metal concentrations in the reference materials determined by FAAS were not statistically different from their certified ones (t-student; $\alpha = 0.05$).

Hydrodynamic modelling and simulations

In this work the hydrodynamic numerical model MOHID (Martins *et al*., 2001), which was designed for coastal and estuarine shallow water applications is used. MOHID is a baroclinic finite volume model that solves the three-dimensional incompressible primitive equations, and assumes the hydrostatic equilibrium as well as the Boussinesq and Reynolds approximations. The model equations were presented in several studies and can be consulted in Vaz (2007), for example. This model has been applied to different coastal and estuarine areas (e.g. Vaz *et al*., 2005, 2007, 2009, 2011; Bernardes, 2007; Malhadas *et al*., 2009; Valentim *et al*., 2013), demonstrating its ability to simulate complex flows features. In the present study, a previously validated set-up of the MOHID model for the Tagus estuary (Vaz *et al*., 2011) was applied. Details about model accuracy in reproducing the tidal dynamics for this application after model's calibration and validation can be consulted in Vaz *et al*. (2007). The model was implemented in a 2D depth integrated mode for the whole estuary. For the Tagus estuary application, a three level nesting model is implemented (Vaz *et al*., 2009). In the first domain (D1, which covers most of the Atlantic coast of Iberia and Morocco), a tidal driven model is applied, which uses the FES2004 global solution as forcing, and has variable horizontal resolution (0.02° - 0.04°). The second domain (D2) has a horizontal resolution similar to D1 and the third domain (D3) encompasses the whole extension of the Tagus estuary. The numerical grid of D3 presents 335 x 212 cells of 200 m each and on its open ocean boundary the model input was the tidal forcing from D2 (Vaz *et al*., 2011). On the bottom, the model uses moving boundaries, which are closed boundaries whose position varies in time. This situation occurs in domains with intertidal areas. In this

case the uncovered cell must be tracked. The model uses a criterion in which a minimum depth (HMIN) is defined. HMIN is the minimum depth below which the cell is deemed to be dry, thus, conserving a thin volume of water above the uncovered cell (Vaz *et al*., 2005). Here, HMIN is 0.10m.

Three scenarios of river inflow were created. Rivers inflow were imposed at the landward boundaries considering three different situations: i) low freshwater discharge, considering 20, 2 and 1 m^3 s^{-1} for Tagus, Sorraia and Trancão Rivers, respectively; ii) a mean discharge of 400, 40 and 5 m^3 s^{-1} for Tagus, Sorraia and Trancão; and iii) a high discharge scenario, considering an inflow of 2000, 200 and 10 m^3 s^{-1} for the three rivers. The time step of the model was 15 s and a horizontal viscosity of 5 m^3 s^{-1} and a friction drag coefficient of 0.0025 were considered. A spin-up time of 4 days for the hydrodynamic model was considered. The velocity predictions were used to determine the residual circulation for each cell of the numerical grid for the whole estuary as well as the average velocity, here represented by the Root Mean Square velocity (V_{rms}), for the areas near the Rosário salt marsh. The V_{rms} was analysed both in Neap and Spring Tide condition.

Also, a Lagrangean particle-tracking module was coupled to the hydrodynamic model and was used to determine the Lagrangean paths of passive particles released in the area near the selected marsh at Tagus Estuary: the Rosário salt marsh. In this module, two main properties are defined: spatial co-ordinates (x, y, z) and the random horizontal/vertical velocities which are responsible for the particle movement, e.g. the particle position is a function of the velocity in each grid cell. Here the particles could be trapped in a dry cell (at low water period) being released when the cell turn wet as the tidal waves progresses during the flood. The particles were released in ebb tide, in Neap and Spring Tide condition, and their path was monitored for several tidal cycles. The movement of the tracers is determined from the velocity field computed by the hydrodynamic model using the procedure followed by (Lopes *et al*., 2006). Two climate scenarios in the numerical simulations were evaluated (present and future (2100)) in order to study the SLR effects in the residual circulation, Lagrangean transport and the root-mean square velocity (V_{rms}). Therefore, the model parameters were kept for both scenarios, except the mean sea level value: 2.08 m was considered for present sea level simulation, while 2.50 m

was adopted for the SLR scenario. This rise of 0.42 m was considered based on local projections of SLR in Portuguese coast for the IPCC A2 storyline (Lopes *et al*., 2011).

Hydrodynamic parameters

Essentially dominated by tidal asymmetries, tidally averaged circulation is generated through the interaction of tidal currents with topographic features. In coastal systems with fast tidal currents such as the Tagus estuary, tidally averaged currents play an important role in the transport of nutrients, sediment and organic matter towards coastal seas or their retention inside the water bodies. As a result of the nonlinearity of these processes, numerical models have been found to be an appropriate tool to investigate tidal and residual flow in several systems, as for instance in the Gulf of California (Dworak and Gómez-Valdés, 2002), the Shark Bay, Western Australia (Burling *et al*., 2003), the Ria de Aveiro, Portugal (Sousa and Dias, 2007; Lopes and Dias, 2011) and the Tagus Estuary (Vaz and Dias, 2014). In the present study, tidally averaged currents were obtained for all grid cells directly from model results by averaging the predicted velocities during a fortnightly simulation period. Once this is a multiple of tidal constituents M2 and S2 periods, the main tidal constituents are filtered, including those related with spring and neap tidal cycle.

The root-mean square velocity (V_{rms}) was determined for the surrounding salt marshes areas from instantaneous velocity values (V_i) determined for full tidal cycles through the application of the equation:

$$V_{rms} = \frac{1}{N}\left(\sum_{i=1}^{N} {V_i}^2\right)^{1/2}$$

where N is the total number of velocity values for each cell in a full tidal cycle (N=118).

Lagrangean transport is a very useful tool to understand estuarine dynamics, allowing the analysis of particles fate through the estimation of its trajectory, being extremely valuable in the sediment and nutrient transport interpretation, by simply following the tracks of selected particles (Lopes *et al*., 2006). Horizontal fields for

tidally averaged currents were determined for both scenarios under analysis. Horizontal fields for V_{rms} and Lagrangean transport were also determinate but, in these cases, specific for Neap and Spring Tide conditions. Percentage differences between the results for present and SLR situations for residual circulation and V_{rms} were calculated in order to assess SLR effects in those hydrodynamic parameters patterns. For the interpretation of the tidally averaged circulation and V_{rms} results, mean values of the salt marsh and the surrounding areas were considered.

Results

Detrital production and exports

As observed in Table 2.2.1 *S. fruticosa* presents the higher biomass production along an annual cycle, whilst *Spartina maritima* presents the lowest values. A higher biomass production generally leads to higher detritus production, as observed in *S. fruticosa*. *H. portulacoides* and *S. perennis* showed very similar biomass and detritus production, with values near to those verified in *S. maritima*. Considering the metal pools of the produced biomass, these differences suffer some changes. Although *S. fruticosa* remains as the species that accumulates higher amounts of all the analysed metals on an area basis, in which concerns the metal exports due to aboveground senescence, some metals present different trends. Cadmium is probably the best example, where all the halophytes analysed presented values of exports within the same order of magnitude. The same could be verified for Cu, with *S. fruticosa* presenting similar exports to those observed to *S. maritima*. In fact, although with the lowest biomass production, *S. maritima* present very high metal accumulations and exports due to the elevated exported biomass percentage. In sum, considering all the exports of each specie for all the extension of the considered marsh, about 80-90% of the metal pools are exported due to senescence, being Zn the more exported, followed by Cu and Pb and finally by Cd with both low accumulation and export values (Table 2.2.1).

Table 2.2.1. Biomass (Kg m^{-2} y^{-1}) and heavy metal (Kg m^{-2} y^{-1}) production and exports of the four most abundant halophytes in Rosário salt marsh (average ± standard deviation, n = 5).

		H. portulacoides	*S. fruticosa*	*S. perennis*	*S. maritima*
Production					
	Biomass	0.74 ± 0.1	4.1 ± 0.5	0.51 ± 0.0	0.4 ± 0.1
	Zn	44.1 ± 9.5	128.2 ± 15.1	23.1 ± 2.1	79.1 ± 7.7
	Cu	3.25 ± 0.4	21.9 ± 11	4.0 ± 0.7	14.7 ± 0.9
	Pb	5.7 ± 0.7	24.2 ± 2.1	3.4 ± 0.4	11.8 ±.1.2
	Cd	0.3 ± 0.1	0.83 ± 0.04	1.0 ± 0.1	0.8 ± 0.1
Exports					
	Biomass	0.58 ± 0.1	3.9 ± 0.7	0.43 ± 0.0	0.28 ± 0.0
	Zn	35.1 ± 7.2	123.3 ± 12.8	21.4 ± 1.6	45.3 ± 5.1
	Cu	2.6 ± 0.1	21.26 ± 0.93	3.8 ± 0.4	10.1 ± 1.0
	Pb	4.4 ± 0.2	23.32 ± 1.32	3.1 ± 0.6	6.5 ± 0.9
	Cd	0.25 ± 0.1	0.81 ± 0.07	0.92 ± 0.1	0.6 ± 0.1

Tidally averaged Circulation

Tidally averaged currents in the Tagus Estuary are very much influenced by the bottom topography and river discharge. These residual flows are depicted in Figure 2.2.2. In general, higher velocities are generated in the deeper areas of the estuary due to the high freshwater discharge, which enhances the existent tidally driven residual circulation (Figure 2.2.2b). Also, higher residual velocities are found in the deeper areas of the estuary for all three cases. The existent tidally averaged currents combined with the freshwater discharge generate residual flows higher than 0.3 m s^{-1} in the deeper channels of the estuary (Figure 2.2.2), reducing to values of about 0.1 (0.05) m s^{-1} in the medium (low) discharge scenario (Figure 2.2.2a). The freshwater inflow act to generate two distinct corridor flows at the upstream and central region of the estuary. In fact, the flow associated with the Tagus and Sorraia River favours the generation of two visible corridor flows near the north margin and central region, respectively, where the estuary is deeper. In the central region of the estuary, outside these corridor flows (shallow region near the south margin), no

influence of the river discharge is visible and the residual flows are mainly driven by the interaction of the tidal flows and local bathymetry. Here, the residual currents are of the order of 0.01 m s^{-1} and practically nullified by the back and forth movement of the tide. Near the estuary mouth a less organized pattern exists. Here, the tidally averaged currents range between 0.1 (medium and low discharge) to 0.3 m s^{-1} in the high discharge scenario (Figure 2.2.2b). Moreover, a noticeable feature of this region is the generation of eddies due to interaction of the estuarine circulation with the complex local bathymetry, which increases the nonlinearity of transport processes in this region. In a previous study of the Tagus Estuary mouth, Fortunato *et al*. (1997) observed the generation of these eddies, relating them with the spring and neap tidal cycle, and highlighting their importance to mixing processes in this region. In the region of the Rosario salt marsh, due to its shallowness, residual flows are quite small, being lower than 0.01 m s^{-1}. Therefore, in this region the residence time tends to be high and strongly modulated by the back and forth movement of the tidal wave.

The main features of the residual flow spatial distribution due to tides, freshwater discharge and wind were presented by Vaz and Dias (2014). In this study the magnitude and location of preferential flow paths in the estuary are highlighted. This is quite important since tidally averaged flows may induce theoretical transport pathways inside the estuary. The results of the tidally averaged flows presented here, are similar to those presented by Vaz and Dias (2014) and allow the definition of different theoretical paths for dissolved properties within the estuary. The river discharge may induce different paths of dispersion and transport of properties through two well-defined corridors passing through the deeper areas of the estuary. The outflow of the Tagus and Sorraia produces a downward transport of properties, which is visible in the central area of the estuary, corresponding to its mixing area. Then, the transport turns more chaotic due to the particular features of the bathymetry of the estuary in the area close to its mouth. Moreover, the corridor flow is highly dependent on the river discharge. A Tagus river discharge of 2000 m^3 s^{-1} (and a 200 m^3 s^{-1} for the Sorraia) produces two well-defined corridor flows, which are not so understandable in the tidal driven residual flow spatial pattern (Figure 2.2.2a). Under the average and no river outflow scenarios, these corridor flows

decrease their extent and are confined to the upstream region of the estuary. The particulate matter with origin in the Rosário salt marsh is influenced by its entrance in the deeper region of the estuary, where its movement is highly influenced not only by the tidal wave, but also by the freshwater inflow from the main tributaries.

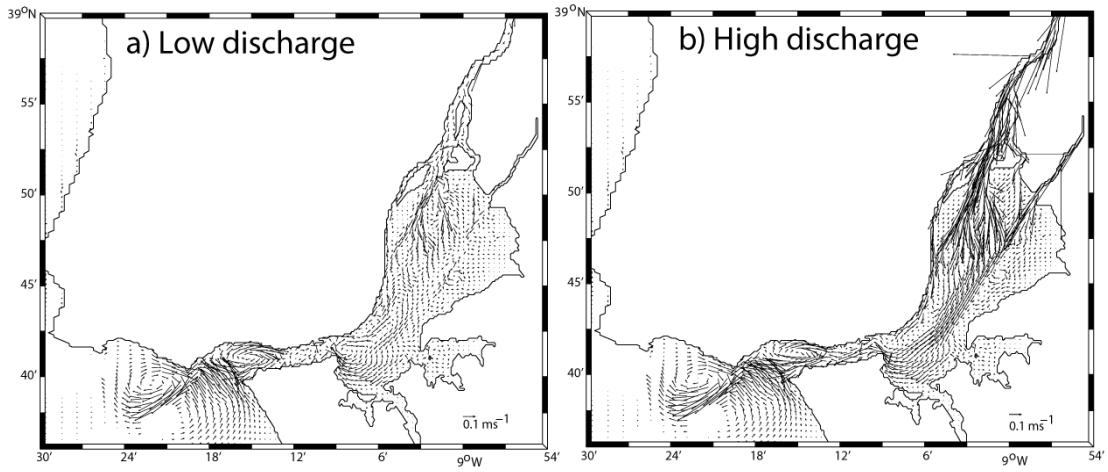

Figure 2.2.2. Residual circulation in the whole Tagus estuary under high and low freshwater discharge (2210 $m^3 s^{-1}$ and 23 $m^3 s^{-1}$ respectively) scenarios.

Root-mean square velocity (V_{rms})

In the surrounding area of the Rosário salt marsh, the main feature influencing the dynamics is the tidal wave propagation. For this reason, the Vrms is computed just for the present sea level scenario and for the SLR scenario previously described. In Figure 2.2.3 the results of V_{rms} at the region surrounding the Rosário salt marsh are depicted, considering the present MSL and SLR scenarios. Also the differences (in percentage) between both scenarios are depicted (Figure 2.2.3c and 2.2.3f). In general, velocities are higher in spring tide than in neaps, which is an expected result since large pressure gradients are expected in the first case. However, these higher values are only visible in the region that connects the region near the Rosário salt marsh to the rest of the estuary. For the present (MSL) scenario, during spring tides, values higher than 0.5 m s^{-1} are visible (Figure 2.2.3d), reducing to values lower than 0.3 during neaps (Figure 2.2.3a). For the SLR scenario, the same patterns are visible, however, there are some differences between the results for the present and SLR scenarios. In the SLR scenario, there is a tendency to

change in V_{rms} of about 40% both in neap and spring tide conditions (Figures 3c,f and 3b,e respectively) (~3.85 cm s^{-1} and ~7.10 cm s^{-1}, respectively). These results are justified by the salt marsh location in a very shallow region of the estuary, where low velocity and high residence time are found. These results also highlight that low stress condition is experimented by the Rosário salt marsh in the SLR scenario.

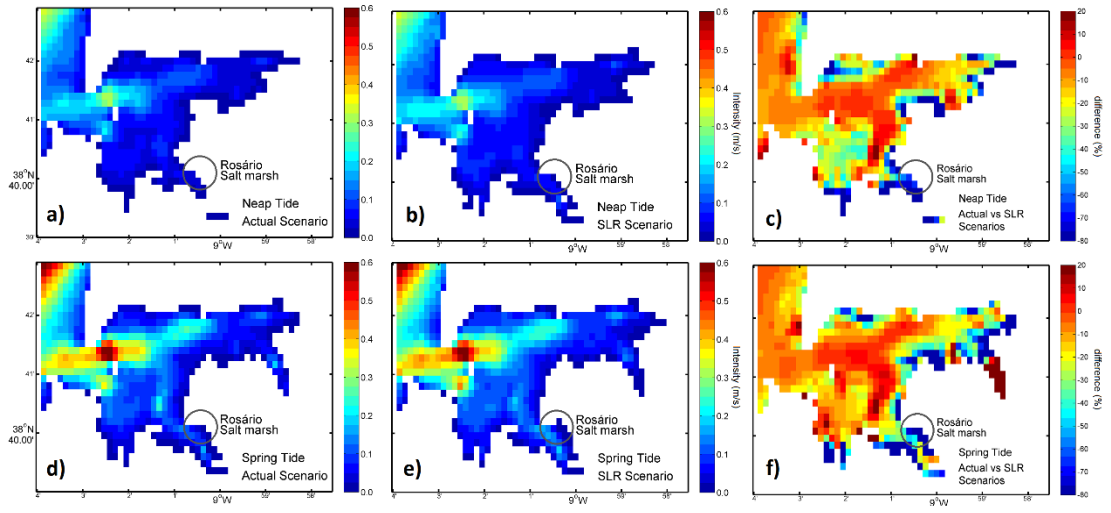

Figure 2.2.3. Residual mean square velocity in the vicinity of Rosário salt marsh in neap and spring tides during normal and future SLR conditions.

Lagrangean particles trajectory

Considering the plant detritus exported as passive particles and according to model results, in Neap Tide, Lagrangean particles remain close to the salt marsh during ~15h in the present scenario (Figure 2.2.4 and 2.2.5). Some particles remain in the surrounding salt marsh area for ~45h and certain particles only begin to disperse and leave the salt marsh channel after ~30h, reaching the central area of the adjacent Montijo channel after ~48h. In SLR scenario, in Neap Tide (Figure 2.2.4 and 2.2.5), particle dispersion is lower than in present scenario. In this case, particles reach far way the salt marsh channel, approaching the cannels head. The SLR increases tidal amplitude, as such, tide could reach more often some areas that weren´t flooded so frequently before. Moreover, there is a lower amount of particles approaching the main area of the Montijo channel (after ~ 48h). In fact, the amount of particles that leaves the surrounding areas of the salt marsh is much smaller. In addition, according to the results present in Figure 2.2.4, the detrital particles

remain close to the salt marsh less time than in present scenario, which may be explained by the higher V_{rms} verified in the SLR condition. As such, the residence time decreases in the SLR condition. Model results also indicate that 2.5 days (60h) are not enough for the particles to reach the Tagus estuary bay, in both sea level cases. During Neap tides, in present scenario tidal currents are weak, contributing to the low dispersion of detrital particles. On the contrary, dispersion is higher in Spring Tide. For the present tidal scenario (MSL), and for low freshwater inflow, the passive particles reach an area in the central region of the estuary, and remain there for all the simulation period. The particles are trapped in this region because tidal velocities are not high enough to advect them to the estuary entrance. On the contrary, for the high freshwater discharge scenario, particles reach the estuary corridor (near the mouth) ~60 hours after their release. This trajectory in modulated by tidal velocities enhanced by a downstream velocity due to the river inflow. Residual circulation results show that in the estuary its intensity increases by one order of magnitude for high freshwater discharge scenarios. Contrarily, in SLR scenario, the particles dispersion is much higher than in present scenario and the amount of particles that concentrates in the salt marsh channel is smaller (Figure 2.2.4 and 2.2.5). The faster dispersion of detrital particles in this climate change context may be justified by the verified increase of the V_{rms} and residual circulation with SLR. Furthermore, the amount of particles reaching the central area of the Montijo channel is much higher. Therefore, model results also indicate that the residence time will decrease in the climate change situation.

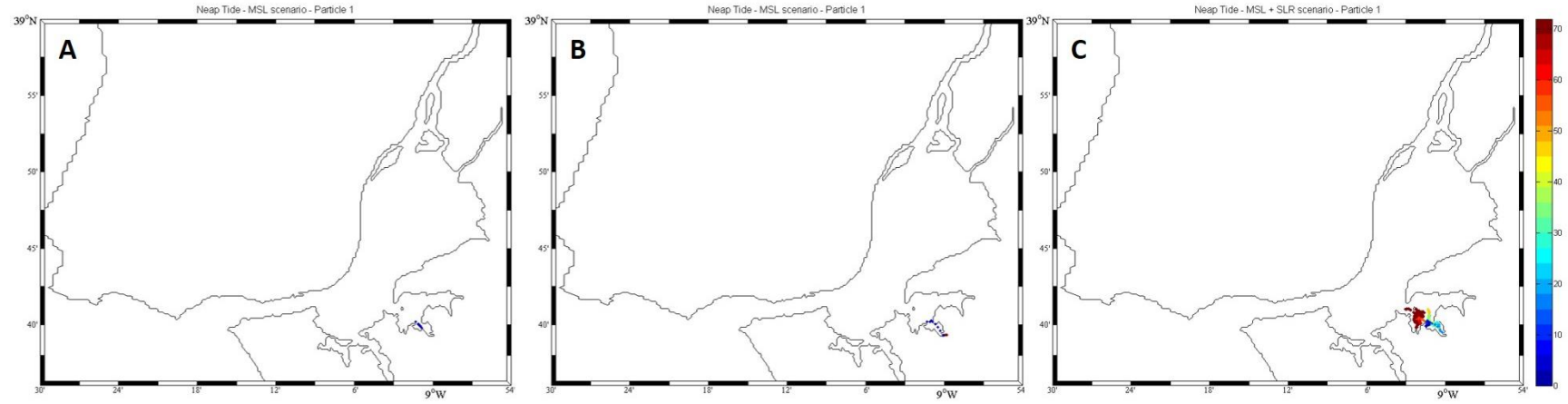

Figure **2.2.4.** Lagrangean transport from Rosário salt marsh in MSL conditions (A), high river discharge (B) and SLR (C) conditions during neap tides.

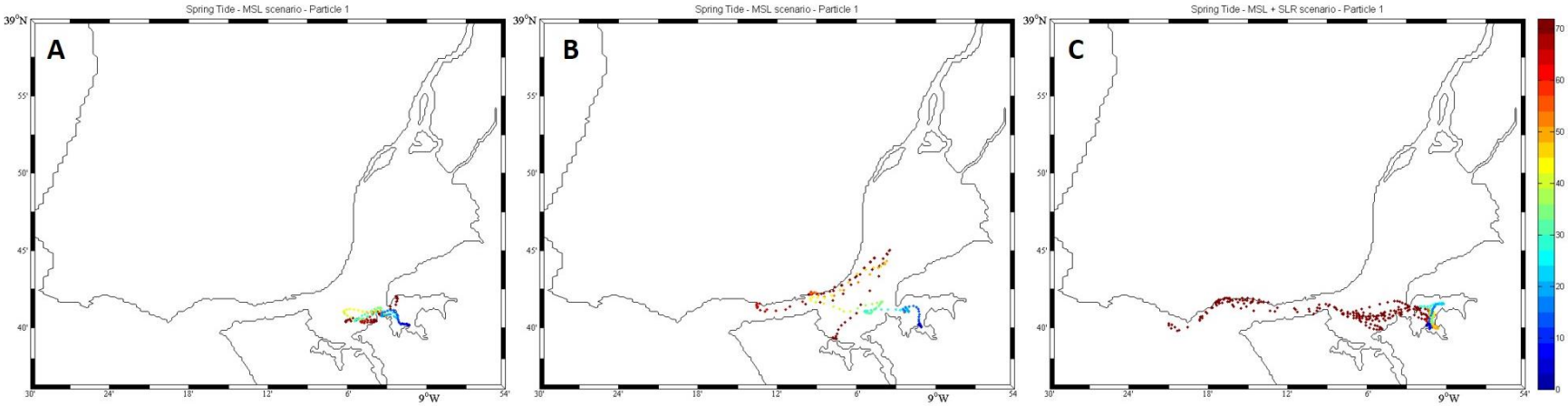

Figure 2.2.5. Lagrangean transport from Rosário salt marsh in MSL conditions (A), high river discharge (B) and SLR (C) conditions during spring tides.

Discussion

Several theories based on statistical and numerical models have been developed aiming towards the ecohydrological understanding of estuarine processes. A large variety of models arisen since the 70s, ranging from tidal prism models (Dyer and Taylor, 1973; Luketina, 1998; Sheldon and Alber, 2006), box models (Miller and McPherson, 1991; Roson *et al*., 1997; Hagy *et al*., 2000; Humborg *et al*., 2000; Kohlmeier and Ebenhoh, 2007), one dimensional models (Flindt and Kamp-Nielsen, 1997; Hinrichsen and Wulff, 1998), two-dimensional models (Canu *et al*., 2003; Ferrarin and Umgiesser, 2005; Inoue *et al*., 2008), to three-dimensional models (Rajar and Cetina, 1997; Solidoro *et al*., 2005; Lin *et al*., 2008). On of the most controversial estuarine processes to which these models were applied was the sink-source function of the estuaries in terms of nutrients but also in terms of contaminants. As estuaries and estuarine marshes are highly productive ecosystems it is also expectable that there is a large generation of detritus resulting from plant senescence. This estuarine exportation was primary focused by Odum (1980) as the ""outwelling"" hypothesis and has been tested several times and applied to several estuaries (Nixon, 1980; Moran *et al*., 1991; Dame and Allen, 1996; Alongi, 1998; Jickells *et al*., 2000; Duarte *et al*., 2014), showing that estuaries export large amounts of organic matter. If organic matter production in estuarine marshes is a significant food source for secondary production in the ocean and this organic matter is significantly contaminated with trace metals, there is potential for this contamination to enter the marine and human food chains. Outwelling may be found to play a role and, perhaps, an increasing role in human health.

However, there are not many studies that crossed hydrodynamic particle tracking data with estimations of the effective amounts of exported material from wetland origin. On the other hand, the new IPCC report (IPCC, 2015) states that extreme climate events such as drought, heat and cold waves and floods are likely to increase not only in intensity but also in frequency, especially in the Mediterranean area. This will not only exacerbate sea level rise but also increase flooding events, known to have impacts on the estuarine metal biogeochemistry (Duarte and Caçador, 2013). Allying these predicted climate-driven hydrological changes with the known salt marsh "outwelling" events (Duarte *et al*., 2014), new insights arise with

increased importance as management tools, for e.g. under the Marine Strategy Framework Directive.

Our results show that in the case the mesotidal Tagus Estuary, the examined contaminated salt marsh exports about 5 kg m^{-2} y^{-1} of dead biomass. Considering the extent of contaminated salt marshes identified in previous studies (Caçador *et al*., 2000; Caçador *et al*., 2013) within the same water body of the Tagus estuary this represents a global exportation in terms of metal burden of about 162 Zn kg y^{-1}, 26 Cu kg y^{-1}, 28 Pb kg y^{-1} and 1 Cd kg y^{-1}. Although these values present a high magnitude in terms of contamination, the Tagus estuary is not among the most contaminated estuaries in Europe, and thus this should be taken into consideration while evaluating "outwelling" process all over the world. The extent to which this metal burden enriched organic matter affects the coastal processes depends mostly on the quality and liability of the organic matter to aquatic decomposition and the hydrodynamic features (Das *et al*., 2010). The biochemical quality of this detritus showed that about 30-40% of the detritus are labile and thus will integrate the dissolved organic matter (Ittekkot, 1988; Spitzy and Leenheer, 1991; Søndergaard and Middelboe, 1995). Nevertheless, a large amount (60-70%) remains on the particulate phase and therefore has Lagrangean behaviour. This assumption allows the application of hydrological tracking models to assess the potential fate of this detritus after marsh exportation, along with all their metal burdens. As general case, during flood tide, material is transported into the marshes, whereas with ebb tide, the flux is to the open estuarine water (Hemminga *et al*., 1996). During neap tides at the present and high river flow conditions the detritus doesn't reach the estuary principal channel. Instead they return to the marsh were they were originated. Thus, part of the detritus transport will be a reflux of material, and may consist of detrital material that was produced in neighbour marshes (Hemminga *et al*., 1996). Similar results were obtained in a coastal salt marsh in the southwest Netherlands (Hemminga *et al*., 1992). Thus this reflux may be considered negligible being the more important transport, in ecological terms, towards the ocean. Even considering the SLR scenario, during neap tides this detritus are not transported into the main channel and continue in the surrounding water body. On the other hand, during Spring tides and considering a high river discharge scenario, the marsh-generated

detritus will reach the estuarine mouth and the main channel within 60 hours after the marsh flooding with a possible reflux into the estuary. If to the spring tide conditions, the SLR scenario is added, it is possible to observe a far more scattered pattern of distribution of detritus in the coastal areas with the particles reaching this area at high velocity, after 3 days. These extreme conditions (SLR and high river discharge) show resemblances, in which concerns the Lagrangean transport of detritus during spring tides, although during high freshwater input from the river, the particles show a smaller dispersion velocity and higher residence time inside the estuarine system. In fact this was already verified by Lopes *et al*. (2008), calculating that about 8.4-17 tons of POC were retained within the estuarine system during neap tides while the more severe spring tides lead to an export of about 57 tons of organic carbon. Also for Ria de Aveiro, a coastal lagoon in the northeast coast of Portugal, was verified that the so called worst case scenario produced a high scattering of detritus into the ocean at high speed with an enormous dispersion of a higher number of particles both to north, west and to south (Duarte *et al*., 2014). In sum neap times produce a reduced number of exported particles to the main estuarine channel and consequently to the ocean shelf adjacent to the estuarine system, while during spring tides some detritus are transported into the main channel. Although in this last case, the contaminated detritus doesn't reach the adjacent ocean shelf, in terms of estuarine contamination these particles can be transported to low contamination sites affecting therefore the metal burden on these destination sites. This is even more exacerbated during a high freshwater input from the upland river system. In this case, there is an apparent decontamination of the estuarine channel mostly due to dilution of contaminated particles in the terrestrial inputs (Duarte and Caçador, 2012). Nevertheless, the contaminated detritus generated within the estuary can be transported to areas with low contamination levels. As above mentioned this will be aggravated by sea level rise. Considering these hydrodynamic features and the nature of the plant detritus, in the present conditions this exposed contaminated salt marsh will act as a detritus exporter but to other areas of the estuarine domain, with a low contribution to the outer oceanic shelf. Only extreme events like storm surges or floods, acting simultaneously with spring tides, enhance this detritus exportation to the ocean.

During these events there is a higher input of contaminated necromass to the ocean increasing this way the degree of contamination of the oceanic food web mainly throughout the deposit feeders (Caçador *et al*., 2012). Nevertheless, at the current conditions these are punctual events occurring mainly during the winter season (Duarte and Caçador, 2012). Similarly, during sea level rise the exports increase only at spring tides, leading to similar effects in terms of contamination of the adjacent coastal waters. In plume regions like the coastal water adjacent to the Tagus Estuary inlet, downward fluxes are extremely elevated (Wysocki *et al*., 2006) and thus this exported detritus will become deposited in the surface sediments near the tidal inlet of the estuarine system (Lopes *et al*., 2008), where deposit feeders and microbial decomposers are likely to be abundant.

Some important ecological outcomes may evolve from this condition. Although flooding events are normally considered as cleansing processes (Vale, 1986; Duarte and Caçador, 2012) this concept must be revisited. During flood events the dilution of metal contamination inside the estuary is mostly due to a dilution of the metal contamination by the freshwater input and by a discharge of organic contaminated material to the mouth of the estuary. Although these are punctual events of annual periodicity the magnitude of contamination in the exported plant detritus should be taken into account. Moreover, this should be considered while dealing with future management plans considering the environmental directives, specially the ongoing Marine Strategy Framework Directive (EU, 2008). These models can thus be an efficient tool for management and predictions of future ecological quality of the estuaries, as well as providing predictions of the changes in terms of ecosystem services during extreme events.

Conclusion

It is widely accepted today that salt marshes work as sinks of the estuarine contamination more than sources. Nevertheless, and although the high retention of contaminants, namely heavy metals, in their sediments, plant necromass detritus should be accounted as a significant source of contamination in management studies of both the estuarine and coastal waters. Tagus estuary has been widely studied in terms of heavy metal contamination both in salt marshes, animas and water column,

but how it circulates within the estuary and to the adjacent coastal shelf, this was rather unknown. Rosário salt marsh produces more than 200 kg of metals per year entrapped in dead aboveground plant detritus. Their presence in the estuarine system is mostly driven by the tidal flooding hydrodynamic features. During neap tides plant detritus are mostly retained in the inner estuary in the vicinity of the marsh of origin, while during spring tides the exportations to the main estuarine channel and ocean increase. Similarly, the sea level rise or extreme events like floods will have a more pronounced effect on the detritus particles movement increasing the estuary contribution to the ocean shelf metal contamination.

References

Alber, M., Swenson, E.M., Adamowicz, S.C and Mendelssohn, I.A., 2008. Salt marsh dieback: An overview of recent events in the US. *Estuarine Coastal and Shelf Science* 80, 1-11.

Alongi, D.M., 1998. Coastal Ecosystem Processes. C.R.C. Press, Boca Raton, FL, USA, 419 pp.

Beeftink, W. G., 1977 The coastal salt marshes of Western and Northern Europe: an ecological and phytosociological approach. In Wet Coastal Ecosystems (Chapman, V. J., ed). Elsevier, Amsterdam, pp. 109–155.

Bernardes, B., 2007. Hydrodynamical and Ecological Modelling of the North Sea. MSc thesis. Technical University of Lisbon, Lisbon, Portugal, p. 81.

Bouchard, V. and Lefeuvre, J.C., 2000. Primary production and macro–detritus dynamics in a European salt marsh: carbon and nitrogen budgets. *Aquatic Botany* 67,23–42.

Bouchard, V., 2007. Export of organic matter from a coastal freshwater wetland to Lake Erie: an extension of the outwelling" hypothesis. *Aquatic Ecology* 41, 1-7.

Brian, G.W., 1971. The Effects of Heavy Metals (other than Mercury) on Marine and Estuarine Organisms. *Proceedings of the Royal Society of London B* 177, 389-410.

Burling, M.C., Pattiaratchi, C.B. and Ivey, G.N., 2003. The tidal regime of Shark Bay, Western Australia. *Estuarine, Coastal and Shelf Science* 57, 725-735.

Caçador, I., Vale, C. and Catarino, F., 1996. The influence of plants on concentration and fractionation of Zn, Pb, and Cu in salt marsh sediments (Tagus Estuary, Portugal). *Journal of Aquatic Ecosystem Health* 5, 193–198.

Caçador, I., Caetano, M., Duarte, B. and Vale, C. 2009. Stock and losses of trace metals from salt marsh plants. *Marine Environmental Research* 67, 75-82.

Caçador, I., Costa, J.L., Duarte, B., Silva, G., Medeiros, J.P., Azeda, C., Castro, N., Freitas, J., Cabral, H. and Costa, M.J., 2012. Macroinvertebrates and fishes as biomonitors of heavy metal concentration in the Seixal Bay (Tagus estuary): which species perform better? *Ecological Indicators* 19, 184-190.

Caçador, I., Neto, J.M., Duarte, B., Barroso, D.V., Pinto, M. and Marques, J.C., 2013. Development of an Angiosperm Quality Assessment Index (AQuA – Index) for ecological quality evaluation of Portuguese water bodies – A multi-metric approach. *Ecological Indicators* 25, 141-148.

Duarte, B., Reboreda, R. and Caçador, I. 2008. Seasonal variation of Extracellular Enzymatic Activity (EEA) and its influence on metal speciation in a polluted salt marsh. *Chemosphere* 73, 1056-1063.

Canu, D.M., Solidoro, C. and Umgiesser, G., 2003. Modelling the responses of the Lagoon of Venice ecosystem to variations in physical forcings. *Ecological Modelling* 170, 265-289.

Costanza, R., d'Arge, R., de Groot, R.S., Farber, S., Grasso, M., Hannon, B., Limburg, K., Naeem, S., O'Neill, R.V., Paruelo, J., Raskin, R.G., Sutton, P. and van den Belt, M., 1997. The value of the world's ecosystem services and natural capital. *Nature* 387, 253–260.

Dagg, M.J., Ammerman, J.W., Amon, R.M.W., Gardner, W.S., Green, R.E. and Lohrenz, S.E., 2007. A review of water column processes influencing hypoxia in the Northern Gulf of Mexico. *Estuaries and Coasts* 30, 735–752.

Dame, R.F. and Allen, D.M., 1996. Between estuaries and the sea. *Journal of Experimental Marine Biology and Ecology* 200, 169-185.

Das, A., Justic, D. and Swenson, E., 2010. Modelling estuarine-shelf exchanges in a deltaic estuary. Implications for coastal budgets and hypoxia. *Ecological Modelling* 221, 978-985.

Deegan, L.A., Hughes, J.E. and Rountree, R.A., 2000. Salt marsh ecosystem support of marine transient species. In: Weinstein, M.P., Kreegers, D.A. (Eds.) Concepts and controversies in tidal marsh ecology. Kluwer Academic Publishers, The Netherlands, pp. 331–363.

Dias, J.M. and Lopes, J.F., 2006. Implementation and assessment of hydrodynamic, salt and heat transport models: the case of Ria de Aveiro Lagoon (Portugal). *Environmental Modelling and Software* 21, 1-15.

Dias, J.M. and Picado, A., 2011. Impact of morphologic anthropogenic and natural changes in estuarine tidal dynamics. *Journal of Coastal Research* 64, 1490-1494.

Duarte, B., Caçador, I., Marques, J.C. and Croudace, I., 2013. Tagus Estuary salt marshes feedback to sea level rise over a 40-year period: insights from the application of geochemical indices. *Ecological Indicators* 34, 268-276.

Duarte, B., Caetano, M., Almeida, P., Vale, C. and Caçador, I., 2010. Accumulation and biological cycling of heavy metal in the root-sediment system of four salt marsh species, from Tagus estuary (Portugal). *Environmental Pollution* 158, 1661-1668.

Duarte, B., Couto, T., Marques, J.C and Caçador, I., 2012. *Scirpus maritimus* leaf pigment profile and photochemistry during senescence: implications on carbon sequestration. *Plant Physiology and Biochemistry* 57, 238-244.

Duarte, B., Reboreda, R. and Caçador, I., 2008. Seasonal variation of Extracellular Enzymatic Activity (EEA) and its influence on metal speciation in a polluted salt marsh. *Chemosphere* 73, 1056-1063.

Duarte, B., Silva, G., Costa, J.L., Medeiros, J.P., Azeda, C., Sá, E., Metelo, I., Costa, M.J. and Caçador, I., 2014. Heavy metal distribution and partitioning in the vicinity of the discharge areas of Lisbon drainage basins (Tagus Estuary, Portugal). *Journal of Sea Research* 93, 101-111.

Dworak, J.A. and Gómes-Valdés, J., 2003. Tide-induced residual current in a coastal lagoon of the Gulf of California. *Estuarine, Coastal and Shelf Science* 57, 99-109.

Dyer, K. and Taylor, P.A., 1973. A simple segmented prism model of tidal mixing in well mixed estuaries. *Estuarine Coastal and Shelf Science* 1, 411-418.

European salt marsh: carbon and nitrogen budgets. *Aquatic Botany* 67, 23–42.

Ferrarin, C. and Umgiesser, G., 2005. Hydrodynamic modelling of a coastal lagoon: the Cabras lagoon in Sardinia, Italy. *Ecological Modelling* 188, 340-357.

Flindt, M.R., Kamp-Nielsen, L., 1997. Modelling estuarine eutrophication gradient. Ecological Modelling 102, 143-153.

Gallagher, J.L., Reimold, R.J., Linthurst, R.A. and Pfeiffer, W.J., 1980. Aerial production, mortality, and mineral accumulation export dynamics in *Spartina alterniflora* and *Juncus roemerianus* plant stands in a Georgia salt marsh. *Ecology* 61, 303–312.

Gross, M., Hardisky, M., Wolf, P. and Klemas, V., 1991. Relationship between aboveground and belowground biomass of *Spartina alterniflora* (smooth cordgrass). *Estuaries* 14, 180–191.

Hagy, J.D., Sanford, L.P. and Boynton, W.R., 2000. Estimation of net physical transport and hydraulic residence times for a coastal plain estuary using box models. *Estuaries* 23, 328-340.

Hemminga, M.A., Cattrijsse, A. and Wielemaker, A., 1996. Bedload and nearbed detritus transport in a tidal saltmarsh creek. *Estuarine Coastal and Shelf Science* 42, 44-62.

Hemminga, M.A., Klap, V.A., van Soelen, J., De Leeuw, J. and Boon, J.J., 1992. Shifts in seston characteristics after inundation of a European coastal salt marsh. *Limnology and Oceanography* 37, 1559–1564.

Hinrichsen, U. and Wulff, F., 1998. Biogeochemical and physical controls of nitrogen fluxes in a highly dynamic marine ecosystem – model and network flow analysis of the Baltic Sea. *Ecological Modelling* 109, 165-191.

Humborg, C., Fennel, K., Pastuszak, M. and Wolfgang, F., 2000. A box model approach for a long-term assessment of estuarine eutrophication, Szczecin Lagoon, Southern Baltic. *Journal of Marine Systems* 25, 387-403.

Inoue, M., Park, D., Justic, D. and Wiseman Jr., W.J., 2008. A High-Resolution Integrated Hydrology-Hydrodynamic Model of the Barataria Basin System. *Environmental Modelling and Software* 23, 1122–1132.

Ittekkot, V., 1988. Global trends in the nature of organic matter in river suspensions. *Nature* 332, 436-438.

Jickells, T., Andrews, J., Samways, G., Sanders, R., Malcom, S., Sivyer, D., Parker, R., Nedwell, D., Mark Trimmer, M. and Ridgway, J., 2000. Nutrient fluxes through the Humber Estuary – past, present and future. *Ambio* 29, 130-135.

Junk, W.J., Bayley, P.B. and Sparks, R.E., 1989. The food pulse concept in river floodplain systems. *Canadian Special Publication of Fisheries and Aquatic Sciences* 106, 110-127.

Kersten M. and Förstner, U., 1986. Chemical Fractionation of Heavy Metals in Anoxic Estuarine and Coastal Sediments. *Water Science and Technology* 18, 121-130.

Kohlmeier, C. and Ebenhoh, W., 2007. Modelling the ecosystem dynamics and nutrient cycling of the Spiekeroog back barrier system with a coupled Euler-Lagrange model on the base of ERSEM. *Ecological Modelling* 202, 297-310.

Lefeuvre, J.C., Bertru, G., Burel, F., Brient, L., Créach, V., Gueuné, Y., Levasseur, J., Mariotti, A., Radureau, A., Retière, C., Savouré, B. and Troccaz, O., 1994. Comparative studies on salt marsh processes: Mont Saint-Michel bay, a multi-disciplinary study. In: Mitsch, W.J. (Ed.), Global Wetlands: Old World and New. Elsevier Science B.V., pp. 215–234.

Lin, J., Xiea, L., Pietrafesac, L.J., Hongzhou Xua, H., Wendy Woods, W., Michael, A., Mallin, M.A. and Durko, M.J., 2008. Water quality responses to simulated flow and nutrient reductions in the Cape Fear River Estuary and adjacent coastal region, North Carolina. *Ecological Modelling* 212, 200-217.

Lopes, C.B., Lillebo, A.I., Pato, P., Dias, J.M., Rodrigues, S.M., Pereira, E. and Duarte, A.C., 2008. Inputs of organic carbon from Ria de Aveiro coastal lagoon to the Atlantic Ocean. *Estuarine Coastal and Shelf Science* 79, 751-757.

Lopes, C.L., Silva, P.A., Dias, J.M., Rocha, A., Picado, A., Plecha, S. and Fortunato, A.B., 2011. Local sea level change scenarios for the end of the 21st century and potential physical impacts in the lower Ria de Aveiro (Portugal). *Continental Shelf Research* 31, 1515-1526.

Lopes, J.F. and Dias, J.M., 2011. Circulação residual, transporte lagrangiano e distribuição de sedimentos na Ria de Aveiro. In: Jornadas da Ria de Aveiro 2011. 2-4/05/ 2011, Aveiro, Portugal.

Lopes, J.F., Dias, J.M. and Dekeyser, I. 2006. Numerical modelling of cohesive sediments transport in the Ria de Aveiro lagoon, Portugal. *Journal of Hydrology* 319, 176-198.

Luketina, D., 1998. Simple tidal prism models revisited. *Estuarine Coastal and Shelf Science* 46, 77-84.

Macintosh, D. J., 1981. The importance of mangrove swamps to coastal fisheries and aquaculture. In Proceedings of the Seminar on Some Aspects of Inland Aquaculture. Mangalore, Karnataka, 14 and 15 July, 1980: 27-33.

Malhadas, M.S., Silva, A., Leitão, P.C. and Neves, R., 2009. Effect of the Bathymetric changes on the hydrodynamic and residence time in Óbidos lagoon (Portugal). *Journal of Coastal Research* 56, 549-553.

Martins, F., Leitão, P., Silva, A. and Neves, R., 2001. 3D modelling in the Sado estuary using a new generic vertical discretization approach. *Oceanologica Acta* 24, 1-12.

Miller, R.L. and McPherson, B.F., 1991. Estimating estuarine flushing and residence times in Charlotte Harnbor, Florida, via salt balance and a box model. *Limnology and Oceanography* 36, 602-212.

Neves, F., 2010. Dynamics and hydrology of the Tagus estuary: results from in situ observations. PhD Thesis, University of Lisbon, Lisbon, Portugal.

Moran, M.A., Pomeroy, L.R., Sheppard, E.S., Atkinson, L.P. and Hodson, R.E., 1991. Distribution of terrestrial derived organic matter on the southeastern U.S. continental shelf. *Limnology and Oceanography* 36, 1134-1149.

Nixon, S.W., 1980. Between coastal marshes and coastal waters – a review of twenty years of speculation and research on the role of salt marshes in estuarine productivity and water chemistry. In. Hamilton, P. and MacDonald, K.B. (Eds.), Estuarine and Wetland Processes. Premium Publishing Corp., New York, NY, USA, pp. 437-525.

Nriagu, J., 1988. A silent epidemic of environmental poisoning. *Environmental Pollution* 50, 139–61.

Odum, E.P., 1968. A research challenge: evaluating the productivity of coastal and estuarine water. In Proceedings of the Second Sea Grant Conference, University of Rhode Island: 63-64.

Odum, E.P., 1980. The status of three ecosystem-level hypotheses regarding salt marsh estuaries: tidal subsidy, outwelling and detritus based food chains. In: Kennedy, V.S. (Ed.), Estuarine Perspectives. Academic Press, New York, USA, pp. 485-495.

Otte, M.L., Bestbroer, S.J., van der Linden, J.M., Rozema, J. and Broekman, R.A., 1991. A survey of zinc, copper and cadmium concentrations in salt marshes plants along the Dutch coast. *Environmental Pollution* 72, 175 – 189.

Pawlowicz, R., Beardsley, B. and Lentz, S., 2002. Classical tidal harmonic analysis including error estimates in MATLAB using T_TIDE. *Computers and Geosciences* 28, 929-937.

Picado, A., Dias, J.M. and Fortunato, A., 2010. Tidal changes in estuarine systems induced by local geomorphologic modifications. *Continental Shelf Research* 30, 1854-1864.

Rajar, R. and Cetina, M., 1997. Hydrodynamic and water quality modelling: an experience. *Ecological Modelling* 101, 195-207.

Roson, G., Alavrez-Salgado, X.A. and Perez, F.F., 1997. A non-stationary box model to determine residual fluxes in a partially mixed estuary, based on both thermohaline properties: application to the Ria de Arousa (NW Spain). *Estuarine Coastal and Shelf Science* 44, 249-262.

Sheldon, J.E. and Alber, M., 2006. The calculation of estuarine turnover times using fresh-water fraction and tidal prism models: a critical evaluation. *Estuaries and Coasts* 29, 133-146.

Snedaker, S.C., 1978. Mangroves: their value and perpetuation. *Natural Resources* 14, 6-13.

Solidoro, C., Pastres, R. and Cossarini, G., 2005. Nitrogen and plankton dynamics in the lagoon of Venice. *Ecological Modelling* 184, 103-124.

Søndergaard, M. and Middelboem M., 1995. A cross-system analysis of labile dissolved organic carbon. *Marine Ecology Progress Series* 118, 283-294.

Sousa, M.C. and Dias, J.M., 2007. Hydrodynamic model calibration for a mesotidal lagoon: the case of Ria de Aveiro (Portugal). *Journal of Coastal Research* SI50, 1075-1080.

Spitzy, A. and Leenheer, J., 1991. Dissolved organic carbon rivers. In: Degens, E.T., Kempe, S., Richey, J.E. (Eds.), Biogeochemistry of Major World Rivers. Wiley, New York, NY, pp. 213-232.

Vale, C., 1986. Transport of particulate metals at different fluvial and tidal energies in the Tagus estuary. Rapports et procès-verbaux des réunions – Conseil international pour l'exploration de la mer 186, 306–312.

Valentim, J.M., Vaz, L., Vaz, N., Silva, H., Duarte, B., Caçador, I. and Dias, J.M., 2013. Sea level rise impact in residual circulation in Tagus estuary and Ria de Aveiro lagoon. *Journal of Coastal Research* SI 65, 1981-1986.

Vaz, N., 2007. Study of Heat and Salt Transport Processes in the Espinheiro Channel (Ria de Aveiro). PhD thesis. Physical Department, University of Aveiro, Portugal, 151 pp. http://hdl.handle.net/10773/2671.

Vaz, N., Dias, J.M. and Leitão, P.C., 2009. Three-dimensional modelling of a tidal channel: the Espinheiro Channel (Portugal). *Continental Shelf Research* 29, 29-41.

Vaz, N. and Dias, J.M., 2014. Residual currents and transport pathways in the Tagus Estuary, Portugal: the role of freshwater discharge and wind. *Journal of Coastal Research*, SI 70, 610-615.

Vaz, N., Dias, J.M., Leitão, P.C. and Martins, I., 2005. Horizontal patterns of water temperature and salinity in an estuarine tidal channel: Ria de Aveiro. *Ocean Dynamics* 55, 416-429.

Vaz, N., Dias, J.M., Leitão, P.C. and Nolasco, R., 2007. Application of the MOHID-2D model to a mesotidal temperate coastal lagoon. *Computers and Geosciences* 33, 1204-1209.

Vaz, N., Mateus, M. and Dias, J.M., 2011. Semidiurnal and spring-neap variations in the Tagus estuary: application of a process-oriented hydro-biogeochemical model. *Journal of Coastal Research* 64, 1619-1623.

Viers, J., Dupré, B. and Gaillardet, J., 2009. Chemical composition of suspended sediments in World Rivers: New insights from a new database. *Science of Total Environment* 407, 853-868.

Wysocki, L.A., Bianchi, T.S., Powell, R.T. and Reuss, N., 2006. Spatial variability in the coupling of organic carbon, nutrients, and phytoplankton pigments in surface waters and sediments of the Mississippi River plume. *Estuarine Coastal and Shelf Science 69*, 47–63.

2.3. BIOPHYSICAL PROBING OF *SPARTINA MARITIMA* PHOTO-SYSTEM II CHANGES DURING PROLONGED TIDAL SUBMERSION PERIODS[1]

Abstract

Submergence is one of the major constrains affecting wetland plants, with inevitable impacts on their physiology and productivity. Global warming as a driving force of SLR, tend to increase the submersion periods duration. Photosynthesis biophysical probing arises as an important tool to understand the energetics underlying plant feedback to these constrains. As in previous studies with *S. maritima*, there was no inhibition of photosynthetic activity in submerged individuals. Comparing both donor and acceptor sides of the PS II, the first was more severely affected during submersion, driven by the inactivation of the OEC with consequent impairment of the ETC. Although this apparent damage in the PS II donor side, the electron transport per active reaction centre was not substantially affected, indicating that this reduction in the electron flow is accompanied by a proportional increase in the number of active reaction centres. These conditions lead to the accumulation of excessive reducing power, source of damaging ROS, counteracted by efficient energy dissipation processes and anti-oxidant enzymatic defences. This way, *S. maritima* appears as a well-adapted specie with an evident photochemical plasticity towards submersion, allowing it to maintain its photosynthetic activity even during prolonged submersion periods.

[1] This section was published in: **Duarte, B.**, Santos, D., Marques, J.C. and Caçador, I., 2014. Biophysical probing of *Spartina maritima* Photo-system II changes during increased submersion periods: possible adaptation to sea level rise. *Plant Physiology and Biochemistry* 77, 122-132.

Introduction

Although salt marshes are widely recognized as one of the major contributors for estuarine primary productivity (Caçador *et al*., 2009), these ecosystems present several environmental constrains that affect the species distribution and zonation (Caçador *et al*., 2007). Tidal flooding is one of the most important stressors shaping these landscapes, while submerging the halophytic vegetation inhabiting salt marshes (Hubbard, 1969; Armstrong *et al*., 1985; Bertness, 1991; Winkel *et al*., 2011). Halophytes are normally defined as "plants that complete their life cycle in a salt concentration of at least 200 mM NaCl under conditions similar to those that might be encountered in the terrestrial environment" (Flowers and Colmer, 2008). Although halophytes can be found in saline deserts, most of the world halophyte populations inhabit coastal areas (like salt marshes and mangroves) prone to tidal flooding (Colmer and Flowers, 2008). Flooding has several consequences not only on halophytes, but also in their rhizosediment (Burdick and Mendelssohn, 1990). With flooding, sediment becomes anoxic with a lower redox potential (Duarte *et al*., 2009). In this case plant survival becomes dependent upon the establishment of an oxygen flow from the atmosphere into the aerial organs and finally pumped into the rhizosphere, supporting root aerobic respiration and enhancing toxic forms detoxification (Burdick and Mendelssohn, 1990; Armstrong, 1979). Several halophytes developed root aerenchyma in order to increase root aeration (Sifton, 1945; Iversen, 1949; Armstrong, 1972). Other types of mechanisms of submergence tolerance include shoot elongation, a quiescence response to conserve energy until water drawbacks, adventitious root formation and traits conferring the ability to preform underwater photosynthesis (Winkel *et al*., 2011; Bailey-Serres and Voesenek, 2008; Colmer and Voesenek, 2009). At the leaf level several constrains arise. Not only the CO_2 gas slow diffusion in the aquatic environment limits its uptake by leaves (Smith and Walker, 1980), but also the decreased light availability, due to light attenuation along the water column (Pedersen and Colmer, 2006), impairs photosynthesis (Sand-Jensen, 1989). This photosynthetic impairment due to low CO_2 or low light, leads to a depletion in the O_2 production, with less O_2 to be diffused from the leaves to the roots, and thus increasing the anoxia driven stress at the sediment level (Colmer and Flowers, 2008). Moreover, plant feedback to

flooding events will be also function of flood duration and water column depth, and of course, plant genotype (Setter and Waters, 2003; Voesenek *et al*., 2004). Due to obvious geographical constrains, the species inhabiting the lower parts of coastal marshes are more exposed both to normal tidal flooding, but also to prolonged flooding events.

Spartina maritima (L.) Loisel (Poaceae), has a very wide distribution in the northern hemisphere, native to the coasts of western and northern Europe and western Africa, with also a disjunct population on the Atlantic coasts of Namibia and South Africa (Marchant and Goodman, 1969). It is typically considered as a pioneer species (Caçador *et al*., 2007) inhabiting the mudflats and lower marshes. Its sediment is often waterlogged and undergo tidal flooding twice per day during, with an average and maximum flooding duration of 2 hours (during spring tides) and 1-1.5 hours (during normal tides) respectively (Serôdio and Catarino, 2000).

Considering the present climatic change projections this subject acquires an even greater importance. Many coastal marshes are prone to storm surges and river flooding, driven by extreme climate events, that in nowadays are becoming more frequent (Egan and Ungar, 2000; Pedersen *et al*., 2006). Also the projections of SLR point out to increased inundations of coastal marshes (Reed, 2002). All these climatic events will increase the frequency and duration of tidal flooding especially on the lower marshes.

In the present study, we examine the photochemical and biochemical adaptations of *S. maritima* to high duration submersion periods, and its photosynthetic ability and underlying photochemical mechanisms during prolonged submersion periods. This will allow understanding the plasticity and adaptation capacity of this specie, in for e.g. climate change scenarios of prolonged tidal flooding due to SLR.

Material and Methods

Plant harvest and mesocosmos setup

Intact turfs of *S. maritima* were collected at in the summer, one day before the experiments start, at Tagus estuary (Alcochete, 38°45'38.78"N, 8°56'7.37"W). The intact turfs were transported to the laboratory of Marine Botany of the Centre

of Oceanography, in air exposed aquariums (60 x 60 x 60 cm) and placed in a normal photoperiod (16h/8h, light/dark) at 20 °C, until the beginning of the experiments. To avoid dryness, sediment was supplemented with ¼ Hoagland solution with the salinity adjusted to 20 PSU (estuarine salinity) to maintain moister conditions from the field.

Two aquariums were prepared by filling the bottom with *S. maritima* transplants in order to simulate the normal displacement within a pure stand of this specie. One of the aquariums was filled with artificial estuarine water supplemented with ¼ Hoagland solution nutrients. The fill up of the aquarium was done slowly (10 min) and gently to avoid sediment ressuspension and water column turbidity. At the end the individuals were completely submersed. In the other aquarium the individuals remained in normal air-exposed conditions. Both aquariums were illuminated with a fluorescent light with a PAR at the leaf level of 400 μmol photons m^{-2} s^{-1} in the air exposed aquarium and of 370 μmol photons m^{-2} s^{-1} in submerged conditions. Both irradiances are within the optimal and maximum productivity range for this specie in Mediterranean marshes (Duarte *et al*., 2013). Leaf samples (for biochemical analysis) were harvest at the beginning of the experiment (T_0) and every 30 min and flash frozen in liquid-N_2. Since each turf included several individuals these were considered as pseudo-replicates in each aquarium. In field conditions this specie undergoes flooding periods of typically 2 hours (Serôdio and Catarino, 2000). In order to evaluate its tolerance to increased submersion periods the submersion experiments were preformed during 3 hours.

PAM fluorometry

All chlorophyll fluorescent measurements (Table 2.3.1) were also performed every 30 min. Modulated chlorophyll fluorescence measurements were made in attached leaves with a FluoroPen FP100 PAM (Photo System Instruments, Czech Republic). All the measurements in the dark-adapted state were made after darkening of the leaves for at least 30 min. The minimal fluorescence (F_0) in dark-adapted state was measured by the measuring modulated light, which was sufficiently low (< 0.1 μmol m^{-2} s^{-1}) not to induce any significant variation in fluorescence. The maximal fluorescence level (F_M) in dark-adapted state was

measured by a 0.8 seconds saturating pulse at 8000 μmol m^{-2} s^{-1}. The maximum photochemical efficiency was assessed as $(F_M-F_0)/F_M$. The same parameters were also measured in light –adapted leaves, being F'_0 the minimum fluorescence, F'_M the maximum fluorescence and the operational photochemical efficiency. Rapid light curves (RLC) measurements, in dark-adapted leaves, were attained using the pre-programed LC1 protocol of the FluoroPen, consisting in a sequence of pulses from 0 to 500 μmol m^{-2} s^{-1}. Shortly, this protocol is based in successive measurements of the sample $\Phi_{PS\ II}$ under various light intensities (20, 50, 100, 200, 300 and 500 μmol m^{-2} s^{-1}) of continuous illumination relating the rate of photosynthesis to photon flux density (PAR). During this protocol the F_0 and F_M as well as the maximum photochemical efficiency were measured. Each $\Phi_{PS\ II}$ measurement was used to calculate the electron transport rate (ETR) through photosystem II using the following equation: ETR = $\Phi_{PS\ II}$ x PAR x 0.5, where PAR is the actinic photosynthetically active radiation generated by the FluoroPen and 0.5 assumes that the photons absorbed are equally partitioned between PS II and PSI (Genty *et al*., 1989). Without knowledge of the actual amount of light being absorbed, fluorescence measurements can only be used as an approximation for electron transport (Beer *et al*., 1998a, Beer *et al*., 1998b and Runcie and Durako, 2004). Rapid light curves (RLC) were generated from the calculated ETRs and the irradiances applied during the rapid light curve steps. Each RLC was fitted to a double exponential decay function in order to quantify the characteristic parameters, alpha and ETR_{max} (Platt *et al*., 1980). The initial slope of the RLC (α) is a measure of the light harvesting efficiency of photosynthesis and the asymptote of the curve, the maximum rate of photosynthesis (ETR_{max}), is a measure of the capacity of the photosystems to utilize the absorbed light energy (Marshall *et al*., 2000). The onset of light saturation (E_k) was calculated as the ratio between ETR_{max} and α. Excitation light of 650 nm (peak wavelength) from array of three light and emitting diodes is focused on the surface of the leaf to provide a homogenous illumination. Light intensity reaching the leaf was 3000 μmol m^{-2} s^{-1}, which was sufficient to generate maximal fluorescence in all individuals. The fluorescence signal is received by the sensor head during recording and is digitized in the control unit using a fast

digital converter. The OJIP transient (or Kautsky curves) depicts the rate of reduction kinetics of various components of PS II. When dark-adapted leaf is illuminated with the saturating light intensity of 3500 µmol m^{-2} s^{-1} then it exhibits a polyphasic rise in fluorescence (OJIP). Each letter reflects distinct inflection in the induction curve. The level O represents all the open reaction centres at the onset of illumination with no reduction of Q_A (fluorescence intensity lasts for 10 ms). The rise of transient from O to J indicates the net photochemical reduction of Q_A (the stable primary electron acceptor of PS II) to Q_A^- (lasts for 2 ms). The phase from J to I was due to all reduced states of closed RCs such as $Q_A^- Q_B^-$, $Q_A Q_B^{2-}$ and $Q_A^- Q_B H_2$ (lasts for 2–30 ms). The level P (300 ms) coincides with maximum concentration of $Q_A^- Q_B^2$ with plastoquinol pool maximally reduced. The phase P also reflects a balance between light incident at the PS II side and the rate of utilization of the chemical (potential) energy and the rate of heat dissipation (Zhu *et al*., 2005). Table 2.3.1 summarizes all the parameters that can be computed from the fluorometric data.

Table 2.3.1. Summary of Fluorometric analysis parameters and their description.

Photosystem II Efficiency	
F'_0 and F_0	Basal Fluorescence under weak actinic light in light and dark-adapted leaves.
F'_M and F_M	Maximum Fluorescence measured after a saturating pulse in light and dark-adapted leaves.
F'_v and F_v	Variable fluorescence light ($F'_M - F'_0$) and dark ($F_M - F_0$) adapted leaves.
PS II Operational and Maximum Quantum Yield	Light and dark-adapted quantum yield of primary photochemistry, equal to the efficiency by which a PS II trapped photon will reduce Q_A to Q^-_A.
Non-Photochemical Quenching (NPQ)	$NPQ = (F_M - F'_M) / F_M$
Rapid Light Curves (RLCs)	
rETR	Relative electron transport rate at each light intensity (rETR = QY x PAR x 0.5).
ETR_{max}	Maximum ETR after which photo-inhibition can be observed.
E_k	The onset of light saturation.
α	Photosynthetic efficiency, obtained from the initial slope of the RLC.

Table 2.3.1. (continuation).

Energy Fluxes (Kautsky curves)	
Area	Corresponds to the oxidized quinone pool size available for reduction and is a function of the area above the Kautsky plot.
V_t	Relative variable fluorescence ($V_t = F_t - F_0)/(F_M - F_0$)
W	Variable fluorescence intensity normalized to the J-step ($W = F_t - F_0) / (F_J - F_0$)
W_K	Amplitude of the K-step ($W_K = V_K – V_J$)
φ_{P0}	Maximum yield of primary photochemistry.
φ_{E0}	Probability that an absorbed photon will move an electron into the ETC.
φ_{D0}	Quantum yield of the non-photochemical reactions.
ψ_0	Probability of a PS II trapped electron to be transported from Q_A to Q_B.
Diving force for photosynthesis	DF ABS = DF RC + DF ψ_{P0} + DFφ)
Driving force for trapping electronic energy	DF ψ_{P0} = log (ψ_{P0} / (1 - ψ_{P0})
Driving force for electron transport	DF φ = log (ψ_0 / (1 - φ_0)
Driving force for energy absorption	DF RC = log (RC/ABS)
M_o	Net rate of PS II RC closure.
δR_0	Electron movement efficiency from the reduced intersystem electron acceptors to the PS I end electron acceptors.
ABS/CS	Absorbed energy flux per leaf cross-section.
TR_0/CS	Trapped energy flux per leaf cross-section.
ET_0/CS	Electron transport energy flux per leaf cross-section.
DI_0/CS	Dissipated energy flux per leaf cross-section.
RC/CS	Number of available reaction centres per leaf cross section.
PI	Performance index.
Grouping Probability (P_G)	The Grouping Probability is a direct measure of the connectivity between the two PS II units (Strasser and Stribet, 2001).

Oxidative stress biomarkers

Briefly, a proportion of 500 mg of fresh leaves for 8 ml of 50 mM sodium phosphate buffer (pH 7.6) with 0.1 mM Na-EDTA, was used for the extraction procedure. The homogenate was centrifuged at 8 890 x g for 20 min, at 4 °C, and the supernatant was used for the enzymatic assays. Catalase (CAT) activity was measured according to the method of Teranishi *et al*. (1974), by monitoring the consumption of H_2O_2, and consequent decrease in absorbance at 240 nm. (ε = 39.4 mM^{-1} cm^{-1}). The reaction mixture contained 50 mM of sodium phosphate buffer (pH 7.6), 0.1 mM of Na-EDTA, and 100 mM of H_2O_2. The reaction was initiated with the addition of the extract. Ascorbate peroxidase (APx) was assayed according to Tiryakioglu *et al.* (2006). The reaction mixture contained 50 mM of sodium phosphate buffer (pH 7.0), 12 mM of H_2O_2, 0.25 mM L-ascorbate. The reaction was initiated with the addition of 100 µL of enzyme extract. The activity was recorded as the decrease in absorbance at 290 nm and the amount of ascorbate oxidized was calculated from the molar extinction coefficient of 2.8 mM^{-1} cm^{-1}. Guaiacol peroxidase (GPx) was measured by the method of Bergmeyer (1974) with a reaction mixture consisting of 50 mM of sodium phosphate buffer (pH 7.0), 2 mM of H_2O_2, and 20 mM of guaiacol. The reaction was initiated with the addition of 100 µL of enzyme extract. The enzymatic activity was measured by monitoring the guaiacol oxidation reflected by an increase in absorbance at 470 nm (ε = 26.6 mM^{-1} cm^{-1}). Superoxide dismutase (SOD) activity was assayed according to Marklund (1974) by monitoring the reduction of pyrogallol at 325 nm. The reaction mixture contained 50 mM of sodium phosphate buffer (pH 7.6), 0.1 mM of Na-EDTA, 3 mM of pyrogallol, Mili-Q water. The reaction was started with the addition of 10 µL of enzyme extract. Control assays were done in the absence of substrate in order to evaluate the auto-oxidation of the substrates. Protein content in the extracts was determined according to Bradford (1976).

Statistical Analysis

Due to the lack of normality and homogeneity, the statistical analysis of the data was based in non-parametric tests. In order to compare the effects of the two

tested environments (air and underwater), the Krustal-Wallis test was performed using Statistica Software (Statasoft).

Results

PS II Quantum Yields

Overlooking the dark-adapted leaves variable fluorescence and quantum yields (Figure 2.3.1B and 2.3.1D) no difference could be detected, neither along the time course nor between the air exposed and the submerged individuals. On the other hand, if the operational yields and light-adapted variable fluorescence are observed (Figure 2.3.1A and 2.3.1C), notorious differences arise. The variable fluorescence in the light-adapted leaves of the air exposed individuals maintained its value almost constant along the time course. As for the submerged leaves, this value rapidly decreased after 30 min of submersion, until a minimum value reached at the end of 60 min of submersion. After this period there could be observed a recovery of these parameters until the end of the time course. Regarding the operational quantum yields, it could also be observed a decrease of its value in the submerged individuals, although in a smaller extent, reaching its minimum at the end of 60 min of time course with a recovery after this period. Considering the non-photochemical quenching (NPQ) of the air exposed individuals it could be observed that it presents a low and almost steady value along all the time course. On the other hand, in the submerged individuals the NPQ (Fig 2.3.1E) increased from the beginning of the experiment until the end of 60 min, after which it started to decrease towards minimum values at the end of 180 min of time course.

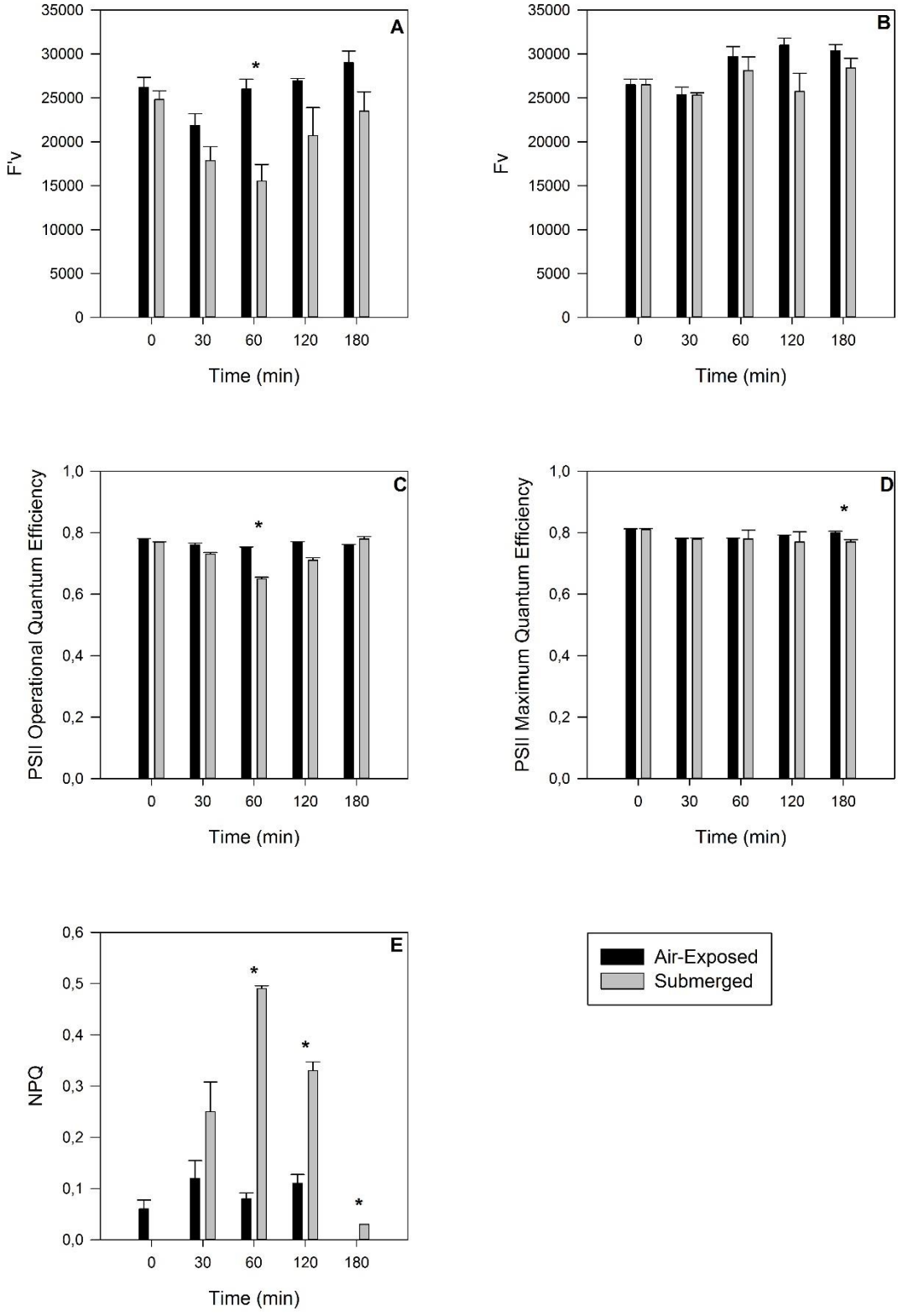

Figure 2.3.1. Variable fluorescence (A, B), PS II quantum yield (C, D) in light and dark-adapted leaves and non-photochemical quenching (E) in submerged and air-exposed *S. maritima* individuals (average ± standard deviation, n = 5; * $p < 0.05$).

Rapid Light Curves (RLCs)

Observing the rETR at different light intensities (Figure 2.3.2A-2E), measured at different moments of the submersion experiment it was possible to assess a similar pattern to the previous reported for the PS II quantum yields.

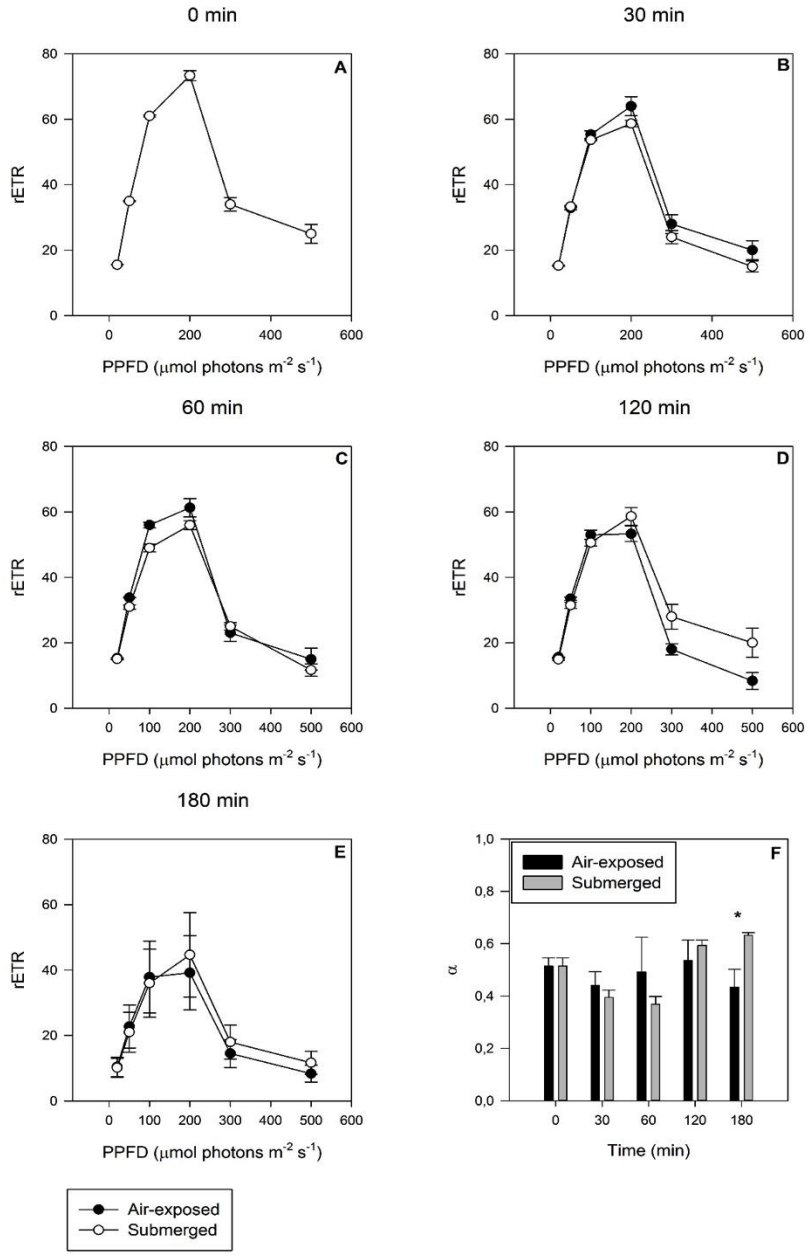

Figure 2.3.2. Rapid Light Curves (A, B, C, D, E) and Photosynthetic Efficiency (F) in dark-adapted leaves of submerged and air-exposed *S. maritima* individuals (average ± standard deviation, n = 5; * $p < 0.05$).

It could be observed that submerged individuals exhibited lower electron transport rates during the first 120 min of submersion at non-photoinibitory light intensities.

After this period, a small increase in the rETR could be observed for all light intensities tested. This was reflected in the photosynthetic efficiency (Figure 2.3.2F), where a significant increase could be detected in the plants submerged after 180 min, relatively to the air-exposed individuals.

Kautsky Curves, Energy Fluxes and Driving Forces

A similar pattern could be observed by plotting Kautsky curves from the examined samples (Figure 2.3.3). Until 120 min of submersion, the air-exposed individuals presented higher values of fluorescence both during the photochemical (O-J-I) and thermal (I-P) phases.

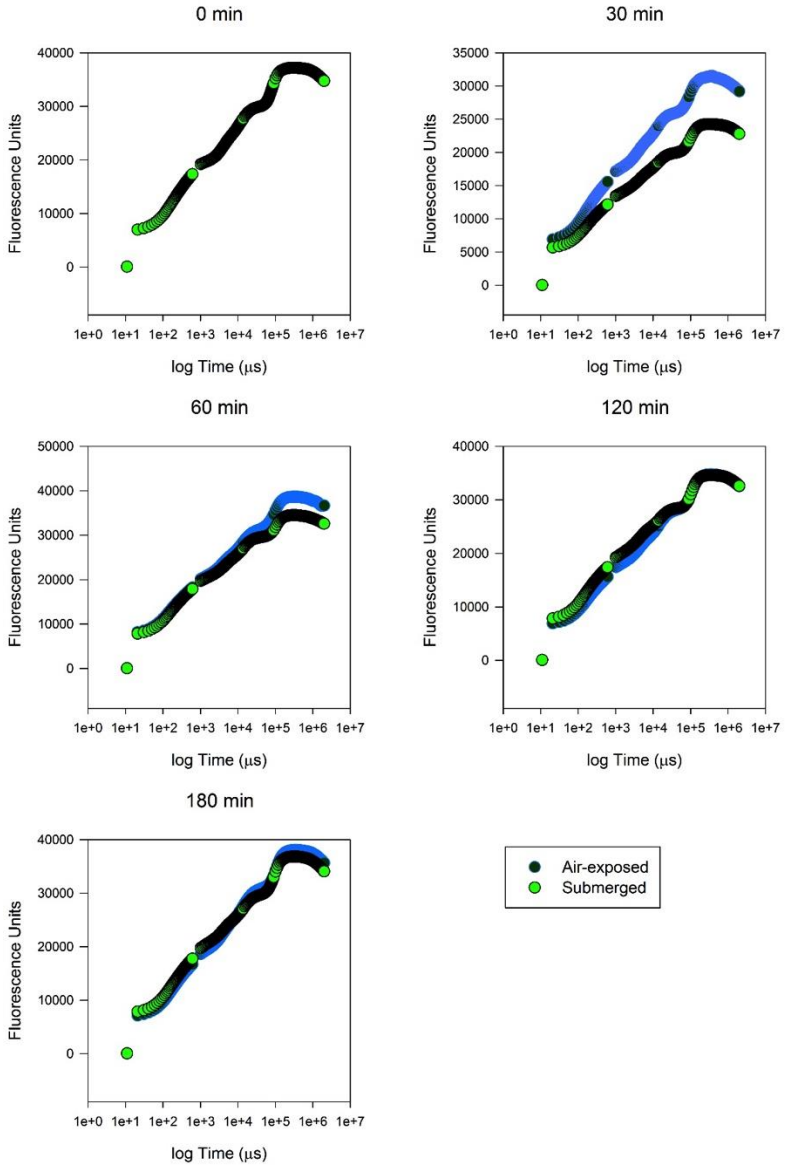

Figure 2.3.3. Average values of the Kautsky curves in dark-adapted leaves of submerged and air-exposed *S. maritima* individuals (average values, n = 5).

This reflects changes in the energy fluxes involved in the light harvesting processes (Figure 2.3.4). It was possible to observe that both the trapped and transported energy fluxes (Figure 2.3.4B and 2.3.4C) were very similar among treatments and during 180 min of experiment. The major differences were observed at the end of 60 min in the absorbed (Figure 2.3.4A) and dissipated energy fluxes (Figure 2.3.4D), showing significant increases in the submerged individuals, especially in which concerns the dissipated energy flux.

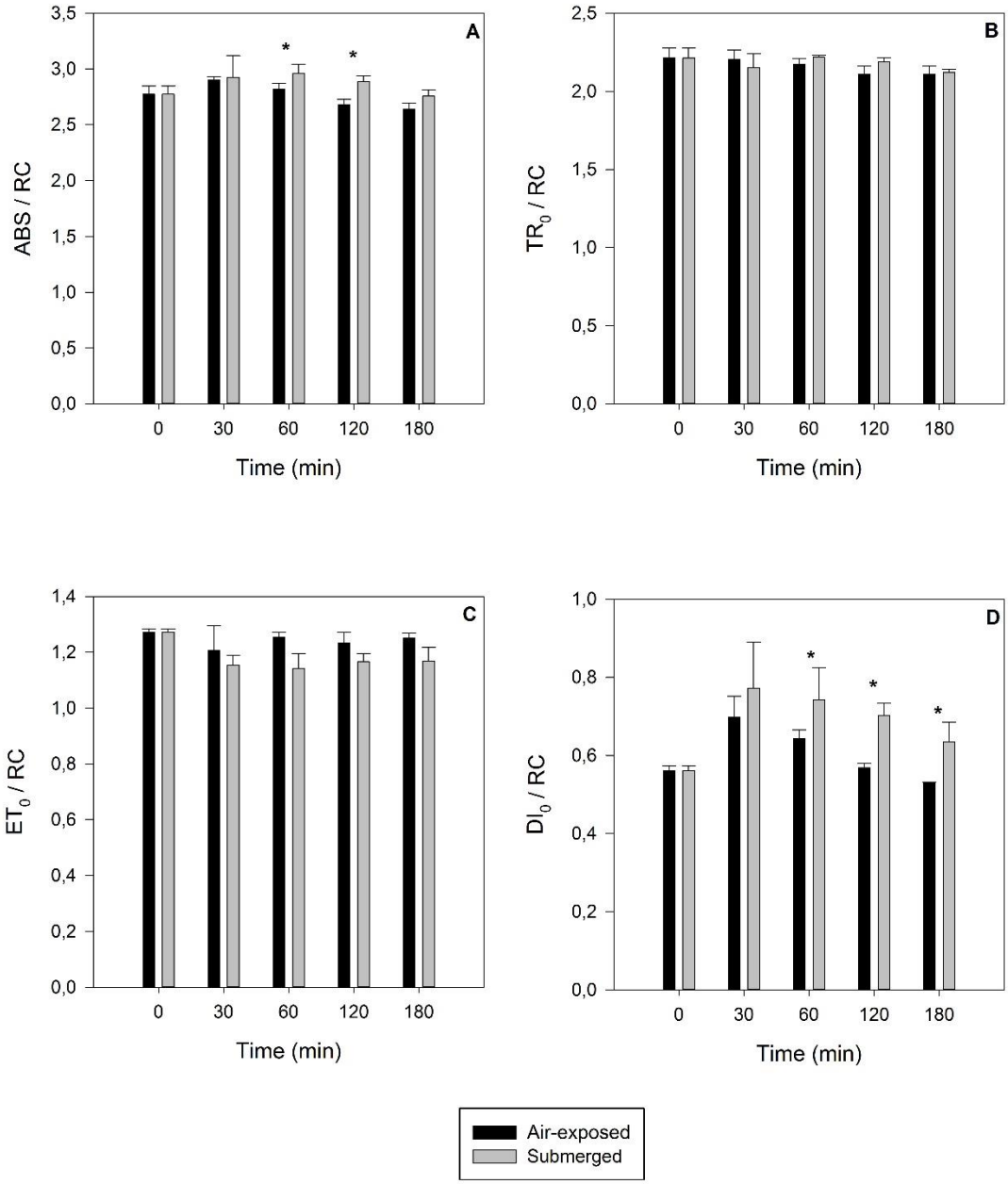

Figure 2.3.4. Absorbed (A), Trapped (B), Transported (C) and Dissipated (D) energy fluxes in dark-adapted leaves of submerged and air-exposed *S. maritima* individuals (average ± standard deviation, n = 5; * $p < 0.05$).

Overlooking the driving forces of each of the processes comprised within the photosynthetic light harvesting process, some interesting differences were noticed (Figure 2.3.5).

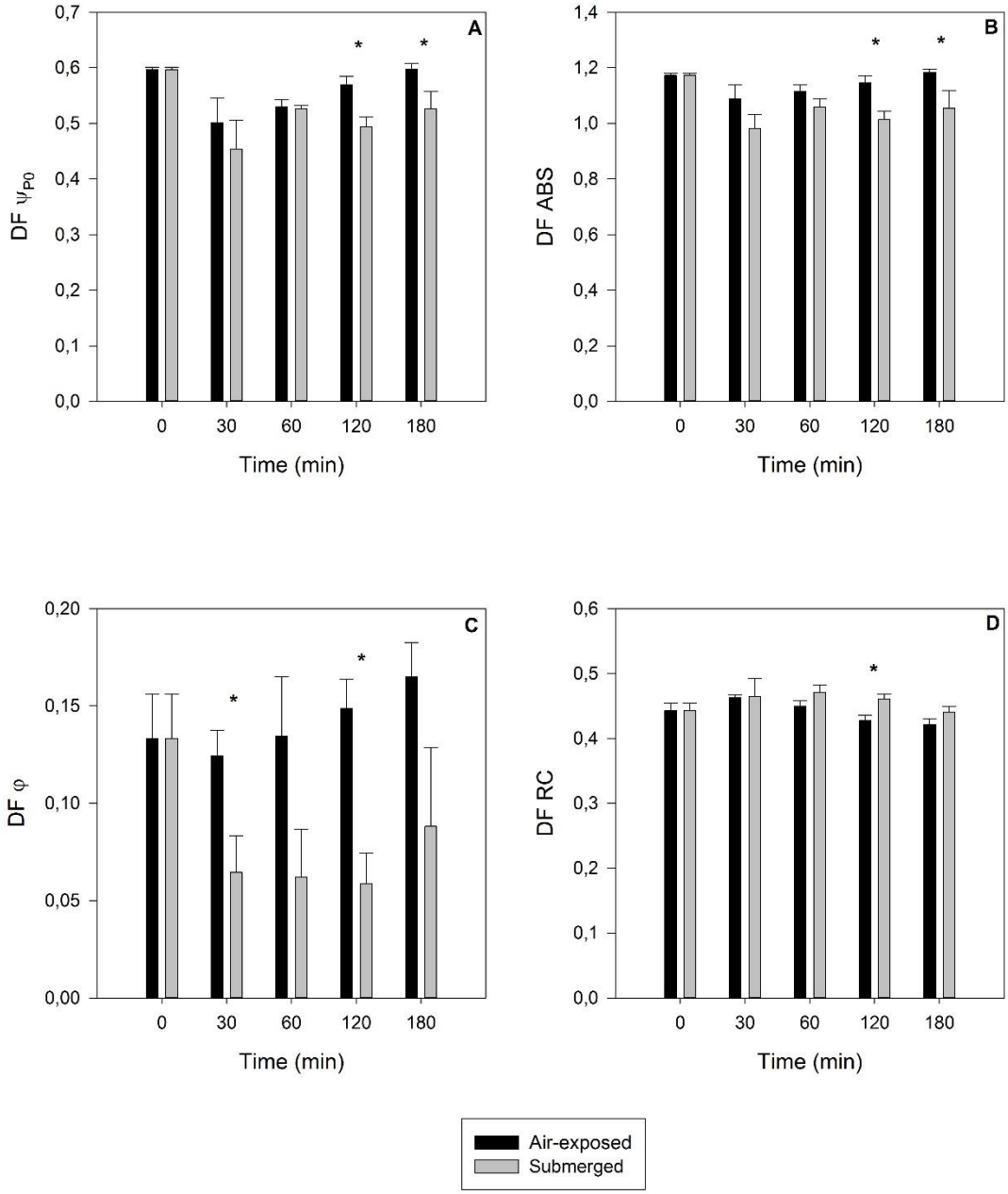

Figure 2.3.5. Driving force for energy trapping (A), for the photosynthesis light harvesting processes (B), for the electron transport throughout the ETC (C) and for energy absorption throughout the PS II (D) in dark-adapted leaves of submerged and air-exposed *S. maritima* individuals (average ± standard deviation, n = 5; * $p < 0.05$).

Again it was possible to observe significant differences in the light energy absorption after 120 min (Figure 2.3.5A), as reported above. Nevertheless, other differences could be found. Both the driving force for energy trapping (Figure 2.3.5B) and for subsequent electron transport (Figure 2.3.5C) showed decreases in the submerged individuals, more markedly after 120 min of submersion. This affects the whole force balance, reflected in the driving force for the overall photosynthetic process (Figure 2.3.5D). Thus, the individuals subjected to submersion periods superior to 120 min showed significantly lower values of these parameters, while compared with the air-exposed individuals.

Investigating deeper into the mechanisms underlying the driving forces and energy fluxes, these processes are enlightened (Figure 2.3.6). It was possible to observe that the maximum quantum yield of the primary photochemical processes occurring in the PS II, showed a significant decrease after 120 min of submersion (Figure 2.3.6E). This was mostly due to a significant decrease in the transport efficiency of the captured electrons, both to the quinone system but also throughout the rest of the ETC (Figure 2.3.6A and 2.3.6C). Concomitant with this and with the increase in the dissipated energy flux, also an increase in the quantum yield of the non-photochemical processes was observed in the submerged individuals and especially after 120 min of underwater treatment (Figure 2.3.6B). Also, it could be noticed that during the first hour of submersion, the individuals exhibited a decrease in the area above the Kautsky curve (Figure 2.3.6D), directly related to the size of the acceptor pool of the PS II, including quinones and plastoquinone. Regarding the connectivity between the two units of the PS II, here evaluated by the grouping probability (Figure 2.3.6F), no significant changes in the connectivity between photosynthetic units were found at this level.

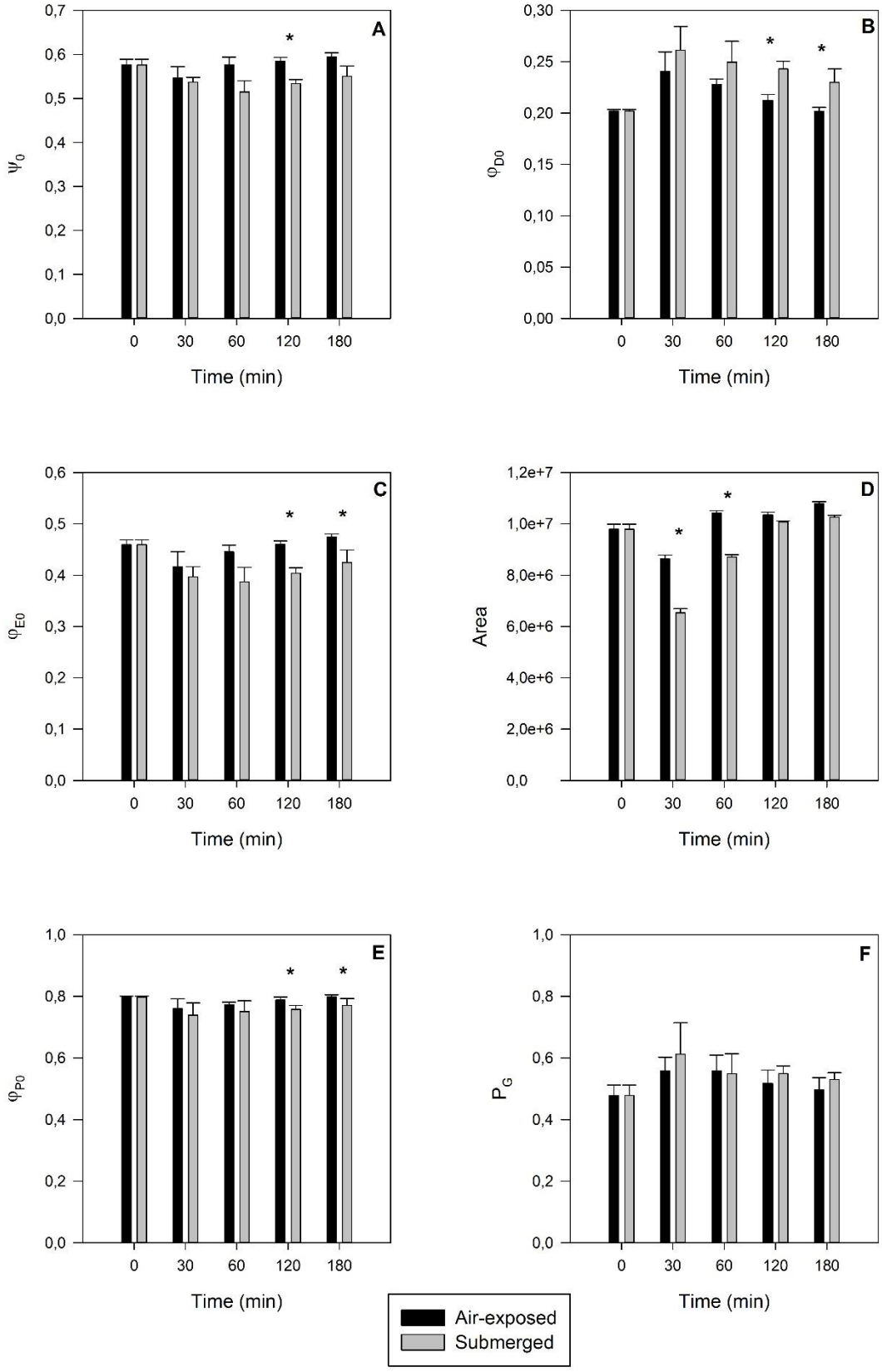

Figure 2.3.6. OJIP transient analysis derived parameters in dark-adapted leaves of submerged and air-exposed *S. maritima* individuals (average ± standard deviation, n = 5; * $p < 0.05$).

Oxidative stress biomarkers

Overall it is possible to observe that superoxide dismutase activity was the most active form of enzymatic counteractive measures (Figure 2.3.7B). During the first 30 to 60 min of submersion there was a significant increase in the activity of all anti-oxidant enzymes (Figure 2.3.7A-D). After this period there is an evident decrease in these activities, reaching values near the observed in the air-exposed individuals at the end of 180 min of submersion.

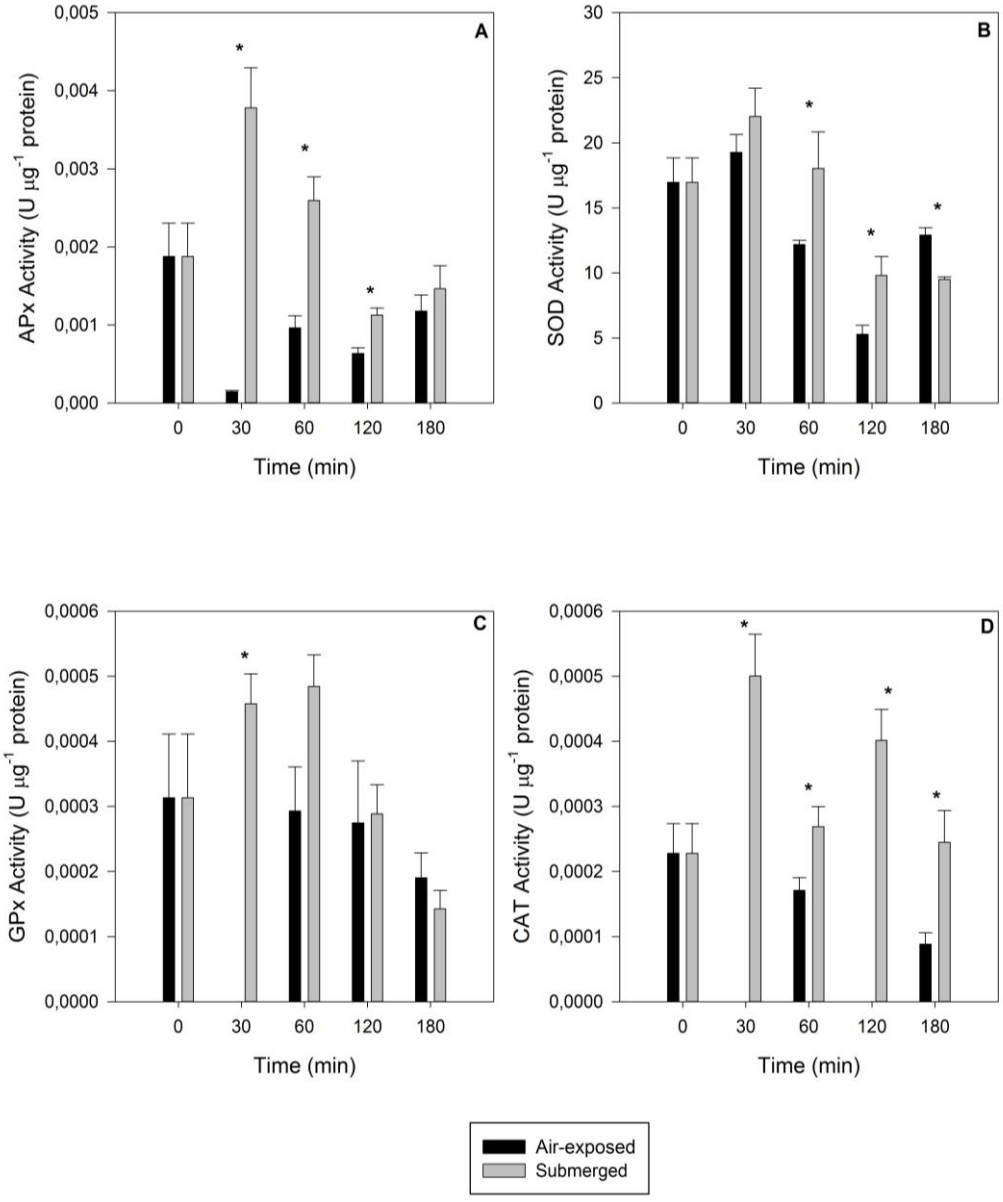

Figure 2.3.7. Antioxidant enzymatic activities in air-exposed and submerged leaves of submerged and air-exposed *S. maritima* individuals (average ± standard deviation, n = 5; * $p < 0.05$).

Discussion

Considering the present predictions of SLR and especially for coastal systems (IPCC, 2002), it is possible that newer or less accreted marshes see their submersion periods increased. During high tide, the lower marsh areas stay flooded for short periods (approximately 2 hours according to Serôdio and Catarino, 2000). With increased sea level heights not only the high tide duration but also the frequency of high low tides is likely to increase, exposing the lower marsh vegetation to increased submersion periods. These changes in the hydrological environment of the species will inevitably impact their photosynthetic physiology. According to recent studies, *S. maritima* will be negatively affected with SLR, decreasing their biomass and thus its coverage area (Valentim *et al*., 2013). This way it becomes important to understand the photobiological causes underlying this projected drawback in the *S. maritima* populations.

As observed in previous studies focusing *S. maritima* communities (Silva *et al*., 2005) although the manly terrestrial characteristics of this specie, there was no inhibition of photosynthetic activity in submerged individuals. These authors found that comparing both communities (submerged and air-exposed), in the terrestrial environment *S. maritima* scavenges about four times more carbon than during submersion (Silva *et al*., 2005).

The shape of the OJIP transient curve is very sensitive to environmental stresses (Zhang and Gao, 1999; Calatayud and Barreno, 2001; Strasser and Tsimilli-Michael; 2001; Sayed, 2003; van Heerden *et al*., 2003; Govindachary *et al*., 2004). During the first hours of submersion the shape of the OJIP transient suffered some alterations resulting in a pronounced decreased on the variable fluorescence of all phases. The rapid O to J rise is a phase controlled by photochemical processes, while J to I is a strictly thermal phase (Schreiber and Neubaeuer, 1987). The release of fluorescence from this phase is controlled by the reactions occurring in the donor side of the PS II. Any abiotic stress that disturbs the structure and function of the oxygen evolving complexes (OECs), affects the rate of oxygen evolution and thus increases the release of fluorescence quenching in the J-I phase (Panda *et al*., 2006). On the other hand, the rise in the O-J phase is due to the PS II quinone pool reduction net photochemical (Prakash *et al*., 2003). Comparing both the donor (J-I)

with the acceptor (O-J) PS II sides, the first was more severely affected during the first hours of submersion, due to the inactivation of the OEC and consequent impairment of the ETC (Panda *et al*., 2006). There could also be verified a reduction in the area above the transient curve, directly related to the size of the quinone pool in the acceptor side of the PS II (Strasser *et al*., 1995; Joliot and Joliot, 2002). This was more evident also during the first hour of submersion. This reduction is in agreement with the overall deleterious effect of submersion on the PS II, as already was described in other plant species (Panda *et al*., 2006; Mateos-Naranjo *et al*., 2007). Inevitably, this decrease of F_M in the transient OJIP affects the F_v/F_M relationship and thus the PS II quantum yields, as could also be verified at the end of one hour of submersion. This reinforces the previous findings, pointing out to a reduction in the PS II capacity to reduce the primary acceptor, Q_A. Although this apparent damage in the donor side of the PS II, this was also verified during the first hour of submersion, not affecting substantially the electron transport per reaction active centre (ET/RC). This indicates that the reduction in the electron flow is accompanied by a proportional increase in the number of active reaction centres (ABS/RC), to overcome this reduction in the electron transport. The increase in the ABS/RC is normally associated to low light levels or significant temperature changes, functioning as a heat radiator, protecting the plant against high temperature and light intensities (Strasser *et al*., 2004; Panda *et al*., 2008). Although the experimental conditions maintained the temperature constant in both treatments, there were differences in the light environment between submerged and non-submerged plants, as normally happens in real-marsh conditions during high tide. This lead to an increase of the number of active reaction centres in order to harvest higher amounts of light. Interesting to notice was the fact that this increase happened at the end of the first hour of submersion, simultaneously with the reduction in the electron transport. From hereafter almost all the parameters showed a recovery, pointing out to a timestamp in the adaptation ability of *S. maritima* to submersion. This increase in active centres, without proportional increase in electron transport efficiency, leads to an accumulation of excessive energy that according to our data, suffered impairment in its transport along the ETC, and thus had to be dissipated. Panda *et al*. (2006) also found a similar mechanism with consequent excessive energy release in

the form of heat dissipation (DI/RC), increasing the quantum yield of the non-photochemical reaction, counteracting the effects of submergence in rice plants. The OJIP-test also provided means to calculate the overall P_G or connectivity between PS II antennae. This parameter accounts for all the energetic communication pathways between neighbour PS II antennae (Strasser and Stirbet, 2001; Panda *et al*., 2006). On the contrary to what could be observed in other terrestrial plants, there was no loss of connectivity between the antennae of the PS II units during submersion, indicating an improved survival strategy for underwater conditions (Panda *et al*., 2006).

The accumulation of energy even with efficient dissipative mechanisms leads to the generation of reactive oxygen species (ROS) that by itself can also damage the PS II and the cellular components of the ETC (Duarte *et al*., 2013). To counteract this damaging effects of ROS, the cell has a machinery mainly composed by enzymatic mechanisms, in order to degrade these molecules and prevent cellular damage, namely at the photosynthetic apparatus level. Similarly, to the observed for the photochemical data, also at the biochemical level these mechanisms follow a similar trend. The majority of the analysed anti-oxidant enzymes showed peaks of activity in the period comprised between 30 and 60 min of submersion. This is in agreement to what as found for the photochemical data. During this period there was higher accumulation of reducing power that had to be dissipated, and thus higher amounts of ROS were generated. The efficient activation of these enzymes points out towards an efficient mechanism, not only for dissipation of the excessive reducing power by the non-photochemical mechanisms, but also for detoxification of the dangerous products resultant of the accumulation of excessive energy. This was also verified in other halophytic species during stress-induced photochemical impairment as a protective measure from the excessive reducing power, even under efficient dissipation (Duarte *et al*., 2013).

Overall a positive feedback to submersion can be observed in *S. maritima* individuals after 60 min of submergence, with increasing values of the processes associated to the photochemical yield and electronic transport and decrease in the non-photochemical processes, like energy dissipation. This points out to a photochemical plasticity in this specie towards submersion, as shown in other

aquatic species like seagrasses (Silva *et al*., 2005). Moreover, the adaptation to the underwater environment appears to be dependent on the duration of the stimulus (submergence). All these biophysical characteristics, confirmed by the biochemical insights provided by the levels of anti-oxidant enzymes, point out to the existence of capable mechanisms triggered in prolonged submersion periods, like the ones expected according SLR projections.

Conclusion

Diurnal tidal flooding imposes to the halophyte community an underwater environment with conditions very different from the terrestrial ones. The predicted SLR increase will have consequences not only on the height of the tidal inundation but also in the duration of the high tides. Thus, becomes important to consider the physiology of each species, and the consequences of their adaptation capacity in terms of ecosystem, towards a changing environment, especially in the case of the species inhabiting the lower marsh, like *S. maritima*. This specie presents a high adaptation capacity to submersion. Although after short periods of submersion an evident reduction of primary PS II photochemistry could be observed mainly due to incapacity to deal with the absorbed light, after prolonged periods it evidences effective mechanisms to dissipate the excessive energy and for detoxification of the accumulated ROS, increasing the photosynthetic efficiency. All these aspects point out to an evident photochemical plasticity of this specie towards prolonged submersion periods like those expected under sea level rise, allowing it to maintain its photosynthetic activity even during prolonged submersion periods, and thus surviving the near future climate change scenarios.

References

Armstrong, W., 1972. A re-examination of the functional significance of aerenchyma. *Physiologia Plantarum* 27, 173-177.

Armstrong, W., 1979. Aeration in higher plants. *Advances in Botanical Research* 7, 225–332.

Armstrong, W., Wright, E.J., Lythe, S. and Gaynard T.J., 1985. Plant zonation and the effects of the spring-neap tidal cycle on soil aeration in a Humber salt marsh. *Journal of Ecology* 73, 323–339.

Bailey-Serres, J. and Voesenek, L., 2008. Flooding stress: acclimations and genetic diversity. *Annual Review of Plant Biology* 59, 313-339.

Beer, S., Ilan, M., Eshel, A., Weil, A. and Brickner I., 1998a. The use of pulse amplitude modulated (PAM) fluorometry for in situ measurements of photosynthesis in two Red Sea Faviid corals. *Marine Biology* 131, 607–612.

Beer, S., Vilenkin, B., Weil, A., Veste, M., Susel, L., and Eshel, A., 1998b. Measuring photosynthesis in seagrasses by pulse amplitude modulated (PAM) fluorometry. *Marine Ecology Progress Series* 174, 293–300.

Bergmeyer, H.U., Gawehn, K., Grassl, M., 1974. Enzymes as biochemical reagents. In: *Methods in enzymatic analysis*. Ed.: Bergmeyer, H. U. Academic press, New York.

Bertness, M.D., 1991. Zonation of *Spartina patens* and *Spartina alterniflora* in New England salt marsh. *Ecology* 72, 138–148.

Bradford, M., 1976. A rapid and sensitive method for the quantification of microgram quantities of protein utilizing the principle of protein-dye-binding. *Analytical Biochemistry* 72, 248–254.

Burdick, D.M. and Mendelssohn, I.A., 1987. Waterlogging responses in dune, swale and marsh populations of *Spartina patens* under field conditions. *Oecologia* 74, 321–329.

Caçador, I., Caetano, M., Duarte, B. and Vale, C. 2009. Stock and losses of trace metals from salt marsh plants. *Marine Environmental Research* 67, 75-82.

Caçador, I., Tibério, S. and Cabral, H., 2007. Species zonation in Corroios salt marsh in the Tagus estuary (Portugal) and its dynamics in the past fifty years. *Hydrobiologia* 587, 205–211.

Calatayud, A. and Barreno, E., 2001. Chlorophyll a fluorescence, antioxidant enzymes and lipid peroxidation in tomato in response to ozone and benomyl. *Environmental Pollution* 115, 283-289.

Colmer, T. and Voesenek, L., 2009. Flooding tolerance: suites of plant traits in variable environments. *Functional Plant Biology* 36, 665-681.

Colmer, T.D. and Flowers, T.J., 2008. Flooding tolerance in halophytes. *New Phytologist* 179, 964-974.

Duarte, B., Couto, T., Freitas, J., Valentim, J., Silva, H., Marques, J. C. and Caçador, I. Abiotic modulation of *Spartina maritima* photosynthetic ecotypic variations in different latitudinal populations. *Estuarine, Coastal and Shelf Science* 130, 127-137.

Duarte, B., Raposo, P. and Caçador, I., 2009. *Spartina maritima* (cordgrass) rhizosediment extracellular enzymatic activity and its role on organic matter decomposition and metal speciation processes. *Marine Ecology* 30, 65-73.

Duarte, B., Santos, D., Marques, J. C. and Caçador, I., 2013. Ecophysiological adaptations of two halophytes to salt stress: photosynthesis, PS II photochemistry and anti-oxidant feedback - Implications for resilience in climate change. *Plant Physiology and Biochemistry* 67, 178-188.

Egan, T.P. and Ungar, I.A., 2000. Mortality of the salt marsh species *Salicornia europaea* and *Atriplex prostrata* (Chenopodiaceae) in response to inundation. *Ohio Journal of Science* 100, 24–27.

Flowers, T.J. and Colmer, T.D., 2008. Salinity tolerance in halophytes. *New Phytologist* 179, 945–963.

Genty, B., Briantais J.-M. and Baker, N., 1989. The relationship between the quantum yield of photosynthetic electron transport and quenching of chlorophyll fluorescence. *Biochimica et Biophysica Acta* 990, 87-92.

Govindachary, S., Bukhov, N.G., Joly, D. and Carpentier, R., 2004. Photosystem II inhibition by moderate light under low temperature in intact leaves of chilling-sensitive and –tolerant plants. *Physiologia Plantarum* 121, 322-333.

Hubbard, J.C.E., 1969. Light in relation to tidal immersion and growth of *Spartina townsendii* (sl). *Journal of Ecology* 57, 795–804.

IPCC, 2002. Climate Change and Biodiversity. IPCC Technical Paper V. Contribution of the Working Group II to the to the Fourth Assessment Report of the Intergovernmental Panel on Climate Change.

Iversen, J. S., 1949. Determinations of the specific gravity of the roots of swamp, meadow and dry-soil plants. *Oikos* 1, 1-5.

Joliot, P. and Joliot, A., 2002. Cyclic electron transport in plant leaf. *PNAS* 99, 10209-10214.

Marchant, C. and Goodman, P., 1969. *Spartina maritima* (Curtis) Fernald. *Journal of Ecology* 57, 287-291.

Marklund, S. and Marklund, G., 1974. Involvement of superoxide anion radical in the autoxidation of pyrogallol and a convenient assay for superoxide dismutase. *European Journal of Biochemistry* 47, 464-469.

Mateos-Naranjo, E., Rendondo-Gómez, S., Silva, J., Santos, R. and Figueroa, E., 2007. Effect of Prolonged Flooding on the Invader *Spartina densiflora* Brong. *Journal of Aquatic Plant Management* 45, 121-123.

Panda, D., Rao, D.N., Sharma, S.G., Strasser, R.J. and Sarkar, R.K., 2006. Submergence effects on rice genotypes during seedling stage: Probing of submergence driven changes of photosystem 2 by chlorophyll a fluorescence induction O-J-I-P transients. *Photosynthetica* 44, 69-75.

Panda, D., Sharma, S.G. and Sarkar, R.K., 2008. Chlorophyll fluorescence parameters, CO_2 photosynthetic rate and regeneration capacity as a result of complete submergence and subsequent re-emergence in rice (*Oryza sativa* L.). *Aquatic Botany* 88, 127-133.

Pedersen, O. and Colmer, T., 2006. Oxygen dynamics during submergence in the halophytic stem succulent *Halosarcia pergranulata*. *Plant Cell and Environment* 29, 1389-1399.

Platt, T., Gallegos, C.L., and Harrison W.G., 1980. Photoinhibition of photosynthesis in natural assemblages of marine phytoplankton. Jo*urnal of Marine Research* 38, 687–701.

Prakash, J.S.S., Srivastava, A., Strasser, R.J. and Mohanty, P., 2003. Senescence-induced alternation in the photosystem II functions of *Cucumis sativus* cotyledons: probing of senescence driven alternation of photosystem II by chlorophyll a fluorescence induction O-J-I-P transients. *Indian Journal of Biochemistry and Biophysics* 40, 160-168.

Reed, D.J., 2002. Sea-level rise and coastal marsh sustainability: geological and ecological factors in the Mississippi delta plain. *Geomorphology* 48, 233–243.

Runcie, J.W. and Durako, M.J., 2004. Among-shoot variability and leaf-specific absorbance characteristics affect diel estimates of in situ electron transport of *Posidonia australis*. *Aquatic Botany* 80, 209–220.

Sand-Jensen, K., 1989. Environmental variables and their effect on photosynthesis of aquatic plant communities. General features to aquatic photosynthesis. *Aquatic Botany* 34, 5-25.

Sayed, O.H., 2003. Chlorophyll fluorescence as a tool in cereal crop research. *Photosynthetica* 41, 321-330.

Schreiber, U. and Neubauer, C., 1987. The polyphasic rise of chlorophyll fluorescence upon onset of strong continuous illumination: Partial control by the photosystem II donor side and possible ways of interpretation. *Zeitschrift für Naturforschung* 42c, 1255-1264.

Serôdio J. and Catarino F., 2000. Modelling the primary production of intertidal microphytobenthos: time scales of variability and effects of migratory rhythms. *Marine Ecology Progress Series* 192, 13-30.

Setter, T.L. and Waters, I., 2003. Review of prospects for germplasm improvement for waterlogging tolerance in wheat, barley and oats. *Plant and Soil* 253, 1–34.

Sifton, H. B., 1945. Air-space tissue in plants. *Botanical Review* 11, 108-43.

Silva, J., R. Santos, M. L. Calleja, and Duarte, C.M., 2005. Submerged versus air-exposed intertidal macrophyte productivity: from physiological to community-level assessments. *Journal of Experimental Marine Biology and Ecology* 317, 87–95.

Smith, F. and Walker, N., 1980. Photosynthesis by aquatic plants: effects of unstirred layers in relation to assimilation of CO_2 and HCO_3^- and to carbon isotopic discrimination. *New Phytologist* 86, 245-259.

Strasser, R.J. and Stirbet, A.D., 2001. Estimation of the energetic connectivity of PS II centres in plants using the fluorescence rise O–J–I–P. Fitting of experimental data to three different PS II models. *Mathematics and Computers in Simulation* 56, 451-461.

Strasser, R.J. and Tsimilli-Michael, M., 2001. Stress in plants, from daily rhythm to global changes, detected and quantified by the JIP test. *Chimie nouvelle* (SRC) 75, 3321-3326.

Strasser, R.J., Srivastava, A. and Govindjee, 1995. Polyphasic chlorophyll a fluorescence transient in plants and cyanobacteria. *Photochemistry and Photobiology* 61, 32-42.

Strasser, R.J., Tsimilli-Michael, M. and Srisvastava, A., 2004. Analysis of the chlorophyll-a fluorescence transients. In: Papageorgiou, G.C. and Govindjee, ed. *Advances in photosynthesis and respiration*. Berlin: Springer p. 321-362.

Teranishi, Y., Tanaka, A., Osumi, M. and Fukui, S., 1974. Catalase activities of hydrocarbon-utilizing Candida yeast. *Agricultural and Biological Chemistry* 38, 1213-1220.

Tiryakioglu, M., Eker, S., Ozkutlu, F., Husted, S. and Cakmak, I., 2006. Antioxidant defence system and cadmium uptake in barley genotypes differing in cadmium tolerance. *Journal of Trace Elements in Medicine and Biology* 20, 181-189.

Valentim, J.M., Vaz, N., Silva, H., Duarte, B., Caçador, I. and Dias, J.M., 2013. Tagus Estuary and Ria de Aveiro Salt Marsh Dynamics and the Impact of Sea Level Rise. *Estuarine, Coastal and Shelf Science* 130, 138-151.

van Heerden, P.D.R., Tsimilli-Michael, M., Krüger, G.H. and Strasser, R.J., 2003. Dark chilling effects on soybean genotypes during vegetative development; parallel studies of CO_2 assimilation, chlorophyll a fluorescence kinetics O-J-I-P and nitrogen fixation. *Physiologia Plantarum* 117, 476-491.

Voesenek, L., Rijnders, J., Peeters, A., van de Steeg, H. and Kroon, H., 2004. Plant hormones regulate fast shoot elongation under water: from genes to communities. *Ecology* 85, 16-27.

Winkel, A., Colmer, T.D. and Pedersen, O., 2011. Leaf gas films of *Spartina anglica* enhance rhizome and root oxygen during tidal submergence. *Plant, Cell and Environment* 34, 2083-2092.

Zhang, S. and Gao, R., 1999. Diurnal changes of gas exchange, chlorophyll fluorescence, and stomatal aperture of hybrid poplar clones subjected to midday light stress. *Photosynthetica* 37, 559-571.

Zhu, X.G., Govindjee, Baker, N.R., Sturler, E.D., Ort, D.R. and Long, S.P., 2005. Chlorophyll a fluorescence induction kinetics in leaves predicted from a model describing each discrete step of excitation energy and electron transfer associated with Photosystem II. *Planta* 223, 114–133.

2.4. IMPACT OF SEA LEVEL RISE INFERRED FROM SEDIMENT DEPOSITION RATES AND GEOCHEMISTRY OVER A 40-YEAR INTERVAL IN THE TAGUS MESOTIDAL ESTUARY (PORTUGAL)[1]

Abstract

Sea level rise has been evaluated using data acquired from two Tagus estuary salt marshes. Sediment accumulation rates over a 40-year study period were determined using ^{137}Cs along with an evaluation of the variations in the sediment elemental geochemistry (including heavy metals). Correlating SLR data from 1963 to 2001 with the sediment accretion rates (SAR) an inverse pattern of interaction was observed, with lower SAR associated to periods of higher mean sea level (MSL) heights. This pointed out to an erosion effect of the salt marsh during higher tidal flooding. Although SLR apparently slows down SAR, it still presents a positive balance with SLR, similar to that identified in most mesotidal estuaries. The geochemical analysis of sediments and chemical alteration index (CAI) also suggest that the major processes inherent to the SAR vary inversely to the MSL and this may be caused mostly by physical disturbances. Both salt marshes did show enhanced high-energy transport driven inputs of sediments, although in the Pancas salt marsh there is a slight evidence of chemical weathering of the sediments. Anthropogenic contamination of the sediments by heavy metals was identified and has been decreasing from 1963 to 2001, mostly linked to a marked reduction of industrial activities in some areas surrounding the Tagus estuary, rather than the sedimentary history of the estuary.

[1] This section was published: **Duarte, B.**, Caçador, I., Marques, J.C. and Croudace, I., 2013. Tagus Estuary salt marshes feedback to sea level rise over a 40-year period: insights from the application of geochemical indices. *Ecological Indicators* 34, 268-276.

Introduction

Climate change is nowadays one major concern spanning across the environmental science community. It is widely accepted that increasing CO_2 levels may induce climate change through the greenhouse effect and holds the potential to affect most ecosystems to some degree. Some direct causes of CO_2 rising concentrations in the atmosphere are increasing temperature values and ocean acidification, but other may result from direct changes to the gas and particle contents within the atmosphere. The impact of an increased greenhouse effect has been widely studied (e.g. IPCC, 1990; Titus and Narayanan, 1995) and the reports of the Intergovernmental Panel on Climate Change (IPCC) in 1990, confirmed in 1995, specify that the global average air and sea surface temperatures are expected to rise by about 2.5°C, within a range of 1.5–4.5°C (Berner and Berner, 1996; Houghton, 1999; IPCC, 1999), although there is a degree of uncertainty about these estimations related to issues of geographical, diurnal and seasonal variability (Gates, 1993; Houghton, 1999). One of the major side-effects of global warming is SLR, due to polar ice meltdown and increasing ocean water supply, but also caused by the thermal expansion of this larger water mass. Inevitably, the most affected areas of the globe and highly vulnerable to SLR are located close to the seashore, including coastal lagoons, estuaries and the shoreline. Estuaries stand out as areas of special concern, because they include some of the most densely populated areas in our planet. Estuarine ecosystems hold therefore great scientific potential in this context and will help us understanding climate change dynamics and their impacts upon these areas.

Salt marshes are often located along estuarine margins and they are particularly vulnerable to SLR (Dyer *et al* 2002). Salt marshes are considered to be among the most productive ecosystems on the planet and they have an essential role as nursing areas for marine fish and invertebrates of great economic value. They are invaluable habitats and feeding sites to many migratory bird species, while sheltering great biodiversity (Reed, 1990; Van Dijkeman *et al*., 1990). The slope of the marsh in relation to the tidal amplitude, and the elevation of the shoreline offering better protection in conditions of increasing storminess (Dyer *et al*., 2002) will be determining factors for the initial set-up and resilience of the salt marsh

communities under increasing conditions of SLR (Simas *et al*., 2001). These areas are described as transitional water bodies in the Water Framework Directive of the European Union, and they are further recognised as ecologically sensible zones according to the Birds and Habitats directives. Locked between landmasses and ocean, rising seawater levels will play an important role in the future ecology of these regions. Sea level rise will also mean higher erosion rates in the outer boundary of the salt marsh (Reed, 1990). However, some mechanisms may counteract the influence of these climatic induced factors, as salt marshes also have the ability to keep their relative elevation above seawater throughout sedimentation (Salgueiro *et al*., 2007). Salt marshes act as sinks for contaminants (Caçador *et al*., 2000; Duarte *et al*., 2010), carbon (Caçador *et al*., 2004) and nitrogen (Caçador *et al*., 2007). The major depositional process for these elements is through sedimentation of particulate matter during tidal flooding (Silva *et al*., 2009), when the halophytic vegetation acts as a baffle and sediment trap, leading to the settling of fine suspended particles transported on the water column that are deposited on the marsh (Silva *et al*., 2009). Furthermore, salt marsh growth is often associated to processes occurring in estuarine areas with high levels of sediment discharge, like mudflats (Simas *et al*. 2001). To counteract the effects of SLR, the marsh elevation must keep on at such a pace that is compatible with the rise. Otherwise flooding is inevitable and will be followed by subsequent marsh erosion. This has already been verified in the Nile and Mississippi rivers (Gornitz, 1991; Blum and Roberts, 2009). Another important factor to consider is the tidal range of the salt marsh. Stevenson *et al*. (1986) suggested that areas with high tidal range are associated with higher sediment transport rates, thus being less affected by SLR. In this case a negative feedback mechanism is observed, where a small increase in sea level leads to higher mineral deposition due to longer submersion periods. This is also associated with less sediment compaction due to reduced decomposition of organic matter in the sediment (Nyman *et al*., 1993; Allen, 1994). However, a rapid SLR, as predicted in some climate change scenarios (IPCC, 2007) increases salt marsh loss caused by the increased submersion periods since salt marsh productivity (organogenic input) is suppressed (Nyman *et al*., 1993; Nyman *et al*. 1994). Recently, an increasing number of numerical modelling studies have appeared aimed at identifying and simulate the

main processes of marsh elevation dynamics in response to changing sea level (Allen, 1990, 1995, 1997; Callaway *et al*., 1996; Chmura *et al*., 1992; Day *et al*., 1999; French, 1993; Krone, 1987; Morris *et al*., 2002; Pont *et al*., 2002; Rybczyk and Cahoon, 2002; Rybczyk *et al*., 1998; Temmerman *et al*., 2003a; Van Wijnen and Bakker, 2001). However, as stated by Allen (2000), these models are at a rather embryonic stage of development. Important information can be obtained meanwhile from empirical studies of saltmarsh systems. By investigating sedimentary records in the context of the climate conditions that produced them it should be possible to understand how salt marsh geochemical characteristics and accretion rates have been responding to changes in sea level. This type of information will be very useful in practice, allowing for better adaptive management of human activities, and hopefully to guide our preparation and protective measures against future scenarios.

This work aims to assess sediment accumulation rates in the Tagus salt marsh over the last 40 years (using ^{137}Cs dating) and to check also for any modifications in elemental geochemistry (including heavy metals) in the context of rising sea level conditions. This may contribute to our knowledge on the impact of SLR and sedimentation rates in a major mesotidal estuarine system, and allows for the possibility of redistributing sediment-bound metal contaminants.

Material and Methods

Study area description

The Tagus estuary is the largest estuary on the west coast of Europe (38°44' N, 9°08' W), located in the most populated area of Portugal (Figure 2.4.1). It is a shallow estuary and its circulation is mainly driven by tides. The Tagus River drains a total area of 86,629 km^2, representing the second most important hydrological basin in the Iberian Peninsula. The river is the main source of freshwater into the estuary. Inflow fluctuates seasonally with an average monthly value varying from 120 m^{-3} s^{-1} in summer to 653 m^{-3} s^{-1} in winter (last 30 years of Water National Institute public database, INAG). Estimated water residence time ranges from 6 to <65 days for winter and summer average river discharge, respectively (Martins *et al*. 1984). It is a mesotidal estuary according to the NOAA classification, with semi-diurnal tides ranging from 0.4 m at neap tide to 4.1 m at spring tide. Seawater enters the estuary

through a deep narrow inlet channel. The tidal influence reaches 80 km inland from Lisbon. Coring took place at Pancas (PAN) salt marsh, located in the southern margin of the Tagus estuary within the Natural Reserve of Tagus Estuary and in S. João da Talha (SJT) salt marsh, located in the northern margin in Lisbon metropolitan zone. Three sediment cores were taken using a tubular probe (6.7 cm diameter) in 2001. The cores were taken along the salt marsh in an area vegetated by *Sarcocornia perennis*. Appropriate measures were taken to avoid compaction during the coring. The position of the cores and vertical level of the coring sites was attained by GPS.

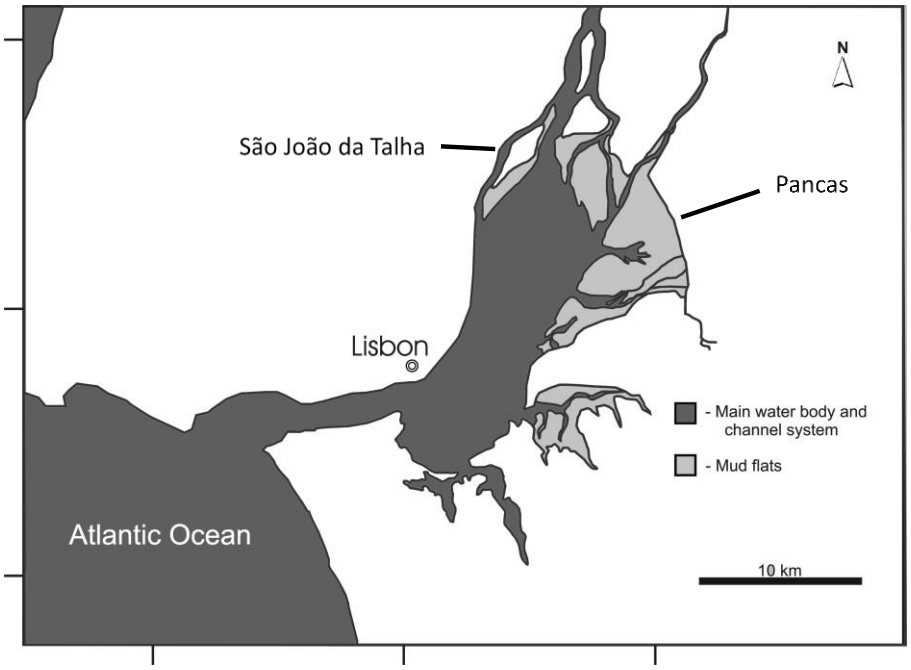

Figure 2.4.1. Tagus Estuary map with Pancas and S. João da Talha salt marshes sampling stations marked.

Laboratory Analysis

The cores obtained at the sampling stations were brought back to the laboratory in refrigerated chambers and sliced. The samples were dried to constant weight at 60 °C. Organic matter content was determined by loss on ignition (LOI) after slowly ashing sub-samples at 600 °C for three hours. The samples were analysed for ^{137}Cs activity, using gamma-spectrometry by way of its peak at 661 keV.

Depth of the 1963 peak (Ritchie and McHenry, 1990) was used to investigate the accumulation rates, while the sediment accumulation rates (SAR) were

computed taking into account the diameter of the corer and an average sediment density of 1020 $kg.m^{-3}$, obtained for the Tagus salt marshes in previous studies (Salgueiro and Caçador, 2007). Sedimentation values were also corrected for organic matter content, considering the organic percentage found in the different layers. These values were taken in account to eliminate for any possible artefacts caused by the fact that each layer in our sample is at a different stage of organic decomposition.

Geochemical analysis of the sediments and their heavy metal content was carried out through X-ray Fluorescence Spectrometry (XRF). The sediments were frozen-dried and compressed into tablets. XRF was performed in a Philips Magix-Pro WD-XRF unit at the National Oceanography Centre (NOC) in Southampton, UK. After knowing the relevant data from the oxides composition it was possible to work out the Chemical Alteration Index (CAI):

$$CAI = \frac{Al_2O_3}{Al_2O_3 + CaO + K_2O + Na_2O}$$

This index gives us information about the kinds of disturbance affecting the sediments. In practice, CAI values below 40 suggest the absence of disturbance, and values from 40 to 70 are typical of physical disturbance only, while index values above 70 essentially are indicators of chemical disturbance of the sediments (Cox and Lowe, 1995).

Sea level data

The Cascais tidal gauge (www.igeo.pt) is the most suitable reference unit nearby and was used to assess sea level data in our study of the Tagus estuary salt marshes. This gauge holds recordings from 1880-present. Only the annual heights dataset from 1963 to 2001 was considered. Tidal heights for the same period were obtained from the Hydrographic Institute (www.hidrografico.pt) and their dataset for the Lisbon station. The annual heights were plotted by linear regression, in order to establish a SLR rate (Andersen *et al*., 2011).

Results

^{137}Cs dating and sediment accumulation rates

The isotopic analysis of the cores showed two major peaks of ^{137}Cs consistent with the recent history of NW Europe. The lower peak corresponds to the input of bomb test material that had its higher activity period in 1963. The upper peak is normally identified as ^{137}Cs deposition resulting from the Chernobyl accident in 1986 (Andersen *et al.*, 2000). These peaks were chosen as markers for those events and allowed us to consider two different time periods for the purpose of this study: from 2001 to 1986 and from 1986 to 1963 (Figure 2.4.2).

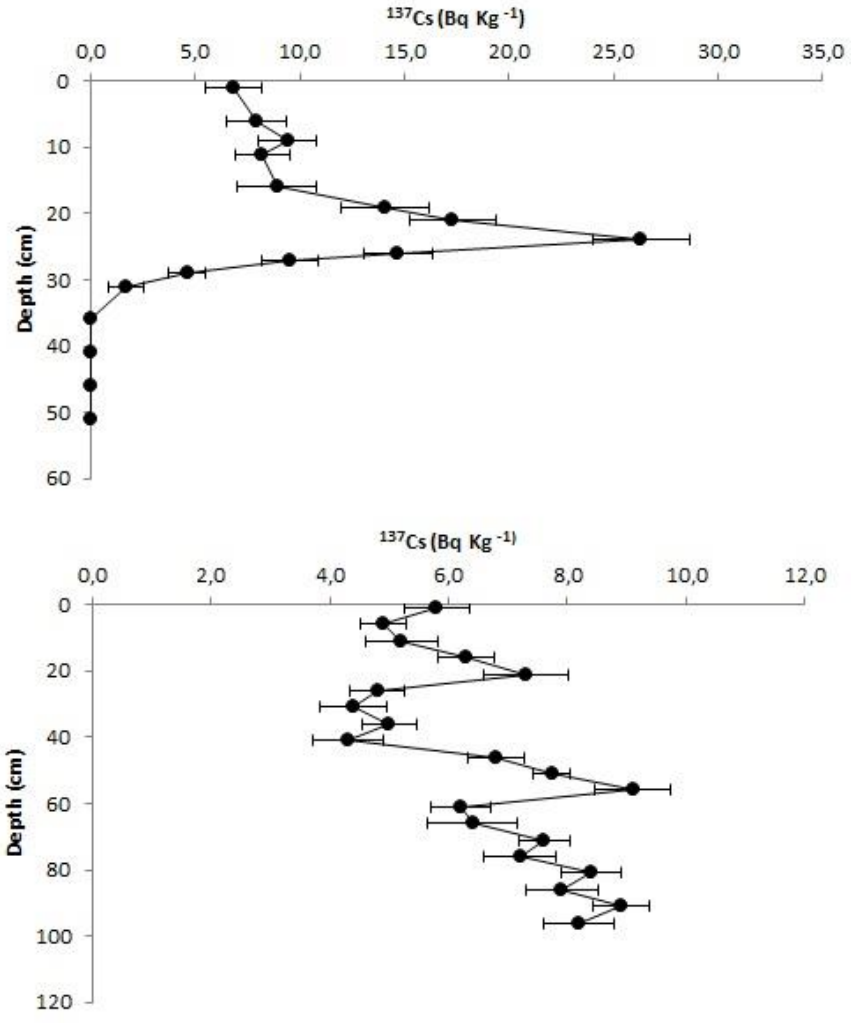

Figure 2.4.2. Vertical profiles of ^{137}Cs activity in salt marsh soil obtained from core samples collected at Pancas (A) and S. João da Talha (B).

Using these radiometric markers, the average SAR were assessed for both time periods (Table 2.4.1) and this allows for increased accuracy in our analysis and better discrimination of the sedimentation history at the two salt marsh stations for the study years (1963 to 2001).

Table 2.4.1. Calculated total and mineral sedimentation ($kg.m^{-2}.y^{-1}$) and accretion ($cm.y^{-1}$) rates based on ^{137}Cs peaks in both salt marshes.

	Pancas (PAN)	**S. João Talha (SJT)**
Apparent Sediment Accumulation Rate		
1963 – 1986	6.65 ± 0.33	15.52 ± 0.78
1986 – 2001	5.44 ± 0.27	13.60 ± 0.68
1963 – 2001	6.17 ± 0.31	14.76 ± 0.74
Real Sedimentation Rate		
1963 – 1986	6.03 ± 0.30	13.17 ± 0.66
1986 – 2001	4.87 ± 0.24	11.06 ± 0.55
1963 - 2001	5.60 ± 0.28	12.25 ± 0.61
Accretion Rate		
1963 – 1986	0.65 ± 0.04	1.52 ± 0.00
1986 – 2001	0.53 ± 0.00	1.33 ± 0.01
1963 – 2001	0.61 ± 0.03	1.45 ± 0.00

The radiometric vertical profile in our cores shows rather obvious peaks of higher ^{137}Cs activity at different depths and these peaks have been observed for the two salt marshes. However, while the 1986 peak was detected at a depth of 9 cm in the Pancas (PAN) salt marsh, the same peak has been detected further down in SJT, occurring at a depth of 21 cm. A similar pattern was found also for the 1963 peak, occurring at a depth of 24 cm in Pancas and 56 cm deep in SJT. The SAR values have been assessed from this type of radiometric dating (Table 2.4.1) and for the years 1963 to 2001 the accretion was always higher in the SJT station when compared to PAN. There was an altitudinal increase of 0.10 cm associated to the accretion rates for the 1963-1986 and 1986-2001 time intervals observed in Pancas salt marsh, and this compares to some 0.20 cm in the SJT station for the same period. This difference

becomes more evident when comparing data in terms of mass deposition by square meter of salt marsh soil area, or total sedimentation rate. Differences among our stations were in the order of 10 kg of sediment deposited on a square meter of salt marsh, further emphasizing the elevated accretion rates observed in the SJT site. Whenever the cores did exhibit different organic matter values due to variations in decomposition rates within the vertical profile, these values of total sedimentation were corrected for its organic matter (as loss on ignition) and expressed as mineral sedimentation rate.

Sea level rise data

The local variation of MSL for the evaluated periods is plotted in Figure 2.4.3. There was a small decrease in MSL from 1963 to 1986, occurring at a mean rate of approximately 1 mm per year. Although, in the following period (1986 to 2001) there has been an increase in MSL, and this was observed occurring at a much higher rate (about 1.76 mm increase per year).

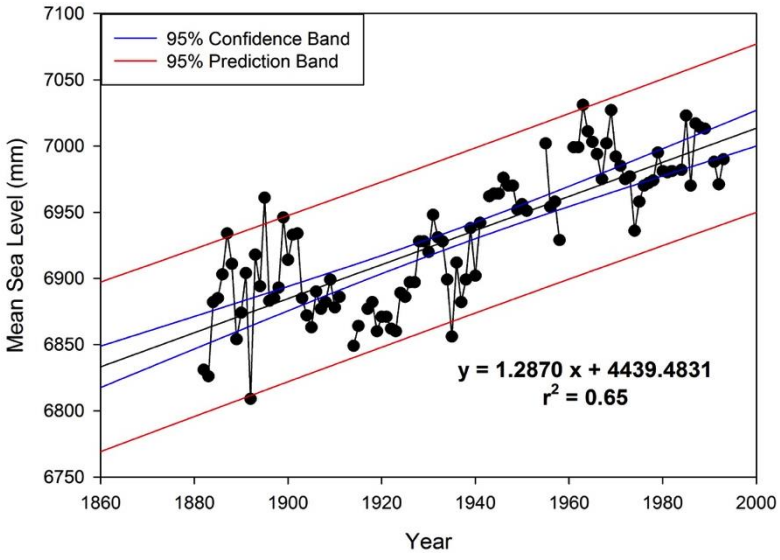

Figure 2.4.3. Changes in Mean Sea Level values (mm) monitored from 1963 to 2001.

Plotting a linear trend for the whole study period (1963-2001) a rate of increase of the MSL was assessed at about 0.75 mm y^{-1} in this area. The yearly mean values did oscillate around 10.5 mm during the study period. The mean water depth in those areas where the lowest part of both salt marshes will be covered by the

incoming tide stays about 1 m above the national chart datum - Portuguese Hydrographic Zero (PHZ). This MSL rise will have major consequences in the ecology of the salt marsh, associated to longer inundation periods during the high tide cycles.

Elemental Analysis

The geochemical analysis of the sediments (Table 2.4.2) revealed that the SiO_2 content has been decreasing from 1963 to 2001, remaining higher in cores from PAN when compared to SJT. Major differences were also observed for CaO in the two salt marshes. In both cases the values for CaO throughout the chronosequence did remain rather stable during the period of our analysis, but SJT showed higher values of CaO when compared to PAN.

Table 2.4.2. Geochemical characterization of the sediment cores of SJT and PAN sites at the depths dated as 1963, 1986 and 2001 (average ± standard Deviation, n = 5).

	SJT site			PAN site		
	1963	**1986**	**2001**	**1963**	**1986**	**2001**
SiO_2	54.5 ± 0.3	54.0 ± 0.4	45.3 ± 8.7	58.7 ± 0.7	57.4 ± 0.7	51.8 ±4.1
Al_2O_3	19.4 ± 0.4	19.1 ± 0.3	16.8 ± 2.7	20.7 ± 0.5	20.7 ± 0.6	17.8 ± 1.8
TiO_2	0.9 ± 0.1	0.9 ± 0.1	0.8 ± 0.1	0.9 ± 0.0	0.9 ± 0.0	0.7 ± 0.1
Fe_2O_3	7.8 ± 0.6	7.9 ± 0.5	6.6 ± 0.5	7.0 ± 0.5	7.7 ± 0.0	6.9 ± 0.6
MnO	0.1 ± 0.0	0.1 ± 0	0.1 ± 0.0	0.1 ± 0.0	0.1 ± 0.0	0.1 ± 0.0
MgO	3.1 ± 0.1	3.0 ± 0.1	2.9 ± 0.1	3.1 ± 0.2	3.1 ± 0.4	3.1 ± 0.2
CaO	4.2 ±0.2	4.4 ± 0.3	4.0 ± 0.4	1.1 ± 0.3	0.9 ± 0.5	1.0 ± 0.5
K_2O	3.8 ±0.3	3.6 ± 0.2	3.3 ± 0.2	3.7 ± 0.1	3.7 ± 0.1	3.3 ± 0.3
Na_2O	2.2 ± 0.2	1.6 ± 0.4	1.7 ± 0.5	1.8 ± 0.2	1.7 ± 0.3	4.8 ± 2.5
P_2O_5	0.2 ± 0.0	0.3 ± 0.0	0.3 ± 0.0	0.2 ± 0.0	0.3 ± 0.1	0.3 ± 0.1
Sum	96.2 ± 1.1	95.1 ± 0.3	81.7 ± 13.2	97.2 ± 0.8	96.5 ± 1.4	89.8 ± 4.1
CAI	65.4 ± 1.2	66.5 ± 0.7	64.9 ± 0.8	75.9 ± 0.9	76.5 ± 0.8	66.2 ± 6.7
Al_2O_3 / SiO_2	2.8 ± 0.1	2.8 ± 0.1	2.7 ± 0.1	2.8 ± 0.1	2.8 ± 0.1	2.9 ± 01

As for Na_2O, there was a decrease of this oxide from 1963-2001 at SJT, while in PAN there was an evident increase from 1986 to 2001. This difference in oxide composition at the two sites is evident also when we look into the CAI values. In both salt marshes there was an increase of the CAI values from 1963 to 1986, and a

subsequent decrease from 1986 to 2001. In this case, the decrease was more evident in Pancas salt marsh. The values observed for both oxides in the two salt marshes are consistent with current interpretation of predominant physical disturbance mechanisms influencing the geochemistry of the sediments (Cox and Lowe, 1995), and this is more evident in Pancas (PAN). The ratios Si/Al and Si/K are dependent upon the proportion of the coarse materials, mainly formed by quartzitic sands containing high percentages of silicon, and fine clays which contain Si, Al and K. Comparing these ratios (Figure 2.4.4), it is possible to observe a strong relationship between the two ratios in Pancas salt marsh, while in SJT the Si/K ratio remains rather stable despite variations in the Si/Al ratio.

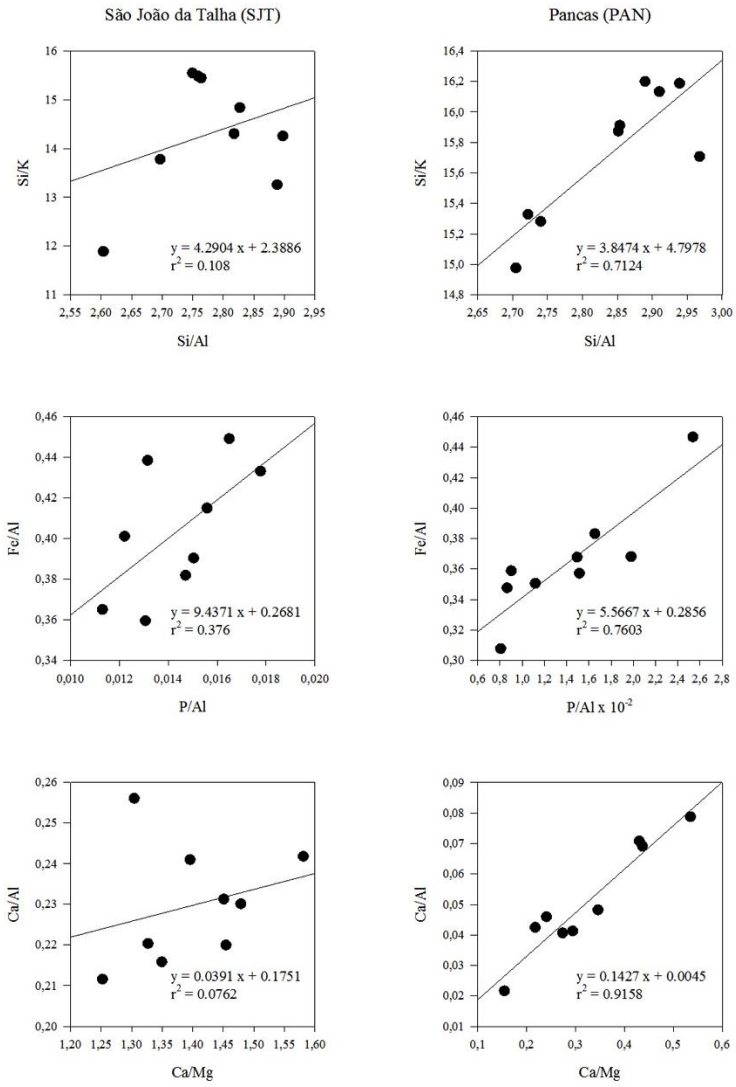

Figure 2.4.4. Geochemical ratios obtained from ^{137}Cs-dated sediments collected at the two salt marsh sampling stations monitored on the Tagus estuary.

Iron and phosphorous are rather abundant elements with high importance on sediment biogeochemistry. A variation on P/Ca and P/Fe ratios indicates an accumulation of organic phosphorus and influences the mechanisms controlling the amount of total phosphorus in sediments. Although the more obvious pattern was found again in the Pancas salt marsh sediments (with a strong correlation between the two ratios), there is also evidence of a correlation between Fe and P (Al normalized values) for the SJT salt marsh, although with smaller variability than found at Pancas. Calcium and magnesium are the most abundant alkaline-earth elements in reservoir sediments, with Ca mainly present as carbonate minerals in this kind of sediments. Similar to the Si/Al and Si/K ratios, analysis of the variation of these elements (Figure 2.4.4) shows also a strong and obvious correlation in the sediments from Pancas salt marsh, while in the SJT salt marsh this relationship was not found.

The heavy metal content in the layers dated by ^{137}Cs did show similar spatial and temporal trends for all metals (Figure 2.4.5). The metal concentrations in SJT samples were always higher than in samples from PAN, except for Ni and Cr in 2001 when both stations had very similar values. It was also possible to observe a temporal trend for all the metals included in our analysis, with concentrations in the sediments decreasing from 1963 to 2001. Comparing the average values determined for both salt marshes included in this study with those provided by Turekian and Wedepohl (1961) for the 'standard shale' may give some indication about the importance of anthropogenic components relative to typical geogenic (non-polluted) components. Lead and Zn are present on the Tagus estuary and they occur at approximately 5 times their typical geogenic concentrations, particularly in the sediments collected in the SJT salt marsh. This indicates anthropogenic introduction of these heavy metals in the Tagus estuarine system, particularly in the northern part of the estuary near the Lisbon metropolitan area.

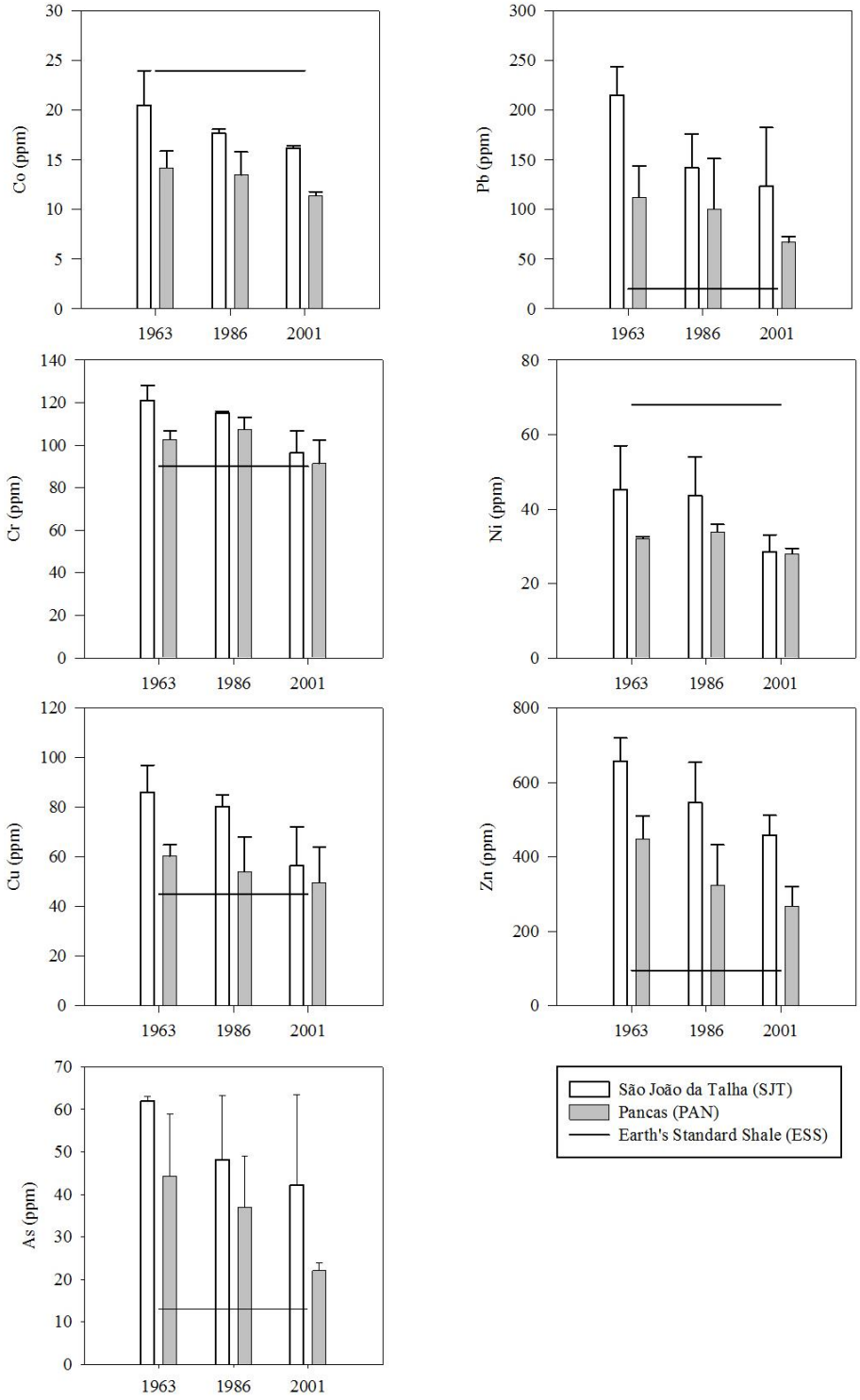

Figure 2.4.5. Heavy metal concentrations measured in ^{137}Cs-dated sediments collected at the São João da Talha (SJT) and Pancas (PAN) salt marsh sampling stations (average ± standard Deviation, n = 5).

Discussion

Sea level rise may have two major influences in salt marshes accretion rates. With higher MSL heights the tidal inundation frequency of a marsh tends to increase, leading to higher suspended sediment supply to the marsh via settling particles. Also, there is an effect of higher erosion rates due to changes in the semidiurnal tidal flooding and drawback of the tidal waters (Roman *et al*., 1997). Evaluating tidal gauge MSL heights and the SAR it is possible to observe an inverse pattern of interaction. From 1963 to 1986 there was a slight decreasing trend in the MSL heights (0.99 mm y^{-1}) on the Tagus Estuary, simultaneous with higher sedimentation and accretion rates in both salt marshes. In contrast, from 1986 to 2001 the MSL heights did show a gradual increase (1.86 mm y^{-1}), and there was a correspondent decrease in the sedimentation and accretion rates for both marshes. Both events point out to the same mechanism of marsh morphodynamics. During periods of high MSL the main effect of tidal inundation is erosion of the marsh. Despite all evidence concomitant with this kind of morphodynamic mechanism some additional factors must also be considered, like storm frequency (Roman *et al*., 1997; Dyer *et al* 2002), elevation in the tidal frame, tidal channel migration (Reed, 1990; Ward *et al*., 1998), exposure to wave attack (Oenema and DeLaune, 1988) and anthropogenic influences such as land reclamation (Sarretta, *et al*., 2010).

Although subsurface sediment compaction could not be estimated in the study area, it seems unlikely to be a significant process contributing to changes in marsh elevation, at least over the time scale investigated (Goodman *et al*., 2007). Considering that SLR apparently slows down the accretion rates in the Tagus salt marshes there is still a positive balance with SLR. This agrees well with other studies about sedimentation in mesotidal marshes (Wood *et al*., 1989), which normally exhibit an obvious relation between SLR and accretion rates, in opposition to macrotidal estuaries (Détriché *et al*., 2011).

In contrast, in macrotidal marshes there is not such an evident relationship (Goodman *et al*., 2007). The fact that most marshes do show a significant build-up of vertical accretion, that exceeds the MSL, is in part attributed to the spatial variation in SAR being influenced by the topography of the estuary itself and consequently influencing the frequency and duration of tidal flooding at each marsh

(French, 2006). Theoretically, it could be expected that as the marsh builds up due to vertical accretion this process would slow down, enabling a larger area of the upper marsh to achieve an elevation close to the equilibrium state between the rates of sedimentation and SLR. However, this cannot be observed over the small time scale considered here but might be if centennial or millennial scales were investigated (French and Burningham, 2003; French, 2006). Allen (1999) also suggests that another key factor influencing the present SAR is the auto-compaction of the Holocene coastal sequences. This will have an important impact in the marsh topographies, enhancing short-term sedimentations. Further insights about the history of the sediments and other phenomena underlying a temporal sequence of sedimentation rates, is the geochemical data concerning the sediment oxides composition. Cox and Lowe (1995) provided an index of chemical alteration (CAI) as a tool for evaluating the nature of sediment disturbance, physical or chemical. Our data further suggests that the major processes inherent to the variations of the sedimentation rates that change inversely to the MSL variation are of physical nature, like the erosion/deposition mechanisms. Using CAI values obtained from the sediment it is also possible to validate this hypothesis, which is more obvious for the SJT sites. All CAI values with a time scale associated that are available from this saltmarsh indicate physical disturbance of the sediment (CAI values falling between 40 and 70), whilst at the PAN sites only sediments from 2001 had values of CAI consistent with physical disturbance. In sediments that have been assigned to years from 1963 to 1986, the CAI values are slightly above 70, indicating some sort of chemical disturbance to the composition of the sediments. The most obvious modification to the composition of sediments was the comparatively high increase of Na_2O incorporated from 1986 to 2003, probably due to the higher flooding frequencies associated to higher MSL. This may be due to a mineral effect of these conditions or to the incorporation of larger amounts of Na coming from longer periods of inundation of the sediments with Na-rich sea water.

Both salt marshes show increases in Si/Al and Si/K and possibly these are related to an enhanced input of quartz, which in turn may be due to Aeolian inputs (Werne *et al*., 2002), but also to higher energy transport. Pancas sediments show signs of weathering, presenting lower values of Si/Al. Therefore, Si/Al ratios in

Pancas salt marsh seem related to chemical weathering rather than hydrodynamics (López, *et al*., 2006), as suggested also by the CAI values.

Ca/Mg ratios in both salt marshes increased with Ca/Al, suggesting that magnesium is mainly associated to the aluminosilicate fraction. The relative abundance of sedimentary calcium, expressed by the Ca/Al ratio, especially in the STJ salt marsh sediments, is clearly related to water mineralization, as expected from the high solubility of calcite (Tardy *et al*., 2004).

The clearest relationship of sedimentary phosphorus with other sedimentary elements appears between iron and phosphorus when concentrations are normalized relative to the aluminium content (i.e. when P/Al and Fe/Al ratios are used instead of rough concentrations). This relationship does not reflect dominance of any particular sedimentary phosphorus fraction. What it really reflects is that the increase of phosphate concentration over the background composition (which in turn may be dominated by calcium, iron or organic phosphorus) is linked with the increase in iron across the same background material. It is well known that autogenic iron oxi-hydroxides have a high capacity to adsorb phosphorus onto their surface (Likjlema, 1980; Lopez *et al*., 1996). Thus, precipitation and accumulation of autogenic iron-oxides causes a corresponding increase in P/Al and Fe/Al and seems to be the main process explaining the global variability observed in Spanish reservoirs (Lopez *et al.,* 1996). Nevertheless, the high variability in the P/Fe ratio observed in the eastern reservoirs also indicate that other processes must be accounted for in order to explain the variability of sedimentary phosphorus within calcareous areas.

Overlooking the potential risk of heavy metals settling associated to higher MSL seems to have the opposite behaviour. Although the fluctuations of MSL did show a small decrease from 1963 to 1986, followed by an increase until 2001, the pattern of contamination by heavy metals in the dated layers does not follow the same pattern. From 1963 until 2001 there is a clear decrease of the heavy metal content in the sediments. This may be associated to the recent history of industries in the area. In fact, the peak of waste dumping and heavy metal introduction in the estuary has occurred in 1970-1980 (Caçador *et al*., 2000), when the heavy industry dominated most of the southern parts of the estuary. Following the introduction of

strict environmental policies, a large number of industries were deactivated since that period and the remaining ones are now subjected to severe measures of contaminant control. This led to a decrease in the incorporation of heavy metals over recent years and is also consistent with values observed in the Pancas salt marsh, which are always lower than in the SJT salt marsh. Pancas is located in the upper eastern part of the estuary and within the Tagus Natural Reserve area, well away from the major centres of industry, while SJT is more subject to anthropogenic pressures due to its location closer to Lisbon and into an area that was highly industrialized until 1990.

The heavy metal contamination of the sediments apparently is not related to the sedimentation process. Although the lower values of sedimentation registered during the higher industrial activity decades, sediment contamination is not affected by the amount of sediment deposited in the marsh but by its contamination, pointing once again to the underlying industrial evolution of the Tagus estuary.

Conclusions

MSL in the Tagus estuary follows a trend already identified in other estuaries around the globe (Blum and Roberts, 2009; Rybczyk *et al*., 1998), with increasing sea heights and higher inundation frequencies. The SAR in the Tagus salt marshes has an inverse pattern of behaviour, showing a decrease in the amount of sediments deposited as the MSL increases. Along with this decrease in sediment supply, also the physical disturbances and chemical weathering are also affecting salt marsh elevation. Although the decreasing rate of marsh elevation, during the study period (1963-2001), there was still a positive feedback to MSL rise increase. It was also noted that heavy metal contamination in dated sediment layers is not related to sedimentary events or disturbance, but rather to changes in industrial inputs to the Tagus estuary. Considering an approximate rate of SLR similar to that observed in 1963 to 2001, we conclude from this study that the Tagus salt marshes (although with slower SAR) may still be able to adjust to SLR and therefore will contribute to protect the nearby shoreline from higher inundation.

References

Allen, J.R.L., 1990. Salt-marsh growth and stratification: a numerical model with special reference to the Severn Estuary, southwest Britain. *Marine Geology* 95, 77–96.

Allen, J.R.L., 1994. A continuity-based sedimentological model for temperate-zone tidal salt marshes. *Journal of the Geological Society* 151, 41–49.

Allen, J.R.L., 1995. Salt-marsh growth and fluctuating sea level: implications of a simulation model for Flandrian coastal stratigraphy and peat-based sea-level curves. *Sedimentary Geology* 100, 21–45.

Allen, J.R.L., 1997. Simulation models of salt-marsh morphodynamics: some implications for high-intertidal sediment couplets related to sea-level change. *Sedimentary Geology* 113, 211–223.

Allen, J.R.L., 1999. Geological impacts on coastal wetland landscapes: some general effects of sediment autocompaction in the Holocene of northwest Europe. *The Holocene* 9, 1–12.

Allen, J.R.L., 2000. Morphodynamics of Holocene salt marshes: a review sketch from the Atlantic and Southern North Sea coasts of Europe. *Quaternary Science Reviews* 19, 1155–1231.

Andersen, T.J., Mikkelsen, O.A., Møller, A.L. and Pejrup, M., 2000. Deposition and mixing depths on some European intertidal mudflats based on ^{210}Pb and ^{137}Cs activities. *Continental Shelf Research* 20, 1569-1591.

Andersen, T. J., Svinth, S. and Pejrup, M., 2011. Temporal variation of accumulation rates on a natural salt marsh in the 20th century – The impact of sea level rise and increased inundation frequency. *Marine Geology* 279, 1-4.

Berner, E.K. and Berner, R.A., 1996. Global Environment: *Water, Air and Geochemical Cycles*. Prentice-Hall, USA.

Blum, M. and Roberts, H., 2009. Drowning of the Mississippi Delta due to insufficient sediment supply and global sea-level rise. *Nature Geoscience* 2, 488-491.

Caçador, I., Costa, A. I. and Vale, C., 2007. Nitrogen sequestration capacity of two salt marshes from the Tagus estuary. *Hydrobiologia* 587, 137-145.

Caçador, I., Costa, A.I. and Vale, C., 2004. Carbon storage in Tagus saltmarsh sediments. *Water, Air and Soil Pollution*: *Focus* 4, 701–714.

Caçador, I., Vale, C. and Catarino, F., 2000. Seasonal variation of Zn, Pb, Cu and Cd concentrations in the root–sediment system of *Spartina maritima* and *Hallimione portulacoides* from Tagus estuary salt marshes. *Marine Environmental Research* 49, 279–290.

Callaway, J.C., DeLaune, R.D. and Patrick Jr., W.H., 1996. Chernobyl ^{137}Cs used to determine sediment accretion rates at selected northern European coastal wetlands. *Limnology and Oceanography* 4, 444-450.

Chmura, G.L., Costanza, R. and Kosters, E.C., 1992. Modelling coastal marsh stability in response to sea level rise: a case study in coastal Louisiana, USA. *Ecological Modelling* 64, 47–64.

Cox, R. and Lowe, D.R., 1995.A conceptual review of regional-scale controls on the composition of clastic sediment and the co-evolution of continental blocks and their sedimentary cover. *Journal of Sedimentary Research* 65, 1-12.

Day, J.W., Rybczyk, J., Scarton, F., Rismondo, A., Are, D. and Cecconi, G., 1999. Soil accretionary dynamics, sea-level rise and the survival of wetlands in Venice Lagoon: a field and modelling approach. *Estuarine, Coastal and Shelf Science* 49, 607–628.

Détriché, S., Susperregui, A-S., Feunteun, E., Lefeuvre, J-C. and Jigorel, A., 2011. Interannual (1999–2005) morphodynamic evolution of macro-tidal salt marshes in Mont-Saint-Michel Bay (France). *Continental Shelf Research* 31, 611-630.

Duarte, B., Caetano, M., Almeida, P.R., Vale, C. and Caçador, I., 2010. Accumulation and biological cycling of heavy metal in four salt marsh species, from Tagus estuary (Portugal). *Environment Pollution* 158, 1661-1668.

Dyer, F.M., Thomson, J., Croudace, I.W., Cox, R. and Wadsworth, R.A., 2002. Records of change in salt marshes: a radiochronological study of three Westerschelde (SW Netherlands) marshes. *Environmental Science and Technology* 36, 854–861.

French, J.R., 2006. Tidal marsh sedimentation and resilience to environmental change: Exploratory modelling of tidal, sea-level and sediment supply forcing in predominantly allochthonous systems. *Marine Geology* 235, 119-136.

French, J.R. and Burningham, H., 2003. Tidal marsh sedimentation versus sea-level rise: a southeast England estuarine perspective. In Davis, R.A. (Ed.) (2003) *Proceedings International Conference on Coastal Sediments 2003*. World Scientific Publishing and East Meets West Productions, Corpus Christi, 1-14.

French, J.R., 1993. Numerical-simulation of vertical marsh growth and adjustment to accelerated sea-level rise, North Norfolk, UK. *Earth Surface Processes and Landforms* 18 (1), 63–81.

Gates, D.M., 1993. *Climate Change and its Biological Consequences*. Sinauer Associates, Inc, USA.

Goodman, J. E., Wood, M. E. and Gehrels, W. R., 2007. A 17-yr record of sediment accretion in the salt marshes of Main (USA). *Marine Geology* 242, 109-121.

Gornitz, V., 1991. Global coastal hazards from future sea level rise. *Palaeogeography, Palaeoclimatology and Palaeoecology*, 89, 379-398.

Houghton, J., 1999. *Global Warming: The Complete Briefing*, Second edition. Cambridge University Press, UK, p. 251.

Intergovernmental Panel on Climate Change (IPCC), 1990. *Climate change*. In: Houghton, J.T., Jenkins G.J., Ephraumus J.J. (Eds.), The IPCC Assessment. Cambridge University Press, UK.

Intergovernmental Panel on Climate Change (IPCC), 1999. *Aviation and the global atmosphere*. A special report of working groups I and III of the Intergovernmental Panel on Climate Change. Summary for policymakers. IPCC, Switzerland.

Intergovernmental Panel on Climate Change (IPCC), 2007. *Climate Change 2007: The Physical Science Basis*. Contributions of Working Group I to the Fourth Assessment Report of the Intergovernmental Panel of Climate Change. Cambridge University Press, New York, NY, 996 pp.

Krone, R.B., 1987. A method for simulating historic marsh elevations. In: Krause, N.C. (Ed.), Coastal Sediments ’87. American Society of Civil Engineers, New York, pp. 316–323.

Lijklema, L., 1980. Interaction of orthophosphate with iron III and aluminium hydroxides. *Environmental Science and Technology*, 14, 537-541.

López, P., Llunch, X., Vidal, M. and Morguí, J. A., 1996. Adsorption of phosphorus on sediments of the Balearic Islands Spain related to their composition. *Estuarine, Coastal and Shelf Science*, 42, 185-196.

Lopez, P., Navarro, E., Marce, R., Ordoñez, J., Caputo, L. and Armendol, J., 2006. Elemental ratios in sediments as indicators of ecological processes in Spanish reservoirs. *Limnetica* 25, 499-512.

Martins, M., Ferreira, J., Calvao, T. and Figueiredo, H. 1984 Nutrientes no estuário do Tejo-comparação da situação em caudais médios e em cheia, com destaque para alterações na qualidade da água, Comunicação I. Simpósio Luso-Brasileiro de engenharia sanitária e ambiental.

Morris, J.T., Sundareshwar, P.V., Nietch, C.T., Kjerfve, B. and Cahoon, D.R., 2002. Responses of coastal wetlands to rising sea level. *Ecology* 83, 2869–2877.

Nyman, J.A., Carloss, M., DeLaune, R.D. and Patrick, W.H. Jr, 1994. Erosion rather than plant dieback as the mechanism of marsh loss in an estuarine marsh. *Earth Surface Processes and Landforms* 19, 69–84.

Nyman, J.A., DeLaune, R.D., Roberts, H.H. and Patrick, W.H. Jr, 1993. Relationship between vegetation and soil formation in a rapidly submerging coastal salt marsh. *Marine Ecology Progress Series* 96, 269–279.

Oenema, O. and DeLaune, R.D., 1988. Accretion rates in saltmarshes in the Eastern Scheldt, south-west Netherlands. *Estuarine, Coastal and Shelf Science* 26, 379–393.

Pont, D., Day, J.W., Hensel, P., Franquet, E., Torre, F., Rioual, P., Ibànez, C. and Coulet, E., 2002. Response scenarios for the deltaic plain of the Rhone in the face of an acceleration in the rate of sea-level rise with special attention to Salicornia-type environments. *Estuaries* 25, 337–358.

Reed, D.J., 1990. The impact of sea-level rise on coastal salt marshes. *Progress in Physical Organic Chemistry* 14, 465–481.

Ritchie, J.C. and McHenry J.R., 1990. Application of radioactive fallout ^{137}Cs for measuring soil erosion and sediment accumulation rates and patterns: A review. *Journal of Environmental Quality* 19, 215–233.

Roman, C.T., Peck, J.A., Allen, J.R., King, J.W. and Appleby, P.G., 1997. Accretion of a New England (U.S.A.) salt marsh in response to inlet migration, storms and sea-level rise. *Estuarine, Coastal and Shelf Science* 45, 717-727.

Rybczyk, J.M. and Cahoon, D.R., 2002. Estimating the potential for submergence for two wetlands in the Mississippi River Delta. *Estuaries* 25, 985–998.

Rybczyk, J.M., Callaway, J.C. and Day, J.W., 1998. A relative elevation model for a subsiding coastal forested wetland receiving wastewater effluent. *Ecological Modelling* 112, 23–44.

Salgueiro, N. and Caçador, I., 2007. Short-term sedimentation in Tagus estuary, Portugal: influence of salt marsh plants. *Hydrobiologia* 587, 187-193.

Sarreta, A., Pillon, S., Molinaroli, E., Guerzoni, S. and Fontolan, G., 2010. Sediment budget in the Lagoon of Venice, Italy. *Continental Shelf Research* 30, 934-949.

Silva, H., J. Dias and I. Caçador 2009. The role of salt marsh vegetation in sedimentation processes. *Hydrobiologia* 621, 33-47.

Simas, T., Nunes, J.P. and Ferreira, J.G., 2001. Effects of climate change on coastal salt marshes. *Ecological Modelling* 139, 1-15.

Stevenson, J.C., Ward, L.G. and Kearney, M.S., 1986. Vertical accretion in marshes with varying rates of sea-level rise. In: Wolfe, D.A. (Ed.), *Estuarine Variability*. Academic press, Orlando, pp. 241–259.

Tardy, Y., Bustillo, V. and Boeglin, J. L., 2004. Geochemistry applied to the watershed survey: hydrograph separation, erosion and soil dynamics: A case study: the basin of the Niger River, Africa. *Applied Geochemistry* 19, 469–518.

Temmerman, S., Govers, G., Meire, P. and Wartel, S., 2003. Modelling long-term tidal marsh growth under changing tidal conditions and suspended sediment concentrations, Scheldt estuary, Belgium. *Marine Geology* 193, 151– 169.

Thomson J., Dyer F.M., and Croudace I.W., 2002. Records of radionuclide deposition in two UK saltmarshes with contrasting redox and accumulation conditions. *Geochimica et Cosmochimica Acta* 66, 1011-1023

Titus, J.G. and Narayanan, V.K. 1995. The probability of Sea-level Rise. Environmental Protection Agency, USA.

Turekian, K.K. and Wedepohl, K.H., 1961. Distribution of the elements in some major units of the Earth's crust. *Geological Society of America Bulletin* 72, 175–191.

Van Dijkeman, K.S., Bossinade, J.H., Bouwema, P. and Glopper, R.J., 1990. Salt marshes in the Netherlands Wadden Sea: rising high-tide levels and accretion enhancement. In: *Expected Effects of Climatic Change on Marine Coastal Ecosystems*. Kluwer Academic Publishers, The Netherlands, pp. 173–188.

Van Wijnen, H.J. and Bakker, J.P., 2001. Long-term surface elevation change in salt marshes: a prediction of marsh response to future sea-level rise. *Estuarine, Coastal and Shelf Science* 52, 381–390.

Ward, L.G., Kearney, M.S. and Stevenson, J.C., 1998. Variations in sedimentary environment and accretionary patterns in estuarine marshes undergoing rapid submergence, Chesapeake Bay. *Marine Geology* 151, 111-134.

Werne, J. P., Sageman, B. B., Lyons, T. W. and Hollander, D. J., 2002. An integrated assessment of a ‘‘type euxinic’’ deposit: evidence from multiple controls on black shale deposition in the Middle Devonian Oatka Creek Formation. *American Journal of Science* 302, 110-143.

Wood, M.E., Kelley, J.T. and Belknap, D.F., 1989. Patterns of sedimentation in the tidal marshes of Maine. *Estuaries* 12, 237–246.

2.5. FINAL REMARKS ON THE SEA LEVEL RISE IMPACTS ON ESTUARINE SALT MARSHES

One particular aspect that acquired a great meaning in the last years is the vulnerability of the coastal areas to SLR, especially salt marshes. Gathering a multidisciplinary approach form geochemistry, to hydrodynamics and ecophysiology, a holistic point of view on this problematic could be attained. Although salt marshes maintain positive sedimentation rates having the mean SLR as comparison, this might not be true in the future do to the increased anthropogenic pressures in the estuarine systems. Additional studies (Valentim *et al*., 2013) showed that SLR scenario could lead to changes in nutrients and sediments patterns around the salt marshes and thus vegetation coverage percentage would be affected. Additionally, as a consequence of flood duration increase, sediment moisture will increase causing a stress condition to plants. Hence, the ratio below/aboveground biomass might increase, becoming critical to plants survival under conditions of accelerated SLR. Accordingly, both SLR and expected changes in vegetation coverage percentage in controlling salt marshes evolution have important implications in their stability and consequently in coastal management. This was lately confirmed by the finding presented in this chapter. Gathering a multidisciplinary approach form geochemistry, to hydrodynamics and ecophysiology a more holistic point of view on this problematic could be addressed. The pioneer *S. maritima* undergoes periods of stress when exposed to prolonged tidal submersion (Duarte *et al.*, 2014a). Thus this will have serious implications on its primary production, corroborating the hypothesis advanced by Valentim *et al*. (2013). This has serious implications not only on the ecosystems services provided on land by salt marsh halophytes but also for the entire estuarine system, as these are important areas with several functions for the whole ecosystem. Some examples of these functions are the contaminant remediative capacity of the salt marshes (Duarte *et al*., submitted) and its nutrient recycling role and food sources for secondary production (Duarte *et al*., 2014b). Due to the increasing stress conditions to which the halophytes are exposed under SLR, the senescence mechanisms will be more evident. Results from these studies point

out an increasing number of necromass particles exported to the oceanic waters adjacent to the estuarine areas, as a combined result of the increased senescence and altered hydrodynamical features. If by one side, this will increase the fuelling of the secondary production of the coastal shelf by supplying higher amounts of particulate organic C and N (Duarte *et al*., 2014b), on the other hand will also contribute to an increasing contamination of these oceanic waters, due to a higher number of contaminated detritus that will not be retained within the estuarine remediative area. (Duarte *et al*., submitted).

Thus becomes important to address SLR from a multidisciplinary approach, as these processes impacts on the halophyte vegetation will condition the whole system at several and different levels. Being trapped between the sea and the urbanized lands, this data points out to a reduction of the salt marshes foundations (by reduction of its pioneer species) with enormous impacts on the coastal erosion, possible eutrophication events and reduced remediative capacity of the ecosystem, making it prone to a possible collapse.

References

Valentim, J.M., Vaz, N., Silva, H., Duarte, B., Caçador, I. and Dias, J.M., 2013. Tagus Estuary and Ria de Aveiro Salt Marsh Dynamics and the Impact of Sea Level Rise. *Estuarine, Coastal and Shelf Science* 130, 138-151.

Duarte, B., Santos, D., Marques, J.C. and Caçador, I., 2014. Biophysical probing of *Spartina maritima* Photo-system II changes during increased submersion periods: possible adaptation to sea level rise. *Plant Physiology ad Biochemistry* 77, 122-132.

Duarte, B., Valentim, J.M., Dias, J.M., Silva, H., Marques, J.C. and Caçador, I., 2014b. Modelling Sea Level Rise (SLR) impacts on salt marsh detrital outwelling C and N exports from an estuarine coastal lagoon to the ocean (Ria de Aveiro, Portugal). *Ecological Modelling* 289, 36-44.

Duarte, B., Vaz, N., Valentim, J.M., Dias, J.M., Silva, H., Marques, J.C. and Caçador, I. (submitted). Revisiting the Outwelling Hypothesis: Modelling Salt Marsh Detrital Metal Exports under Extreme Climatic Events. *Marine Chemistry*.

CHAPTER III

EFFECTS OF CO_2 RISING ON SALT MARSH ECOPHYSIOLOGY AND BIOGEOCHEMISTRY

CHAPTER III

3.1. EFFECTS OF CO_2 RISING ON SALT MARSH ECOPHYSIOLOGY AND BIOGEOCHEMISTRY

Atmospheric CO_2 represents the main atmospheric phase of the global carbon cycle. The global carbon is composed by a serie of reservoirs of carbon, connected by exchange fluxes of carbon. Two domains in the global carbon cycle can be distinguished. The first is a fast domain with large exchange fluxes and relatively 'rapid' reservoir turnovers, which consists of carbon in the atmosphere, the ocean, sediments and on land in vegetation, soils and freshwaters. A second, slow domain consists of the huge carbon stores in rocks and sediments which exchange carbon with the fast domain through volcanic emissions, chemical weathering, erosion and sediment formation on the sea floor (Sundquist, 1986). Natural exchange fluxes between both domains are relatively small (< 0.3 Pg C yr^{-1}) (Raymond and Cole, 2003). The terrestrial biosphere reservoir contains carbon in organic compounds in vegetation living biomass (450 to 650 Pg C; Prentice *et al*., 2001) and in dead organic matter in litter and soils (1500 to 2400 Pg C; Batjes, 1996). There is an additional amount of old soil carbon in wetland soils (300 to 700 Pg C; Bridgham *et al*., 2006) and in permafrost soils (~1700 Pg C; Tarnocai *et al*., 2009). CO_2 is mainly removed from the atmosphere by plant photosynthesis (Gross Primary Production (GPP), 123±8 Pg C yr^{-1}, (Beer *et al*., 2010)) being lately released back into the atmosphere by autotrophic (plant) and heterotrophic (soil microbial and animal) respiration and additional disturbance processes (e.g., sporadic fires). Atmospheric CO_2 is exchanged with the surface ocean through gas exchange, driven by the partial CO_2 pressure difference between the air and the sea. In the ocean, carbon is available predominantly as Dissolved Inorganic Carbon (DIC, ~38,000 Pg C), in the form of carbonic acid, bicarbonate and carbonate ions. In addition, the ocean contains a pool of Dissolved Organic Carbon (DOC, ~700 PgC) (Hansell *et al*., 2009). The change in oceanic carbonate chemistry could explain the slow atmospheric CO_2 increase during the Holocene. Two theories support these processes: (1) a shift of oceanic carbonate

sedimentation from deep sea to the shallow waters due to SLR onto continental shelves causing accumulation of $CaCO_3$ on shelves including coral reef growth, a process that releases CO_2 to the atmosphere (Ridgwell *et al*., 2003; Kleinen *et al*., 2010), (2) a 'carbonate compensation' in response to the release of carbon from the deep ocean during deglaciation and to the build-up of terrestrial biosphere in the early Holocene (Broecker *et al*., 1999; Joos *et al*., 2004; Elsig *et al*., 2009; Menviel and Joos, 2012). Several studies (Hemminga and Duarte, 2000; Wu *et al*., 2008; McKee *et al*., 2012) point out that ocean acidification will enhance the production of seagrass, macroalgae, salt marsh plants, and mangrove trees through the fertilization effect of CO_2. Increased CO_2 concentrations are already pointed out as the main reason for the increased seagrass photosynthetic rates by 20 % (Hemminga and Duarte, 2000; Hendriks *et al*., 2010). Although elevated CO_2 and ocean acidification are expected to increase productivity of vegetated coastal habitats in the future, this will come accompanied by a simultaneous warming effect. In which concerns seagrasses, there is limited evidence that elevated CO_2 will increase the survival or resistance to this warming effect (Alexandre *et al*., 2012; Jordá *et al*., 2012). Coastal wetlands and seagrass meadows experience coastal squeeze in urbanized coastlines, without any chance to migrate inland with rising sea levels. However, increased CO_2 and warming can stimulate marsh elevation gain, counterbalancing moderate increases in SLR rates (Langley *et al*., 2009; Kirwan and Mudd, 2012). Climate change tends to increase carbon burial rates on salt marshes during the first half of the 21st century, provided sufficient sediment supply, with carbon-climate feedbacks diminishing over time (Kirwan and Mudd, 2012). The increase of atmospheric CO_2 levels are expected to reduce the efflux of CO_2 from estuaries (Borges, 2005; Chen and Borges, 2009).

With such a complex network of interactions driven from CO_2 increase there is a great need to understand how the different salt marsh compartments will cope with this change. Salt marshes are colonized by different plants mostly with C_3 and C_4 mechanisms and different photosynthetic rates. It is expected that CO_2 will not affect all species in the same way. Similarly increased dissolved CO_2 will also affect plants in different extents. Alongside sediment biogeochemistry will also be directly affected by increased atmospheric CO_2 with implications on its biogeochemical

services. Considering this, the present chapter intents to make physiological and biogeochemical approach of the effects of CO_2 rising on Mediterranean marshes, focusing the primary productivity of the main colonizing species and the organic matter biogeochemical cycling processes, from the ecosystem point of view.

References

Alexandre, A., Silva, J., Buapet, P., Bjšrk, M. and Santos, R., 2012. Effects of CO_2 enrichment on photosynthesis, growth, and nitrogen metabolism of the seagrass *Zostera noltii*. *Ecology and Evolution* 2, 2625-2635.

Batjes, N.H., 1996. Total carbon and nitrogen in the soils of the world. *European Journal of Soil Science* 47, 151–163.

Beer, C., *et al*., 2010. Terrestrial gross carbon dioxide uptake: Global distribution and covariation with climate. *Science* 329, 834-838.

Bridgham, S.D., Megonigal, J.P., Keller, J.K., Bliss, N.B. and Trettin, C., 2006. The carbon balance of North American wetlands. *Wetlands* 26, 889–916.

Broecker, W.S., Clark, E., McCorkle, D.C., Peng, T.-H., Hajdas, I. and Bonani, G., 1999. Evidence for a reduction in the carbonate ion content of the deep sea during the course of the Holocene. *Paleoceanography* 14, 744–752.

Elsig, J., *et al*., 2009. Stable isotope constraints on Holocene carbon cycle changes from an Antarctic ice core. *Nature* 461, 507–510.

Hansell, D.A., Carlson, C.A., Repeta, D.J. and Schlitzer, R., 2009. Dissolved organic matter in the ocean: A controversy stimulates new insights. *Oceanography* 22, 202–211.

Hemminga, M.A., and Duarte, C.M., 2000. Seagrass Ecology. Cambridge Univ. Press, Cambridge.

Hendriks, I.E., Duarte, C.M. and Álvarez, M., 2010. Vulnerability of marine biodiversity to ocean acidification: a meta-analysis. *Estuarine, Coastal and Shelf Estuarine Science* 86, 157–164.

Joos, F., Gerber, S., Prentice, I.C., Otto-Bliesner, B.L. and Valdes, P.J., 2004. Transient simulations of Holocene atmospheric carbon dioxide and terrestrial carbon since the Last Glacial Maximum. *Global Biogeochemical Cycles* 18, Gb2002.

Jordà, G., Marbà, N. and Duarte, C.M., 2012. Mediterranean seagrass vulnerable to regional climate warming. Nature Climate Change 2, 821-824.

Kleinen, T., Brovkin, V., von Bloh, W., Archer, D. and Munhoven, G., 2010. Holocene carbon cycle dynamics. *Geophysical Research Letters* 37, L02705.

Langley, J.A., McKee, K.L., Cahoon, D.R., Cherry, J.A. and Megonigal, J.P., 2009. Elevated CO_2 stimulates marsh elevation gain, counterbalancing sea-level rise. *Proceedings of the National Academy of Sciences of the United States of America*, 106(15), 6182-6186.

McKee, K., K. Rogers, and N. Saintilan, 2012: Response of salt marsh and mangrove wetlands to changes in atmospheric CO_2, climate, and sea level. In: [Middleton, B.A. (ed.)]. Springer, pp. 63-96.

Menviel, L., and Joos, F., 2012. Toward explaining the Holocene carbon dioxide and carbon isotope records: Results from transient ocean carbon cycle-climate simulations. *Paleoceanography* 27, PA1207.

Prentice, I.C., *et al*., 2001. The carbon cycle and atmospheric carbon dioxide. In: Climate Change 2001: The Scientific Basis. Contribution of Working Group I to the Third Assessment Report of the Intergovernmental Panel on Climate Change [J. T. Houghton, Y. Ding, D. J. Griggs, M. Noquer, P. J. van der Linden, X. Dai, K. Maskell and C. A. Johnson (eds.)]. Cambridge University Press, Cambridge, United Kingdom and New York, NY, USA, pp. 183–237.

Raymond, P.A., and Cole, J.J., 2003. Increase in the export of alkalinity from North America's largest river. *Science* 301, 88–91.

Ridgwell, A.J., Watson, A.J., Maslin, M.A. and Kaplan, J.O., 2003. Implications of coral reef buildup for the controls on atmospheric CO_2 since the Last Glacial Maximum. *Paleoceanography* 18, 1083.

Sundquist, E.T., 1986. Geologic analogs: Their value and limitations in carbon dioxide research. In: *The Changing Carbon Cycle*. J. R. Trabalka and D. E. Reichle (eds.), Springer-Verlag, New York, pp. 371–402.

Tarnocai, C., Canadell, J.G., Schuur, E.A., Kuhry, P., Mazhitova, G. and Zimov, S., 2009. Soil organic carbon pools in the northern circumpolar permafrost region. *Global Biogeochemical Cycles* 23, Gb2023.

Wu, H.Y., Zou, D.H. and Gao, K.S., 2008. Impacts of increased atmospheric CO_2 concentration on photosynthesis and growth of micro- and macro-algae. *Science in China Series C: Life Sciences* 51, 1144-1150.

3.2. PHOTOCHEMICAL AND BIOPHYSICAL FEEDBACKS OF C_3 AND C_4 MEDITERRANEAN HALOPHYTES TO ATMOSPHERIC CO_2 ENRICHMENT CONFRIMED BY THEIR STABLE ISOTOPE SIGNATURES [1]

Abstract

According the latest predictions, an increase of about two times in atmospheric CO_2 concentrations is expected to occur by the end of this century. In order to understand the effects of this atmospheric composition changes on two abundant Mediterranean halophytes (*H. portulacoides* and *S. maritima*), mesocosmos trials were performed simulating two atmospheric CO_2 environments (380 ppm and 760 ppm of CO_2 respectively). The two chosen halophyte species present different metabolic characteristics: *H. portulacoides*, is a C_3 specie while *S. maritima* is a C_4 species. Distinct feedbacks were obtained for each of the studied species. Stable Isotope discrimination showed that both species showed an enhancement of the Rubisco carboxylation capacity and photosynthetic efficiency mostly due to an increase in intracellular [CO_2]. In *H. portulacoides* CO_2 fertilization induced an enhancement of ETR and a decrease in non-photochemical quenching and in dissipated energy fluxes. On the other hand, the C_4 grass *S. maritima*, already at full capacity, showed no photosynthetic enhancement. In fact, this highly productive grass presented lower photosynthetic efficiencies accompanied by increases in dissipated energy fluxes mostly due to reductions in energy flux associated with the transport of reducing power throughout the quinone pool. The accumulation of reducing power led to oxidative stress, and thus the photosynthetic ability of this grass was greatly reduced. Both these feedbacks to realistic future CO_2 concentrations are important consideration for in future primary productivity models, indicating a possible reduced abundance of pioneer *S. maritima* and an

[1] This section was published in: **Duarte, B.**, Santos, D., Silva, H., Marques, J.C. and Caçador, I., 2014. Photochemical and Biophysical feedbacks of C_3 and C_4 Mediterranean halophytes to atmospheric CO_2 enrichment confirmed by their stable isotope signatures. Plant *Physiology and Biochemistry* 80, 10-22.

increased abundance of the sediment stabilizer *H. portulacoides*, inevitably affecting the morphology and function of the salt marshes imposed by these atmospheric changes, both in terms of ecosystem functioning and loss of biodiversity.

Introduction

According to the latest predictions, atmospheric CO_2 concentrations are expected to double from 380 to 760 ppm until the end of this century (IPCC, 2007). The increasing atmospheric CO_2 is expected to have a number of effects (global warming, SLR, ocean acidification, etc.) on the biosphere (Lenssen *et al*., 1995). Such a significant change in one of the major resources for plant growth will have significant implications on its own (Ziska, 2008). In addition, the increasing concentrations of atmospheric CO_2, has also the inevitable greenhouse side effect, leading to an increase of the global temperature (Houghton, 2001) and thus resulting into severe climatic changes such as more frequent and drastic drought events (Mpelasoka *et al*., 2008). This way, plant growth and metabolism will be profoundly affected by such changes, putting not only the plant biodiversity at risk, but also the global primary production (Tausz-Posch *et al*., 2013). Salt marshes and its halophytic species are not aside from these implications. These ecosystems are among the planet most productive ones, retaining about 1/2 to 1/3 of the fixed carbon and providing important ecosystem services to the estuarine system, namely nutrient regeneration, primary production, habitat for wildlife and as shoreline stabilizers (Caçador *et al.*, 2009). Their known high productivity have been attributed to the large abundance of several halophytic species. Salt marshes plant species occupy specific habitats in a well-defined distribution, resultant from inter-specific relationships between the halophytes and competition for specific and optimal habitats (Mendelssohn and Morris, 2000). The exposure of these species to several abiotic (for e.g. climate driven) and anthropogenic (for e.g. pollution) constrains have an evident modelling role, shaping the species expansion, growth and productivity. The knowledge on plant stress responses and adaptations, namely at molecular, cellular, physiological and biochemical levels, becomes this way a top priority to understand the impact of these constrains on the future plant biodiversity (Urano *et al*., 2010; Yamaguchi-Shinozaki and Shinozaki, 2006). Plant biodiversity outcomes in

a diversity of photosynthetic mechanisms, one of the primary targets affected by CO_2 rising (Lenssen *et al*., 1995; Rozema *et al*., 1991; Geissler *et al*., 2009). Gaastra (1959) reported that, for e.g., C_3-plants have a stronger response to CO_2 fertilization than C_4-species. Elevated atmospheric CO_2 concentration steepens the diffusion gradient needed for photosynthetic uptake and can therefore stimulate growth and the development of several species (Ghannoum *et al*., 2000). Increased [CO_2] enhances the photosynthetic efficiency, due to reduction of carbon limitation, thereby increasing the supply of photo-assimilates and biomass (Hao *et al*., 2013). On the other hand, higher [CO_2] increases the carboxylation reaction of Rubisco, but will simultaneously decrease the oxygenation reaction. Although this would be the generalized behaviour among the plant kingdom, C_4 plants with its highly efficient CO_2 concentration mechanism keeping Rubisco near CO_2 saturation, are expected to benefit less from this CO_2 increase (Cousins *et al*., 2002). Changes in carbon assimilation require the maintenance of the balance between absorbed light, heat dissipation and photochemistry (Pammenter *et al*., 1993; Drake *et al*., 1997). Over-excitation of the photosynthetic apparatus tends to produce oxidative stress and thus reduce the primary production process (Horton, 2000). Being one of most important primary producers in estuarine ecosystems (Duarte *et al*., 2012a), it is also important to consider the effects of [CO_2] increase in carbon allocation patterns (Guy *et al*., 1986). These impacts on carbon assimilation and allocation inevitably affect $\delta^{13}C$ stable isotope of C_3 and C_4 species. Nevertheless, these signatures are influenced by the surrounding environmental conditions especially atmospheric [CO_2], since stable isotopes are a reflection of the source and fixation of carbon in the plant (Guy *et al*., 1986). This way, C_4 plants normally present less negative values of $\delta^{13}C$ while compared to C_3 plants (Guy *et al*., 1980).

Halimione portulacoides (L.) Allen occupies approximately 24% of all Portuguese salt marshes in both estuaries and coastal lagoons, being one of the most abundant halophytes in the Mediterranean salt marshes (Caçador *et al*., 2013). On the other hand, *Spartina maritima* (Curt.) occupies only approximately 12% of the salt marshes in the Portuguese transitional systems (Caçador *et al*., 2013), presenting a key role as pioneer species, intervening in shoreline stabilization and salt marsh accretion (Duarte *et al*., 2009). Alongside these different ecological

aspects, these two species exhibit different photosynthetic pathways, with *H. portulacoides* presenting C_3 type photosynthesis and *S. maritima* presenting the typical fast-growing C_4 mechanism characteristic of highly productive grasses (Duarte *et al*., 2012b; Duarte *et al*., 2013a).

Recently several papers have focused on the impacts of CO_2 on halophyte photosynthesis and carbon allocation, although most of them mainly directed their attention to the photosynthetic gas exchanges in CO_2 environments (Mateos-Naranjo *et al*., 2010; Geissler *et al*., 2010 and 2009; Farnsworth *et al*., 1996; Ball and Munns, 1992). In the present work, the effects of CO_2 enrichment on these two halophytes are addressed, focusing mainly their photochemical systems and their light harvesting mechanisms under normal (380 ppm) and increased CO_2 (760 ppm) levels as predicted for 2100 by the IPCC. This study is complemented with the analysis of the plants elemental and stable isotope composition as proxy of their carbon incorporation and intercellular carbon concentration. This will provide new insights on the influence of this ongoing climate change driver on both species and on their role as ecosystem service providers in an estuarine context.

Material and Methods

Study area, sampling and mesocosmos setup

Sampling took place at Tagus estuary Rosário salt marshes. Rosário (38°40' N, 9°01' W) is a mature salt marsh (Valiela *et al*. 2000) located in the southern part of the Tagus estuary, in the vicinity of various urbanized and industrialized zones. The upper marsh is mainly colonized by *H. portulacoides* (Chenopodiaceae) and undergoes short submersion episodes during high tide. *Spartina maritima* (Curt.) Fernald is an herbaceous perennial plant (Poaceae) that colonizes estuarine intertidal mudflats widely distributed throughout the coasts of western, southern, and southeastern Europe, as well as in western Africa. From the 17.24 km^2 of salt marshes existent in Tagus estuary, about 2.41 km^2 are colonized by *S. maritima* and 5.32 km^2 by *H. portulacoides* (Caçador *et al*., 2013).

Ten sediment cores were collected in *S. maritima* pure stands (each core containing one *S. maritima* shoot; the inter-core plant biomass was as similar as possible) using a Plexiglas core (Ø = 8 cm; 30 cm height). Each sediment core was 15

cm in depth. The *in situ* air temperatures and PAR were recorded, and all samples were taken to the laboratory within 1h. At the laboratory the cores were sealed with a Plexiglas lid with a rubber stopper to prevent gas-exchange and placed in a Fytoscope 130 RGBIR (Photon System Instruments, Czech Republic). For *H. portulacoides* grafts were propagated in the greenhouse in sediment from the salt marsh during 2 months in order to be fully developed and adapted. After this period, they were also inserted in Plexiglas cores as described above. For both species each core contained only one individual. The chamber was programmed to replicate the average field air temperatures (25 ± 2 °C), relative humidity (50 ± 2 %) and the PAR evolution along the day (16 h light/8h dark sine function with a maximum PAR of 500 μmol photons m^{-2} s^{-1}), considering the light attenuation inside the core. The experiment had the duration of 30 days to allow new biomass development. The cores subjected to the CO_2 increase were connected to the chamber throughout specially designed connectors on their lid (Figure 3.2.1). A CO_2 gas bottle was connected to a gas-mixing unit (Waltz, Germany) mixing pure CO_2 (Linde, Hollriegelskreuth, Germany) into CO_2–free atmospheric air (passed over soda lime) at the desired concentrations and flow rates. This allowed maintaining the reaming atmospheric characteristics intact while manipulating only the CO_2 concentration. An IrGA (Li-COR) was connected at the outlet of the gas-mixing unit preforming continuous measures of CO_2 and relative humidity of the air injected inside the cores. Relative humidity values recorded inside the chamber during the whole experiment were setup to 50 ± 2%. Five cores were connected to the chamber inlet, receiving CO_2, while other five were maintained in the same condition but with a normal atmosphere. At the end of 30 days plants were harvested and for all analyses 5 individuals were sampled (one leave each) from each treatment.

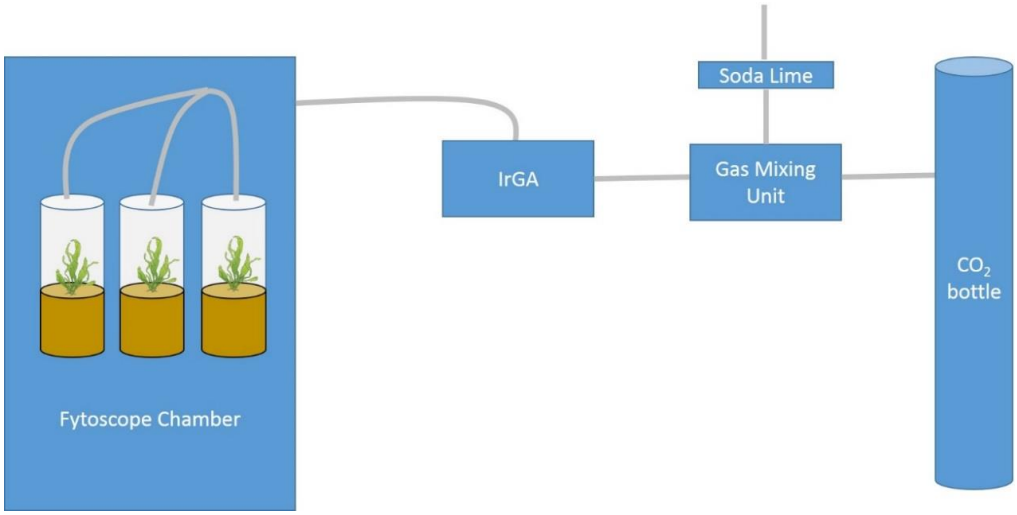

Figure 3.2.1. Experimental setup design for the CO_2 manipulation experiments.

Stable Isotope Analysis

The carbon isotopic composition of the pulverized dry leaf samples was determined using a Flash EA 1112 Series elemental analyser coupled on line via Finningan conflo III interface to a Thermo delta V S mass spectrometer. The carbon isotope ratio are expressed in delta (δ) notation, defined as the parts per thousand (‰) deviation from a standard material (PDB limestone) throughout the formula: $\delta^{13}C$ or $\delta^{15}N = [(R_{sample}/R_{standard})-1] \times 10^3$, where R is $^{13}C/^{12}C$. The analytical precision for the measurement was 0.2‰. Carbon and nitrogen contents (%) were determined simultaneously using the same procedure. From the stable isotope discrimination, intracellular [CO_2] was determined using the Farquhar *et al*. (1989) model:

$$\delta^{13}C_{plant} = \delta^{13}C_{atm} - a - (b - a)\,(C_i / C_{atm})$$

where $\delta^{13}C_{plant}$ is the plant $\delta^{13}C$ value, $\delta^{13}C_{atm}$ is the atmosphere $\delta^{13}C$ value (normally -7.8 ‰ for normal air and -53.2 ‰ for CO_2 enriched air, relatively to PDB), “a” is the discrimination associated with diffusion (+4.4 ‰), “b” is the discrimination at carboxylation by Rubisco (+27 ‰), C_i is the intracellular [CO_2] and C_{atm} is the atmospheric [CO_2]. Although this model was developed for C_3 plants, it can also be applied to C_4 plants, if optimal temperatures are ensured and thus there is no CO_2 leakage from the leaves derived from temperature (Caemmerer, 2013).

Gauss Peak Spectra Pigment Analysis

Leaves for pigment analysis were freeze-dried in the dark during 48 h, after which they were grinded in pure acetone with a glass rod. To ensure complete disaggregation of the leaf material, samples with acetone were subjected to a cold ultra-sound bath during 2 min. Extraction occurred at – 20 °C during 24 h in the dark to prevent pigment degradation. After extraction samples were centrifuged at 1 780 x g during 15 min at 4 °C. For pigment analysis it was employed the Gauss-Peak Spectra (GPS) method (Kupper *et al*., 2007). Samples were scanned in a dual beam spectrophotometer from 350 nm to 750 nm at 0.5 nm steps. The absorbance spectrum was introduced in the GPS fitting library, using SigmaPlot Software, allowing the determination of all the target pigments.

In order to better evaluate the light harvesting and photo-protection mechanisms the De-Epoxidation State (DES) was calculated as:

$$DES = \frac{[\text{Antheraxanthin}] + [\text{Zeaxanthin}]}{[\text{Violaxanthin}] + [\text{Antheraxanthin}] + [\text{Zeaxanthin}]}$$

PAM fluorometry

Fluorometric analysis were preformed according to the described in Chapter II, Section 3 as described in Duarte *et al*. (2014). All derived variables were computed as described in Table 2.3.1.

Anti-oxidant enzyme assays

All enzymatic analyses were performed by UV-Vis spectrophotometry using specific substrates as described in Chapter II, Section 3 (Duarte *et al*., 2014).

Statistical Analysis

Due to the lack of normality and homogeneity, the statistical analysis of the data was based in non-parametric tests. In order to compare the effects of the two tested CO_2 concentrations, the Krustal-Wallis test was performed using Statistica Software (Statasoft).

Results

Elemental Analysis and $\delta^{13}C$ Stable Isotope

Tissue C and N composition in both species (Figure 3.2.2) showed that independently of their CO_2 environment, *S. maritima* had higher C and N contents than *H. portulacoides*. If the CO_2 treatments are considered, an asymmetric response arise. While *H. portulacoides* increased its C and N contents with increasing atmospheric CO_2 levels, in *S. maritima*, only small differences could be detected, especially concerning its C content. Evaluating the tissue stable isotope composition these differences become more evident (Figure 2). The C_3 *H. portulacoides* increased significantly $\delta^{13}C$ signature ($p < 0.05$) under 760 ppm of CO_2, while the C_4 *S. maritima* maintained its isotopic signature almost unaffected ($p > 0.05$).

Applying the Farquhar *et al*. (1989) model it was possible to assess the intracellular [CO_2] concentration (Table 3.2.2). Both species diffusion ratio was significantly different among CO_2 treatments, concomitant with the simultaneous and significant increase in the intracellular [CO_2] concentration at increased levels of atmospheric CO_2.

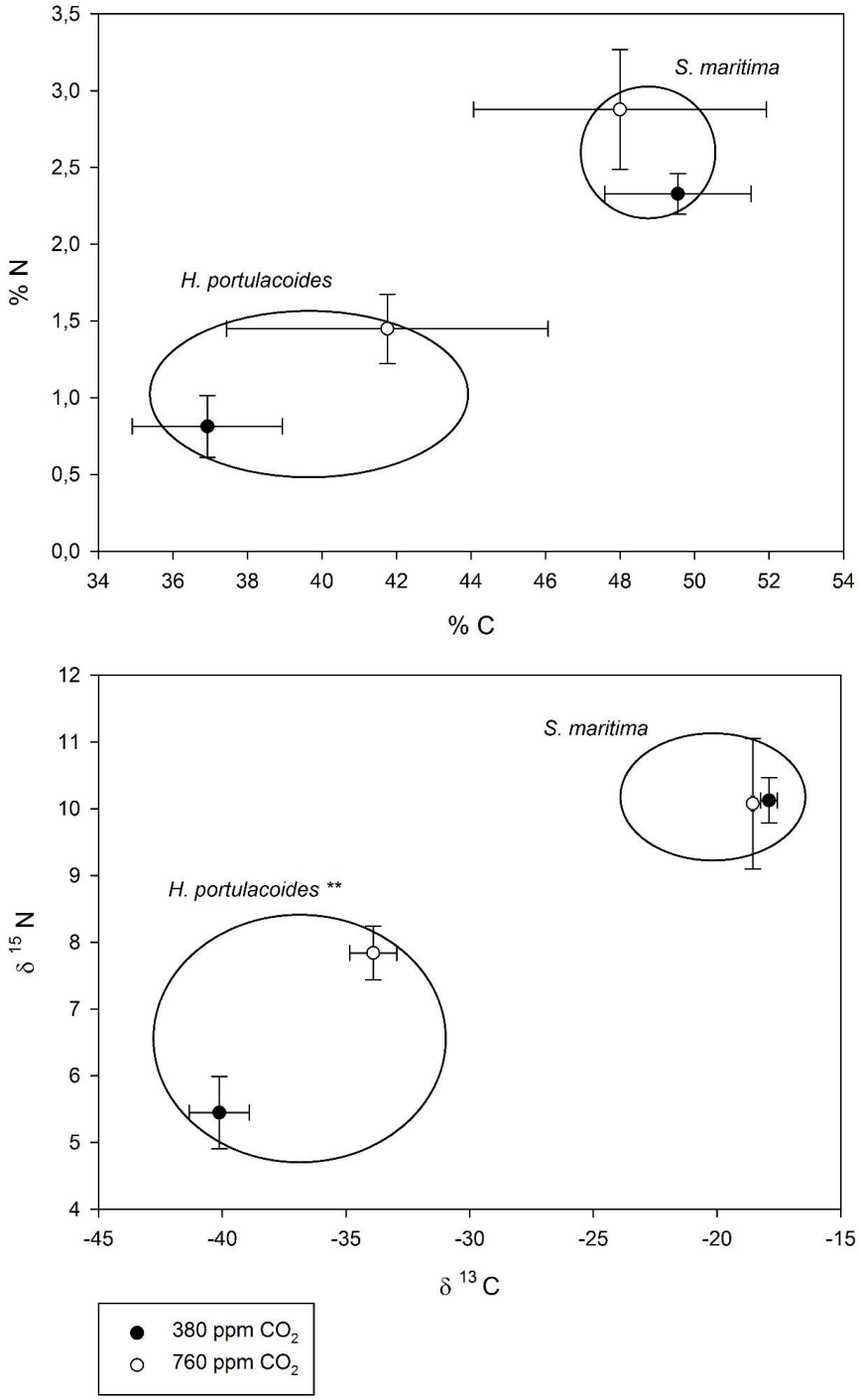

Figure 3.2.2. Carbon and nitrogen concentrations (w/w) and stable carbon isotope signature in *H. portulacoides* and *S. maritima* individuals at both CO_2 tested concentrations (average ± standard deviation, n = 5; * $p < 0.05$, ** $p < 0.01$).

Table 3.2.2. Diffusion ratio (C_i/C_{atm}) ratio and C_i of both *H. portulacoides* and *S. maritima* exposed to 380 and 760 ppm of CO_2 (average ± standard deviation; [a] $p < 0.01$, [b] $p < 0.05$).

	H. portulacoides		***S. maritima***	
	380 ppm	**760 ppm**	**380 ppm**	**760 ppm**
C_i/C_{atm}	1.15 ± 0.19 [a]	0.64 ± 0.19 [a]	0.51 ± 0.01 [b]	0.35 ± 0.04 [b]
C_i (ppm)	366.23 ± 11.55 [a]	548.14 ± 11.76 [a]	195.46 ± 3.62 [a]	265.10 ± 31.27 [a]

PAM fluorometry

Regarding light adapted leaves variable fluorescence (F'_v) and operational PS II quantum yield (Figure 3.2.3) no differences among individuals subjected to a normal and to a CO_2 enriched atmosphere could be detected. On the other hand, variable fluorescence on dark-adapted state showed a smaller increase in both species individuals exposed to 760 ppm CO_2. Overlooking the maximum PS II quantum yield, while in *H. portulacoides* there was a small increase at high CO_2 levels, in *S. maritima* both treatment groups presented very similar values. Considering the non-photochemical quenching energy dissipation mechanism, a very significant decrease in the *H. portulacoides* individuals subjected to 760 ppm of CO_2 was observed. As for *S. maritima,* a small but significant increase of the non-photochemical quenching values could be detected.

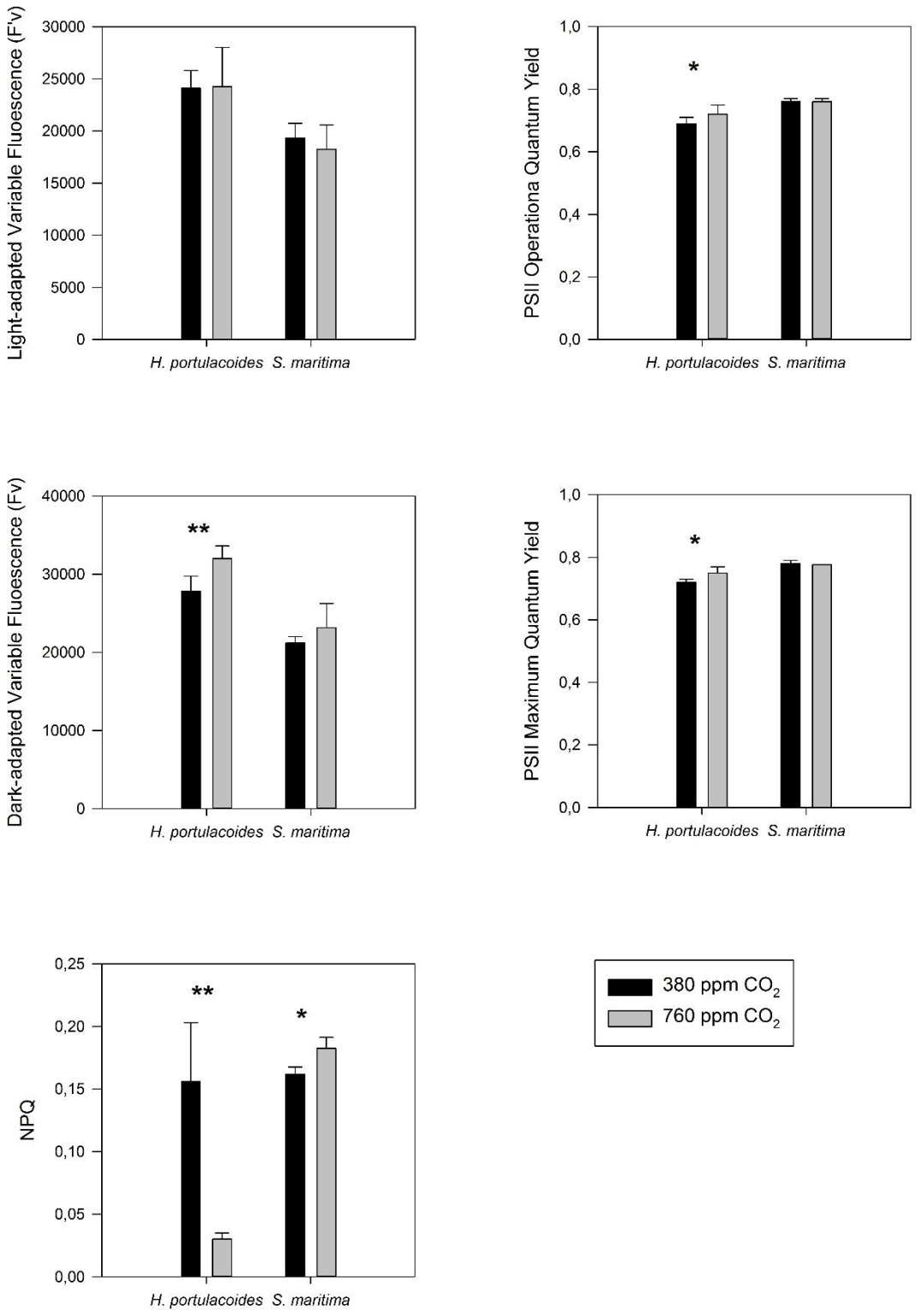

Figure 3.2.3. Operational and maximum variable fluorescence and PS II quantum efficiency and non-photochemical quenching in *H. portulacoides* and *S. maritima* individuals at both CO_2 tested concentrations (average ± standard deviation, n = 5; * $p < 0.05$, ** $p < 0.01$).

Considering the rapid light curves of both species subjected to 380 and 760 ppm of CO_2, differences among species and treatments become more visible (Figure 3.2.4). Under high (above 50 μmol photons m^{-2} s^{-1}) light intensities, *H. portulacoides* individuals exposed to 760 ppm of CO_2, showed higher rETR, even under photoinibitory light intensities (above 200 μmol photons m^{-2} s^{-1}).

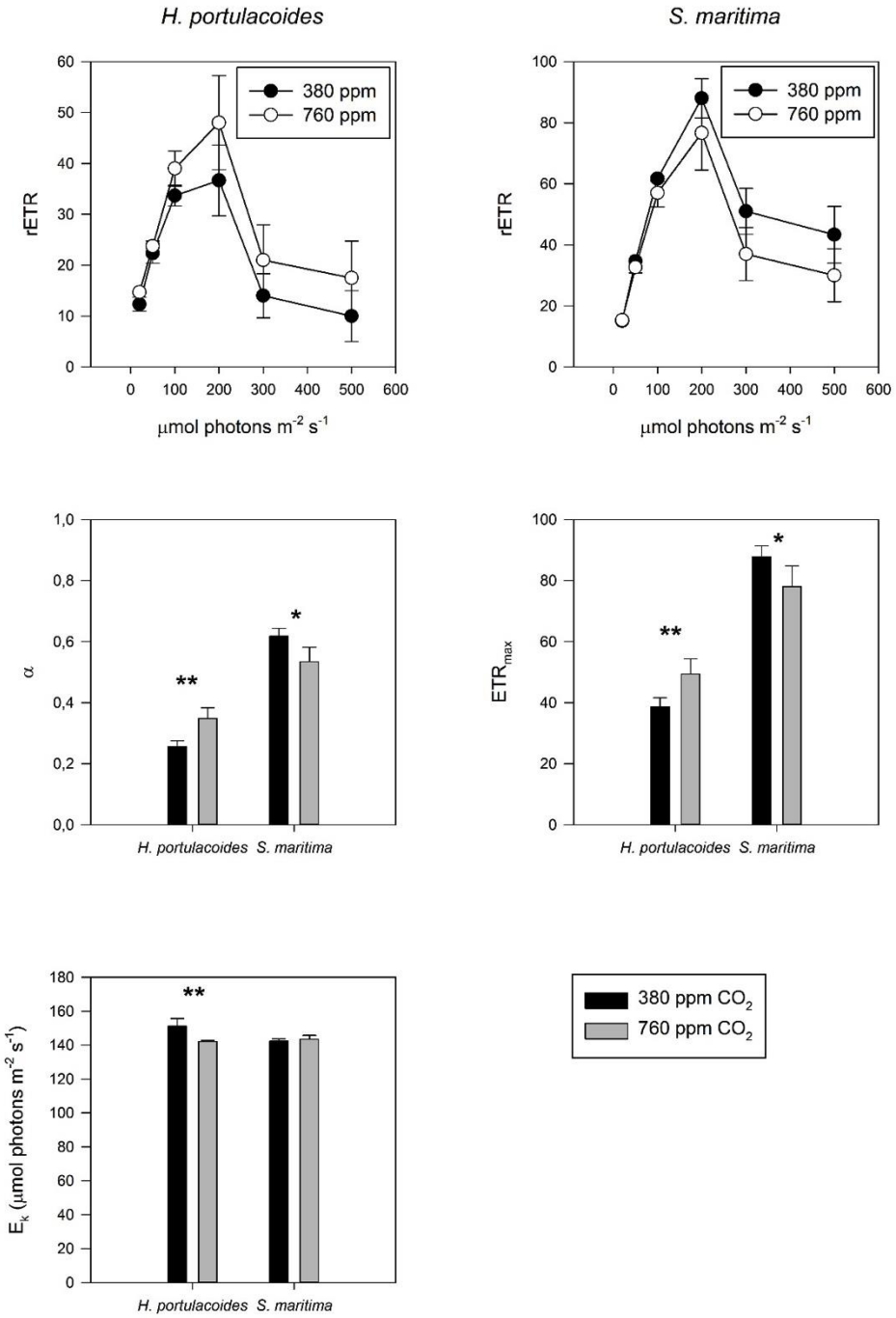

Figure 3.2.4. Rapid light curves, photosynthetic efficiency, maximum ETR and onset of light saturation in *H. portulacoides* and *S. maritima* individuals at both CO_2 tested concentrations (average ± standard deviation, n = 5; * $p < 0.05$, ** $p < 0.01$).

Consequently, these individuals showed a higher maximum ETR as well as a lower Ek, mostly due to a higher PS II light saturation threshold and photosynthetic efficiency (α). On the other hand, *S. maritima* showed an opposite pattern. Plants exposed to higher levels of atmospheric CO_2, showed lower ETRs at all tested light intensities, and consequently lower maximum ETR and photosynthetic efficiencies.

A similar behaviour was evidenced by the Kautsky curves derived from the OJIP transient analysis (Figure 3.2.5). *Halimione portulacoides* individuals exposed to 760 ppm of atmospheric CO_2 showed thermal and photochemical phases with higher fluorescence values, while *S. maritima* showed the inverse pattern.

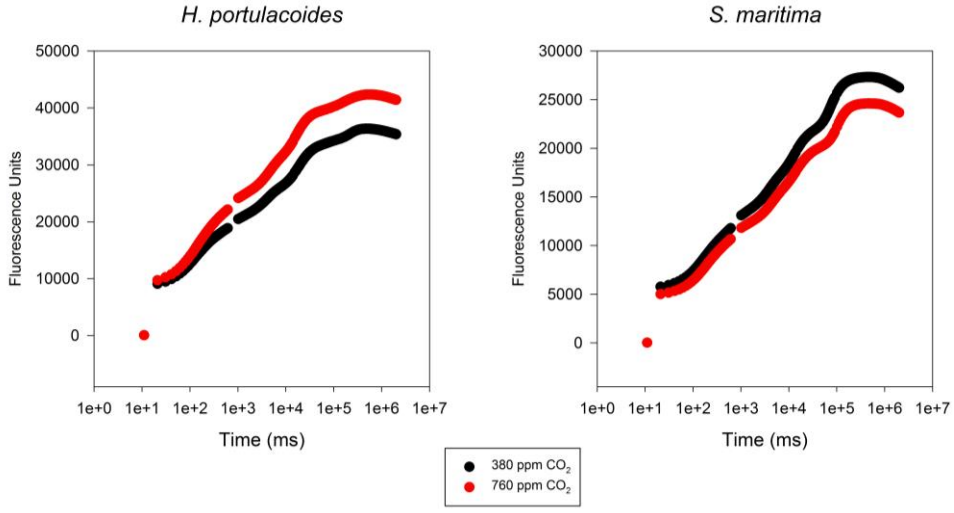

Figure 3.2.5. Transient (OJIP) light curves in *H. portulacoides* and *S. maritima* individuals at both CO_2 tested concentrations (average fluorescence values, n = 5).

Decomposing the transient curves into their derived parameters normalized to the leaf cross-section, the energy pathways could be discriminated (Figure 3.2.6). No significant changes in both absorbed and trapped electron fluxes were observed in either species under normal or elevated CO_2 levels. On the other hand, *S. maritima* electron transport flux per cross section under elevated CO_2 levels was significantly increased. The same could be observed for the dissipated energy flux. Conversely, in *H. portulacoides* the dissipated energy was found to be significantly lower in individuals subjected to higher CO_2 concentrations.

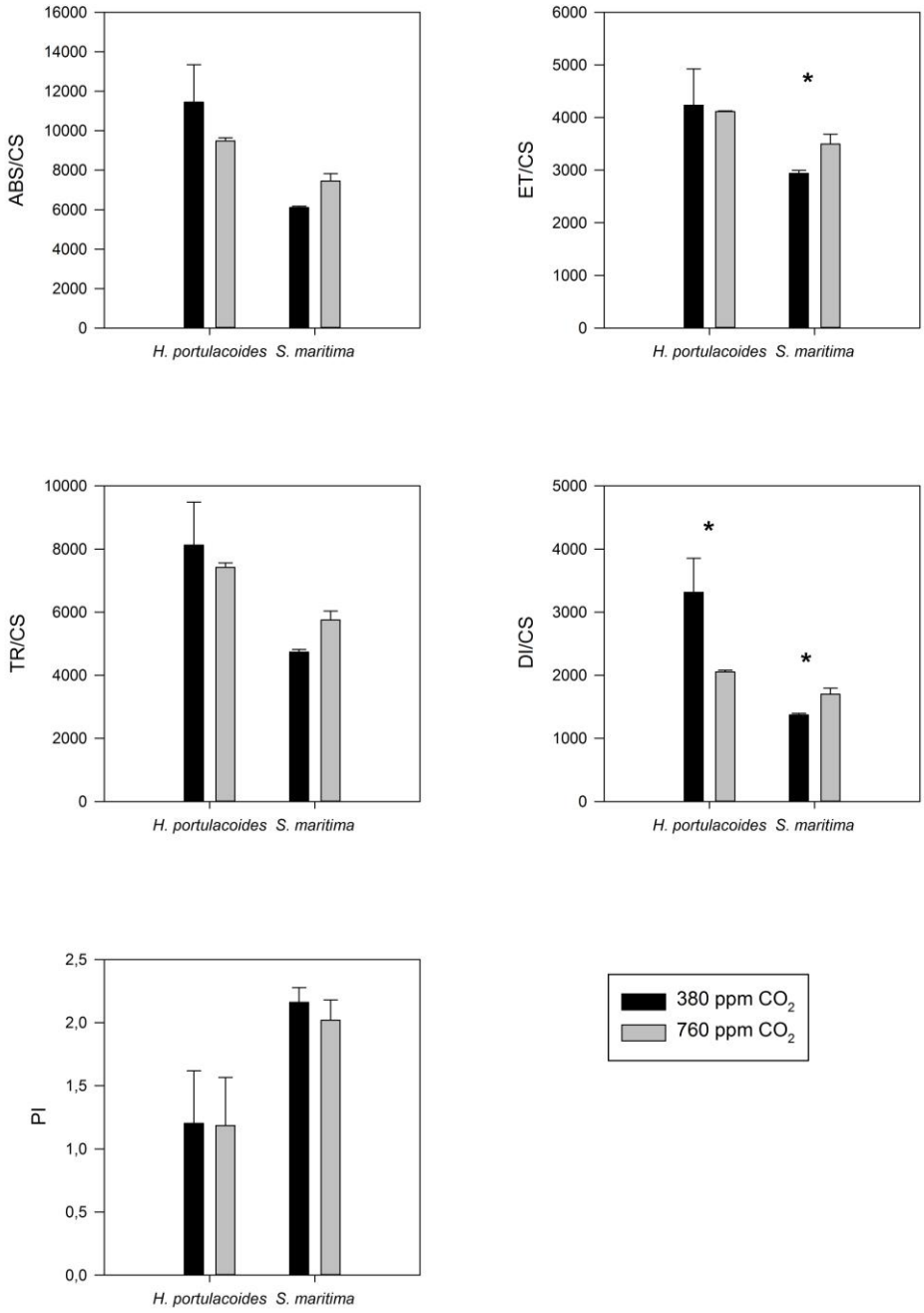

Figure 3.2.6. Energy fluxes and Performance Index (PI) in *H. portulacoides* and *S. maritima* individuals at both CO_2 tested concentrations (average ± standard deviation, n=5; * $p < 0.05$, ** $p < 0.01$).

Leaf pigment composition

Both *H. portulacoides* experimental groups showed very similar leaf Chl a concentration. On the other hand, in *S. maritima* the differences are more evident, with the individuals exposed to normal CO_2 levels exhibiting higher leaf Chl a concentration (Figure 3.2.7).

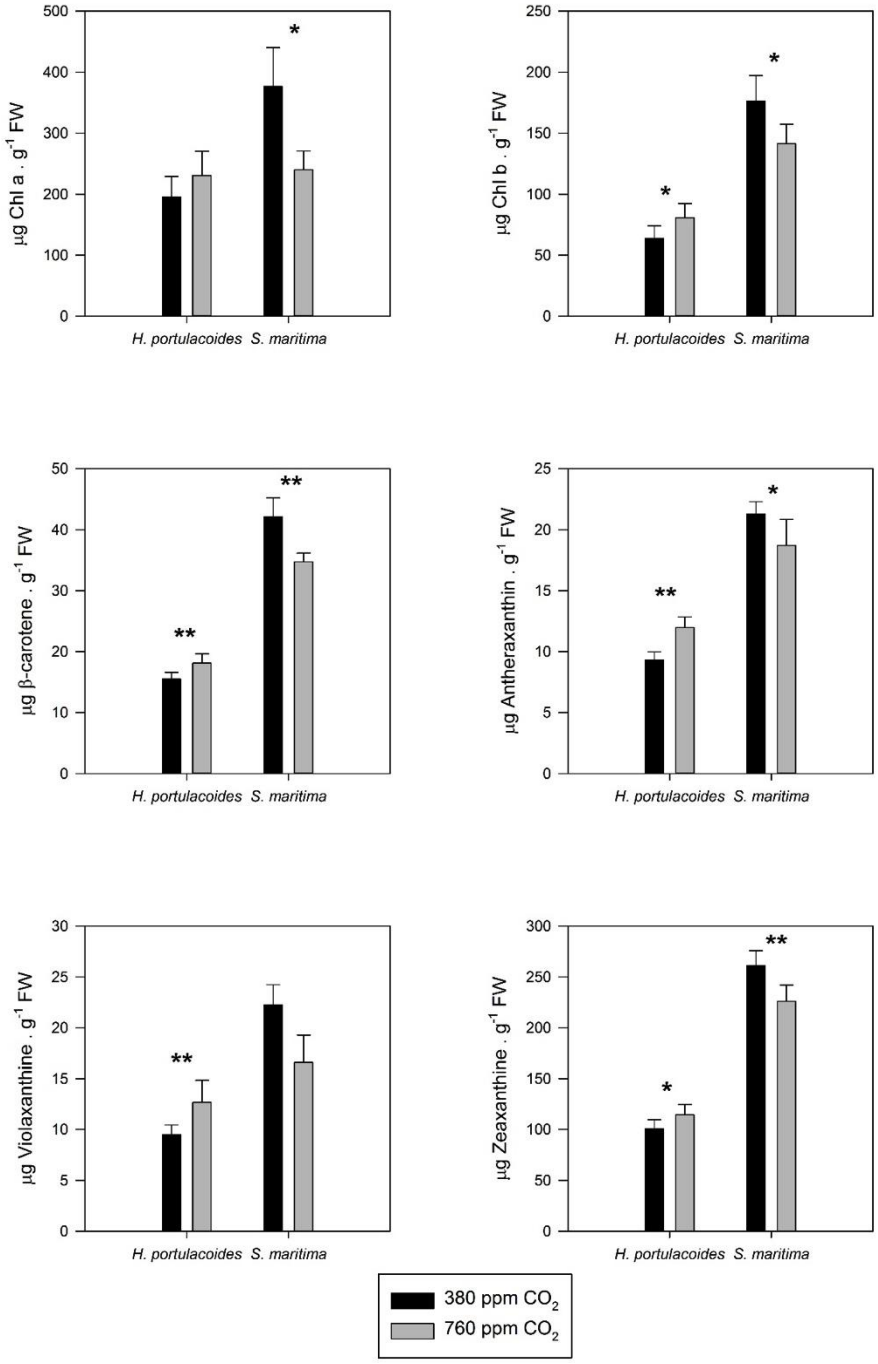

Figure 3.2.7. Chlorophylls and carotenoids contents in *H. portulacoides* and *S. maritima* individuals at both CO_2 tested concentrations (average ± standard deviation, n = 5; * $p < 0.05$, ** $p < 0.01$).

This was also true for the remaining analysed pigments. Overlooking the pigment ratios (Figure 3.2.8) only the chlorophyll a/b ratio showed significant differences between CO_2 treatments. In both species the individuals exposed to a CO_2 enriched atmosphere presented lower chlorophyll a/b values. None of the remaining analysed ratios showed any differences among treatments.

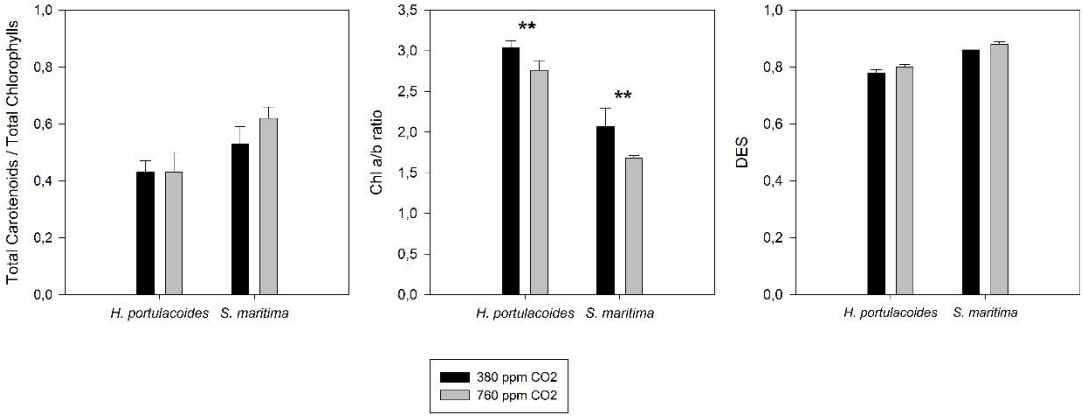

Figure 3.2.8. Pigment ratios in the leaves of *H. portulacoides* and *S. maritima* individuals at both CO_2 tested concentrations (average ± standard deviation, n = 5; * $p < 0.05$, ** $p < 0.01$).

Antioxidant enzymatic activities

Overlooking the activity of three antioxidant enzymes, different feedback patterns could be observed between species and treatments (Figure 3.2.9). Considering *H. portulacoides* individuals exposed to 760 ppm of CO_2, a significant decrease in their antioxidant enzymatic defence activities occurred, being this more evident for APx activity. On the other hand, CO_2 enrichment led to a different feedback from *S. maritima* enzymatic defences. While SOD and APx presented an increased activity in leaves exposed to 760 ppm CO_2, GPx showed a marked decreased under elevated CO_2. Concerning leaves total protein content, *H. portulacoides* individuals exposed to higher CO_2 concentration, showed a significant increase in its protein content, while *S. maritima* individuals under CO_2-enrichement presented a small but significant decrease in their leaves protein content.

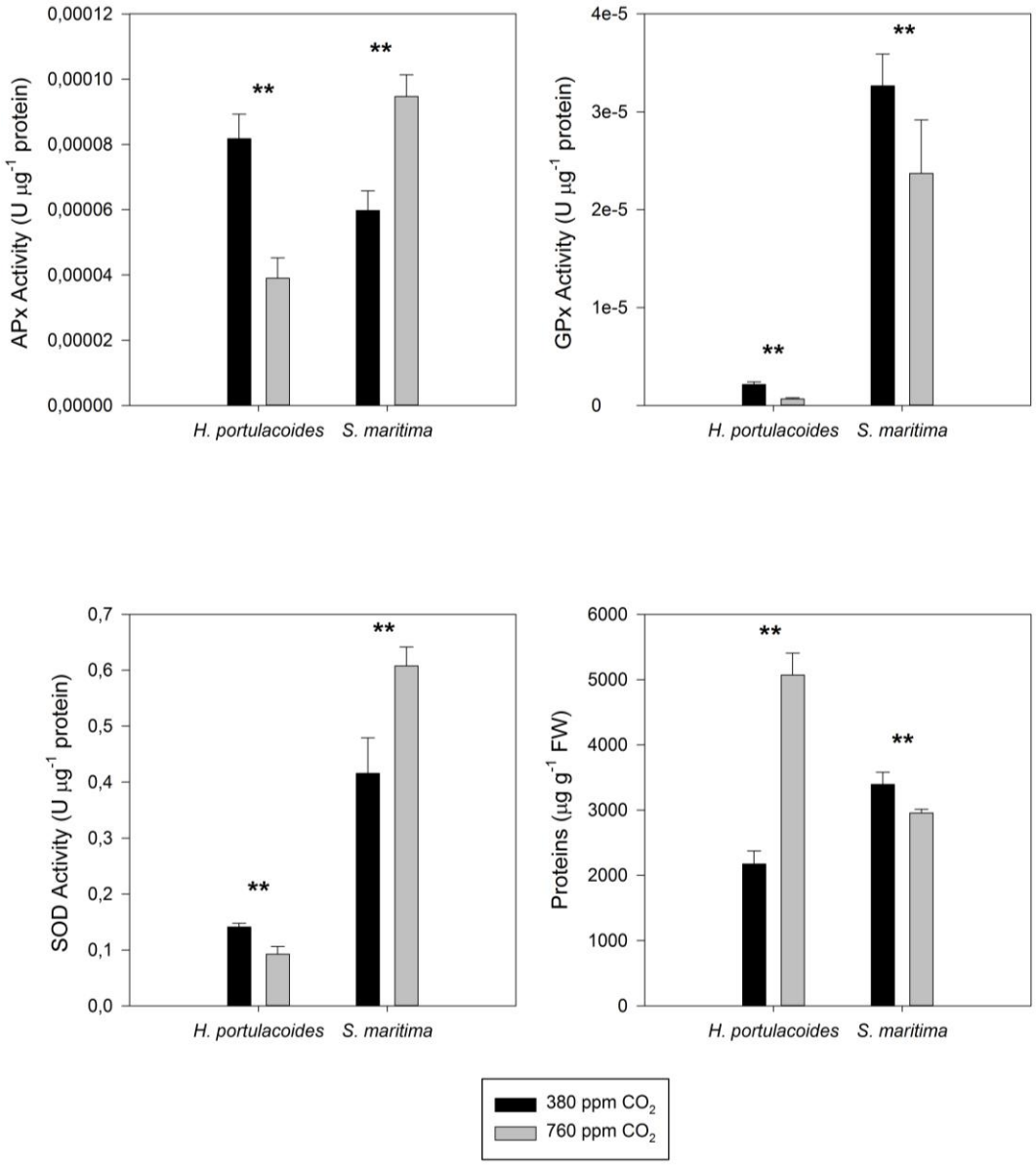

Figure 3.2.9. Anti-oxidant enzymatic activities in the leaves of *H. portulacoides* and *S. maritima* individuals subjected to both tested CO_2 concentrations (average ± standard deviation, n = 5; * $p < 0.05$, ** $p < 0.01$).

Discussion

In the last years several studies have been developed in order to evaluate the effects of CO_2 enrichment in different plant species, although there is still no consensus on a generalization of CO_2 effects based on plant functional type (Newingham *et al.*, 2013; Nowak *et al.*, 2004). It becomes this way important to address different species in different habitats evaluating constrains associated to CO_2 rising case by case. *H. portulacoides* is a coastal small shrub with a C_3

photosynthetic pathway typically found in the middle and upper areas of salt marshes (Duarte *et al*., 2012b). *S. maritima* on the other hand is a grass with a C_4 photosynthetic pathway inhabiting the lower marshes (Duarte *et al*., 2013a). As observed throughout this experiment, CO_2 enrichment has some similar effects on both species. Both species showed a decrease in the diffusion ratio from the atmosphere to the intracellular spaces dropping to values bellow one, indicating that intracellular CO_2 concentration stays bellow ambient one. In this case, the diffusion ratio decreases (to values bellow one) as Rubisco full carboxylation is reached (Guy *et al.*, 1986). Holtum *et al*. (1983) already found a similar pattern, and attributed it to stomatal aperture adjustments in response to ambient CO_2 changes. This was shown to be a common mechanism in both C_3 and C_4 species (Holtum *et al.*, 1983). At a given environmental [CO_2] this diffusion coefficient is inversely proportional to the [CO_2] outside the plant, driving the diffusion towards the leaf interior (Guy *et al.*, 1986). This is either due to an increase in photosynthetic capacity or to a decrease in stomatal conductance. Increased photosynthetic activity has as primary consequence a larger incorporation of atmospheric carbon in the plant tissues, thus increasing the $\delta^{13}C$ discrimination (Newingham *et al*., 2013). This was more evident in *H. portulacoides* and it is in agreement with higher increase in cellular CO_2 concentration, supporting the hypothesis of Rubisco full carboxylation capacity and photosynthetic enhancement. On the other hand, in *S. maritima* intracellular [CO_2] concentration of the individuals exposed to CO_2 enrichment, showed only a small enhancement, while compared to the observed in *H. portulacoides*. Alongside, the $\delta^{13}C$ discrimination also didn't show any increased carbon incorporation, indicating that there was no photosynthetic capacity enhancement.

Observing the photochemical traits underlying these elemental evidences, this differential behaviour is elucidated. Overlooking the photochemical process and analysing it through a perspective of PS II quantum efficiency, some differences arose. In *H. portulacoides* individuals exposed to high CO_2 levels there was a small increase in the maximum quantum efficiency, consistent to the findings from Cousins *et al*. (2002) and Wall *et al*. (2001). These authors suggested that this increased of PS II maximum efficiency is due to an increased ETR as a result of a higher efficiency transporting absorbed quanta from the light-harvesting complexes

(LHCs) to the PS II reaction centres, rather than a higher availability of electron acceptors downstream of PS II. This is supported by the higher values verified for maximum ETR rates inferred from the light curves. On the other hand, this species also showed low energy dissipation values, indicating a higher efficiency in the electronic transport under higher CO_2 levels. This fact has been attributed to an increasing demand for NADPH upon increasing CO_2 levels (Hymus *et al*., 1999). In this case, elevated CO_2 concentration under natural irradiance supports a higher electron transport rate (Long *et al*., 2004). As for *S. maritima* under CO_2 fertilization, it showed reduced PS II photosynthetic efficiencies (α) and ETR, with a simultaneous increase of dissipated energy. As can be seen, changes were not mediated by alterations in electron fluxes, but by changes in redox-regulated NPQ mechanisms, implying that, for a C_4 plant, photosynthesis is not substrate limited (Wall *et al*., 2001). At midday conditions, high CO_2 availability increased linear electron transfer as well as dissipated the large variation in the stroma pH across thylakoid membranes as photosynthetic rates increased (Cousins *et al*., 2002). This accumulation of excessive reducing power has to be dissipated or it will damage thylakoid membrane system. NPQ and DES variations can be attributed to treatment effects on electron transport capabilities and on the redox state of the photosynthetic membrane (Föster *et al*., 2001). Excess of light energy leads inevitably to a decrease in lumen pH, attributed to NPQ activation through protonation of the LHC proteins associated with the PS II (Cousins *et al*., 2002). Consequently, this will induce the activation of the xanthophyll cycle in order to dissipate excessive energy and therefore reduce PS II and associated proteins protonation. In fact, this was clearly observed in both species during exposure to elevated levels of CO_2. In *H. portulacoides* leaves subjected to CO_2 fertilization, the photosynthetic efficiency were higher independently of the light intensity, leading to higher ETR and thus reducing the need to dissipate excessive energy, decreasing NPQ and DES. This clearly points out for a substrate limitation of this C_3 species, with increasing CO_2 levels favouring the carbon harvest capacity and allowing an enhancement of the light harvesting efficiency. On the other hand, *S. maritima* highly efficient C_4 carbon concentration mechanism was already functioning at its full power. Subsequently, increased CO_2 levels lead to an overload of the

photosynthetic light harvesting apparatus, inducing a reduction of ETR and this way, to the activation of the xanthophyll cycle dissipating the elevated reducing power accumulated within the stroma and avoiding photo-inhibition (Demming-Adams, 1990). Nevertheless, both species showed an increase in the number of PS II LHC, as inferred by the decrease observed in Chl a/b ratio (Habash *et al*., 1995). As a result there was an evident increase in the photosynthetic efficiencies in *H. portulacoides*, while in *S. maritima* this increase in LHC number is rapidly supressed by low ETRs, having as a result a lower photosynthetic rate (Gutiérrez *et al*., 2009).

Inevitably these modified photosynthetic performances have severe consequences on the cellular redox state and thus, will have its feedback reflected at the oxidative-stress enzymes level. Nevertheless, these enzymes are not exclusively linked to stress processes as they are part, for example, of the normal photosynthetic process. This seems to be the case of APx. The impairment of light harvesting process in *S. maritima* led to a restriction on the carbon harvesting processes. In these conditions, it is known that occurs a significant water-water cycle (Mehler ascorbate peroxidase) activity, where APx plays a key role (Ort and Baker, 2002). This could be observed in *S. maritima* individuals exposed to 760 ppm of CO_2. Still, it must be considered that these plants are under stress due to accumulation of excessive reducing power, one of the causes for reactive oxygen species (ROS) generation, as previously observed in photo-inhibited halophytes (Duarte *et al*., 2013b). Supporting this last hypothesis, SOD activity in *S. maritima* individuals under CO_2 fertilization was also elevated. On the other hand, *H. portulacoides* showed comparatively reduced levels of anti-oxidant enzymes activity. The observed reductions in anti-oxidant defences support the theory that growing under elevated CO_2 concentrations decreases intrinsic oxidative stress. Under these conditions, a lower production of ROS is likely to occur due to an enhanced use of reducing power for assimilation in photosynthesis and also to a decrease of photo-respiratory rate. Nonetheless, the suppression of superoxide dismutase activity, suggests that the stress relaxation is not only confined to chloroplasts and peroxisomes but also occurs in other subcellular compartments (Schwanz and Polle, 1998), where SOD isoforms are present. With SOD activity reduction, lower levels of H_2O_2 are generated via superoxide decomposition leading to a reduction of the activity of

both peroxidases (Duarte *et al*., 2013b). Only GPx activity, in *S. maritima* individuals exposed to elevated CO_2 levels and presumably under stress, was not consistent with an oxidative stress condition. Guaiacol-type peroxidases participate in a number of important processes in plants, other than oxidative stress, like lignification and auxin metabolism (Hiraga *et al*., 2001). This decrease in GPx activity in *S. maritima* individuals exposed to 760 ppm of CO_2 was not related to a reduction of oxidative stress levels (as shown by the APx and SOD), but is probably due to a reduction of the acid-soluble lignin, as found in previous works (Riikonen *et al*., 2005; Tegelberg *et al*., 2001).

Conclusions

The ongoing atmospheric CO_2 concentration rising are known to have implications throughout the entire biosphere. Halophyte species inhabiting wetlands will also be affected. As in other ecosystems, underlying their feedback to environmental changes, there is a metabolic variability. While C_3 species appear to respond positively to increasing atmospheric CO_2 levels, enhancing its light harvesting mechanisms and its photosynthetic efficiency, C_4 halophytes appear to suffer from stress induced by CO_2 rising. In *H. portulacoides,* CO_2 fertilization induced Rubisco full carboxylation capacity and photosynthetic enhancement, mostly due to an enhancement of ETR and lower amounts of dissipated energy. On the other hand, C_4 grasses like *S. maritima* are normally working at full potential and presenting none photosynthetic enhancement under CO_2 fertilization. In fact, this highly productive grass presented signs of photochemical and oxidative stress, reducing this way its global photosynthetic ability. Both these feedbacks to realistic future CO_2 concentrations are important to be considered in future primary productivity models, as they are indicative of a possible abundance reduction of pioneer *S. maritima* and an increased biomass spreading of the sediment stabilizer, *H. portulacoides*. This way, it is important to consider the inevitable changes in morphology and function of salt marshes, imposed by these atmospheric changes, both in terms of ecosystem functioning and loss of biodiversity.

References

Ball, M.C. and Munns, R., 1992. Plant responses to salinity under elevated atmospheric concentrations of CO_2. *Australian Journal of Botany* 40, 515-525.

Caçador, I., Caetano, M., Duarte, B. and Vale, C. 2009. Stock and losses of trace metals from salt marsh plants. *Marine Environmental Research* 67, 75-82.

Caçador, I., Neto, J.M., Duarte, B., Barroso, D.V., Pinto, M. and Marques, J.C., 2013. Development of an Angiosperm Quality Assessment Index (AQuA – Index) for ecological quality evaluation of Portuguese water bodies – A multi-metric approach. *Ecological Indicators* 25, 141-148.

Caemmerer, S., 2013. Steady-state models of photosynthesis. *Pant Cell and Environment* 36, 1617-1630.

Cousins, A., Adam, N., Wall, G., Kimball, B., Pinter, P., Ottman, M., Leavitt, S. and Webber, A., 2002. Photosystem II energy use, non-photochemical quenching and the xanthophyll cycle in *Sorghum bicolor* grown under drought and free-air CO_2 enrichment (FACE) conditions. *Plant, Cell and Environment* 25, 1551-1559.

Demmig-Adams, B., 1990. Carotenoids and photoprotection in plants: a role for the xanthophyll zeaxanthin. *Biochimica et Biophysica Acta* 1020, 1–24.

Drake, B., Gonzalez-Meler, M. and Long S.P., 1997. More efficient plant: a consequence of rising atmospheric CO_2. A*nnual Review of Plant Physiology and Plant Molecular Biology* 48, 609–639.

Duarte, B., Couto, T., Freitas, J., Valentim, J., Silva, H., Marques, J. C. and Caçador, I., 2013a. Abiotic modulation of *Spartina maritima* photosynthetic ecotypic variations in different latitudinal populations. *Estuarine, Coastal and Shelf Science* 130, 127-137.

Duarte, B., Couto, T., Marques, J.C and Caçador, I., 2012a. *Scirpus maritimus* leaf pigment profile and photochemistry during senescence: implications on carbon sequestration. *Plant Physiology and Biochemistry* 57, 238-244.

Duarte, B., Raposo, P. and Caçador, I., 2009. *Spartina maritima* (cordgrass) rhizosediment extracellular enzymatic activity and its role on organic matter decomposition and metal speciation processes. *Marine Ecology* 30, 65-73.

Duarte, B., Santos, D., Marques, J. C. and Caçador, I., 2013b. Ecophysiological adaptations of two halophytes to salt stress: photosynthesis, PS II photochemistry and anti-oxidant feedback - Implications for resilience in climate change. *Plant Physiology and Biochemistry* 67, 178-188.

Duarte, B., Silva, V. and Caçador, I., 2012b. Hexavalent chromium reduction, uptake and oxidative biomarkers in *Halimione portulacoides*. *Ecotoxicology and Environmental Safety* 83, 1-7.

Farnsworth, E.J., Ellison, A.M. and Gong, W.K., 1996. Elevated CO_2 alters anatomy, physiology, growth, and reproduction of red mangrove (*Rhizophora mangle* L.). *Oecologia* 108, 599-609.

Farquhar, G. D., Ehleringer, J. R., and Hubick, K. T., 1989. Carbon isotope discrimination and photosynthesis. *Annual Review of Plant Physiology and Plant Molecular Biology* 40, 503–537.

Förster, B., Osmond, C.B. and Boynton, J.E., 2001. Very high light resistant mutants of *Chlamydomonas reinhardtii*: Responses of Photosystem II, nonphotochemical quenching and xanthophyll pigments to light and CO_2. *Photosynthesis Research* 67, 5–15.

Gaastra, P., 1959. Photosynthesis of crop plants as influenced by light, carbon dioxide, temperature and stomatal diffusion resistance. -Meded. *Landbouwhogesch. Wageningen* 59, 1-68.

Geissler, N., Hussin, S. and Koyro, H.-W., 2009. Elevated atmospheric CO_2 concentration ameliorates effects of NaCl salinity on photosynthesis and leaf structure of *Aster tripolium* L. *Journal of Experimental Botany* 60, 137–151.

Geissler, N., Hussin, S. and Koyro, H.-W., 2010. Elevated atmospheric CO_2 concentration enhances salinity tolerance in *Aster tripolium* L. *Planta* 231, 583-594.

Ghannoum, O., von Caemmerer, S., Ziska, L.H. and Conroy, J.P., 2000. The growth response of C_4 partial pressure: a reassessment. *Plant, Cell and Environment* 23, 931–942.

Gutierrez, D., Gutierrez, E., Perez, P., Morcuende, R., Verdejo, A.L. and Martinez-Carrasco, R., 2009. Acclimation to future atmospheric CO_2 levels increases photochemical efficiency and mitigates photochemistry inhibition by warm temperatures in wheat under field chambers. *Physiologia Plantarum* 137, 86–100.

Guy, R.D., Reid, D.M. and Krouse, H.R., 1980. Shifts in carbon isotope ratios of two C_3 halophytes under natural and artificial conditions. *Oecologia* 44, 241-247.

Guy, R.D., Reid, D.M. and Krouse, H.R., 1986. Factors affecting $^{13}C/^{12}C$ ratios of inland halophytes. I. Controlled studies on growth and isotopic composition of *Puccinellia nuttalliana. Canadian Journal of Botany* 64, 2693-2699.

Habash, D.Z., Paul, M.J., Parry, M.A.J., Keys, A.J and, Lawlor, D.W., 1995. Increased capacity for photosynthesis in wheat grown at elevated CO_2 – the relationship between electron-transport and carbon metabolism. *Planta* 197, 482–489.

Hao, X., Li., P., Feng, Y., Han, X., Gao., J., Lin, E. and Han, Y., 2013. Effects of fully open-air [CO_2] elevation on leaf photosynthesis and ultrastructure of *Isatis indigotica* Fort. *PLoS ONE* 8, e74600.

Hiraga, S., Sasaki, K., Ito, H., Ohashi, Y., Matsui, H., 2001. A large family of class III plant peroxidases. *Plant Cell Physiology* 42, 462–468.

Holtum, I.A.M., O'Leary, M.H. and Osmond, C.B., 1983. Effect of varying CO_2 partial pressure on photosynthesis and on carbon isotope composition of carbon-4 of malate from the Crassulacean acid metabolism plant *Katanchoe daigremontiana* Hamet et Perr. *Plant Physiology* 71, 602-609.

Horton P., 2000. Prospects for crop improvement through the genetic manipulation of photosynthesis: morphological and biochemical aspects of light capture. *Journal of Experimental Botany* 51, 475–485.

Houghton, J., 2001. The science of global warming. *Interdisciplinary Science Reviews* 26, 247–257.

Hymus, G.J., Ellsworth, D.S., Baker, N.R. and Long, S.P., 1999. Does free-air carbon dioxide enrichment affect photochemical energy use by evergreen trees in different seasons? A chlorophyll fluorescence study of mature loblolly pine. *Plant Physiology* 120, 1183–1191.

IPCC, 2007. Summary for policymakers. In: Climate Change 2007: The Physical Science Basis. Contribution of Working Group I to the Fourth Assessment Report of the Intergovernmental Panel on Climate Change (Solomon S, Qin D, Manning M, Chen Z, Marquis M, Averyt KB, Tignor M, Miller HL eds). Cambridge University Press, Cambridge and New York, NY.

Kupper, H., Seibert, S. and Aravind, P., 2007. A fast, sensitive and inexpensive alternative to analytical pigment HPLC: quantification of chlorophylls and carotenoids in crude extracts by fitting with Gauss-peak-spectra. *Analytical Chemistry* 79, 7611-7627.

Lenssen, G.M., van Duin, W.E., Jak, P. and Rozema, J., 1995. The response of *Aster tripolium* and *Puccinellia maritima* to atmospheric carbon dioxide enrichment and their interactions with flooding and salinity. *Aquatic Botany* 50, 181–192.

Long, S.P., Ainsworth, E.A., Rogers, A. and Ort, D.R., 2004. Rising atmospheric carbon dioxide: plants FACE the future. *Annual Review of Plant Biology* 55, 591-628.

Mateos-Naranjo, E., Redondo-Gómez, S., andrades-Moreno, L., Davy, A.J., 2010. Growth and photosynthetic responses of the cordgrass *Spartina maritima* to CO_2 enrichment and salinity. *Chemosphere* 81, 725-731.

Mendelssohn, I. and Morris, J., 2000. Eco-Physiological Controls on the Productivity of *Spartina alterniflora* Loisel in Concepts and Controversies in Tidal Marsh Ecology. Springer Netherlands. 59-80.

Mpelasoka, F., Hennessy, K., Jones, R. and Bates, B., 2008. Comparison of suitable drought indices for climate change impacts assessment over Australia towards resource management. *International Journal of Climatology* 28, 1283–1292.

Newingham, B., Vanier, C., Charlet, T., Ogle, K., Smith, S. and Nowak, R., 2013. No cumulative effect of 10 years of elevated [CO_2] on perennial plant biomass components in the Mojave Desert. *Global Change Biology* 19, 2168-2189.

Nowak, R.S., Ellsworth, D.S. and Smith, S.D., 2004. Functional responses of plants to elevated atmospheric CO_2 – do photosynthetic and productivity data from FACE experiments support early predictions? *New Phytologist* 162, 253–280.

Ort, D.R. and Baker, N.R., 2002. A photoprotective role for O_2 as an alternative electron sink in photosynthesis? *Current Opinion in Plant Biology* 5, 193–198.

Pammenter, N.W., Loreto F. and Sharkey, T.D., 1993 End product feed-back effects on photosynthetic electron transport. *Photosynthesis Research* 35, 5–14.

Riikonen, J., Holopainen, T., Oksanen, E. and Vapaavuori, E., 2005. Leaf photosynthetic characteristics of silver birch during three years of exposure to elevated CO_2 and O_3 in the field. *Tree Physiology* 25, 621–632.

Rozema, J., Dorel, F., Janissen, R., Lenssen, G., Broekman, R., Arp, W. and Drake, B.G., 1991. Effect of elevated atmospheric CO_2 on growth, photosynthesis and water relations of salt marsh grass species. *Aquatic Botany* 39, 45–55.

Schwanz, P. and Polle, A., 1998. Antioxidative systems, pigment and protein contents leaves of adult Mediterranean oak species (*Quercus pubescens* and *Q. ilex*) with life-time exposure to elevated CO_2. *New Phytologist* 140, 411-423.

Tausz-Posch, S., Borowiak, K., Dempsey, R., Norton, R., Seneweera, S., Fitzgerald, G. and Tausz, M., 2013. The effect of elevated CO_2 on photochemistry and antioxidative defence capacity in wheat depends on environmental growing conditions – A FACE study. *Environmental and Experimental Botany* 88, 81-92.

Tegelberg, R., Julkunen-Tiitto, R. and Aphalo, P.J., 2001. The effects of long-term elevated UV-B on the growth and phenolics of field-grown silver birch (*Betula pendula*). *Global Change Biology* 7, 839–848.

Urano, K., Kurihara, Y., Motoaki, S., and Shinozaki, K., 2010. 'Omics' analyses of regulatory networks in plant abiotic stress responses. *Current Opinion in Plant Biology* 13, 132-138.

Valiela, I., Cole, M., McClelland, J., Cebrian, J. and Joye, S. B., 2000. Role of salt marshes as part of coastal landscapes. In Weinstein, M. P. and D. A. Kreeger (eds), Concepts and Controversies in Tidal Marsh Ecology. Kluwer Academic Publishers, London.

Wall, G.W., Brooks, T.J., Adam, N.R., Cousins, A.B., Kimball, B.A., Pinter, P.J., LaMorte, R.L., Triggs, J., Ottman, M.J., Leavitt, S.W., Mathias, A.D., Williams, D.G and Webber, A.N., 2001. Elevated atmospheric CO_2 improved sorghum plant water status by ameliorating the adverse effects of drought. *New Phytologist* 152, 231–248.

Yamaguchi-Shinozaki, K. and Shinozaki, K., 2006. Transcriptional regulatory networks in cellular responses and tolerance to dehydration and cold stresses. *Annual Reviews in Plant Biology* 57, 781-803.

Ziska, L.H., 2008. Rising atmospheric carbon dioxide and plant biology: the overlooked paradigm. *DNA and Cell Biology* 27, 165–172.

3.3. LIGHT-DARK O_2 DYNAMICS IN SUBMERGED LEAVES OF C_3 AND C_4 HALOPHYTES UNDER INCREASED DISSOLVED CO_2[1]

Abstract

Waterlogging and submergence are major constrains to which wetland plants are subjected, with inevitable impacts on their physiology and productivity. Global warming and climate change, as driving forces of sea level rise, tend to increase such submersion periods and also modify the carbonate chemistry of the water column due to the increased concentration of CO_2 in the atmosphere. In the present work, the underwater O_2 fluxes in the leaves of three abundant Mediterranean halophytes were evaluated at different levels of dissolved CO_2, showing very different responses to the conditions imposed. Photosynthetic enhancement due to increased dissolved CO_2 was confirmed for *H. portulacoides* and *S. maritima*, probably due to the high tissue porosity and the formation of leaf gas films and reduction of the oxygenase activity of Rubisco. Enhancement of the photosynthetic rates in *H. portulacoides* and *S. maritima* were concomitant with an increase in energy trapping and transfer, mostly due to the enhancement of the carboxylation reaction of Rubisco, leading to a reduction of the energy costs for carbon fixation.

Transposing these findings to the ecosystem, and assuming increased dissolved CO_2 concentration scenarios, the halophyte community displays a new ecosystem function, increasing the water column oxygenation and thus reinforcing their role as principal primary producers of the estuarine system.

[1] This section was published in: **Duarte, B.**, Silva, H., Marques, J.C., Caçador, I. and Sleimi, N., 2014. Light-dark O_2 dynamics in submerged leaves of C_3 and C_4 halophytes under increased dissolved CO_2: Clues for saltmarsh response to climate change. *Annals of Botany Plants* 6, plu067.

Introduction

Wetlands are among the most productive ecosystems of the planet, retaining about 1/2 to 1/3 of the carbon fixed and providing important ecosystem services to the estuarine system, namely nutrient regeneration, primary production, and shoreline stabilization as well as a habitat for wildlife (Caçador *et al.*, 2009). Estuarine wetlands are known for their high productivity, which has been attributed to the high degree of halophyte coverage and diversity, with a specific zonation, resulting from inter-specific relationships between species and competition for specific optimal habitats (Mendelssohn and Morris, 2000). Another key factor defining species expansion, growth and productivity is their exposure to abiotic stresses, both environmental (for example climate driven) and anthropogenic (for example, pollution with heavy metals). If the future of these ecosystems is to be predicted in the face of climate change, it is of great importance to understand plant stress responses and adaptations at the molecular, biochemical levels, cellular and physiological levels (Urano *et al*., 2010; Yamaguchi-Shinozaki and Shinozaki, 2006).

Waterlogging and submergence are two major features to which wetland plants, especially salt marsh halophytes are subjected, with severe impacts on their survival and productivity (Pedersen *et al*., 2010; Bailey-Serres and Voesenek, 2008). Due to tidal flooding, shoots and leaves can become completely submerged, restricting gas exchange and light harvesting (Colmer and Voesenek, 2009). The frequency, duration and depth of tidal flooding can influence the species distribution in salt marshes, this being determined by, for example, their ecophysiological tolerance to flooding (Voesenek *et al*., 2004; Pedersen and Colmer, 2006). Not only does the slow diffusion of CO_2 in the aquatic environment limit its uptake by leaves (Smith and Walker, 1980), but also the decreased light availability, due to attenuation down the water column, impairs photosynthesis (Sand-Jensen, 1989; Pedersen *et al*., 2006). Several plant species have developed leaf adaptations to these constraints in order to enhance underwater CO_2 uptake - by reducing morphologically the boundary-layer and cuticle resistance or by acquiring HCO^-_3 directly from the water column (Colmer and Pedersen, 2008). In submerged leaves of halophytes, CO_2 limitation becomes severe when concentrations are near air equilibrium, due to the elevated saturation point of underwater photosynthesis (20

to 75-fold the water-air equilibrium conditions; Pedersen *et al*., 2010). Taking into account the present projections made by the Intergovernmental Panel for Climate Change (IPCC), it is expected that the increased levels atmospheric CO_2 will lead to an inevitable increase in the dissolved CO_2 in the water bodies (IPCC, 2002), in this way altering the availability of CO_2 underwater.

Spartina maritima (L.) Loisel (Poaceae) and *H. portulacoides* (L). Allen (Amaranthaceae) are two of the most abundant and productive halophytic plants present in the Mediterranean estuaries (Duarte *et al*., 2010; Caçador *et al*., 2013). These species typically colonize the lower marsh mudflats and the sides of the network of channels within the marshes, being subjected to tidal flooding twice per day (Duarte *et al*., 2009; Duarte *et al*., 2014a). Nevertheless, these are photosynthetically different species: *H. portulacoides* undergoes C_3 photosynthesis (Duarte *et al*., 2012; Duarte *et al.*, 2014b), while *S. maritima* is a C_4 plant (Duarte *et al*., 2013; Duarte *et al*., 2014b). Previous works showed that these species present very different dynamics under atmospheric CO_2 enrichment as well as under submersion (Duarte *et al*., 2014a; Duarte *et al*., 2014b).

In the present paper, we report the O_2 dynamics both during light and dark periods of the leaves of the C_3 *H. portulacoides* and the C_4 *S. maritima* under different dissolved CO_2 concentrations. This has provided insights not only on the species tolerance to submersion but also how CO_2 can ameliorate the imposed submersion stress and its consequences in the ecosystem services provided, namely in terms of water column oxygenation.

Material and Methods

Plant harvest

Intact turfs of the target species were collected at the end of the growing season (October), one day before the experiments started, from the Tagus estuary (Alcochete, 38°45'38.78"N, 8°56'7.37"W). All the turfs of the same species were of similar height to ensure similar ages. The intact turfs and their rhizosediment were transported to the laboratory, in air-exposed trays and placed in a FytoScope Chamber (Photon-System Instruments, Czech Republic), in a photoperiod (16h / 8h light/dark) at 20 °C, until the beginning of the experiments. Sediment was

supplemented with ¼ Hoagland solution with the salinity adjusted to 20‰ (estuarine salinity) to maintain moisture conditions from the field.

Underwater Net Photosynthesis and Respiration

The experimental setup was based on that of Colmer and Pedersen (2008). Fully expanded leaves (n=3) were excised from their base in the stem. In the case of *S. maritima* leaves, samples were sliced into similar rectangular segments (approximately 5 cm) by cutting their extremities. For *H. portulacoides,* intact excised leaves were used, as their approximate length was 5 cm. The segments were immediately placed in 50 mL plastic gas-tight bottles with rubber stopper (3 bottles containing 3 leaf segments each, per treatment). Hoagland solution (¼ strength was used as incubation medium with salinity adjusted to 20‰ (estuarine salinity) with sea salt mixture and supplemented with $KHCO_3$ in order to attain the desired dissolved CO_2 levels (0.05, 0.5, 1.0 and 2.0 mM) and the pH adjusted to 6.00 with KOH, according to field measurements (Duarte *et al*., 2014c). Three replicate bottles per treatment were maintained in the light (PAR 400 μmol photons m^{-2} s^{-1} inside the bottle), while the remaining three replicate bottles were darkened. Both groups were maintained at 25 °C. Bottles containing only incubation medium were placed in the same conditions to confirm that the O_2 concentrations were maintained constant in the absence of leaves. Underwater Net Photosynthesis (P_N) and Respiration (R_N) were measured using a dissolved oxygen probe (WTW Oxi 330i/SET) after 2 h. Due to the lack of homogeneity in the morphology and succulence of the leaves of the two species, the O_2 fluxes were expressed on the basis of dry weight. To determine the dry weight (DW) of the leaves, 20 samples per species, from the same intact turfs used in the experiments, were collected and dried at 60 °C until constant weight and re-weighted. This normalization was adopted instead of using chlorophyll since during stress conditions chlorophyll content can be affected and thus affect the normalization.

In order to achieve a projection of the O_2 production/consumption rates in the Tagus estuarine system, the rates determined in this work were combined with the known biomasses and areas colonised by each of the studied species in the Tagus estuary (Caçador *et al*., 2010; Duarte *et al*., 2010; Caçador *et al*., 2013). The

computed values were expressed on a daily basis, considering two high tides per day (one in daytime and another during the night) with a maximum period of plant submersion of 3 h (Serôdio and Catarino, 2000; Duarte *et al*., 2014b). The calculations were made for the four dissolved CO_2 scenarios tested in the present work and the O_2 production/consumption rates obtained experimentally.

PAM fluorometry

Fluorometric analysis were preformed according to the described in Chapter II, Section 3 as described in Duarte *et al*. (2014). All derived variables were computed as described in Table 2.3.1.

Anti-oxidant enzyme assays

All enzymatic analyses were performed by UV-Vis spectrophotometry using specific substrates as described in Chapter II, Section 3 (Duarte *et al*., 2014).

Statistical Analysis

In order to compare the results of the different ecophysiological parameters between species at different treatments the Kruskal–Wallis test was employed. Statistical analyses were carried out using the Statistica Software version 10 (Statsoft).

Results

Underwater Light-Dark O_2 Fluxes

For *H. portulacoides*, an increase in dissolved CO_2 led to an increase in O_2 production (photosynthesis) in the light-exposed leaves and a decrease in the O_2 consumption (respiration) in the presence of increasing dissolved CO_2 concentrations in dark-incubated leaves (Figure 3.3.1). For *S. maritima*, however, increased dissolved CO_2 lead to a decrease in O_2 consumption rates (respiration) in light-exposed leaves. In fact, underwater photosynthetic O_2 production could only be observed under higher dissolved CO_2 concentrations. Regarding the dark-adapted leaves of *S. maritima* there was no distinct pattern of variation in O_2 consumption rates with change of dissolved CO_2 concentration. The highest underwater O_2

production (4 μmol O_2 g^{-1} DW h^{-1}) was recorded in *H. portulacoides* at 0.5 mM dissolved CO_2, while *S. maritima* showed the lowest (1.6 μmol O_2 g^{-1} DW h^{-1}) even at elevated dissolved CO_2 concentrations (2 mM). On the other hand, and concerning O_2 dark-consumption, *S. maritima* exhibited the highest respiratory rates, independently of the applied dissolved CO_2 concentration.

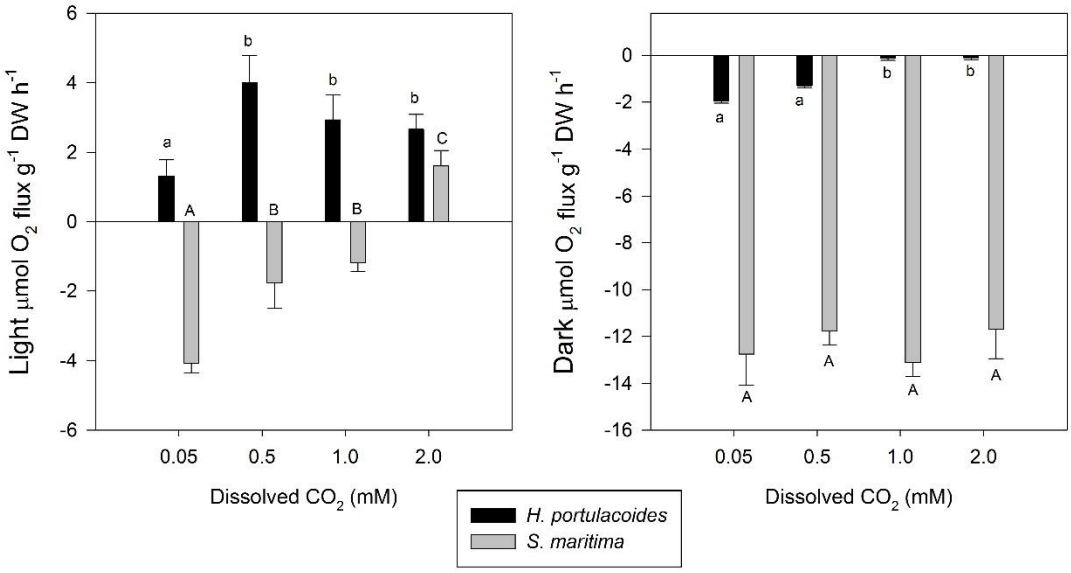

Figure 3.3.1. Oxygen production (positive values) and consumption (negative values) by the two tested species in light and dark conditions, at different levels of dissolved CO_2 (average ± standard deviation, n=9. Letters indicate significant differences among CO_2 treatments at $p < 0.05$).

PS II Quantum Efficiencies and Variable Fluorescence

The maximum PS II quantum efficiencies (dark-adapted leaves) showed no evident differences among the dissolved CO_2 treatments for both tested species (Figure 3.3.2). As for the operational PS II quantum efficiencies, there was a tendency for reduction with increasing dissolved CO_2 concentrations. The variable fluorescence (F_v) in both dark and light adapted leaves of *H. portulacoides* showed a decrease in both with increasing CO_2 treatments, presenting a maximum at 0.5 mM dissolved CO_2. On the other hand, in *S. maritima* the F_v in dark-adapted leaves showed an evident increase along with increasing dissolved CO_2 concentrations. Nevertheless, there was no distinguishing pattern in the variable fluorescence data in light-adapted leaves of *S. maritima*.

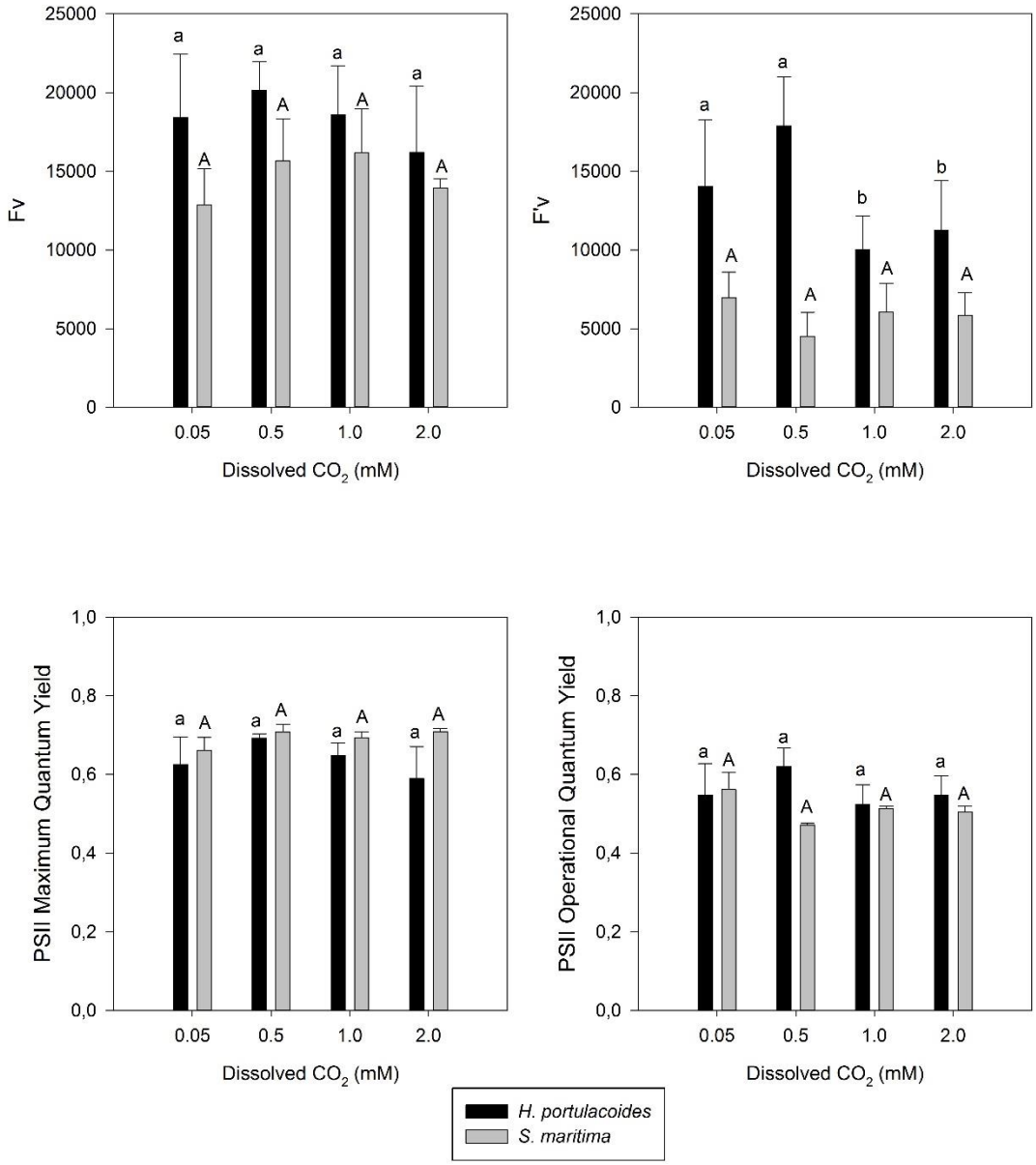

Figure 3.3.2. Photosystem II variable fluorescence and quantum efficiencies (operational and maximum) by the two tested species in light and dark conditions, at different levels of dissolved CO_2 (average ± standard deviation, n=9. Letters indicate significant differences among CO_2 treatments at $p < 0.05$).

Kautsky Curves and Transient OJIP parameters

The O-J phase of the Kautsky curves of all samples presented similar patterns, independently of the dissolved CO_2 concentrations (Figure 3.3.3). In *H. portulacoides* the more evident differences were observed during the thermal phase (J-I-P), with higher values in the samples exposed to higher dissolved CO_2 concentrations. During the photochemical phase (O-J), there was generally an overlap of the Kautsky plots

among treatments. For *S. maritima* leaves, the increase in dissolved CO_2 lead to an increase in the intensity of both the photochemical and thermal phases, the latter being more pronounced in leaves subjected to the higher concentration of dissolved CO_2.

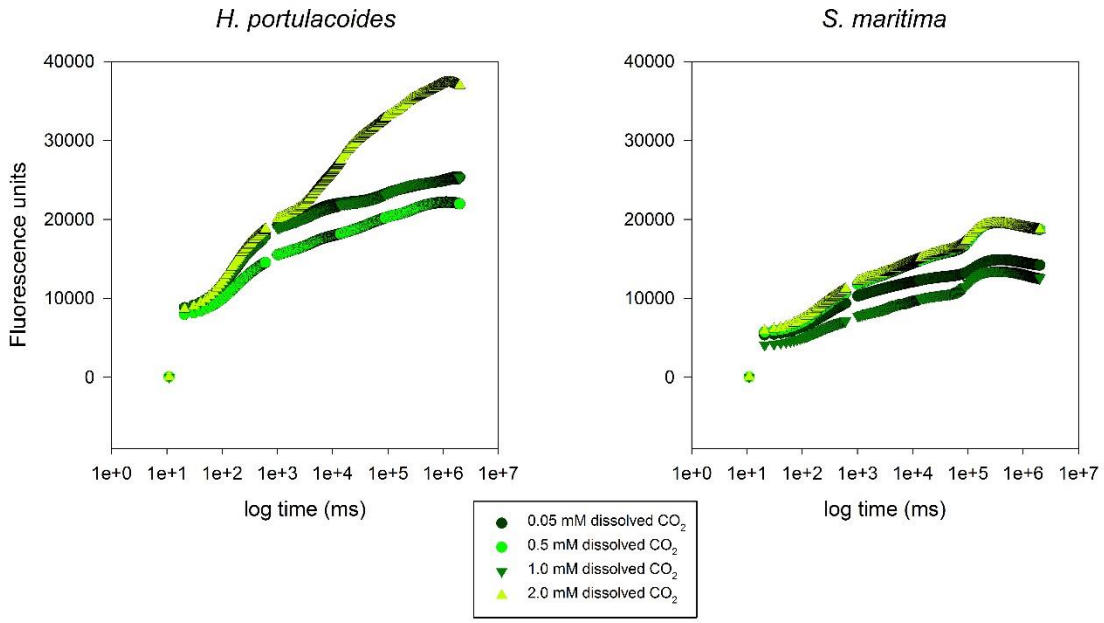

Figure 3.3.3. Kautsky OJIP curves of the two tested species in light and dark conditions, at different levels of dissolved CO_2 (average, n=9).

Regarding the OJIP-derived photochemical parameters, as well as the energy flux variables, some differences were evident (Figure 3.3.3 and 3.3.4). The maximum quantum yield of primary PS II photochemistry (φ_{Po}) was generally maintained both among CO_2 treatments and species. On the other hand, in *H. portulacoides*, small fluctuations were observed in the probability of a PS II trapped electron being transferred from Q_A to Q_B (ψ_0) as well as in the electronic transport quantum yield (φ_{Eo}) across the different applied CO_2 treatments. In *S. maritima*, both parameters, showed an increase in their relative fluorescence with increasing dissolved CO_2. The quantum yield of the non-photochemical reactions (φ_{Do}), decreased only in *S. maritima* with increasing CO_2.

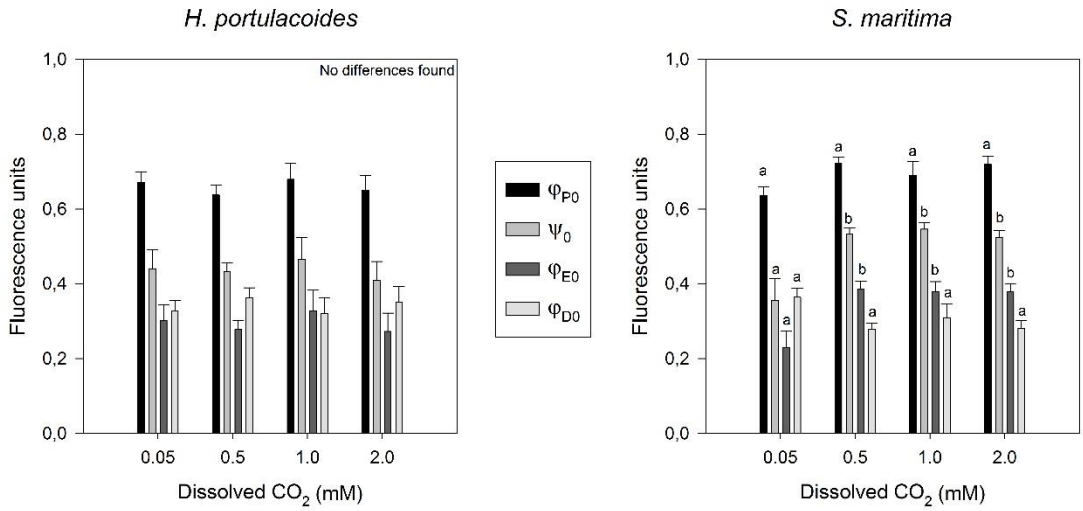

Figure 3.3.4. OJIP-driven photochemical parameters in the two tested species in light and dark conditions, at different levels of dissolved CO_2 (average ± standard deviation, n=9. Letters indicate significant differences among CO_2 treatments at $p < 0.05$).

If the driving forces variation at the various concentrations of dissolved CO_2 are analysed (Figure 3.3.5), *H. portulacoides* and *S. maritima*, showed a decrease in the driving force for photosynthesis (DF_{ABS}) mainly due to a decrease in the trapping ($DF\psi$) of the excitation energy and in the conversion of this excitation energy into electron transport ($DF\varphi$). The DF_{RC} (light energy absorption) was not affected by the increase in dissolved CO_2, in both these species. Nevertheless, in *H. portulacoides* there was a recovery of the DF_{ABS} at the highest CO_2 level, driven by a simultaneous increase in both the $DF\psi$ and $DF\varphi$.

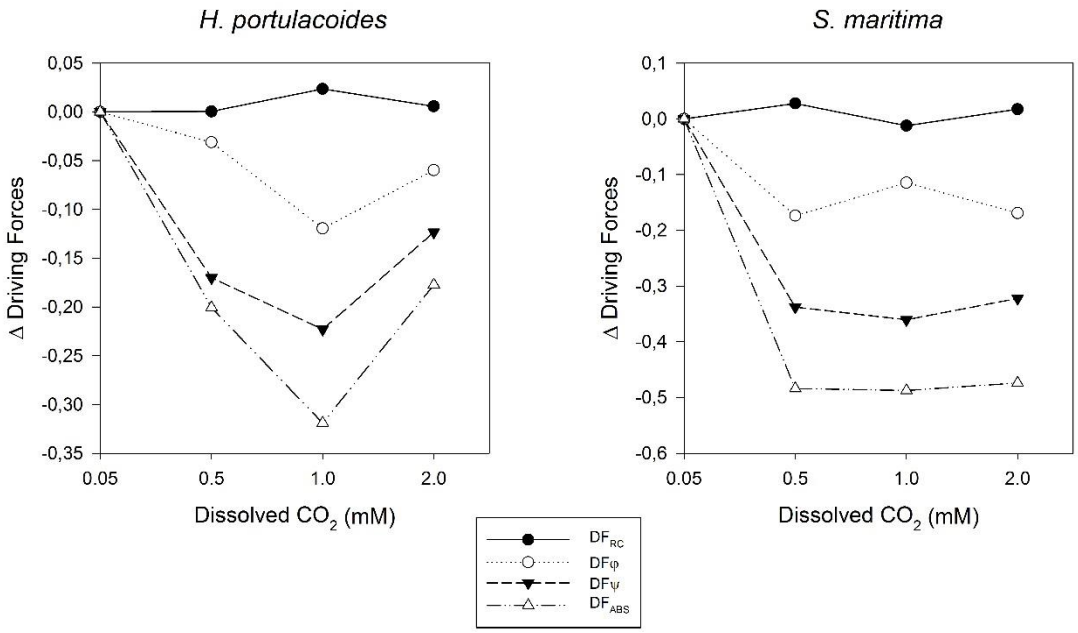

Figure 3.3.5. Photochemical reactions driving forces in the two tested species in light and dark conditions, at different levels of dissolved CO_2 (average, n=9).

Normalizing the data on a leaf cross-section basis provided new insights (Figure 3.3.6). It was possible to see that neither of the studied species presented differences in the number of available PS II reaction-centres (RC) for light harvesting (RC/CS), or in the absorbed (ABS/CS) or trapped (TR/CS) energy fluxes. On the other hand, the energy fluxes for electron transport (ET/CS) in *S. maritima* showed a marked increase upon CO_2 supplementation, while *H. portulacoides* leaves did not show any significant difference in this parameter or in the dissipated energy fluxes (DI/CS). *S. maritima*, on the other hand, showed a marked reduction in the dissipated energy values at above-ambient CO_2 concentrations. This analysis also provided insights on the connectivity between PS II antennae (P_G) and thus the PS II harvesting efficiency. While in *H. portulacoides* the increase of the antennae connectivity only occurred at the highest tested CO_2 concentrations, in *S. maritima* this could be observed in all CO_2 levels above ambient concentrations.

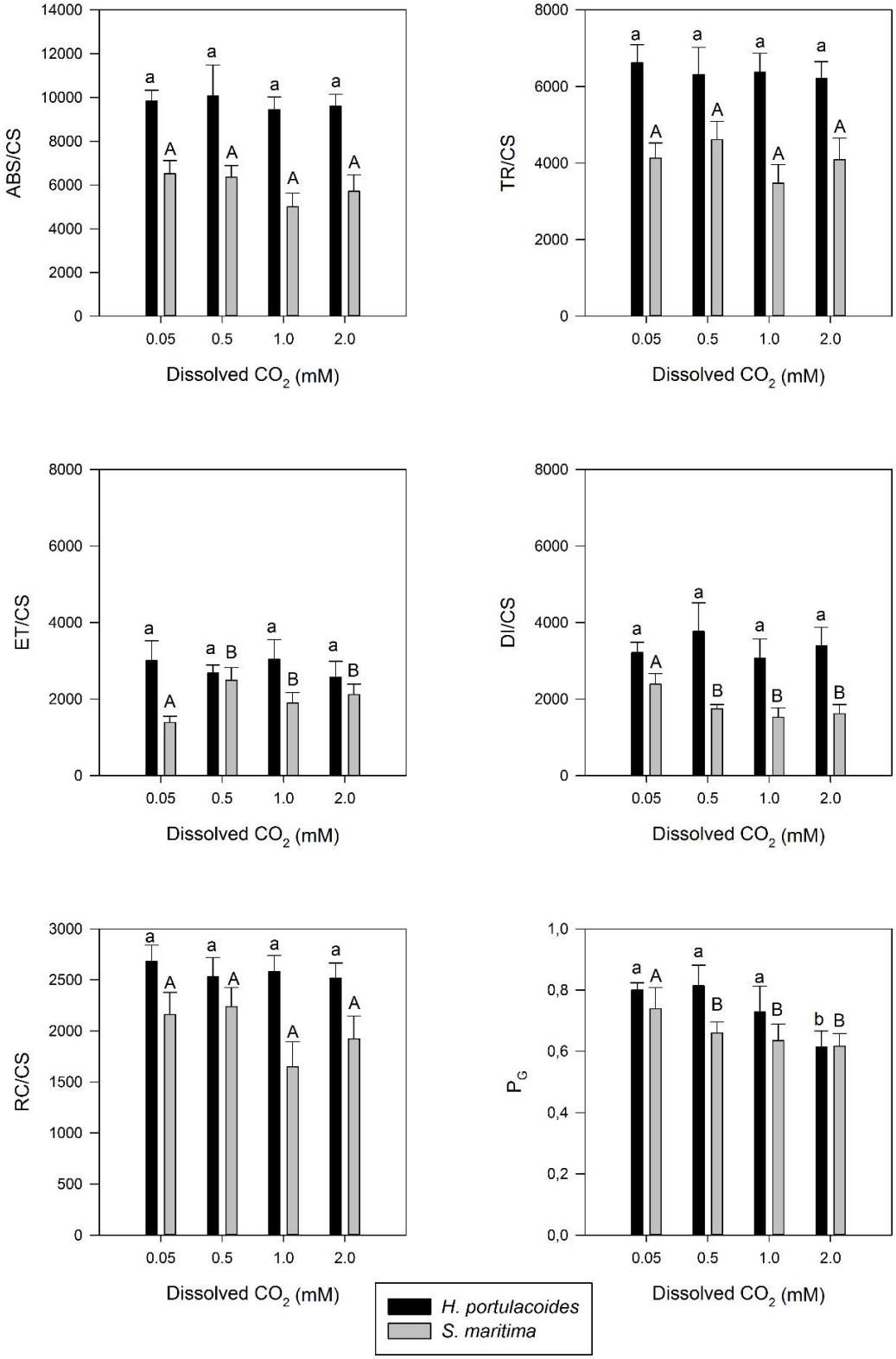

Figure 3.3.6. PS II antennae connectivity (P_G) and energy fluxes on a leaf cross-section basis, in the leaves of the two tested species in light and dark conditions, at different levels of dissolved CO_2 (average ± standard deviation, n=9. Letters indicate significant differences among CO_2 treatments at $p < 0.05$).

Anti-oxidant enzyme activities

Anti-oxidant enzymatic defences are presented in (Figure 3.3.7). *Halimione portulacoides* showed a marked increase in both CAT and SOD activities with the increasing dissolved CO_2 supply and in *S. maritima* leaves there was a decreasing trend in APx and GPx activities along with the increasing dissolved CO_2, while SOD activity increased at the highest dissolved CO_2 concentration.

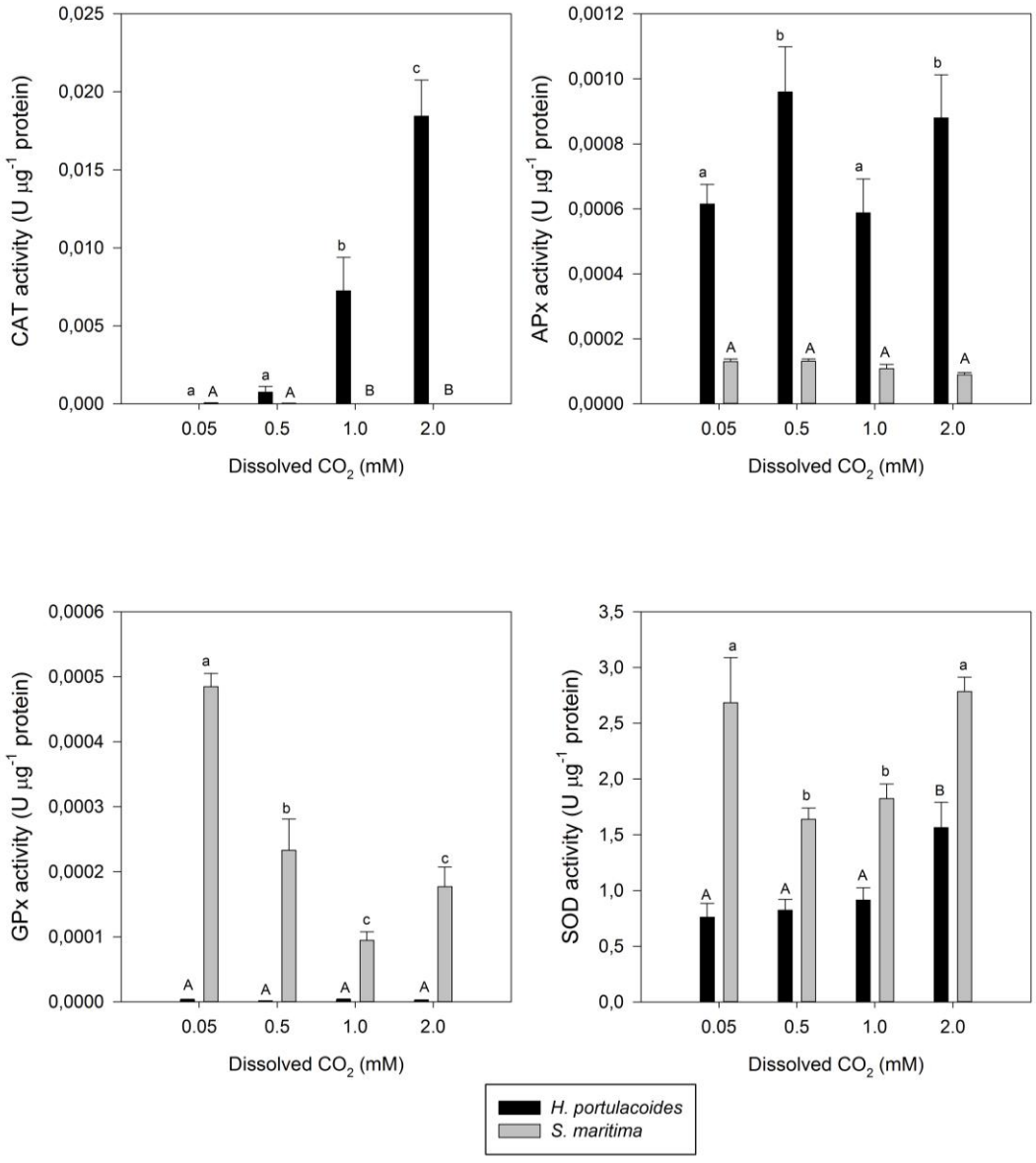

Figure 3.3.7. Peroxidase (CAT, APx and GPx) and Superoxide Dismutase (SOD) activity in the leaves of the two tested species in light and dark conditions, at different levels of dissolved CO_2 (average ± standard deviation, n=9. Letters indicate significant differences among CO_2 treatments at $p < 0.05$).

(De)Oxygenation of the water column

Considering the biomass values per square meter and the total abundance of each of the analysed species, the underwater estuarine oxygen consumption/production rates were calculated per m^2 on a daily basis, for four tested scenarios (Table 3.3.2). It was possible to calculate that *S. maritima* was responsible for the highest O_2 consumptions in the estuarine system. On the other hand, *H. portulacoides* appears as the major contributor for water column oxygenation, with high rates of O_2 production and very low rates of respiration during the night-time. Overall at the community level, as represented by these two species, an increase in the dissolved CO_2 concentrations in the water column tended to increase the oxygenation of the water column by these halophytes.

Table 3.3.2. O_2 (mol) produced (+)/consumed (-) by each halophyte (considering all the coverage area in the Tagus estuary) at the four different considered scenarios per day, during the day and night-time and considering all the estuarine halophyte community (Tagus Estuary), composed by these three species.

	Dissolved CO_2 concentration (mM)			
	0.05	**0.5**	**1**	**2**
Daytime				
H. portulacoides	3 952 ± 1397	12 050 ± 1 397	8 816 ± 2 140	7 990 ± 1 301
S. maritima	- 2 039 ± 135	- 8 79 ± 368	- 590 ± 124	801 ± 224
Night				
H. portulacoides	- 5 872 ± 196	- 3 882 ± 193	- 316 ± 224	- 297 ± 210
S. maritima	- 6 379 ± 465	- 5 885 ± 214	- 6 557 ± 207	- 5 840 ± 449
Daily Budget				
	-10 338	1 404	1 353	2 654

Discussion

Aquatic plants submerged in different coastal ecosystems, are often flooded by water with CO_2 concentrations above the air-water equilibrium (Sand-Jesen *et al*., 1992; Keeley, 1998; Ram *et al*., 1999; Pedersen *et al*., 2010; Duarte *et al*., 2014b). The dissolved CO_2 concentration is a key factor, as its availability controls underwater net photosynthesis, in both terrestrial and aquatic plants (Colmer and Pedersen, 2008; San-Jensen *et al.*, 1992). In estuaries populated with halophytes, not only is their growth controlled by dissolved CO_2, but also their function as oxygen providers/consumers. The tolerance of these plants to submersion has often been described on a basis of a quiescence response – the lack of shoot elongation conserves the carbohydrates during submersion periods (Bailey-Serres and Voesenek, 2008). At night-time an increased O_2 deficit arises as another stressor in submerged conditions due to the plants dependency on dissolved O_2 entry from flood waters, for night respiration (Waters *et al*., 1989; Pedersen *et al*., 2009; Pedersen *et al*., 2006).

In the present study, two of the more abundant halophyte species in the Portuguese estuarine ecosystems showed very different feedbacks to dissolved CO_2 increases. *H. portulacoides* submerged at low CO_2 concentrations (near the air-equilibrium), seems to have its photosynthetic rate inhibited. On the other hand, *S. maritima* proved to be highly adapted to submersion with high plasticity to this condition, allowing a quickly recovery from the stress imposed by this submersion, in agreement with recent studies (Duarte *et al*., 2014b). In this recent study the plasticity of *S. maritima* is demonstrated as an efficient adaptation to submersion, allowing it to quickly recover from the stress imposed by this condition. The photosynthetic enhancement, verified for *H. portulacoides* and *S. maritima*, has already been described for rice and for *Hordeum marinum* (Setter *et al*., 1998a; Pedersen *et al*., 2010). These authors suggested enhancement was driven by the presence of gas biofilms on the leaf surface and high tissue porosity, allowing higher rates of gas exchange according to CO_2 availability (Pedersen *et al*., 2010). Also, an increase in $[CO_2]/[O_2]$ ratio can improve CO_2 use-efficiency, due to a reduction in Rubisco oxygenase activity (Lorimer, 1981; Bowes 1993; Andersen and Pedersen, 2002). Although this enhancement was detected even at low dissolved CO_2

concentrations in *H. portulacoides*, for *S. maritima* it was only achieved at high CO_2 concentrations. Being a C_4 species, these results for *S. maritima* point to a reduction of the oxygenase activity of Rubisco driven by diffusion limitations for CO_2 entry, due to extremely high $[CO_2]/[O_2]$, and thus restricting underwater photosynthesis (Colmer *et al*., 2011). Although *S. maritima* has a high specific leaf area (SLA) compared with *H. portulacoides*, the presence of a thicker cuticle is probably the factor responsible for this reduced diffusion underwater (Mommer *et al*., 2007). On the other hand, the presence of wax-rich cuticles is a well-known factor for the formation of leaf gas micro-layers (Wagner *et al*., 2003). The presence of these wax-rich cuticles has been reported in *H. portulacoides* hydrophobic leaves (Grossi and Raphel, 2003) and can result in an improvement in gas film formation at the leaf surface, thus promoting gas exchange (Setter *et al*., 1989; Colmer and Pedersen, 2008). All these facts indicate, that, while submerged, these species are C_i-limited at normal inorganic carbon concentration in estuarine water.

Nevertheless, the anatomical differences along with the photosynthetic and electronic processes, showed marked differences in light harvesting and processing mechanisms. One important fluorescence parameter, normally associated with stress conditions is the variable fluorescence (F_v). The maximum photosynthetic O_2 production in *H. portulacoides*, verified at 0.5 mM dissolved CO_2, also showed the highest value of F'_v, an indicator of low stress conditions (Duarte *et al*., 2012). The same was true, but to a smaller extent, for the operational quantum yield of this species.

Since CO_2 and O_2 compete for the same Rubisco active sites (Taiz and Zeiger, 2002), favouring of the carboxylation process and reduction of the oxygenation capacity of Rubisco also implies a decrease in the energy costs for CO_2 fixation and consequent increase in PS II quantum yield for photosynthesis (Furbank, 1998; Taiz and Zeiger, 2002). This was confirmed by analysing the principal driving forces underlying the electronic photosynthetic processes. In *H. portulacoides* and *S. maritima* there was not only an increase in the driving forces related to the trapping of excitation energy, but also in the transfer of this energy to the electron transport chain. Both these increases, lead to an enhancement in total driving force for photosynthesis. It was also interesting to note that, in both species there were no

changes in the light energy absorption ability, confirming the above-mentioned hypothesis (increased PS II efficiency induced by higher Rubisco carboxylation rates) and pointing to an increase in photosynthetic activity due to higher CO_2 availability. In fact, in *S. maritima* this was related to an increase in the probability of a PS II trapped electron being transferred from Q_A to Q_B (ψ_0) as well as for the quantum yield of this transport between quinones (φ_{Eo}).

All these findings are confirmed by the analysis of the energy fluxes on a cross-sectional area basis. Both species maintained their number of available PS II RC constant and thus the absorbed and trapped energy fluxes did not suffer any changes. Differences arise if the integrity of the PS II antennae is observed and are the basis of the increased energy processing efficiency observed in *S. maritima* leaves. This parameter accounts for all the energetic communication pathways between neighbour PS II antennae (Strasser and Stirbet, 2001; Panda *et al*., 2006). On the contrary to what has been observed in other terrestrial plants, there was no loss of connectivity between the antennae of the PS II units during submersion, indicating an improved survival strategy for underwater conditions (Panda *et al*., 2006; Duarte *et al*., 2014b). The increased PS II antennae integrity in *S. maritima* leads to an enhanced efficiency in transporting energy and thus reduction of the dissipated energy. Although this was also noticed in *H. portulacoides* leaves subjected to the highest dissolved CO_2 concentrations tested, it did not result in a significant improvement of the energy fluxes use-efficiency, indicating that the increasing dissolved CO_2 concentrations does not affect *H. portulacoides* leaves at the energy processing but in deeper processes.

Comparing the data on anti-oxidant enzymatic activities with the data from the oxygen production, *H. portulacoides* showed a maximum photosynthetic O_2 production at 0.5 mM CO_2 decreasing towards higher CO_2 concentrations, concomitantly with an increase in catalase activity. This O_2 production decrease or increase consumption during daytime conditions as well as increased CAT activity is in agreement with photorespiratory activation. It is known that activation of photorespiration is an important part of the abiotic stress feedback as a means to dissipate the excessive energy trapped (Voss *et al*., 2013). With the activation of this mechanism, H_2O_2 is generated and scavenged by the increased CAT activity. In fact,

looking at the data from the principal driving forces, the increase in CAT activity is appears simultaneously with a decrease in the driving forces for trapping excitation energy and for photosynthesis. In the C_4 *S. maritima*, peroxidase activity (APx and GPx) showed a concomitant decrease along with the increase in O_2 production. On the other hand, SOD showed two marked peaks driven by distinct and opposite mechanisms. The first peak at 0.05 mM CO_2, is concomitant with high respiratory activity and increased non-photochemical activity, indicating a need to dissipate excessive photon energy, due to the C_i limitation, similar to that observed in plants exposed to increased atmospheric CO_2 (Geissler *et al*., 2009; Duarte *et al.*, 2014a). The second observed SOD peak, observed in individuals exposed 2 mM dissolved CO_2, is coincident with the increase in the photosynthetic activity, and consequent superoxide radical production (Taiz and Zeiger, 2002).

Nevertheless, previous studies (Duarte *et al*., 2014a) with CO_2-enriched air showed a very different trend, pointing to different stress mechanisms, occurring during submersion. While the C_3 *H. portulacoides* showed an enhancement of the photosynthetic rates while exposed to atmospheric CO_2 enrichment, the same was not observed for the C_4 *S. maritima*. In the present study this grass showed a very significant improvement in its photosynthetic rates upon dissolved CO_2 fertilization that was not observed in immersed conditions (Duarte *et al*., 2014b). This points to two interesting aspects: 1) *S. maritima* is probably C_i limited in submersed conditions and 2) CO_2 in fact ameliorates the stress imposed by submersion (Duarte *et al.*, 2014a).

All these ecophysiological responses have their repercussions for the ecosystems services provided by the salt marshes, namely in terms of O_2 and CO_2 production for the water column. Considering the average temperature used in these experiments and the biomass production drawn from the literature (Duarte *et al*., 2010; Caçador *et al*., 2009) as well as the species coverage (Caçador *et al.*, 2013), a very simple and basic extrapolation was made for the Tagus estuary salt marshes. It was possible to calculate that there is a general trend for increasing water column oxygenation during the daily tidal cycle (two tides, one in the day-time and another during the night-time), driven by plant underwater photosynthesis. This becomes of great importance if we consider salt marshes as one of the most important primary

producers in an estuarine system (Caçador *et al.*, 2007; Duarte *et al*., 2010; Caçador *et al*., 2013). Oxygen production by the halophytes becomes a key player overcoming the low rates of air-water O_2 diffusion, and thus introduces important amounts of oxygen, required for the heterotrophic species (fishes, macro-invertebrates and bacteria). According to this conclusion, a new salt-marsh service arises as a crucial O_2 producer for the estuarine aquatic community to accompany the role of these marshes as important carbon-harvesting primary producers.

Conclusions

The diurnal tidal flooding imposes on the halophyte community an underwater environment where gas concentrations are very different from the atmospheric ones. The predicted atmospheric CO_2 increase will have consequences not only on the atmospheric composition, but also in the carbonate chemistry of estuarine waters. It is important to consider the physiology of each species, and the consequences that their adaptations to altered CO_2 concentration have in terms of the ecosystem they inhabit. The presence of leaf gas films, lack of tissue porosity or other morphological traits of the leaf, as well as photochemical differences and biochemical responses to the imposed condition, are very important characteristics that from a holistic point of view have enormous impacts on the estuarine water column chemistry as a habitat for heterotrophic species. Salt marshes will play a crucial role in counterbalancing the effects of climate change, in terms of water column oxygenation and in buffering its acidification by withdrawing excess CO_2.

References

Andersen, T. and Pedersen, O., 2002. Interactions between light and CO_2 enhance the growth of *Riccia fluitans*. *Hydrobiologia* 477, 163-170.

Bailey-Serres, J. and Voesenek, L., 2008. Flooding stress: acclimatations and genetic diversity. *Annual Review of Plant Biology* 59, 313-339.

Bowes, G, 1993. Facing the inevitable: plants and increasing atmospheric CO_2. *Annual Review in Plant Physiology and Plant Molecular Biology* 44, 309–332.

Caçador, I., Caetano, M., Duarte, M. and Vale, C., 2009. Stock and losses of trace metals from salt marsh plants. *Marine Environmental Research* 67, 75-82.

Caçador, I., Neto, J.M., Duarte, B., Barroso, D.V., Pinto, M. and Marques, J.C., 2013. Development of an Angiosperm Quality Assessment Index (AQuA – Index) for ecological quality evaluation of Portuguese water bodies – A multi-metric approach. *Ecological Indicators* 25, 141-148.

Caçador, I., Tibério, S. and Cabral, H., 2007. Species zonation in Corroios salt marsh in the Tagus estuary (Portugal) and its dynamics in the past fifty years. *Hydrobiologia* 587, 205–211.

Colmer, T. and Pedersen, O., 2008. Underwater photosynthesis and respiration in leaves of submerged wetland plants: gas films improve CO_2 and O_2 exchange. *New Phytologist* 177, 918-926.

Colmer, T. and Voesenek, L., 2009. Flooding tolerance: suites of plant traits in variable environments. *Functional Plant Biology* 36, 665-681.

Colmer, T., Winkel, A. and Pedersen, O., 2011. A perspective on underwater photosynthesis in submerged terrestrial plants. *AoB Plants* plr030, 1-14.

Duarte, B., Caetano, M., Almeida, P., Vale, C., Caçador, I., 2010. Accumulation and biological cycling of heavy metal in the root-sediment system of four salt marsh species, from Tagus estuary (Portugal). *Environmental Pollution* 158, 1661-1668.

Duarte, B., Couto, T., Freitas, J., Valentim, J., Silva, H., Marques, J. C. and Caçador, I., 2013b. Abiotic modulation of *Spartina maritima* photosynthetic ecotypic variations in different latitudinal populations. *Estuarine, Coastal and Shelf Science* 130, 127-137.

Duarte, B., Raposo, P., Caçador, I., 2009. *Spartina maritima* (cordgrass) rhizosediment extracellular enzymatic activity and its role on organic matter decomposition and metal speciation processes. *Marine Ecology* 30, 65-73.

Duarte, B., Santos, D., Marques, J. C. and Caçador, I., 2013a. Ecophysiological adaptations of two halophytes to salt stress: photosynthesis, PS II photochemistry and anti-oxidant feedback - Implications for resilience in climate change. *Plant Physiology and Biochemistry* 67, 178-188.

Duarte, B., Silva, V. and Caçador, I., 2012. Hexavalent chromium reduction, uptake and oxidative biomarkers in *Halimione portulacoides*. Ecotoxicology and Environmental Safety 83, 1-7.

Duarte, B., Santos, D., Silva, H., Marques, J.C. and Caçador, I., 2014a. Photochemical and Biophysical feedbacks of C_3 and C_4 Mediterranean halophytes to atmospheric CO_2 enrichment confirmed by their stable isotope signatures. *Plant Physiology ad Biochemistry* 80, 10-22

Duarte, B., Santos, D., Marques, J.C. and Caçador, I., 2014b. Biophysical probing of *Spartina maritima* Photo-system II changes during increased submersion periods: possible adaptation to sea level rise. *Plant Physiology ad Biochemistry* 77, 122-132.

Duarte, B., Silva, G., Costa, J.L., Medeiros, J.P., Azeda, C., Sá, E., Metelo, I., Costa, M.J. and Caçador, I., 2014c. Heavy metal distribution and partitioning in the vicinity of the discharge areas of Lisbon drainage basins (Tagus Estuary, Portugal). *Journal of Sea Research* 93, 101-111.

Furbank, R. T., 1998. C4 pathway. Pp. 123–135 in A. S. Raghavendra, ed. *Photosynthesis, a comprehensive treatise*. Cambridge Univ. Press, Cambridge, U.K.

Geissler, N., Hussin, S. and Koyro, H-W., 2009. Elevated atmospheric CO_2 concentration ameliorates effects of NaCl salinity on photosynthesis and leaf structure of *Aster tripolium* L. *Journal of Experimental Botany* 60, 137-151.

Grossi, V. and Raphel, D., 2003. Long-chain (C19-C29) 1-chloro-n-alkanes in leaf waxes of halophytes of the Chenopodiaceae. *Phytochemistry* 63, 693-698.

IPCC, 2002. Climate Change and Biodiversity. IPCC Technical Paper V. Contribution of the Working Group II to the to the Fourth Assessment Report of the Intergovernmental Panel on Climate Change.

Kalaji, H., Govindjee, Bosa, K., Koscielniak, J., and Zuk-Golaszewska, K., 2011. Effects of salt stress on photosystem II efficiency and CO_2 assimilation of two Syrian barley landraces. *Environmental and Experimental Botany* 73, 64-72.

Lorimer, G. H., 1981. The carboxylation and oxygenation of Ribulose-1,5-Biphosphate Carboxylase: the primary event in photosynthesis and photorespiration. *Annual Reviews in Plant Physiology* 32, 349–383.

Mendelssohn, I. and Morris, J., 2000. Eco-Physiological Controls on the Productivity of *Spartina alterniflora* Loisel in *Concepts and Controversies in Tidal Marsh Ecology*. Springer Netherlands. 59-80.

Mommer, L., Wolters-Arts, M., Andersen, C., Visser, E.J.W. and Pedersen, O., 2007. Submergence-induced leaf acclimation in terrestrial species varying in flooding tolerance. *New Phytologist* 176, 337–345.

Panda, D., Rao, D.N., Sharma, S.G., Strasser, R.J. and Sarkar, R.K., 2006. Submergence effects on rice genotypes during seedling stage: Probing of submergence driven changes of photosystem 2 by chlorophyll a fluorescence induction O-J-I-P transients. *Photosynthetica* 44, 69-75.

Pedersen, O. and Colmer, T., 2006. Oxygen dynamics during submergence in the halophytic stem succulent *Halosarcia pergranulata*. *Plant Cell and Environment* 29, 1389-1399.

Pedersen, O., Malik, A., and Colmer, T., 2010. Submergence tolerance of *Hordeum marinum*: dissolved CO_2 determines underwater photosynthesis and growth. *Functional Plant Biology* 37, 524-531.

Pedersen, O., Rich, S.M. and Colmer, T.D., 2009. Surviving floods: leaf gas films improve O_2 and CO_2 exchange, root aeration, and growth of completely submerged rice. *The Plant Journal* 58, 147–156.

Ram, P.C., Singh, A.K., Singh, B.B., Singh, V.K., Singh, H.P., Setter, T.L., Singh, V.P. and Singh, R.K., 1999. Environmental characterization of floodwater in Eastern India: relevance to submergence tolerance of lowland rice. *Experimental Agriculture* 35, 141–152.

Sand-Jensen, K., 1989. Environmental variables and their effect on photosynthesis of aquatic plant communities. General features to aquatic photosynthesis. *Aquatic Botany* 34, 5-25.

Sand-Jensen, K., Pedersen, M.F. and Nielsen, S.L., 1992. Photosynthetic use of inorganic carbon among primary and secondary water plants in streams. *Freshwater Biology* 27, 283–293.

Serôdio J. and Catarino F., 2000. Modelling the primary production of intertidal microphytobenthos: time scales of variability and effects of migratory rhythms. *Marine Ecology Progress Series* 192, 13-30.

Setter, T.L., Waters, I., Wallace, I., Bhekasut, P. and Greenway, H., 1989. Submergence of rice I. Growth and photosynthetic response to CO_2 enrichment of floodwater. *Australian Journal of Plant Physiology* 16, 251–263.

Smith, F. and Walker, N., 1980. Photosynthesis by aquatic plants: effects of unstirred layers in relation to assimilation of CO_2 and HCO^-_3 and to carbon isotopic discrimination. *New Phytologist* 86, 245-259.

Strasser, R.J. and Stirbet, A.D., 2001. Estimation of the energetic connectivity of PS II centres in plants using the fluorescence rise O–J–I–P. Fitting of experimental data to three different PS II models. *Mathematics and Computers in Simulation* 56, 451-461.

Taiz, L., and Zeiger, E., 2002. Plant physiology. 3rd ed. Sinauer Associates, Inc., Publishers, Sunderland, MA.

Urano, K., Kurihara, Y., Motoaki, S., and Shinozaki, K., 2010. 'Omics' analyses of regulatory networks in plant abiotic stress responses. C*urrent Opinion in Plant Biology* 13, 132-138.

Voesenek, L., Rijnders, J., Peeters, A., van de Steeg, H. and Kroon, H., 2004. Plant hormones regulate fast shoot elongation under water: from genes to communities. *Ecology* 85, 16-27.

Voss, I., Sunil, B., Scheibe, R. and Raghavendra, S., 2013. Emerging concept for the role of photorespiration as an important part of abiotic stress response. *Plant Biology* 15, 713-722.

Wagner, P., Furstner, R. and Barthlott, W., 2003. Quantitative assessment to the structural basis of water repellency in natural and technical surfaces. J*ournal of Experimental Botany* 54, 1295-1303.

Waters, I., Armstrong, W., Thomson, C.J., Setter, T.L., Adkins, S., Gibbs, J. and Greenway, H., 1989. Diurnal changes in radial oxygen loss and ethanol metabolism in roots of submerged and non-submerged rice seedlings. *New Phytologist* 113, 439–451.

Yamaguchi-Shinozaki, K. and Shinozaki, K., 2006. Transcriptional regulatory networks in cellular responses and tolerance to dehydration and cold stresses. *Annual Review in Plant Biology* 57, 781-803.

3.4. SHIFTS IN SALT MARSH SEDIMENT BIOGEOCHEMICAL FUNCTIONS EXPOSED TO ELEVATED CO_2 [1]

Abstract

The increase in atmospheric CO_2 concentration resulting from increase of anthropogenic activities are known to interfere with sediment microbial communities, via plant rhizosphere. The present work intended to evaluate this interaction in *Spartina maritima* rhizosediments. For this purpose, mesocosmos trial was conducted exposing cores with *S. maritima* and its sediments to 380 and 760 ppm of CO_2 and while assessing the sediment microbial activities. There was an evident increase in the dehydrogenase activity directly linked to the microbial respiratory activity indicating a CO_2 priming effect in the rhizosphere community. Phosphatase showed a marked increase in rhizosediments exposed to elevated CO_2, indicating a higher requirement of phosphate for maintaining higher respiratory rates. The high sulphatase activity suggests a possible S-limitation as a result of elevated CO_2, probably due to higher sulphur needs for protein synthesis and thus increasing the need to acquire more labile forms of sulphur. Concomitantly with this need to acquire and synthetize amino acids, also a marked decrease in protease activity was detected. Overall a shift in the microbial activity and in their abundance (this last inferred from the dehydrogenase data) could be observed upon CO_2 fertilization, mostly due to priming effects of DOC concentration and not due to changes in the quality of carbon substrates, as shown by the sediment stable isotope signature. The improvement of recycling activity of organic N and P compounds, accompanied by a simultaneous depletion on the C recycling capacity, unbalances these biogeochemical cycles, shifting the ecosystem functions of this microbial community with inevitable changes at the ecosystem services level.

[1] This section was published in: Caçador, I., **Duarte, B.**, Marques, J.C. and Sleimi, N., 2015. Carbon mitigation: a salt marsh ecosystem service in times of change. Halophytes for Food Security in Dry Lands. Muhammad Ajmal Khan, Munir Ozturk, Bliquees Gul and Muhammad Zaheer Ahmed (Eds.) Elsevier.

Introduction

The increasing anthropogenic activities initiated with the industrial revolution, have increased atmospheric CO_2 concentration from 280 ppm to 369 ppm (Kang *et al.,* 2005), and recent projections from the Intergovernmental Panel for Climate Change (IPPC) point out to an increase to approximately 600 ppm until 2100 (IPCC, 2007). Several studies, mostly focusing on agricultural crops, have recognized the fertilization potential of elevated CO_2 increasing productivity in terrestrial ecosystems (Hunt *et al.,* 1991; Baxter *et al.,* 1994; Ainsworth and Long, 2005; Rasse *et al.,* 2005). Although there is still some controversy, it seems that elevated CO_2 will increase net primary productivity, mainly by increasing belowground carbon allocation (Kang *et al.,* 2001). Although some reports point out changes in plant C:N ratio exposed to high CO_2 concentrations, due to starch content increase and reduction of N-compounds (Cotrufo and Ineson, 1995), leaf litter chemistry did not show changes under elevated CO_2 (Hirschel *et al.,* 1997). This way, most of the possible and expectable effects of high CO_2 concentrations on soils will probably be due to interactions between root and microbial communities, rather than by differences in plant litter chemistry (Jung *et al.,* 2010).

Salt marshes are very important areas in terms of estuarine biodiversity, with elevated primary production, supporting a large number of habitats as feeding areas, shelters, nurseries, matting and reproduction sites, and as migration points (Williams *et al.,* 1994; Doyle and Otte, 1997; Vinagre *et al.,* 2008; Caçador *et al.,* 2009). Microorganisms inhabiting the halophytic species rhizosphere appear as key players in estuarine biogeochemical cycling (Duarte *et al.,* 2008). Although the adverse haline environment and potentially anoxic salt marsh sediments, these microbial communities are stimulated by the aerobic environment created in the halophyte rhizosphere throughout oxygen pumping from the atmosphere (Ludemann *et al.,* 2000). These communities have a fundamental role in the ecosystem functions, with an essential role in nutrient regeneration and organic matter decomposition. Salt marshes located at estuarine systems frequently receive large inputs of nutrients (Tobias *et al.,* 2001), and also of particulate and dissolved organic matter. The large amounts of particulate organic matter that enter the salt marsh during tidal flooding, settles in the sediments where it may be buried and serve as substrate to

decomposition processes. Microbial-mediated mechanisms play a key role in these mineralization processes (Rauch and Dennis, 2008). This large spectrum of intervention in sediment biogeochemistry makes microbial activities a very important mechanism to be considered in terms of ecosystem health (Duarte *et al*., 2012 and 2013). Recent studies suggest that marsh vegetation allocates biomass according to resource availability and capture, interconnecting this way marsh productivity with sediment mineralization and nutrient recycling processes (White *et al*., 2012). This straight relationship between sediment microbial communities and halophytes, acquire a reinforced importance if high CO_2-driven changes in primary production are considered. Therefore, changes in primary production in these estuarine ecosystems will have inevitable consequences, not only in the salt marsh community itself, but also in the adjacent areas (Jung *et al.,* 2010). About 30-60% of the net photosynthetic C is allocated in the root system, from which about 40-90% enter the sediments through rhizodeposition (Lynch and Whipps, 1990; Marschner, 1996; Duarte *et al.,* 2010; Couto *et al*., 2013). In flooded sediments, root-derived DOC may serve as a C source to the microbial community stimulating its activity (Dalenberg and Jager, 1989; Kim and Kang, 2008; Duarte *et al.,* 2008).

In the last decades, sediment extracellular enzymatic activities (EEAs) have acquired a very important role as tools for salt marsh biogeochemical functions evaluation (Kim and Kang, 2008; Duarte *et al.,* 2012; Duarte *et al.,* 2013). Extracellular enzymes serve as proxies of organic matter decomposition agents with their key activities directly linked to the mineralization of complex organic molecules of carbon, nitrogen, phosphorous and sulphur into nutrient forms easily up taken by the primary producers (Sinsabaugh *et al.,* 2008, Duarte *et al.,* 2009; Freitas *et al*., 2014). All together these enzymes can give very good insights on the microbial demand for carbon, nitrogen and phosphorous (Sinsabaugh and Moorhead, 1994; Freitas *et al*., 2014).

Microbial feedback to increasing CO_2 levels in terrestrial environments have been widely studied, both in terms of structure and community function (Mooney *et al.,* 1991), however for aquatic environments its effects are almost unknown, especially in terms of wetlands. In this study, the impacts of the predicted increase

of atmospheric [CO_2] on salt marsh sediment extracellular enzymes will be investigated as well as its effects on salt marsh biogeochemical functions.

Material and Methods

Study area, sampling and mesocosmos setup

Sampling took place at Tagus estuary Rosário salt marshes (Portugal) in the end of the summer of 2013. Rosário (38°40'N, 9°01'W) is a mature salt marsh (Valiela *et al*. 2000) located in the southern part of Tagus estuary, in the vicinity of various urbanized and industrialized zones. The upper marsh is mainly colonized by *H. portulacoides* (Chenopodiaceae) and *S. fruticosa* (Chenopodiaceae) and undergoes short submersion episodes during high tide. *Spartina maritima* (Curt.) Fernald is an herbaceous perennial plant that colonizes estuarine intertidal mudflats and is distributed throughout the coasts of western, southern, and south-eastern Europe, as well as in western Africa. It is one of the most common halophytes colonizing salt marshes in Tagus estuary, occupying approximately 2.41 km^2 from a total of 17.24 km^2 of salt marsh area (Caçador *et al.,* 2013). Sampling was performed at the end of the halophyte growing season, when the microbial community is more active (Duarte *et al*., 2008 and 2009). Ten sediment cores were collected in *S. maritima* pure stands (each core containing one *S. maritima* shoot; the inter-core plant biomass was as similar as possible) using a Plexiglas core (Ø = 8 cm; 30 cm height). Each sediment core was 15 cm in depth. The *in situ* air temperatures and PAR were recorded in order to allow an accurate replication of the environmental characteristics in the mesocosmos trials. All samples were taken to the laboratory within 1 h. At the laboratory, cores were sealed with a Plexiglas lid with a rubber stopper to prevent gas-exchange and placed in a Fytoscope 130 RGBIR (Photon System Instruments, Czech Republic). The chamber was programmed to replicate the average field air temperatures (25 ± 2 °C), relative humidity (50 ± 2 %) and the PAR evolution along the day (16 h light/8h dark sine function with a maximum PAR of 500 μmol photons m^{-2} s^{-1}), considering the light attenuation inside the core. The cores subjected to the CO_2 increase were connected to the chamber throughout specially designed connectors on their lid (Figure 3.4.1). A CO_2 gas bottle was connected to a gas-mixing unit (Waltz, Germany) mixing pure CO_2 (Linde,

Hollriegelskreuth, Germany) into CO_2–free atmospheric air (passed over soda lime) at the desired concentrations and flow rates. This allowed maintaining the reaming atmospheric characteristics intact, while manipulating atmospheric CO_2 concentration. An IrGA (Li-COR) was connected at the outlet of the gas-mixing unit preforming continuous measures of CO_2 and relative humidity of the air injected inside the cores. Relative humidity values recorded inside the chamber during the whole experiment were setup to 50 ± 2 %. Five cores were connected to the chamber inlet, receiving CO_2-enriched air, while other five were maintained in the same condition but with a normal atmosphere. At the end of 30 days, cores were sacrificed and the plants rhizosediment was collected. For all analyses 5 individuals were considered in each treatment group. Sediments for extracellular enzymatic analysis were frozen and immediately stored at - 20 °C, with the exception of the samples for dehydrogenase analysis.

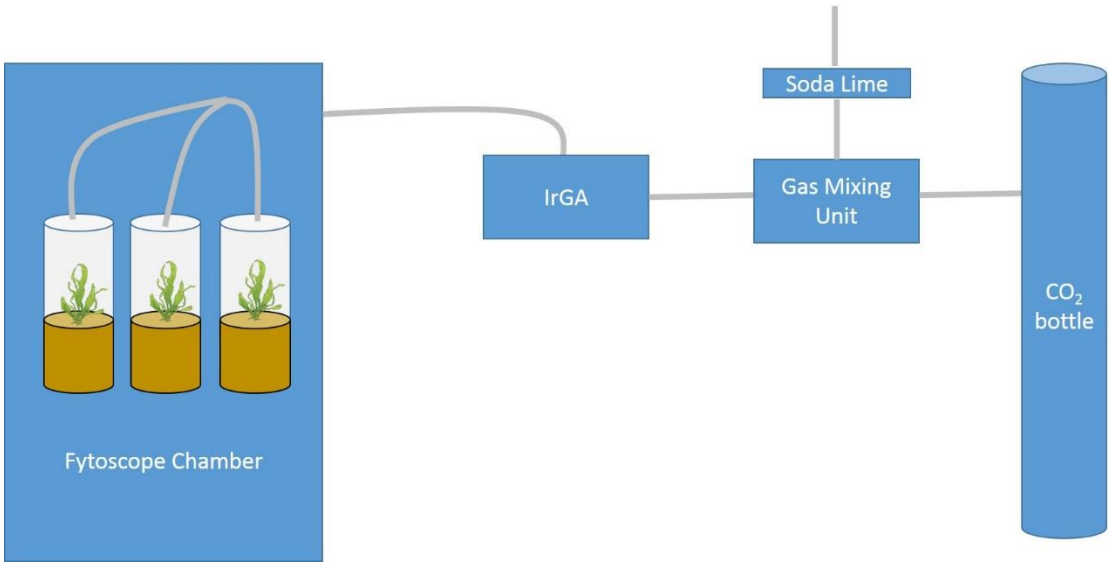

Figure 3.4.1. Experimental mesocosmos setup.

Sediment physicochemical characterization

All analyses were carried out in sediment samples from 5-8 cm depth, due to the high influence of the root system at this depth (Duarte *et al.,* 2008 and 2009). Sediment relative water content (RWC) was determined by drying sediment samples at 60 °C until constant weight. Pore water salinity was measured with a hand refractometer, after pore water extraction by centrifugation at 14,000 g for 15 min at 4 °C. Organic matter was determined by the loss on ignition (LOI) method by

burning 1 g of air-dried pulverized sediment at 600 °C for 2 h (Duarte *et al*., 2008). Sediment pH was measured using an HANNA pH/mV (HI 9025) electrode directly in the sediment. The pH calibration was performed using buffer solutions of pH 4 and pH 7.

Stable Isotope analysis

The stable isotope composition of the pulverized samples was determined as described in Chapter 3, Section 2 (Duarte *et al*., 2014).

Dehydrogenase and Extracellular Enzymatic Activities (EEA)

All enzymatic determinations were carried out with colorimetric methods and the absorbance was read on a TECAN Absorbance Microplate Reader (SPECTRA Rainbow). The use of microplates allowed performing three readings (analysis replicates) of the same sample replicate, giving a total of 15 replicate readings. In all samples the roots were sorted out for the enzymatic assays. Dehydrogenase activity (DHA) was determined using the TTC method according to Thalmann (1968) immediately after sampling. Briefly, approximately 5 g of frozen sediment were incubated with 5 ml of TTC solution (1 %). Samples without the substrate were also prepared with 5 ml Tris-HCl buffer (100 mM) instead of the TTC solution. Incubation was made at 30 °C for 24 h. After incubation, 40 ml of acetone were added to each tube and shaken. The tubes were kept in the dark for 2 h and centrifuged at 14,000 g for 15 minutes, at 4 °C. The clear supernatant absorbance was read on a TECAN Absorbance Microplate Reader (SPECTRA Rainbow) at 546 nm. All extracellular enzymatic analysis were carried out within a week after storage. Prior to assay sediments were warmed at room temperature while mixed in the respective assay buffer. For urease activity (UA) determination all lab wares were soaked for two days in HCl (10%) and rinsed with distilled water to avoid ammonia contaminations. Urease activity was assayed according to Askin and Kizikaya (2006). Briefly approximately 2 g of sediment were incubated with 3.75 ml of citrate buffer (50 mM, pH 6.7) and 5 ml of urea 10% (w/v). Samples without the substrate were also prepared in order to subtract the citrate-extractable ammonia. The incubation was made at 37 °C, for 3 h. After this period the samples were centrifuged at 4,000 g for

15 min, at 4 °C. One ml of supernatant was diluted to a final volume of 10 ml with distilled water. This solution was used for ammonia determination using the iodophenol-blue method (Koroleff, 1969). Ammonia concentrations were read at 630 nm and urease activity expressed as μmol NH_4 formed per gram of sediment fresh weigh per hour. Peroxidase, β-glucosidase, phosphatase and sulphatase were assayed according to Ravit *et al.,* (2003) with a modification in the incubation temperature and without dilution of the supernatant (Duarte *et al.,* 2008). Briefly, 75 ml of sodium acetate buffer (pH 5) was added to 5 g of fresh sediment, and mixed for 1 min in order to obtain the sediment slurry. The substrates (5 mM) used were p-nitrophenyl-glucoside, p-nitrophenyl-phosphate and p-nitrophenyl-sulphate, respectively for β-glucosidase, phosphatase and sulphatase. Two ml of each substrate were added to 2 ml of slurry and incubated at 30 °C with gentle agitation for 60 min (sulphatase, β-glucosidase and peroxidase) and 30 min (phosphatase). After the incubation, samples were centrifuged at 6 530 x g for 15 min, at 4 °C and 0.2 ml of 1 N NaOH was added in order to stop the reaction and reveal the p-nitrophenol (pNP) formed. Absorbance of the supernatant was read at 410 nm and compared with the calibration curve for pNP. The activity was expressed as μg of pNP released per gram of sediment dry weight per hour. Peroxidase was assayed using 5 mM L-DOPA (L-3,4-dihydroxyphenylalanine) as substrate. 2 ml were added to 2 ml of slurry and 0.1 ml of 0.3 % H_2O_2 and incubated for 60 min. After incubation samples were centrifuged as described above. Absorbance of supernatant was read at 460 nm and the activity was expressed as μmol L-DOPA oxidized per gram sediment dry weight per hour, by comparison with the L-DOPA standard curve. Protease activity was assayed according to Ladd *et al.,* (1976). Briefly, 1 g of fresh sediments was incubated with 5 ml of Tris (Trishydroxymethyl-aminomethane) buffer (0.05 M, pH 8.1) and a 2% (w/v) casein solution, for 2 h at 50 °C. After incubation the reaction was stopped with 1 ml of thichloroacetic acid 17.5 % (w/v) and centrifuged at 14 690 x g for 15 min, at 4 °C. For photometric analysis, 1 ml of supernatant was added to 1 ml of Folin-Ciocalteu's phenol reagent (0.2 N) and 2.5 alkali reagent, and left to stand for 90 min. The colour developed was measured at

700 nm and compared with a calibration curve for tyrosine. Activity was expressed as μg tyrosine equivalents per gram of sediment dry weight per hour.

Statistical Analysis

Due to the lack of normality and homogeneity, the statistical analysis of the data was based in non-parametric tests. In order to compare the similarities between the two treatments tested a Similarity Percentage test (SIMPER) was performed using Primer 6 software (Clarke and Gorley, 2006). For this purpose the data was first log (x+1) transformed and normalised using Primer normalisation algorithms, to avoid interference of the different orders of greatness of each of the input variables. The SIMPER analysis has the propose of identify variables primarily responsible for differences between two or more groups of ecological samples, having has output a measure of the distance among the tested groups (d^2) as well as the contribution in percentage of each variable to the overall distance among sample groups (Clarke and Gorley, 2006). The ANOSIM coupled analysis provided the overall significance of the distance among treatment groups.

Results

Physic-Chemical sediment characteristics and stable isotope signatures

As it can be observed in Figure 3.4.2, both groups of sediments present very similar values of all analysed physic-chemical parameters (SIMPER d^2 = 9.83). It is possible to observe that the variability inside each treatment group is very reduced, presenting high similarity values among samples exposed to ambient (SIMPER d^2 = 0.96) and to elevated CO_2 (SIMPER d^2 = 4.75), although in this last case there is a lower degree of similarity. The pH and redox potential appear as the factors with higher contribution for the resemblances between CO_2 treatments (cumulative contribution = 61.28 %).

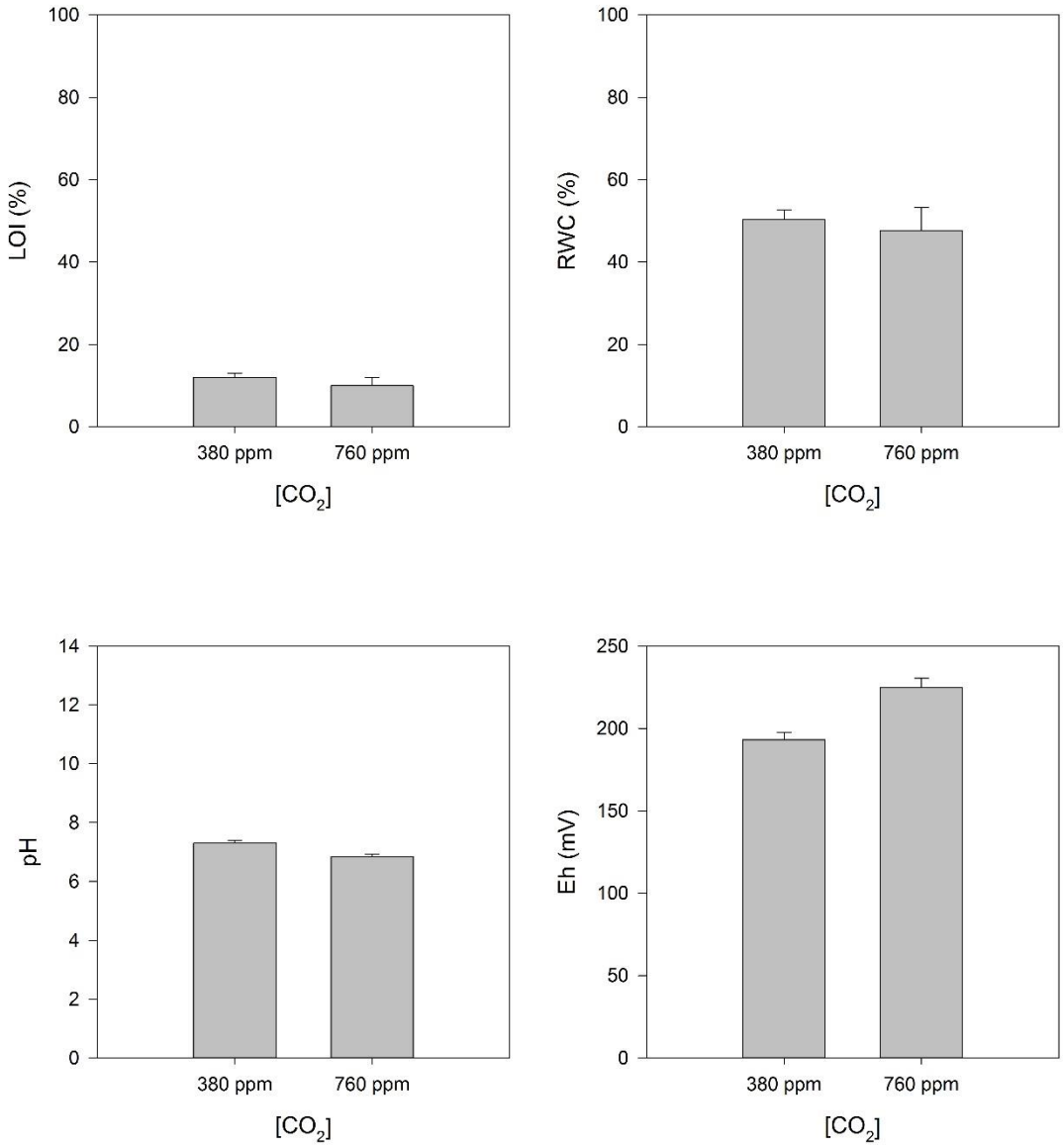

Figure 3.4.2. Physic-chemical parameters of both groups of sediments (n = 5) exposed to 380 ppm (ambient) and to 760 ppm (elevated) of CO_2 (average ± standard deviation).

Regarding the stable isotope analysis of the organic matter present in the sediment (Figure 3.4.3), it is possible to observe that there is an overlap of the isotopic signatures of the sediments from both the tested atmospheric CO_2 concentrations (d^2 = 0.57), indicating a very similar organic matter quality in both sediment groups.

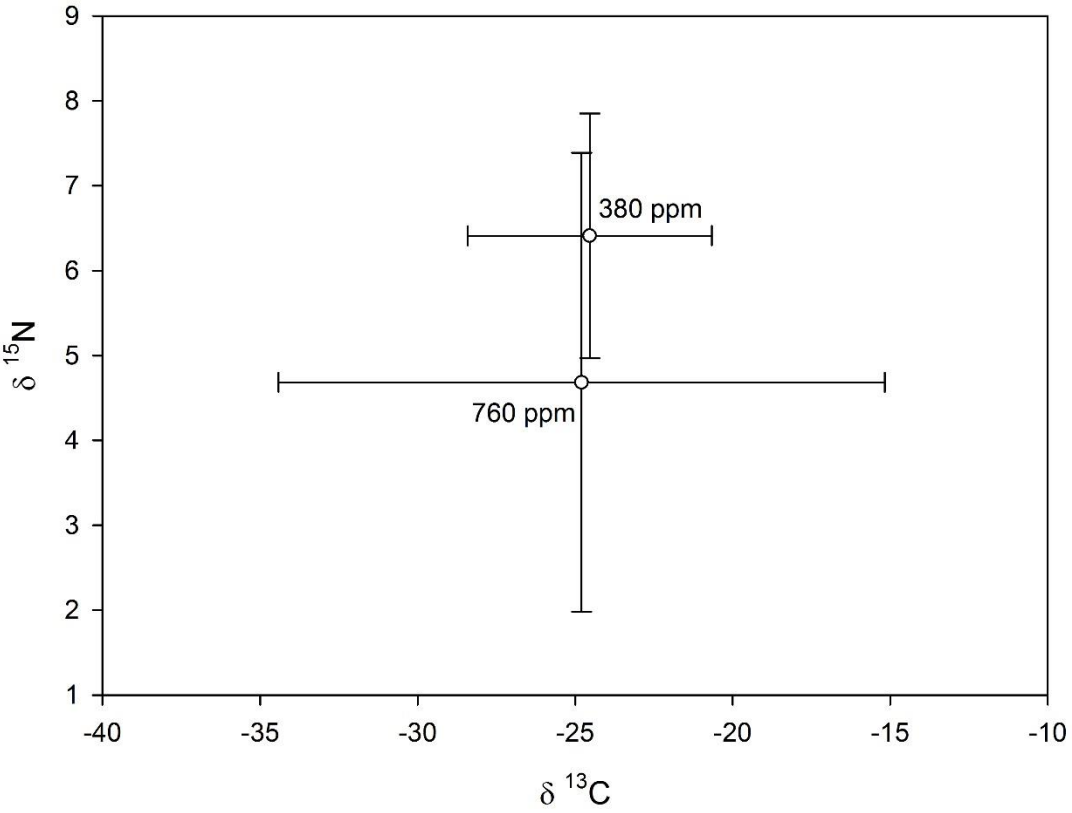

Figure 3.4.3. $\delta^{13}C$ and $\delta^{15}N$ Stable isotope signatures of both sediments (n = 5) exposed to 380 ppm (ambient) and to 760 ppm (elevated) of CO_2 (average ± standard deviation).

Active microbial cells measured by Dehydrogenase

As shown in Figure 3.4.4, sediments exposed to elevated CO_2 presented a very high dehydrogenase activity, a proxy of active microbial cells. Also in this case, there is a high degree of similarity among samples subjected to the same treatment (d^2_{380ppm} = 0.52; d^2_{760ppm} = 0.60. Ranking this activity along with the remaining enzymatic variables, dehydrogenase appears, not only, as the variable that contributes more to the similarity among samples subjected to the same treatment, but also as the variable with higher contribution for the differences observed among CO_2 treatments (d^2 = 4.05, contribution = 20.57%).

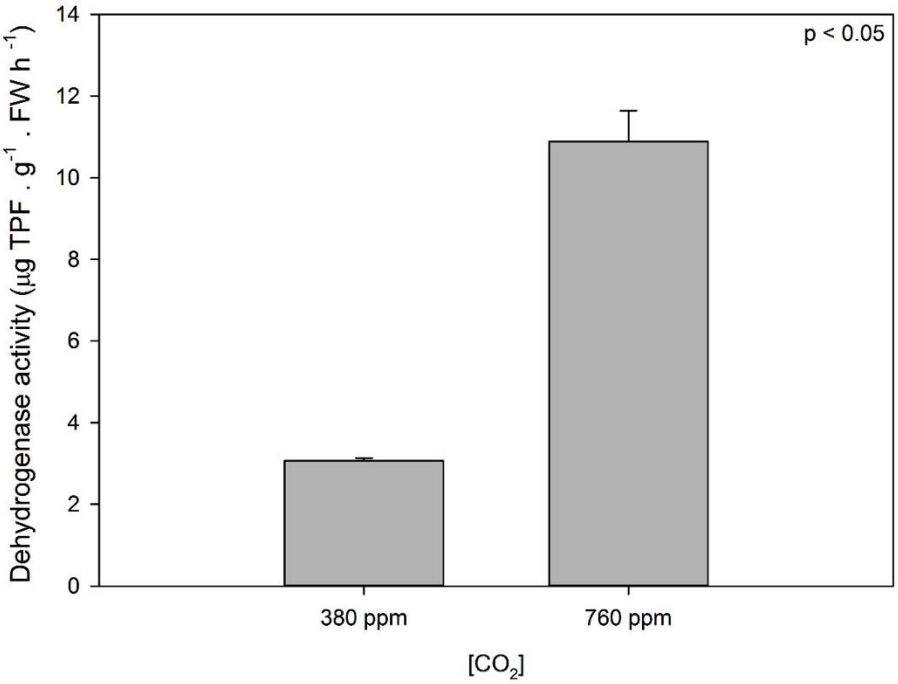

Figure 3.4.4. Dehydrogenase activity in both groups of sediments (n = 5) exposed to 380 ppm (ambient) and to 760 ppm (elevated) of CO_2 (average ± standard deviation).

Extracellular Enzymatic Activities

Two different patterns of activity could be observed between CO_2 treatments (Figure 3.4.5). While sulphatase, protease and phosphatase showed an increase in activity upon exposure to 760 ppm CO_2, protease, β-glucosidase and urease showed a decrease in its activities in sediments exposed to elevated atmospheric CO_2 concentrations. The major dissimilarities between the two treatment groups were found to be on protease (d^2 = 2.84, contribution 16.46 %), urease (d^2 = 2.69, contribution 15.62 %) and sulphatase (d^2 = 2.22, contribution 12.90%) activities. Although some differences can be observed in phosphatase, β–glucosidase and peroxidase activities, the dissimilarities were not significant among CO_2 concentrations. In fact, these enzymes activities contributed with 34.35% to the similarity among treatments (d^2 = 1.91, 1.96 and 2.07 respectively).

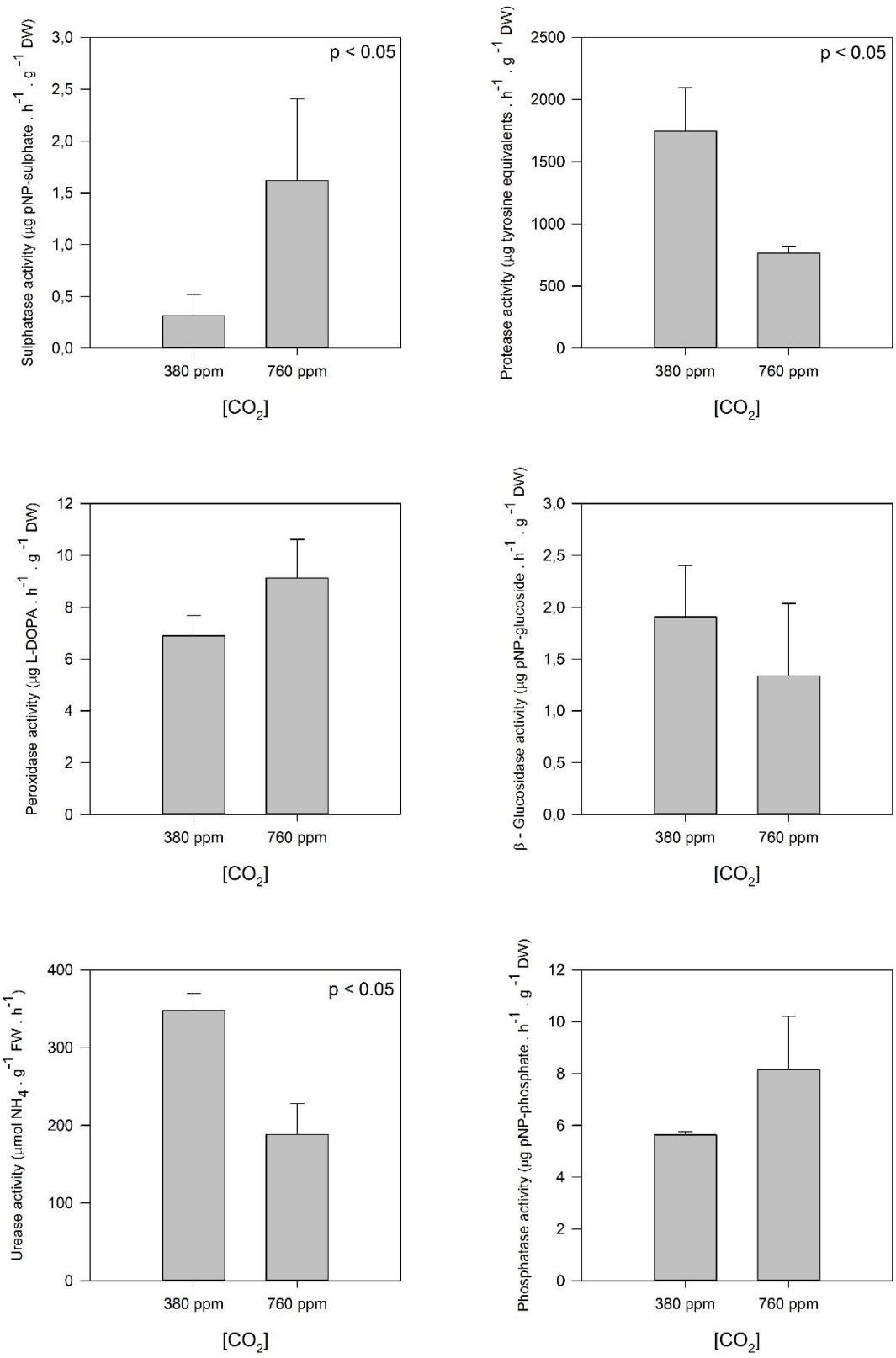

Figure 3.4.5. Extracellular Enzymatic Activities (EEA) in both groups of sediments (n = 5) exposed to 380 ppm (ambient) and to 760 ppm (elevated) of CO_2 (average ± standard deviation).

Discussion

In the last years, several studies have addressed the effects of elevated CO_2 on plant productivity and soil biota, focusing mainly on terrestrial environments. Only more recently, this issue has been addressed for aquatic environments. Previous studies have suggested that marsh vegetation increases root-driven DOC release under CO_2 fertilization (Kim ad Kang, 2008). DOC increase is expected to enhance organic matter decomposition through a priming effect (Allard *et al.,* 2006). According to these last authors, the priming effect would result an increase of sediment organic matter, driven by plant rhizodepositon of organic carbon forms. These plant-driven carbon sources are not metabolized but their increase stimulates the decomposition of sediment organic matter (Allard *et al*., 2006). In addition, an increase in DOC concentrations will also lead to an enhancement of the activity of several extracellular enzymatic activities involved, not only in the carbon cycle, but also in the mineralization of other nutrient forms (Shackle *et al*., 2006). Generally, rhizospheres accumulate higher labile carbon amounts than in bulk sediments, due to the exudation of photosynthesis products into the rhizosphere (Domanski *et al.,* 2001; Jung *et al.,* 2010). This way, DOC increase in the rhizosphere will enhance microbial activities, due to its normal C limitation (Jung *et al.,* 2010). Another key factor, regulating sediment carbon pool under elevated CO_2, is nitrogen concentration. In N-limited systems there is no observable activity increase under elevated CO_2 (Hungate *et al.,* 2009). In the present study, there was an evident increase in dehydrogenase activity, directly linked to microbial respiratory activity, pointing out to a priming effect of elevated CO_2 in the rhizosphere community. Simultaneously, it could be observed that the type of organic matter, here evaluated by its isotopic signature, did not change substantially, indicating that there were no changes in the organic molecules chemical composition introduced into the rhizosphere. Although these effects are markedly observable in the abundance and respiratory activity of the microorganisms inhabiting the halophyte rhizosphere, also their ecosystem functions suffered shifts, as observed by its EEAs. Unlike some carbon and nitrogen enzymes, phosphatase showed a marked increase in the rhizosediments exposed to elevated CO_2, pointing out to an enhancement of the production of higher amounts of inorganic phosphate allowing microbial growth at

higher rates (Kang *et al.,* 2005). This was already reported for several other ecosystems like in *Sphagnum*-dominated wetlands (Kang *et al.,* 2005), tundra (Moorhead and Linkins, 1997), Mediterranean ecosystems (Dhillion *et al.,* 1996) and grasslands (Ebersberger*et al.,* 2003). This is in accordance to another mechanism of CO_2 interference in rhizosphere microbes. Increased concentrations of easily usable carbon sources, like monosaccharides, may inhibit some carbon-related enzymes (e.g. β-glucosidase) whilst other enzyme activities (e.g. phosphatase) may be increase to relieve the limitation by other nutrients (Moorhead and Linkins, 1997; Barret *et al.,* 1998; Kang *et al.,* 2001). Furthermore, actively growing vegetation under high atmospheric CO_2 can compete with microbes for organic nutrients, resulting in an activity decrease in some functional microbial groups (Freeman *et al.,* 1998). Sulphatase also showed a marked increase under high CO_2. Sulphur is an essential component of several amino acids, like cysteine and methionine. The high activity of this enzyme, suggests a possible S-limitation as result of CO_2 fertilization (Kelley *et al.,* 2011). The increase in microbial biomass and/or activity (as suggested by its proxy, dehydrogenase) increases the requirements in sulphur for protein synthesis and thus the needs to acquire more labile sulphur forms, like SO_4^{2-}(Kelley *et al.,* 2011). Concomitantly with this need to acquire and synthetize amino acids, there was also a marked decrease in protease activity. This is in accordance with the conclusions withdrawn from dehydrogenase activity, suggesting that there are no signs of N-limitation since N-linked enzymes all showed activity decreases under elevated CO_2 (Kelley *et al.,* 2011; Kampichler *et al.,* 1998). The same can be inferred if urease activity is observed. This enzyme produces NH_4 and CO_2 from urea hydrolysis (Askin and Kizikaya, 2006). In this case, there could have been an inhibitory effect driven from excessive reaction products accumulation in the medium (Kampichler *et al.,* 1998), mostly high NH_4 concentrations (Duarte *et al.,* 2012), impairing urease activity. This is in agreement with the hypothesis provided by Langley and Megonigal (2010), pointing out not to a local response from the plant or from the sediments, but to a concerted feedback from the plant-sediment system. According to these authors, excessive phytoavailable N-forms, like NH_4, would lead to a negative feedback from C_4 plants to CO_2 increase. Also, the exposure of sediments to elevated CO_2 concentrations could have contributed to a similar effect,

since CO_2 is also a reaction product from urease activity. Overall, a shift in the microbial activity and possible in their abundance (this last inferred from the dehydrogenase data) could be observed upon CO_2 fertilization, mostly due the priming effects of plant-driven DOC rhizodeposition stimulating microbial activity and not due to the variations in the quality of the carbon substrates, as could be expected.

Conclusions

Sediment microorganisms are known to be affected by elevated CO_2 concentrations, due to its interactions with plants, especially in its rhizosphere. High carbon supplies from plants, resulting from CO_2 increase, changes microbial activities whether decreasing or enhancing it. Since these microorganisms are key players in the biogeochemical cycles occurring in salt marshes, these shifts will have impacts on the marsh and even on the estuarine system. The improvement of the recycling activity of organic N and P compounds and simultaneous depletion on the recycling capacity of C, will unbalance the interconnections between these biogeochemical cycles, affecting nutrient regeneration and supply to the primary producers, not only of the marsh but of all the estuarine system.

References

Ainsworth, E. A. and Long, S. P., 2005. What have we learned from 15 years of free-air CO_2 enrichment (FACE): a meta-analytic review of the responses of photosynthesis, canopy properties and plant production to rising CO_2. *New Phytologist* 165, 351–372.

Allard, V., Robin, C., Newton, P. C. D., Lieffering, M. and Soussana, J. F., 2006. Short and long-term effects of elevated CO_2 on *Lolium perenne* rhizodeposition and its consequences on soil organic matter turnover and plant N yield. *Soil Biology and Biochemistry* 38, 1178–1187.

Askin, T. and Kizilkaya, R., 2006. Assessing spatial variability of soil enzyme activities in pasture topsoils using geostatistics. *European Journal of Soil Biology* 42, 230-237.

Barrett, D.J., Richardson, A.E. and Gifford, R.M., 1998. Elevated atmospheric CO_2 concentrations increase wheat root phosphatase activity when growth is limited by phosphorus. *Australian Journal of Plant Physiology* 25, 87-93.

Baxter, R., Gantley, M., Ashenden, T.W. and Farrar, J.F., 1994. Effects of elevated carbon dioxide on 3 grass species from montane pasture. 2. Nutrient-uptake, allocation and efficiency of use. *Journal of Experimental Botany* 45, 1267-1278.

Caçador, I., Caetano, M., Duarte, B. and Vale, C., 2009. Stock and losses of trace metals from salt marsh plants. *Marine Environmental Research* 67, 75-82.

Caçador, I., Neto, J.M., Duarte, B., Barroso, D.V., Pinto, M. and Marques, J.C., 2013. Development of an Angiosperm Quality Assessment Index (AQuA – Index) for ecological quality evaluation of Portuguese water bodies – A multi-metric approach. *Ecological Indicators* 25, 141-148.

Clarke, K.R., Gorley, R.N., 2006. PRIMER v6: User Manual/Tutorial. PRIMER-E, Plymouth.

Cotrufo, M.F. and Ineson, P., 1995. Effects of enhanced atmospheric CO_2 and nutrient supply on the quality and subsequent decomposition of the fine roots of *Betula pendula* Roth. and *Piceas itchensis*(Bong.) Carr. *Plant and Soil* 170, 267-277.

Couto, T., Duarte, B., Caçador, I., Baeta, A. and Marques, J.C., 2013. Salt marsh plants carbon storage in a temperate Atlantic estuary illustrated by a stable isotopic analysis based approach. *Ecological Indicators* 32, 305-311.

Dalenberg, J. W. andJager, G., 1989. Priming effect of some organic additions to ^{14}C-labeled soil. *Soil Biology and Biochemistry* 21, 443–448.

Dhillion, S., Roy, J. and Abrams, M., 1996. Assessing the impact of elevated CO_2 on soil microbial activity in a Mediterranean model ecosystem. *Plant and Soil* 187, 333–342.

Domanski, G., Kuzyakov, Y., Siniakina, D. and Stahr, K., 2001. Carbon flows in the rhizosphere of ryegrass (*Lolium perenne*). Jou*rnal of Plant Nutrition and Soil Science* 164, 381-387.

Doyle, M. and Otte, M., 1997. Organism-induced accumulation of Fe, Zn and As in wetland soils. *Environmental Pollution* 96, 1-11.

Duarte, B., Caetano, M., Almeida, P., Vale, C. and Caçador, I., 2010. Accumulation and biological cycling of heavy metal in the root-sediment system of four salt marsh species, from Tagus estuary (Portugal). *Environmental Pollution* 158, 1661-1668.

Duarte, B., Freitas, J. and Caçador, I., 2012. Sediment microbial activities and physic-chemistry as progress indicators of salt marsh restoration processes. *Ecological Indicators* 19, 231-239.

Duarte, B., Freitas, J., Couto, T., Silva, H., Marques, J. C. and Caçador, I., 2013. New multi-metric Salt marsh Sediment Microbial Index (SSMI) application to salt marsh sediments ecological status assessment. *Ecological Indicators* 29, 390-397.

Duarte, B., Raposo, P., Caçador, I., 2009. *Spartina maritima* (cordgrass) rhizosediment extracellular enzymatic activity and its role on organic matter decomposition and metal speciation processes. *Marine Ecology* 30, 65-73.

Duarte, B., Reboreda, R. and Caçador, I., 2008. Seasonal variation of Extracellular Enzymatic Activity (EEA) and its influence on metal speciation in a polluted salt marsh. *Chemosphere* 73, 1056-1063.

Ebersberger, D., Niklaus, P. A. and Kandeler, K., 2003. Long term CO_2 enrichment stimulates N-mineralisation and enzyme activities in calcareous grassland. *Soil Biology and Biochemistry* 35, 965–972.

Freeman, C., Baxter, R., Farrar, J.F., Jones, S.E., Plum, S., Ashendon, T.W. and Stirling, C., 1998. Could competition between plants and microbes regulate plant nutrition and atmospheric CO_2 concentration? *Science of Total Environment* 220, 181-184.

Freitas, J., Duarte, B. and Caçador, I. Biogeochemical drivers of phosphatase activity in salt marsh sediments. *Journal of Sea Research* 93, 101-111.

Hirschel, G., Korner, C. and Arnone, J.A. 3rd., 1997. Will rising atmospheric CO_2 affect leaf litter quality and in situ decomposition rates in native plant communities? *Oecologia* 110, 387-392.

Hungate, B.A., van Groenigen, K.J., Six, J., Jastrow, J.D., Luo, Y., de Graaff, M.A., van Kessel, C. and Osenberg, C.W., 2009. Assessing the effects of elevated carbon dioxide on soil carbon: a comparison of four meta-analyses. *Global Change Biology* 15, 2020-2034.

Hunt, R., Hand, D.W., Hannah, M.A. and Neal, A.M., 1991. Response of CO_2 enrichment in 27 herbaceous species. *Functional Ecology* 5, 410-421.

IPCC. 2007. Summary for policymakers. In: Climate Change 2007: The Physical Science Basis. Contribution of Working Group I to the Fourth Assessment Report of the Intergovernmental Panel on Climate Change (Solomon S, Qin D, Manning M, Chen Z, Marquis M, Averyt KB, Tignor M, Miller HL eds). Cambridge University Press, Cambridge and New York, NY.

Jung, S., Lee, S-H., Park, S-S. and Kang, H., 2010. Effects of elevated CO_2 on organic matter decomposition capacities and community structure of sulfate-reducing bacteria in salt marsh sediment. *Journal of Ecology and Field Biology* 33, 261-270.

Kampichler, C., Kandeler, E., Bardgett, R.D., Jones, T.H. and Thompson, J., 1998. Impact of elevated atmospheric CO_2 concentration on soil microbial biomass and activity in a complex, weedy field model ecosystem. *Global Change Biology* 4, 335-346.

Kang, H. J., Freeman, C. and Ashendon, T. W., 2001. Effects of elevated CO_2 on fen peat biogeochemistry. *Science of the Total Environment* 279, 45–50.

Kang, H., Kim, S.-Y., Fenner, N. and Freeman, C., 2005. Shifts of soil enzyme activities in wetlands exposed to elevated CO_2. *Science of the Total Environment* 337, 207–212.

Kelley, A.M., Fay, P.A., Polley, H.W., Gill, R.A. and Jackson, R.B., 2011. Atmospheric CO_2 and soil extracellular enzyme activity: a meta-analysis and CO_2 gradient experiment. *Ecosphere* 2, 1-20.

Kim, S-Y. and Kang, H., 2008. Effects of elevated CO_2 on below—ground processes in temperate marsh microcosms. *Hydrobiologia* 605, 123-130.

Koroleff, F., 1969. Direct determination of ammonia in natural waters as indophenol blue, *International Conference in the Exploration of the Sea*. ICES, Denmark.

Ladd, J.N., Brisbane, P.G. and Butler, J.H.A., 1976. Studies on soil fumigation. 3. Effects on enzyme-activities, bacterial numbers and extractable ninhydrin reactive compounds. Soil *Biology and Biochemistry* 8, 255–260.

Langley, J.A. and Megonigal, J.P., 2010. Ecosystem response to elevated CO2 levels limited by nitrogen-induced plant species shift. *Nature* 466, 96-99.

Ludemann H., Arth I. and Wiesack W., 2000. Spatial changes in the bacterial community structure along a vertical oxygen gradient in flooded paddy soil cores. *Applied and Environmental Microbiology* 66, 754–762.

Lynch, J. M. and Whipps, J. M., 1990. Substrate flow in the rhizosphere. *Plant and Soil* 129, 1–10.

Marschner, H., 1996. Mineral Nutrition of Higher Plants.Academic Press, London.

Mooney, H.A., Drake, B.G., Luxmoore, R.J., Oechel, W.C. and Pitelka, L.F., 1991. How will terrestrial ecosystems interact with changing CO_2 concentration of the atmosphere and anticipated climate change? *BioScience* 41, 96-104.

Moorhead, D.L. and Linkins, A.E., 1997. Elevated CO_2 alters belowground exoenzyme activities in tussock tundra. *Plant and Soil* 189, 321-329.

Rasse, D. P., Peresta, G. and Drake, B. G., 2005. Seventeen years of elevated CO_2 exposure in a Chesapeake Bay Wetland: sustained but contrasting responses of plant growth and CO_2 uptake. *Global Change Biology* 11, 369–377.

Rauch, M. and Dennis, L., 2008. Spatio-temporal variability in benthic mineralization processes in the eastern English Channel. *Biogeochemistry* 89, 163–180.

Ravit, B., Ehrenfeld, J.G. and Haggblom, M.M., 2003. A comparison of sediment microbial communities associated with *Phragmites australis* and *Spartina alterniflora* in two brackish wetlands of New Jersey. *Estuaries* 26, 465–474.

Shackle, V., Freeman C. and Reynolds, B., 2006. Exogenous enzyme supplements to promote treatment efficiency in constructed wetlands. *Science of the Total Environment* 361, 18–24.

Sinsabaugh, R. L., Laber, C.L., Weintraub, M.N., Ahmed, B., Allison, S.D., Crenshaw, C., Contosta, A.R., Cusack, D., Frey, S., Gallo, M.E., Gartner, T.B., Hobbie, S.E., Holland, K., Keeler, B.L., Powers, J.S., Stursova, M., Takacs-Vesbach, C., Waldrop, M.P., Wallenstein, M.D., Zak, D.R. and Zeglin, L.H. 2008. Stoichiometry of soil enzyme activity at global scale. *Ecology Letters* 11, 1252–1264.

Sinsabaugh, R.L. and Moorhead, D.L., 1994. Resource allocation to extracellular enzyme production: a model for nitrogen and phosphorus control of litter decomposition. *Soil Biology and Biochemistry* 26, 1305– 1311.

Thalmann, A. 1968. Zur Methodik der Bestimmung der Dehydrogenase Aktivität in Boden Mittels Triphenyltetrazoliumchlorid (TTC). Landwirtsch. Forsch. 21, 249-258.

Tobias C., Macko S., Anderson I. and Canuel E., 2001. Tracking the fate of a high concentration groundwater nitrate plume through a fringing marsh: a combined groundwater tracer and in situ isotope enrichment study. *Limnology and Oceanography* 46, 1977–1989.

Valiela, I., Cole, M., McClelland, J., Cebrian, J. and Joye, S.B., 2000. Role of salt marshes as part of coastal landscapes. In: Weinstein, M.P., Kreeger, D.A. (Eds.), *Concepts and Controversies in Tidal Marsh Ecology*. Kluwer Academic Publishers, London.

Vinagre, C., Cabral, H. and Caçador, I., 2008. Influence of halophytes and metal contamination on salt marsh macro-benthic communities. *Estuarine, Coastal and Shelf Science* 76, 715-722.

White, K.P., Langley, J.A., Cahoon, D.R. and Medonigal, J.P., 2012. C3 and C4 Biomass Allocation Responses to Elevated CO_2 and Nitrogen: Contrasting Resource Capture Strategies. *Estuaries and Coasts* 35, 1028-1035.

Williams, T.P., Bubb, J.M. and Lester, J.N., 1994. Metal accumulation within salt marsh environments: A review. *Marine Pollution Bulletin* 28, 277-290.

3.5. OUT COMINGS FROM THE EFFECTS OF CO_2 RISING ON SALT MARSH ECOSYSTEM SERVICES

On the background of several climatic changes and consequences is the greenhouse effect promoted by the increasing atmospheric GHGs concentration, such as CO_2. Changes in the atmospheric CO_2 concentrations will have direct and indirect effects on the primary producers, due to its carbon-fixation based metabolism. As described for terrestrial ecosystem, also in coastal ecosystems the changes will be manly dependent on the plant metabolism. In sum C_3 plants growth will be promoted by the increasing concentration of this atmospheric carbon source, while C_4 species have their metabolism working at near maximum rates, and thus won't see their primary productivity enhanced. In fact, C_4 grasses show evident signs of photochemical stress under elevated CO_2 concentrations, reducing this way its global photosynthetic ability (Duarte *et al*., 2014a). On the other hand these estuarine environments divide their diel cycles between emersion and submersion conditions. Taking into account the present projections made by the Intergovernmental Panel for Climate Change (IPCC), it is expected that the increased levels atmospheric CO_2 will lead to an inevitable increase in the dissolved CO_2 in the water bodies, altering this way the availability of CO_2 underwater. Under submersion halophytes have their photosynthesis under non-saturated levels, being evident an increasing primary production along the increasing dissolved CO_2 concentrations. At this level, the estuarine halophyte communities act as a counterbalancing force, decreasing the dissolved CO_2, buffering estuarine water and increasing the oxygenation of the water column, an important service as a life support system (Duarte *et al*., 2014b). On the opposite of the equation in the estuarine energy web, also the decomposition processes will be affected by changes in atmospheric CO_2. There is an evident shift in the biogeochemical function of salt marshes as organic matter recyclers, providing unbalanced amounts of nutrients to the nearby primary producers. All this points out to evident changes in the whole ecosystem. The

reduction of area of the ecosystem engineer *S. maritima* and expansion of C_3 halophytes will not only reduce the carbon live stocks of the salt marshes as effective sinks, but also reduce the counteracting force of these halophytes as buffers of the estuarine waters. Aside from this, the deficient supply of inorganic nutrients due to altered biogeochemical cycles will also impact the primary productivity of the estuarine water column.

References

Duarte, B., Santos, D., Silva, H., Marques, J.C. and Caçador, I., 2014a. Photochemical and Biophysical feedbacks of C_3 and C_4 Mediterranean halophytes to atmospheric CO_2 enrichment confirmed by their stable isotope signatures. *Plant Physiology ad Biochemistry* 80, 10-22.

Duarte, B., Silva, H., Marques, J.C., Caçador, I. and Sleimi, N., 2014b. Light-dark O_2 dynamics in submerged leaves of C_3 and C_4 halophytes under increased dissolved CO_2: Clues for saltmarsh response to climate change. *Annals of Botany Plants* 6, plu067.

Caçador, I., Duarte, B., Marques, J.C. and Sleimi, N., 2015. Carbon mitigation: a salt marsh ecosystem service in times of change. *Halophytes for Food Security in Dry Lands.* Muhammad Ajmal Khan, Munir Ozturk, Bliquees Gul and Muhammad Zaheer Ahmed (Eds.) Elsevier.

CHAPTER IV

BIOPHYSICAL AND BIOCHEMICAL CONSTRAINS IMPOSED BY SALT STRESS

CHAPTER IV

4.1. BIOPHYSICAL AND BIOCHEMICAL CONSTRAINS IMPOSED BY SALT STRESS

If we take a good look to our planet we will conclude that it is in fact a salt planet. About 70 % of its surface is covered by salt water, with concentrations of Na^+ around 500 mM and contrasting low K^+ concentrations of 9 mM (Flowers, 2004). Alongside, the remaining 30 % of the Earth's surface is severely affected by increased salinization, enhanced by improper agricultural soil use and irrigation practices (Zhan and Shi, 2014). We live in a time of changes. The ongoing climate-driven changes must also be considered as well as their consequences, such as increasing drought frequency and intensity, air temperature and salt water intrusion in coastal soils (Duarte *et al*., 2013). All these aspects impose severe constraints to the Earth primary production. Vegetation constitutes the foundation of most wetland habitat structures and food chains (Valiela *et al*., 2004). As referred before wetlands, mangroves, and scrubs provide sediment stability for smaller vegetation, and they provide niches for many fauna species. In general, mangroves and salt marshes occupy, respectively the seaward and inland margins of wetlands. While fluvial discharge or precipitation runoff provides wetlands with most of their freshwater supplies, seawater intrusion determines flora's salinity optimums. Sea level rise will cause optimum saline conditions to shift inland. In addition, most halophyte species have elevation optimums. Elevation optimums will also shift inland unless sedimentation enables vertical migration. Halophytes will likely track these optima either by vertical or horizontal range shifts or in a worse case scenario, extinction. Second, SLR raises salinity of high ground areas, which can exogenously decrease their resident populations. Using 2500 years of macrofossil data, Donnelly and Bertness (2001) found that SLR brought increasingly saline conditions to high ground areas, leading to a decline in high ground vegetation. This opened a new habitat space for cordgrasses, like *S. maritima*. If unchanged, current SLR rates would allow seaward species to continue to replace high ground species (Donnelly and Bertness 2001). However, if SLR accelerate, then both cordgrasses and high ground species

will drown. Although their abundance, pioneer wetland vegetation such as cordgrasses contribute relatively little to biomass production (Donnelly and Bertness 2001), and thus replacement of high ground species with less productive pioneer species will likely lower overall biomass production, and thus reduce the carbon sink provided by a well structured salt marsh. Additionally, global warming will also enhance this salinization process. McKee *et al*. (2004) suggests that increases in temperature and decreases in rainfall associated with climate change may dramatically affect tidal marshes. Increased temperature may interact with other stressors damaging coastal marshes. For example, during the spring to fall period of 2000 the Mississippi delta experienced large areas of salt marsh that were stressed and dying (Day *et al*., 2005). This appears to be the result the synergistic effects related to a strong La Niña event, resulting in low water levels, prolonged and extreme drought, and high air temperatures. This combination of factors apparently raised soil salinities to stressful toxic levels.

Salinity-induced constraints in plants are associated with reductions in leaf expansion, stomatal closure, reduced primary production, biomass losses and nutritional deficiencies, like K^+ deficiency (James *et al*., 2011; Rahnama *et al*., 2010; Mahajan and Tuteja, 2005). Halophytes are an exception, being highly productive under saline conditions. The typical definition of halophyte is a plant species that can survive and reproduce under growth conditions with more than 200 mM NaCl (Flowers and Colmer, 2008). For this, halophytes developed morphological and biochemical adaptations to survive under extreme haline conditions. Nevertheless, all these morphological adaptations have implications at both biophysical and biochemical levels. This way, and considering the projected increased soil salinization and SLR rates, becomes important to understand how these salt-adapted plants will cope with increasing sediment salinities in a near future and how this will affect their primary productivity and physiological processes. Moreover, with the changing in these saline habitats becomes also imperative to assess the vulnerability of these habitats to NIS, by replacement of the native species with lower fitness under these altered environments.

References

Day, J.W., Narras, J., Clairain, E., Johnston, J., Justic, D., Kemp, G.P., Ko, J.Y., Land, R., Mitsch, W.J., Steyer, G., Templet, P. and Yanez-Arancibia, A., 2005. Implications of global climatic change and energy cost and availability for the restoration of the Mississippi delta. *Ecological Engineering* 24, 253–265.

McKee, K., Mendelssohn, I.A. and Materne, M.D., 2004. Acute salt marsh dieback in the Mississippi River deltaic plain: a drought induced phenomenon? *Global Ecology and Biogeography* 13, 65–73.

Flowers, T.J., 2004. Improving crop salt tolerance. *Journal of Experimental Botany* 55, 307–319.

Zhang, J.-L., and Shi, H., 2014. Physiological and molecular mechanisms of plant salt tolerance. *Photosynthesis Research* 115, 1–22.

Duarte, B., Caçador, I., Marques, J. C., and Croudace, I., 2013. Tagus Estuary salt marshes feedback to sea level rise over a 40-year period: insights from the application of geochemical indices. *Ecological Indicators* 34, 268–276.

Valiela, I., Rutecki, D. and Fox, S., 2004. Salt marshes: biological controls of food webs in a diminishing environment. *Journal of Experimental Marine Biology and Ecology* 300, 131-159.

Donnelly, J.P. and Bertness, M.D., 2001. Rapid shoreward encroachment of salt marsh cordgrass in response to accelerated sea-level rise. *Proceedings of the National Academy of Sciences of the United States of America* 98, 14218-14223.

James, R. A., Blake, C., Byrt, C. S., and Munns, R., 2011. Major genes for Na^+ exclusion, Nax1 and Nax2 (wheat HKT1;4 and HKT1;5), decrease Na^+ accumulation in bread wheat leaves under saline and waterlogged conditions. *Journal of Experimental Botany* 62, 2939–2947.

Rahnama, A., James, R. A., Poutini, K., and Munns, R., 2010. Stomatal conductance as a screen for osmotic stress tolerance in durum wheat growing in saline soil. *Functional Plant Biology* 37, 255–263.

Mahajan, S., and Tuteja, N., 2005. Cold, salinity and drought stresses: an overview. *Archives in Biochemistry and Biophycs* 444, 139–158.

Flowers, T. J., and Colmer, T. D., 2008. Salinity tolerance in halophytes. *New Phytologist* 179, 945–963.

4.2. ECOPHYSIOLOGICAL ADAPTATIONS OF TWO HALOPHYTES TO SALT STRESS: PHOTOSYNTHESIS, PS II PHOTOCEMISTRY AND ANTI-OXIDANT-FEEDBACK[1]

Abstract

Halimione portulacoides and *S. fruticosa* commonly exhibit a reddish coloration especially in high evaporation periods, due to betacyanin production in response to stress. Although sharing the same area in salt marshes, they present different strategies to overcome salinity stress. While *S. fruticosa* present a dilution strategy, increasing succulence, *H. portulacoides* appears to have developed an ionic compartmentalization strategy. Nevertheless, there's still a decrease in the photosynthetic activity in different extents. While in *S. fruticosa*, the impairment of photosynthetic activity is due to a decrease in the flow from the electron transport chain to the quinone pool; in *H. portulacoides* the process is affected far more early, with high amounts of energy dissipated at the PS II light harvesting centres. This photosynthetic impairment leads to energy accumulation and consequently to the production of reactive oxygen species (ROS). SOD was particularly active in stressed individuals, although this increment is rather more significant in *S. fruticosa* than in *H. portulacoides* suggesting that *H. portulacoides* may have a maximum salt concentration at which can sustain cellular balance between ROS production and scavenging. These different ecophysiological responses have great importance while evaluating the impacts climate change driven increase of sediment salinity on halophyte physiology and on the marsh community, structure and ecosystem services.

[1] This section was published in: **Duarte, B.**, Santos, D., Marques, J. C. and Caçador, I., 2013. Ecophysiological adaptations of two halophytes to salt stress: photosynthesis, PS II photochemistry and anti-oxidant feedback - Implications for resilience in climate change. Plant *Physiology and Biochemistry* 67, 178-188.

Introduction

A decrease in photosynthesis capacity is very common in salt stressed plants (Munns and Termaat, 1986; Munns, 1993; Jaleel *et al*., 2007; Qiu *et al*., 2003), mostly due to a low osmotic potential of the soil solution (osmotic stress), specific ion effects (salt stress), nutritional imbalances or more usually, a combination of these factors (Zhu, 2003). Similarly, to other stress factors, these induce plant biochemical and physiological disturbances (Munns, 2002). One of the consequences of salinity induced limitation of photosynthetic capacity, is the exposure of plants to excess of light energy with inevitable consequences on the PS II, if the dissipation mechanisms are not efficient enough (Demming-Adams and Adams, 1992; Qiu *et al*., 2003), since plants under salt stress have lower light use efficiencies (Megdiche *et al*., 2008). The effects of salinity on photosynthesis include several other consequences besides the damage on PS II. Also the photosynthetic carbon harvesting is affected by disturbances on leaf water relations and osmotic potential (Munns, 2002; Zhao *et al*., 2007), on the chloroplast membrane systems and on the pigment composition (carotenoids and chlorophyll). To avoid damages to the PS II, plants have developed several strategies to dissipate excessive energy, protecting the photosynthetic apparatus. One of these mechanisms is the dissipation of energy throughout the xanthophyll cycle already described for several photosynthetic organisms as a stress response mechanism (Demimg-Adam and Adams, 1992; Gilmore, 1997; Li *et al*., 2000). During this cycle, excessive energy is dissipated in the form of heat through the formation of zeaxanthin by violaxanthin de-epoxidation via antheraxanthin (Reinhold *et al*., 2008).

Halophytes are typically considered to be plants able to complete their life cycle in environments where the salt concentration is around 200 mM NaCl or higher, representing 1% of the world flora (Flowers and Colmer, 2008). *Halimione portulacoides* and *S. fruticosa* are two Amaranthaceae widely distributed on the Portuguese and European salt marshes. They present different strategies against salt stress. While *H. portulacoides* has specific salt glands on the leaves to excrete the excess of salt, *S. fruticosa* increases its water content in the photosynthetic stems, becoming turgid, promoting this way salt dilution (Liphschitz and Waisel, 1982).

Considering these differences of defence against salt stress and on the photosynthetic mechanisms, this study aims to investigate *in situ* how the photosynthesis of these halophytes is affected under salt stress and how this will affect the carbon sequestration rates, in order to understand the defence and tolerance mechanisms towards salt stress.

Material and Methods

Plant collection and leaf harvest

Leaves were harvested in July 2011 in an undisturbed salt marsh of Tagus estuary within the Tagus Estuary Natural Reserve. Due to the relatively high temperatures (25-30 °C) verified in the previous weeks, the salt content in the sediments increased due to evaporation. Several stands of both target species exhibited red leaves. Red and green leaves of *H. portulacoides* and *S. fruticosa* were harvested randomly along all the salt marsh. To study the salt effects on *H. portulacoides* fully developed leaves were harvested while in *S. fruticosa* the photosynthetic stems were used for this propose. Samples for biochemical and chemical analysis were immediately stored in liquid nitrogen and brought back to the laboratory.

Elemental analysis

Leaves or photosynthetic steams for Na, K and Ca content were washed with ultra-pure water to eliminate salts in the surface of the leaf. Subsequently samples were treated and analysed by FAAS as described in Chapter 2, Section 2 (Duarte *et al*., 2013).

Leaf Water Status

Leaf Relative Water Content (RWC) was calculated as: RWC (%) = (FW-DW)/(TW-DW) x 100, where FW is the fresh weight, TW is the turgid weight after rehydrating samples for 24 h in ultra-pure water, and DW is the Dry Weight after oven-drying samples at 60 °C until constant weight.

Photosynthetic carbon fluxes

An infrared gas analyser (S151, Qubit, EUA) was used to estimate net CO_2 assimilation rate by an open system. Measurements were made at summer midday PAR (1000 photons μmol m^{-2} s^{-1}) on attached photosynthetic organs. CO_2 net assimilation rates were measured using ambient humidity and CO_2 concentrations. Due to the lack of true leaves in *S. fruticosa* and to the cylindrical morphology of the photosynthetic steams, all the photosynthetic carbon fluxes were normalized for the leaf DW instead of the leaf area.

PAM fluorometry

Fluorometric analysis were preformed according to the described in Chapter II, Section 3 as described in Duarte *et al*. (2013). All derived variables were computed as described in Table 2.3.1.

Anti-oxidant enzyme assays

All enzymatic analysis (APx, GPx and SOD) were performed by UV-Vis spectrophotometry using specific substrates as described in Chapter II, Section 3 (Duarte *et al*., 2013).

Gauss Peak Spectra Pigment Analysis

Samples for pigment analysis were extracted using pure acetone after freeze-drying and analysed by UV-Vis spectrophotometry as described in Chapter III, Section 2 (Kupper *et al*., 2007).

Anthocyanin and Betacyanin concentration

Leaves for both anthocyanins and betacyanins quantification were also freeze-dried for 48h. For anthocyanins quantification, leaves were grinded in 99 % methanol acidified at 1% with HCl. To ensure complete disaggregation of the leaf material, samples were subjected to a cold ultra-sound bath during 2 min. Extraction occurred at – 20 °C during 24 h in the dark. After extraction samples were centrifuged at 1 780 x g during 15 min at 4 °C and the absorbance of the extract was read at 530 nm (Sepúlveda-Jiménez *et al*. 2004). For betacyanins quantification

leaves were grinded in 80 % methanol added with 50 mM of ascorbic acid. To ensure complete disaggregation of the leaf material, samples were also subjected to a cold ultra-sound bath during 2 min. Extraction occurred at – 20 °C during 30 min in the dark. After extraction, samples were centrifuged at 1 780 x g during 15 min at 4 °C and the absorbance of the extract was read at 536 nm (Francis, 1989).

Results

Leaf elemental content

All stressed individuals showed higher Na concentrations (Figure 4.2.1) in the photosynthetic tissues, independently from the analysed specie. When comparing both species, stressed *H. portulacoides* individuals presented higher Na concentrations when compared with *S. fruticosa* stressed individuals. In which concerns non-stressed individuals, the opposite trend could be verified, with higher Na concentrations in *S. fruticosa* photosynthetic organs.

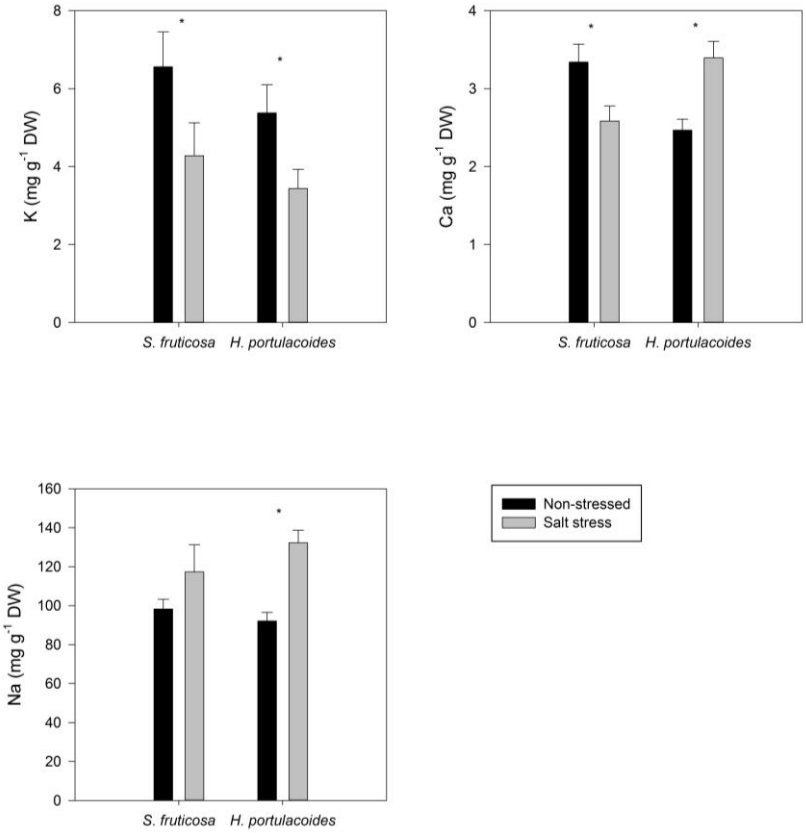

Figure 4.2.1. Potassium, Calcium and Sodium leaf concentrations in stressed and non-stressed individuals of *S. fruticosa* and *H. portulacoides* species (average ± standard deviation, n = 10, * $p < 0.05$).

Concerning K, the exact same pattern was observed between species, although with higher concentrations in non-stressed individuals. Calcium exhibited a distinct pattern between species. While in *S. fruticosa* the Ca content was higher in non-stressed individuals, in *H. portulacoides* the higher concentrations were observed in stress individuals.

Leaf Water Status

Leaf relative water content (Figure 4.2.2) showed both differences between species and within the same specie between stressed and non-stressed individuals. *Sarcocornia fruticosa* stressed individuals showed lower water contents than the non-stressed ones, while in *H. portulacoides* the opposite behaviour was observed, with higher water contents in the individuals subjected to higher salinities. Beside this, *S. fruticosa* had slightly higher water content than *H. portulacoides*, under normal circumstances.

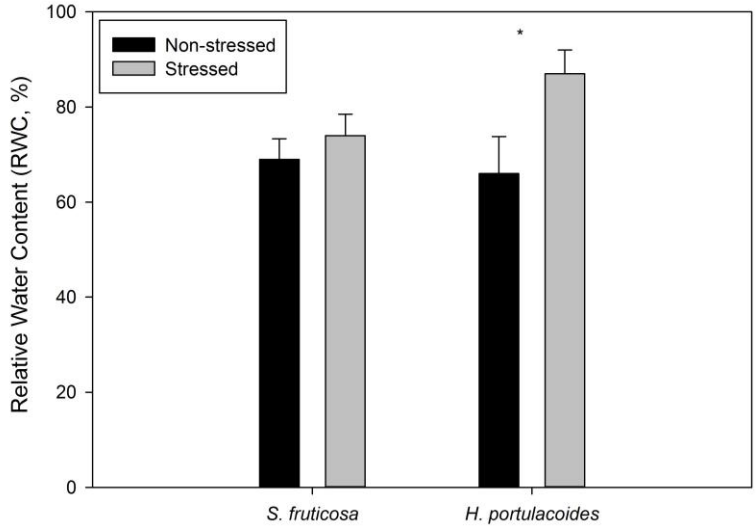

Figure 4.2.2. Leaf Relative Water Content (RWC) in stressed and non-stressed individuals of *S. fruticosa* and *H. portulacoides* species (average ± standard deviation, n = 10, * $p < 0.05$).

Photosynthetic gas exchange and PS II activity

Independently of their stress levels, *S. fruticosa* individuals showed always-higher gas exchange rates than *H. portulacoides* (Figure 4.2.3). Comparing the stressed individuals with the non-stressed, it is possible to observe that these last

ones presented always lower gas exchange rates than the non-stressed, being this difference more evident in the *S. fruticosa* individuals.

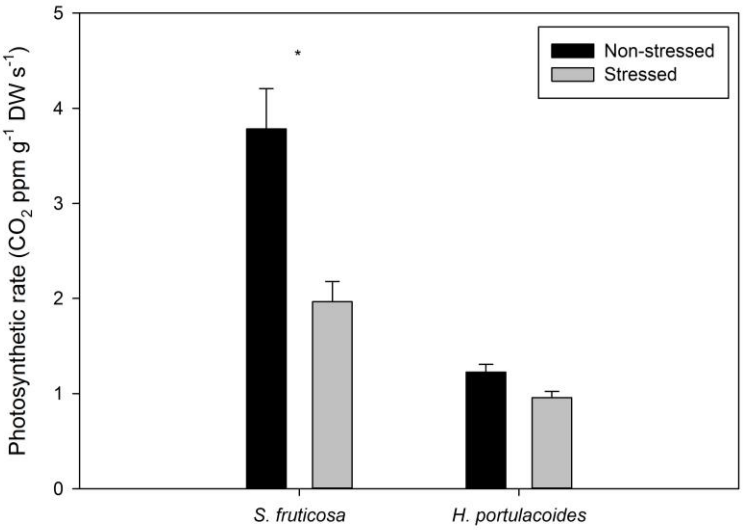

Figure 4.2.3. Photosynthetic rate (ppm CO_2 g^{-1} DW s^{-1}) in stressed and non-stressed individuals of *S. fruticosa* and *H. portulacoides* species (average ± standard deviation, n = 10, * $p < 0.05$), measured at a PAR of 500 μmol photons m^{-2} s^{-1}.

As observed in other evaluated parameters, the stressed individuals showed lower quantum yields in both dark and light adapted leaves (Figure 4.2.4). Among species, stressed *S. fruticosa* individuals presented high quantum yields if compared with the homologous *H. portulacoides* individuals. In healthy individuals the contrary was observed, with higher quantum yields observed in the analysed *H. portulacoides* leaves. Similarly, to the observed with the gas exchange rates also the non-photochemical quenching (NPQ) was always higher in the *S. fruticosa* individuals, independently of their health condition (Figure 4.2.4). Considering stressed and non-stressed individuals, in both species heathy individuals showed lower NPQ.

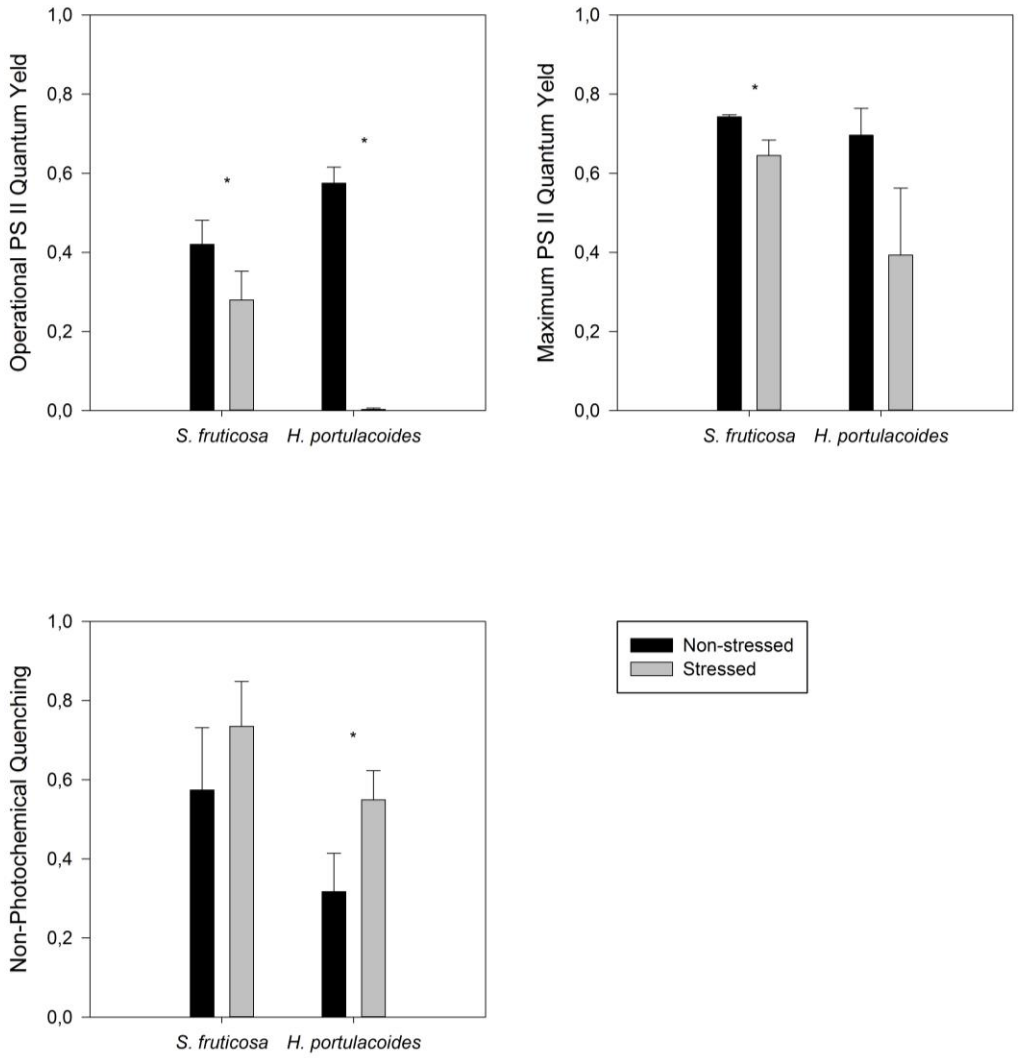

Figure 4.2.4. Operational, Maximum PS II photosynthetic and Non-photochemical Quenching (NPQ) in stressed and non-stressed individuals of *S. fruticosa* and *H. portulacoides* species (average ± standard deviation, n=10, * $p < 0.05$).

Observing the rapid light curves (Figure 4.2.5 and Table 4.2.1) obtained for both species at different stress levels it is possible to observe that there are evident differences either between species and, in particular for *H. portulacoides*, between stress levels. In *S. fruticosa* the maximum ETR, photosynthetic efficiency and the onset of light saturation are very similar among healthy and stressed individuals (Table 4.2.1), presenting only small differences regarding the rETR at different light exposures (Figure 4.2.5).

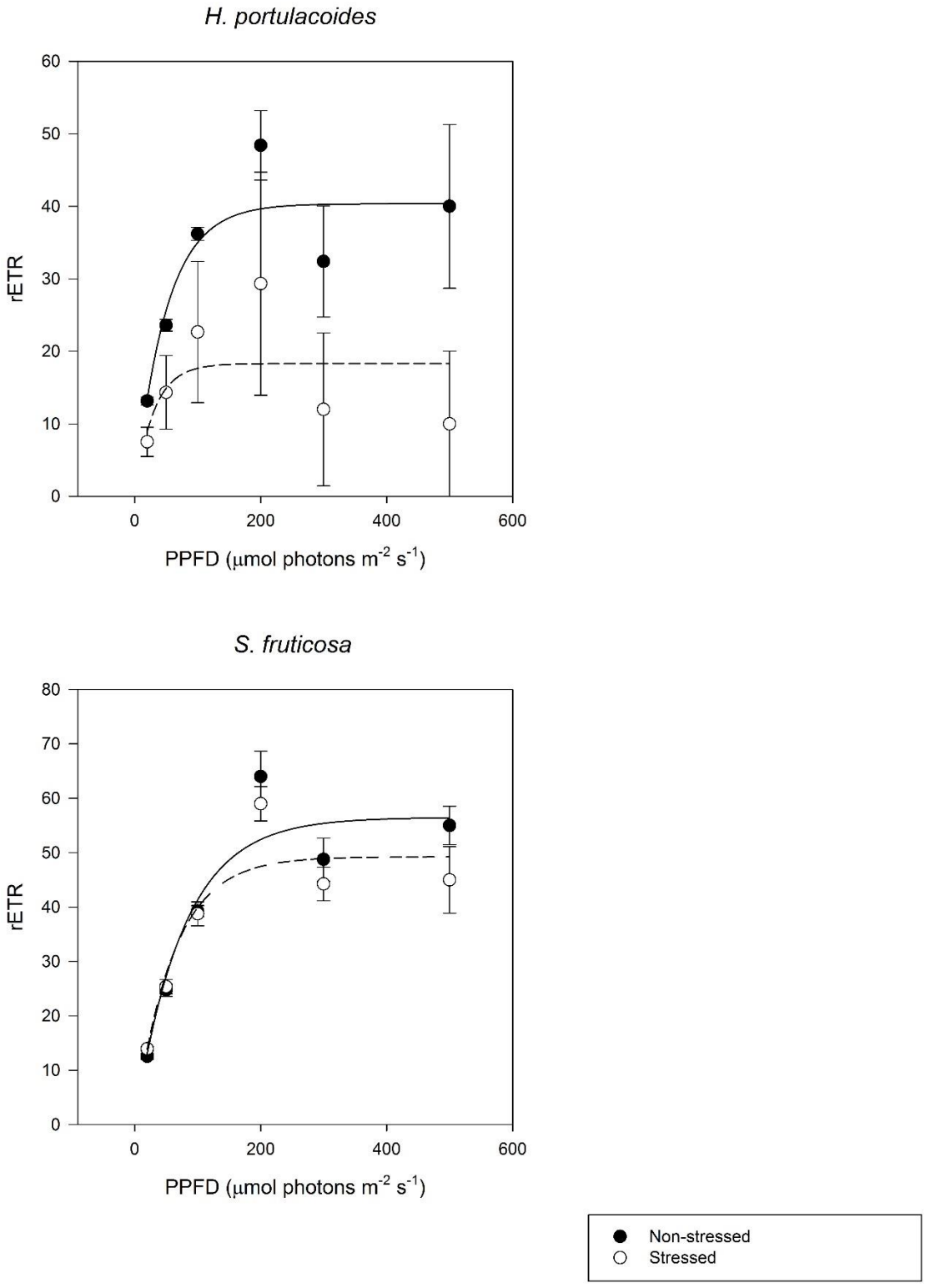

Figure 4.2.5. Relative electron transport rate (rETR) in stressed and non-stressed individuals of *S. fruticosa* and *H. portulacoides* species (average ± standard deviation, n=10).

On the other hand, *H. portulacoides* stressed and healthy individuals exhibited very distinct photosynthetic parameters. Not only the photosynthetic efficiency and the onset of light saturation were reduced to zero, but also the maximum electron transport rate was lower in stressed individuals.

Table 4.2.1. Rapid light curve parameters contents in leaves of *S. fruticosa* and *H. portulacoides* stressed and healthy individuals (average ± standard deviation, n=10, * $p < 0.05$).

	S. fruticosa		***H. portulacoides***	
	Stressed	**Non-stressed**	**Stressed**	**Non-stressed**
$\mathbf{ETR_{max}}$	49.25 ± 4.28	56.49 ± 4.89	18.33 ± 4.27*	40.37 ± 3.60*
α	0.41 ± 0.07	0.46 ± 0.03	0.00 ± 0.01*	0.32 ± 0.09*
$\mathbf{E_k}$	120.12 ± 12.35	122.80 ± 11.28	0.00 ± 0.00*	126.16 ± 10.36*

Concerning the data relative to the rapid transient curves (Figure 4.2.6), both healthy and salt stressed *S. fruticosa* individuals showed similar trapping and dissipating energy fluxes. On the other hand, *H. portulacoides* individuals showed marked differences between stressed and non-stressed individuals. Healthy specimens showed higher trapping and lower dissipating fluxes, in opposition to the salt stressed individuals. These similar trapping abilities, found in *S. fruticosa* individuals, are confirmed if the probability of an absorbed photon to move an electron throughout the electronic transport chain is observed, leading this way to similar maximum primary photochemistry yields. Alongside also a reduction in the ability to reduce the quinone pool and with this start the electronic flow between the quinone pool and the electronic transport chain, was found in stressed individuals. Observing *H. portulacoides* individuals, the lower trapping fluxes and high dissipated energy fluxes decreased the probabilities of an absorbed photon to move an electron throughout the electronic transport chain as well as the maximum primary photochemistry yields. Regarding the quinone turnover in *H. portulacoides* individuals, both salt stressed and healthy individuals present similar values, although in non-stressed individuals there is a slightly higher electronic flow rate from the reduced quinone pool to the ETC.

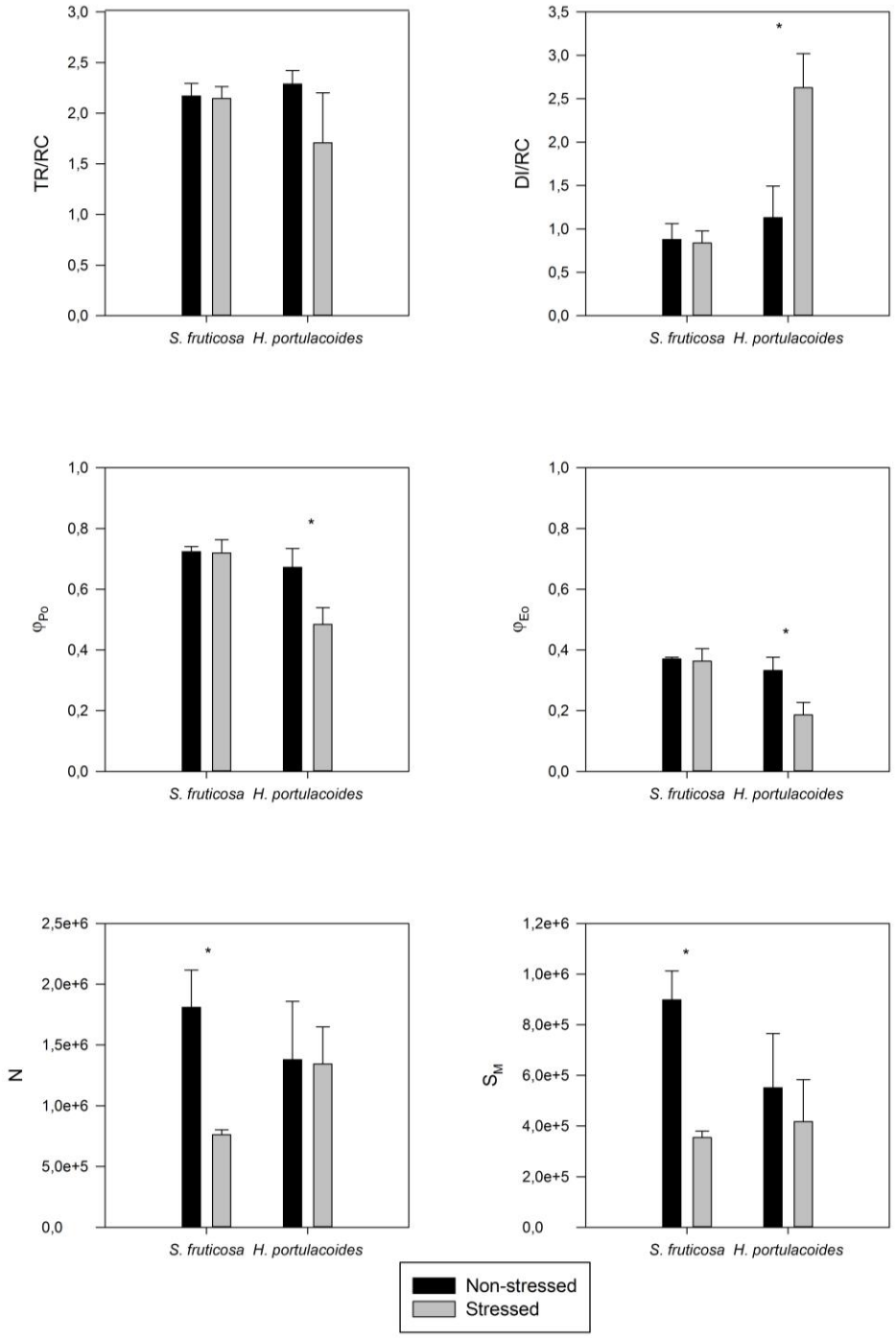

Figure 4.2.6. Transient OJIP curve derived parameters in stressed and non-stressed individuals of *S. fruticosa* and *H. portulacoides* species (average ± standard deviation, n=10, * $p < 0.05$).

Applying an integrative variable, as it is the Performance Index (Figure 4.2.7), it was possible to more markedly observe the differences both between species and stress levels. All the stressed individuals regardless from the specie presented lower performance index values, although this decrease was more evident in the *H. portulacoides* individuals.

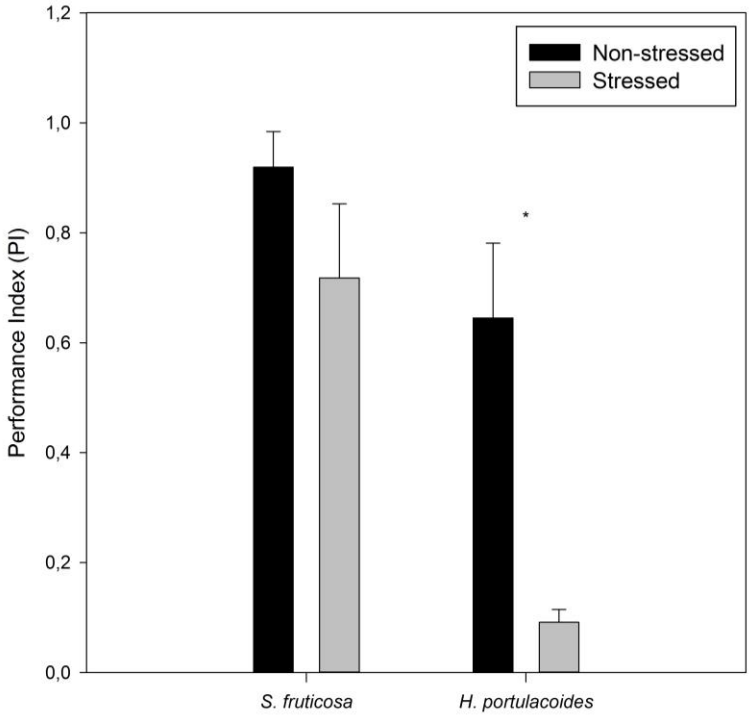

Figure 4.2.7. Performance Index (PI) in stressed and non-stressed individuals of *S. fruticosa* and *H. portulacoides* species (average ± standard deviation, n=10, * $p < 0.05$).

Pigment concentrations

One of the more evident differences between stressed and non-stressed individuals is the reduced concentration of chlorophyll a and b in salt affected individuals (Table 4.2.2).

Table 4.2.2. Chlorophylls, Carotenoids, Anthocyanins (μg g^{-1} FW) and Betacyanins (meq betain x 10^6 g^{-1} FW) contents in leaves of *S. fruticosa* and *H. portulacoides* stressed and healthy individuals (average ± standard deviation, n=10, * $p < 0.05$).

	S. fruticosa		***H. portulacoides***	
	Non-stressed	**Stressed**	**Non-stressed**	**Stressed**
Chlorophyll a	80.00 ± 13.81*	27.99 ± 7.53*	66.78 ± 15.74*	14.72 ± 5.99*
Chlorophyll b	22.01 ± 4.42*	9.37 ± 1.88*	28.26 ± 7.73*	6.10 ± 2.51*
Pheophytin a	0.63 ± 0.21	0.49 ± 0.21	1.33 ± 0.50*	0.21 ± 0.06*
Antheraxanthin	3.82 ± 1.70	5.66 ± 3.58	11.79 ± 3.51*	2.19 ± 0.82*
β - carotene	5.73 ± 0.94	3.31 ± 1.33	7.60 ± 2.06*	1.81 ± 0.51*
Lutein	14.93 ± 3.91*	7.51 ± 1.16*	17.09 ± 6.04*	3.29 ± 0.89*
Violaxanthin	4.20 ± 1.49	3.67 ± 1.42	5.72 ± 2.07*	0.70 ± 0.10*
Zeaxanthin	6.07 ± 0.99	3.20 ± 1.27	9.27 ± 4.08	4.65 ± 1.27
Anthocyanins	0.04 ± 0.00*	0.08 ± 0.02*	0.03 ± 0.01*	0.06 ± 0.01*
Betacyanins	0.02 ± 0.00*	0.08 ± 0.02*	0.00 ± 0.00*	0.05 ± 0.01*

In fact, the chlorophyll a/b ratio (Figure 4.2.8), a common stress indicator, supports these findings, with higher values for healthy individuals in both species. With the exception of antheraxanthin, the photosynthetic stems of stressed *S. fruticosa* individuals, exhibited low carotenoid concentrations in stressed individuals independently of the specie, as it can be confirmed by the total carotenoid concentration (Figure 4.2.8). Also when comparing healthy individuals of both species, they have similar concentrations of all the pigments (chlorophylls and carotenoids), while when comparing both species stressed individuals, *S. fruticosa* individuals presented almost twice the concentration of the referred pigments (Table 4.2.2). This can be also observed while overlooking the carotenoid/chlorophyll ratio, with lower differences between stressed and non-stressed *S. fruticosa* individuals, due to the high amounts of carotenoids concentration, even under stress (Figure 4.2.8). Another important pigment index directly related with the light use efficiency and with the energy dissipation is the DES (Figure 4.2.8). As expected and in accordance with the data from chlorophyll fluorescence and OJIP curves, the DES of salt stressed leaves presented higher

values. In order to understand the origin of the reddish coloration of salt stressed leaves, also the anthocyanin and betacyanin content was evaluated (Table 4.2.2). Both pigments exhibited the same trend with higher concentrations in stressed plants than in healthy samples. Nevertheless, this common pattern, betacyanin content proved to be much higher than anthocyanin, being the predominant pigment in salt stressed leaves.

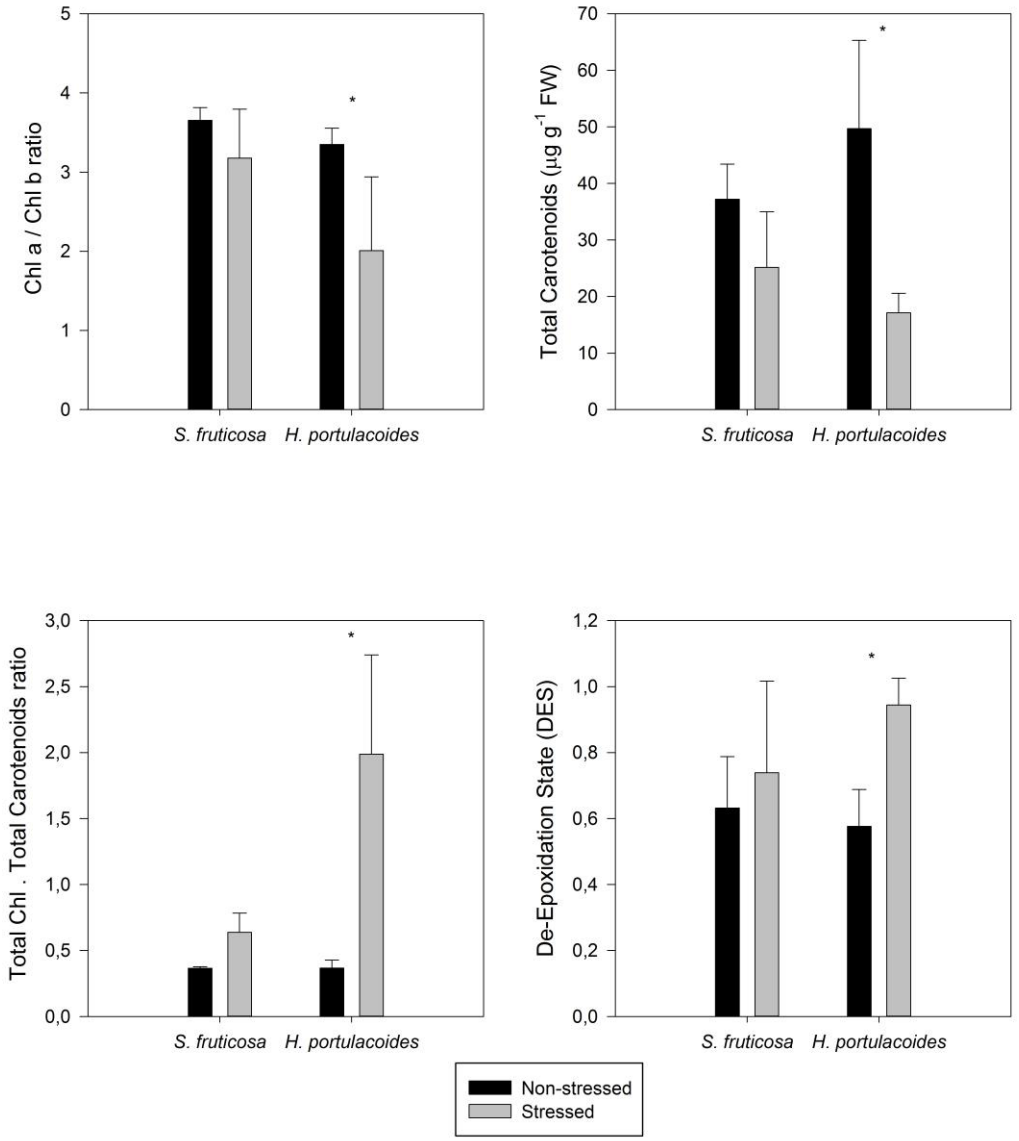

Figure 4.2.8. Pigment ratios in stressed and non-stressed individuals of *S. fruticosa* and *H. portulacoides* species (average ± standard deviation, n=10, * $p < 0.05$).

Anti-oxidant enzymatic activities

Overlooking all the anti-oxidant enzymes evaluated (Figure 4.2.9), in both levels of stress independently of the specie, stressed individuals present an increased enzymatic activity. These differences are more evident in the GPx and SOD activity, although APx also showed enhanced activities in individuals suffering from salt stress. The predominant anti-oxidant peroxidase in *S. fruticosa* was found to be the GPx while in *H. portulacoides* was found to be the APx. Nevertheless, SOD was the predominant form of enzymatic anti-oxidant defence in both species.

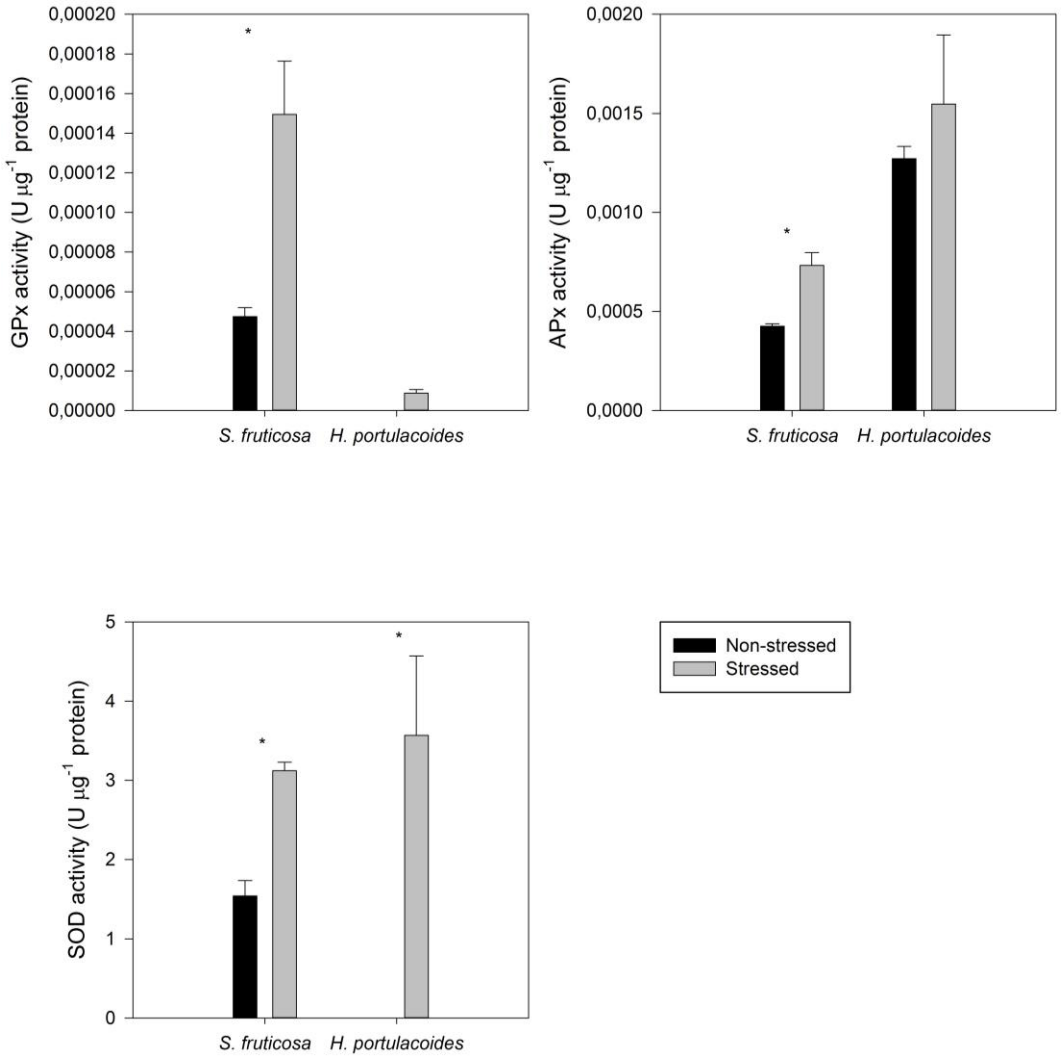

Figure 4.2.9. Guaiacol peroxidase (GPx), Ascorbate Peroxidase (APx) and Superoxide Dismutase (SOD) in stressed and non-stressed individuals of *S. fruticosa* and *H. portulacoides* species (average ± standard deviation, n=10, * $p < 0.05$).

Discussion

Salt marshes sometimes arid environment leads to the development of some physiological adaptations by some elements of the Amaranthaceae family. One of these adverse abiotic factors is the high salinity sometimes verified in the sediments, due to evaporation and consequent reduction of sediment water content, and increased salt concentration. Both *Halimione* and *Sarcocornia* genus are characterized by succulent plants, well adapted to the arid middle-upper salt marsh environment. Some of these ecophysiological feedback mechanisms to salt stress includes the increase of the tissues water content, in order to dilute salt concentration within the photosynthetic organs. Other tolerance and defence mechanisms include glandular salt excretion, trichome salt accumulation, salt leaching and guttation, salt transport to the roots, xylem ion loading, vacuolar ion sequestration and control of stomata aperture (Waisel, 1972; Shabala and Mackay, 2011). This increase in the fresh weight is well described for several halophyte families and is still matter of discussion although several authors point out some hypothesis involving interactions of ion uptake, cell water relations, and cell wall metabolism. (Black, 1954; Greenway, 1968; Gale and Poljakoff-Mayber, 1970; Poljakoff-Mayber and Gale, 1975; Flowers *et al*., 1977; Osmond *et al*., 1980). This increase in succulence aims to reduce the apoplastic salinity, maintaining this way cell turgor. From this point of view *S. fruticosa* seems to have a lower ability to increase its succulence, mostly due to the fact that its water content is already higher (under normal conditions) than in *H. portulacoides*. The major physiologically adverse effects of salinity are mostly due to the high ionic content and its consequent toxicity. At low concentrations the verified elemental concentrations of both species are in accordance with the assessed for other halophytic species (Laudadio *et al*., 2009). The increase in Na concentration in sediments, as it is, in case of excess salinity, has impacts not only in plant physiology, but also in the soil chemistry with consequent metabolic impact. Sodium increase leads to a high depolarization of the root plasma membrane, making K an essential element for plant nutrition (Marschener, 1995), less accessible to the roots (Khan *et al*., 2000; Shabala and Cuin, 2008). Stressed individuals from both species exhibited lower K concentrations in their tissues. Sodium can also affect K metabolism, by interfering

with several K-cofactor enzymes (Khan *et al*., 2000). Sodium excess can also lead to the displacement of membrane-bound Ca, essential in cell signalling (Cramer *et al*., 1985). Furthermore, elevated cytosolic Na/K ratio leads to activation of caspase-like proteases and endonucleases triggering rapid programmed cell death in salinity-exposed roots (Demidchik *et al*., 2010). At this point *H. portulacoides* and *S. fruticosa* exhibited different behaviours. While in *S. fruticosa* seems to exist a displacement effect on Ca, in *H. portulacoides* this element also increased along with the increase in the Na concentration. These differences point out to different salinity tolerance strategies. *H. portulacoides* ionic content in saline conditions appear to be higher, indicating that similarly to the verified for *Atriplex spp*. (De Araùjo *et al*., 2006), this specie probably protects its subcellular structures throughout an efficient salt ions compartmentalisation mechanism. On the other hand, the permanent high succulence and lower ionic content observed in *S. fruticosa*, points out to a dilution-based strategy.

Beyond succulence, another morphologically evident characteristic that could be observed in both species salt-stressed individuals was an intense reddish pigmentation. Since all carotenoids exhibited a decrease in concentration, the presence pigments sensitive to pH changes was investigated. Anthocyanins and betacyanins have similar colorations and are well described as being produced by some species as feedback to stress conditions (Chang-Quan *et al*., 2006). Also the polarity of both these classes of pigments make them different; while anthocyanins are highly soluble in organic solvents and hardly on water, betacyanins are easily extracted by water and difficultly by organic solvents (Chang-Quan *et al*., 2006). Also their ecophysiological role is different. Anthocyanins are normally produced in response to light stress, while betacyanins are normally produced as response to salinity, anoxia or thermal stresses (Chang-Quan *et al*., 2006). At this level, both species under salt stress, presented high concentrations of betacyanins, concomitant with the high RWC and salt concentrations in their tissues. As an analogue of anthocyanins, betacyanins play an important role scavenging ROS (Stintzing and Carle, 2004), generated under environmental stress conditions. Chang-Quan *et al*. (2006) found similar results for other Amaranthaceae species (*Sueda salsa*),

suggesting that this betacyanin production is part of a common defence mechanism against environmental stresses, namely salinity.

Overlooking both the light-harvesting pigments (chlorophylls) and light-protecting pigments (carotenoids) there is a generalized significant decrease of all pigments in both species stressed individuals, at similar extents. Another evident signal of environmental stress is the xanthophyll cycle activation, as revealed by the increase in the DES index. When the absorbed light exceeds the plant photochemical capacity (as revealed above by the decrease in the chi a/b ratio), even in normal light conditions, this excess energy may be transferred to the ever-present oxygen. In this context, the conversion of violaxanthin to zeaxanthin throughout the xanthophyll cycle is considered to be one of the most effective energy dissipation mechanisms (Demmig-Adams and Adams, 1992). Also the total chlorophyll to total carotenoids ratio, points out in the same direction. In stressed individuals of both species occurred an increase in this ratio, indicating that although all pigments suffered a drastic decrease under stress, chlorophylls decreased in a smaller proportion than carotenoids, enhancing the light harvesting efficiency, counteracting stress. All these pigment characteristics are evidenced overlooking the photochemical process in detail. Contrarily to the observed in other species (Zinnert *et al*., 2012) the photosynthetic net rate was limited mostly by damage in the PS II, rather than by stomatal closure. This can be seen not only by the reduced operational PS II efficiency, but also by the increase in NPQ and in the previously mentioned change in pigment profile verified in both *H. portulacoides* and *S. fruticosa* stressed individuals. Looking deeper into the photochemical mechanisms, it can be observed that in *S. fruticosa* the major factor responsible by the decrease in the photosynthetic rate is due to salinity adverse effects in the quinone pools. Both the electron flow from the ETC to the quinone pool and the quinone reduction turnover rate was rather decreased, leading to an excess of energy accumulated at this level (Kalaji *et al*., 2011). In *H. portulacoides*, the negative effects driven by salt stress leads to higher amounts of energy dissipated rather than trapped in the photochemical reactions, ultimately having as consequence the destruction of the D1 protein (Rintamäki *et al.,* 1995). In these individuals there is a small probability that an incident photon can move an electron throughout the ETC and also a

reduced efficiency of a trapped electron to move further than the oxidized quinone, reducing this way the maximum yield of primary photochemistry (Kalaji *et al*., 2011). Although excessive salt acts at different levels in the two different analysed species (in the photon reception in *H. portulacoides* and in the reduction of the quinone pool in *S. fruticosa*), all these effects are well summarized overlooking the reduced Performance Index (PI) in stressed individuals, due to its dependency on the efficiency, yield of energy transfer and primary photochemistry. The rapid light curves reinforce these assumptions. Observing *S. fruticosa* healthy and stressed individuals there are no major differences neither between the ETR nor in the onset of light saturation, indicating a normal functioning in the ETC. As for *H. portulacoides*, not only the ETR is rather decreased in stressed individuals, but also these individuals have a smaller onset for light saturation, indicating an incapacity to use the absorbed photons into primary photochemistry. This inevitably leads to an accumulation of large amounts of lethal energy that, as stated before, can destroy the D1 protein, impairing the photochemical apparatus. Again two tolerance mechanisms are evidenced between these two Amaranthaceae species. *Sarcocornia fruticosa* has salinity tolerance mechanisms that allow the photosystems to absorb light even at high Na concentrations, while in *H. portulacoides* these mechanisms appear to absent or inactivated, leading to lower light and carbon harvesting efficiencies. These photoinibitory processes although with different extents in the two analysed species, lead to energy accumulation and consequent production of ROS, especially singlet oxygen and superoxide anions (Hideg *et al*., 1998) that inhibits the repair cycle of PS II by protein synthesis arrest in the chloroplast (Nishiyama *et al*., 2006). Furthermore, salt stress as any other excessive accumulation of cations, also leads to additional direct ROS production. Anti-oxidant enzymatic defences play a key role detoxifying the chloroplast from ROS. The production of these toxic molecules is regulated by their generation rates, reaction with target substances, degradation, and scavenging/neutralizing by enzymatic and/or non-enzymatic antioxidants (Triantaphylides *et al*., 2008). Aside from their destructive nature, ROS play an important role in protection induction mechanisms during salt stress (Buchert and Forreiter, 2010). Both species salt stressed individuals exhibited elevated SOD activities. This enzyme directly modulates the amount of ROS

accumulated inside the cell. The increase in leaf SOD activity may reflect an overproduction of superoxide radical, likely as product of electron leakage from the ETC (Gill and Tuteja, 2010). It is possible that the significant increase in leaf SOD activity under salt stress is correlated with both the temporal regulation of specific isoenzymes, as well as the induction of new isoforms (Anthony *et al*., 2005). Although this important role in the detoxification mechanism, one of the products of SOD activity is hydrogen peroxide, which has also damaging effects at cellular level. In order to proceed to the cell detoxification from ROS, the cell has specific peroxidases, which, in this case study, present a high but different activity considering both analysed species. An interesting aspect is that the induction of SOD activity is concomitant with changes in the specific peroxidases activity, very different in both species. Thus, in *S. fruticosa* stressed individuals, the expected increase in H_2O_2 as product of the SOD activity was accompanied by an increased GPx enzymatic capacity to decompose it. On the other hand, in *H. portulacoides* stressed samples, only a small increase in both enzymes was detected. These results suggest that in *H. portulacoides* may exist a threshold NaCl concentration, above which, an imbalance between ROS-generating and –scavenging systems occurs, similar to what was detected in other plants (Hernandez *et al*., 1999, 2000; Chaparzadeh *et al*., 2004). The correspondent impairment of APx activity suggests that ascorbate levels are insufficient for maintaining this enzyme activity, as it can be irreversibly damaged when ascorbic acid concentration falls (Miyagawa *et al*. 2000). All these results point out to an efficient enzymatic defence mechanism against ROS chloroplastic generation in *S. fruticosa*, while in *H. portulacoides* these defences are rather low and could justify the evident damage verified in the remaining analysed physiological processes.

Conclusions

Salinity increase on salt marshes is on of the expected consequences of the ongoing climate change events either due to increases in heat waves duration and frequency or due to higher salt intrusion, driven from SLR. Although *H. portulacoides* and *S. fruticosa* are both member species of the Amaranthaceae family highly

adapted to elevated salinities sharing the same habitat in salt marshes, they present different strategies to overcome this salinity increase. Both species exhibit a reddish coloration driven from betacyanin accumulation, typical of stands exposed increased sediment salt concentrations. The increased succulence of *S. fruticosa* contrasts with *H. portulacoides* ionic compartmentalization. The high betacyanin production, important to removal of reactive oxygen species (ROS), indicate a common defence mechanism against salinity stress. Nevertheless, these strategies to survive with such conditions, these species experience a decrease in the photosynthetic activity in different extents. While in *H. portulacoides* the photosynthetic process is affected at the first phases of light harvesting occurring in the PS II with high energy wastes, in *S. fruticosa*, the impairment of photosynthetic activity is mostly felt at the ETC with a decrease of the electron flow. This excessive energy leads to ROS production and activation of anti-oxidant enzymatic defences especially SOD and GPx. However, this increment is rather more significant in *S. fruticosa* than *H. portulacoides* indicating that *H. portulacoides* may have a maximum concentration of salt at which can sustain cellular balance between ROS production and scavenging. All evidences point out to more efficient salt tolerance mechanisms in *S. fruticosa*, having consequences at the ecosystem level. Higher adaptation capacity to salinity and a deficient ability to counteract high ionic contents will lead inevitably to changes in the middle-upper marsh halophytic community and consequently in the ecosystem services provided, that must be accounted in climate change scenarios.

References

Anthony, J.R., Warczak, K.L. and Donohue, T.J., 2005. A transcriptional response to singlet oxygen, a toxic by-product of photosynthesis. *PNAS* 102, 6502-6507.

Black, R.F, 1954. The leaf anatomy of Australian members of the genus *Atriplex*, I. *Atriplex vescaria* Hewaxd and *A. nummularia* Lindl. *Australian Journal of Botany* 2, 269–286.

Buchert, F. and Forreiter, C., 2010. Singlet oxygen inhibits ATPase and proton translocation activity of the thylakoid ATP synthase CF1CFo. *FEBS Letters* 584, 147-152.

Chang-Quan, W., Ji-Qiang, Z., Min, C. and Bao-Shan, W., 2006. Identification of betacyanin and effects of environmental factors on its accumulation in halophyte *Suaeda salsa*. *Journal of Plant Physiology and Molecular Biology* 32, 195-201.

Chaparzadeh, N., D'amico, M.L., Khavari-Nejad, R.A., Izzo, R. and Navari-Izzo, F., 2004. Antioxidative responses of *Calendula officinalis* under salinity conditions. *Plant Physiology and Biochemistry* 42, 695–701.

Cramer, G.R., Lauchli, A. and Polito, V.S., 1985. Displacement of Ca^{2+} by Na^{+} from the plasmalemma or root cells: a primary response to stress. *Plant Physiology* 79, 207-211.

De Araùjo, S.A.M., Silveira, J.A.G., Almeida, T.D.A., Rocha, I.M.A., Morais, D.L. and Viegas, R.A., 2006. Salinity tolerance of halophyte *Atriplex nummularia* L. grown under increasing NaCl levels. *Revista Brasileira de Engenharia Agricola e Ambiental* 10, 848–854.

Demldchlk, V., Culn, T., Svistunenko, D., Smith, S., Miller, A., Shabala, S., Sokollk, A. and Yurin, V., 2010. *Arabidopsis* root K^{+}-efflux conductance activated by hydroxyl radicals: single-channel properties, genetic basis and involvement in stress-induced cell death. *Journal of Cell Science* 123, 1468-1479.

Demmig-Adams, B. and Adams, WW II., 1992. Photoprotection and other responses of plants to light stress. *Annual Review of Plant Physiology and Plant Molecular Biology* 43, 599-626.

Flowers T. and Colmer T., 2008. Salinity tolerance in halophytes. *New Phytologist* 179, 945–63.

Flowers, T., Troke, P. and Yeo, A., 1977. The mechanism of salt tolerance in halophytes. *Annual Review of Plant Physiology* 28, 89–121.

Francis, F., 1989. Food colourants: Anthocyanins. *Critical Reviews in Food Science and Nutrition* 28, 273-314.

Gale, J. and Poljakoff-Mayber, A., 1970. Interrelationships between growth and photosynthesis of saltbush (*Atriplex halimus* L.) grown in saline media. *Australian Journal of Biological Sciences* 23, 937–945.

Gill, S. and Tuteja, N., 2010. Reactive oxygen species and antioxidant machinery in abiotic stress tolerance in crop plants. *Plant Physiology and Biochemistry* 48, 909-930.

Gilmore, A.M., 1997. Mechanistic aspects of xanthophyll cycle dependant photoprotection in higher plant chloroplast and leaves. *Physiologia Plantarum* 99, 197-209.

Greenway, H., 1968. Growth stimulation by high chloride concentrations in halophytes. *Israel Journal of Botany* 17, 169–177.

Hernández, J.A., Campillo, A., Jimenez, A., Alarcón, J.J. and Sevilla, F., 1999. Response of antioxidant systems and leaf water relations to NaCl stress in pea plants. *New Phytologist* 141, 241–251.

Hernández, J.A., Jimenez, A., Mullineaux, P. and Sevilla, F., 2000. Tolerance of pea (*Pisum sativum* L.) to long-term salt stress is associated with induction of antioxidant defences. *Plant, Cell and Environment* 23, 853–862.

Hideg É., Kálai, T., Hideg, K. and Vass, I., 1998. Photoinhibition of photosynthesis in vivo results in singlet oxygen production detection via nitroxide-induced fluorescence quenching in broad bean leaves. *Biochemistry* 37, 11405–11411.

Jaleel, C.A., Gopi, R., Manivannan, P. and Panneerselvam, R., 2007.Antioxidative potentials as a protective mechanism in *Catharanthus roseus* (L.) G. Don. plants under salinity stress. *Turkish Journal of Botany* 31, 245-251.

Kalaji, H., Govindjee, Bosa, K., Koscielniak, J., and Zuk-Golaszewska, K., 2011. Effects of salt stress on photosystem II efficiency and CO_2 assimilation of two Syrian barley landraces. *Environmental and Experimental Botany* 73, 64-72.

Khan, M.A., Ungar, I.A. and Showalter, M., 2000. Effects of salinity on growth, water relations and Ion accumulation of the subtropical perennial Halophyte, *Atriplex griffithii var. stocksii*. *Annals of Botany* 85, 225–232.

Küpper, H., Seibert, S. and Aravind, P., 2007. A fast, sensitive and inexpensive alternative to analytical pigment HPLC: quantification of chlorophylls and carotenoids in crude extracts by fitting with Gauss-Peak-Spectra. *Analytical Chemistry* 79, 7611-7627.

Laudadio, V., Tufarelli, V., Dario, M., Hammadi, M., Seddik, M., Lacalandra, G. and Dario, C., 2009. A survey of the chemical and nutritional characteristics of halophytes plants used by camels in Southern Tunisia. *Tropical Animal Health and Production* 41, 209-215.

Liphschitz, N. and Waisel, Y., 1982. Adaption of the plants to saline environments: salt excretion and glandular structure. In D.N. Sen and Rajpurohit (ed.). *Contribution to the ecology of halophytes*. Dr. W. Junker Publishers. The Hague.

Marschner, H., 1995. Mineral Nutrition in Higher Plants, 2nd Ed. Academic Press Limited, London.

Megdiche, W., Hessini, K., Gharbi, F., Jaleel, C., Ksouri, R. and Abdelly, C., 2008. Photosynthesis and photosystem 2 efficiency of two salt-adapted halophytic seashore *Cakile maritima* ecotypes. *Photosynthetica* 46, 410-419.

Miyagawa, Y., Tamori, M. and Shigeoka, S., 2000. Evaluation of the defence system in chloroplasts to photo-oxidative stress caused by paraquat using transgenic tobacco plants expressing catalase from *Escherichia coli*. *Plant Cell Physiology* 41, 311–320.

Munns, R. and Termaat, A., 1986. Whole plant responses to salinity. *Australian Journal of Plant Physiology* 13, 143-160.

Munns, R., 1993. Physiological processes limiting plant growth in saline soils: some dogmas and hypotheses. *Plant, Cell and Environment* 16, 15-24.

Nishiyama, Y., Allakhverdiev, S. I. and Murata, N., 2006. A new paradigm for the action of reactive oxygen species in the photoinhibition of photosystem II. *Biochimica et Biophysica Acta* 1757, 742-749.

Li, X., Bjorkman, O., Shih, C., Grossman, A., Rosenquist, M., Jansson, S. and Niyogi K., 2000. A pigment-binding protein essential for regulation of photosynthetic light harvesting. *Nature* 403, 391–395.

Osmond, C.B., Bjorkman, O. and Anderson, D.J., 1980. Physiological processes in plant ecology: toward a synthesis with *Atriplex*. Ecological Studies, vol. 36. Springer Verlag, Berlin, p. 468.

Poljakoff-Mayber, A. and Gale, J., 1975. Plants in Saline Environments. Springer-Verlag, NY.

Qiu, N., Lu, Q. and Lu, C., 2003. Photosynthesis, photosystem II efficiency and the xanthophyll cycle in the salt-adapted halophyte *Atriplex centralasiatica*. *New Phytologist* 159, 479-486.

Reinhold, C., Niczyporuk, S., Beran, K. And Jahns, P., 2008. Short-term down-regulation of zeaxanthin epoxidation in *Arabidopsis thaliana* in response to photo-oxidative stress conditions. *Biochimica et Biophysica Acta – Bioenergetics* 1777, 462-469.

Rintamaki, E., Salo, R., Lehtonen, E. and Aro, E., 1995. Regulation of D1 protein-degradation during photoinhibition of photosystem-II in vivo— phosphorylation of the D1 protein in various plant groups. *Planta* 195, 379–386.

Sepulveda-Jimenez, G., Rueda-Benitez, P., Porta, H. and Rocha-Sosa, M., 2004. Betacyanin synthesis in red beet (*Beta vulgaris*) leaves induced by wounding and bacterial infiltration is preceded by an oxidative burst. *Physiological and Molecular Plant Pathology* 64, 125–133.

Shabala, S. and Cuin, T., 2008. Potassium transport and plant salt tolerance. *Physiologia Plantarum* 133, 651-669.

Shabala, S. and Mackay, A., 2011. Ion Transport in Halophytes. *Advances in Botany* 57, 151-199.

Stintzing, F. and Carle, R., 2004. Functional properties of anthocyanins and betalains in plants, food, and in human nutrition. *Trends in Food Science and Technology* 15, 19-38.

Triantaphylides, C., Krischke, M., Hoeberichts, F.A., Ksas, B., Gresser, G., Havaux, M., Van Breusegem, F. and Mueller, M.J., 2008. Singlet oxygen is the major reactive oxygen species involved in photo-oxidative damage to plants. *Plant Physiology* 148, 960-968.

Waisel, Y., 1972. Biology of Halophytes. Academic Press, NY.

Zhao, G.Q., Ma, B.L. and Ren, C.Z., 2007. Growth, gas exchange, chlorophyll fluorescence, and ion content of naked oat in response to salinity. *Crop Science* 47, 123-131.

Zhu, J-K., 2003. Regulation of ion homeostasis under salt stress. *Current Opinion in Plant Biology* 6, 441-445.

Zinnert, J., Nelson, J. and Hoffman, A., 2012. Effects of salinity on physiological responses and photochemical reflectance index in two co-occurring coastal shrubs. *Plant and Soil* 354, 45-55.

4.3. ECOPHYSIOLOGICAL CONSTRAINTS OF TWO INVASIVE PLANT SPECIES UNDER A SALINE GRADIENT: HALOPHYTES VERSUS GLICOPHYTES [1]

Abstract

Salt marsh environments are harsh environments where salinity comprises one of the most important species distribution shaping factor, presenting sediment salinities from 0 to 855 mM (0 to 50 ppt). Invasive species have often a high colonizing potential, due to its high plasticity and adaptation ability. *Spartina patens* is an invasive species already spread along several Mediterranean countries, like France and Spain. *Cyperus longus* is typically a freshwater species that has been spreading across the Mediterranean. In order to evaluate the ecophysiological fitness of these species, mesocosmos trials were performed subjecting both species to increasing realistic salinity levels and their photochemical and biochemical feedback was evaluated. Both species presented very different behaviours. *Spartina patens* appears to be insensitive to salt stress, mostly due to elevated proline concentrations in its leaves allowing it to maintain its osmotic balance, and thus preventing the damaging of its photochemical mechanisms. *Cyperus longus*, on the other hand, was highly affected by elevated salt levels mostly due to the lack of osmotic balance driven by an incapacity to counteract the elevated ionic strength of the external medium by osmocompatible solutes. *Spartina patens* is physiologically highly adapted to saline environments and thus is capable to colonize all the marsh saline environments, while *C. longus* appears to be an opportunistic invader colonizing the marsh during periods of lower salinities typical from rainy seasons.

[1] This section was published in: **Duarte, B.**, Santos, D., Marques, J.C. and Caçador, I., 2015. Ecophysiological constraints of two invasive plant species under a saline gradient: halophytes versus glycophytes. *Estuarine Coastal and Shelf Science* 167, 154-165.

Introduction

About 70% of the Earth's surface is covered by salt water, the oceans, with concentrations of Na^+ around 500 mM, contrasting with the low K^+ concentrations of 9 mM (Flowers, 2004). Also, the remaining 30% of the Earth's surface is severely affected by an increased salinization phenomenon, mostly due to the increased soil use on agriculture and its irrigation procedures (Zhan and Shi, 2014). The ongoing climatic changes are increasing drought, air temperature and salt-water intrusion in coastal soils (Duarte *et al*., 2013). Soil and water salinity substantially constrain crop and biomass production. Above 400 million hectares of land are affected by salinity and this area is increasing day by day due to the excessive irrigation practices, and to the tremendous increase of world population and consequent increasing demand for food supply. Crops cannot be grown on salt-affected soils, but nature has provided us with a unique group of plants that can, the halophytes (Aslam *et al*., 2011). Salinity-induced damage in plants includes reduction of leaf expansion, stomata closure, reduce primary production, biomass losses due to water deficit and deficiency in essential nutrients like K^+ (James *et al*., 2011; Rahnama *et al*., 2010; Mahajan and Tuteja, 2005). Although this is true for most of the Earth's flora, halophytes are the exception, being highly productive under saline conditions. Halophytes are defined as plant species that can survive and reproduce under growth conditions with more than 200 mM NaCl, comprising only 1% of world flora (Flowers and Colmer, 2008). By opposition, glycophytes are defined as species that cannot survive in a saline environment. The recent on-going environmental changes tend to modify the climatic habitats available for colonization of the ecosystems. Salt marshes are no exception to these changes. In these environments species distribution is mostly modulated by marsh elevation, being this last a key factor affecting sediment flooding, redox potential, pH and salinity (Caçador *et al*., 2007). In fact, this last abiotic driver is one of the most important shapers of the salt marsh morphology, conditioning species distribution according to their salinity tolerance. Nevertheless, within the halophytes group, several salt tolerance mechanisms are known. Some species have specific salt glands on the leaves to excrete the excess of salt, others increases its water content in the photosynthetic stems, becoming turgid and this way promotes salt dilution (Liphschitz and Waisel, 1982; Duarte *et al*.,

2013). At the biochemical level halophytes can also accumulate quaternary nitrogen compounds like proline, betain or sorbitol to counteract in the increasing water potential of salty soils (Hassine *et al*., 2008). Besides these adaptations, halophytes are still affected by excessive ionic contents and thus depend on efficient energy dissipation mechanism in order to avoid the overload of the photosynthetic apparatus, mostly based on the xanthophyll cycle and electronic processes at the electron transport chain level (Duarte *et al*., 2013).

Spartina patens is an invasive species already spread along several Mediterranean countries, like France and Spain (Ainouche *et al*., 2004 and 2009). Recently there has been verified an increased invasion of *S. patens* in the Portuguese marshes competing for habitats normally occupied by endemic Chenopodiaceae species (like *Halimione portulacoides* and *Sarcocornia* sp.). Although in a rather small extent, also *Cyperus longus* has recently being detected in some Portuguese salt marshes. According to the Invasive Species Compendium (www.cabi.org) this species is also considered as an invader in European marshes. These two species differ greatly in their salinity tolerance, being *S. patens* a halophyte while *C. longus* is a glycophyte. From this point of view, salinity will be a determining factor establishing the extent to which each of these species will penetrate within the marsh competing with native species.

In the present work the authors aimed to test the ecophysiological constrains in both these species to saline environments similar to those found in field. Since the success of these species colonizing the marshes greatly depend on its biomass production, a special attention was given to their photosynthetic biophysical mechanisms, as well as to some biochemical feedback stress mechanisms. Although there are several salinity tolerance studies on a wide number of halophytes and specially focusing species from the *Spartina* genus, the behaviour of the invasive *S. patens*, along a salinity gradient, lacks of information. Similarly, the papyrus *C. longus* although a glycophyte appears as a potential invasive species and thus the studies of its ecophysiological behaviour on a saline environment acquire this way a renewed importance. This will bring some light into the potential of each species as a possible invader threatening the marsh native species considering sediment salinity

as one of the major abiotic factors shaping the species distribution along a marsh elevation transect.

Materials and Methods

Study area, sampling and mesocosmos setup

Sampling took place at Tagus estuary Alcochete salt marshes. Alcochete (38° 40' N, 9° 01' W) is a young salt marsh (Duarte *et al*., 2013) located in the southern part of the Tagus estuary, within the Tagus Estuary Natural Reserve (Figure 1). The upper marsh is mainly colonized by *H. portulacoides* (Chenopodiaceae) and undergoes short submersion episodes during high tide. *Spartina maritima* (Curt.) Fernald is an herbaceous perennial plant that colonizes estuarine intertidal mudflats widely distributed throughout the coasts of western, southern, and south-eastern Europe, as well as in western Africa. From the 17.24 km^2 of salt marshes existent in Tagus estuary, about 2.41 km^2 are colonized by *S. maritima* and 5.32 km^2 by *H. portulacoides* (Caçador *et al*., 2013).

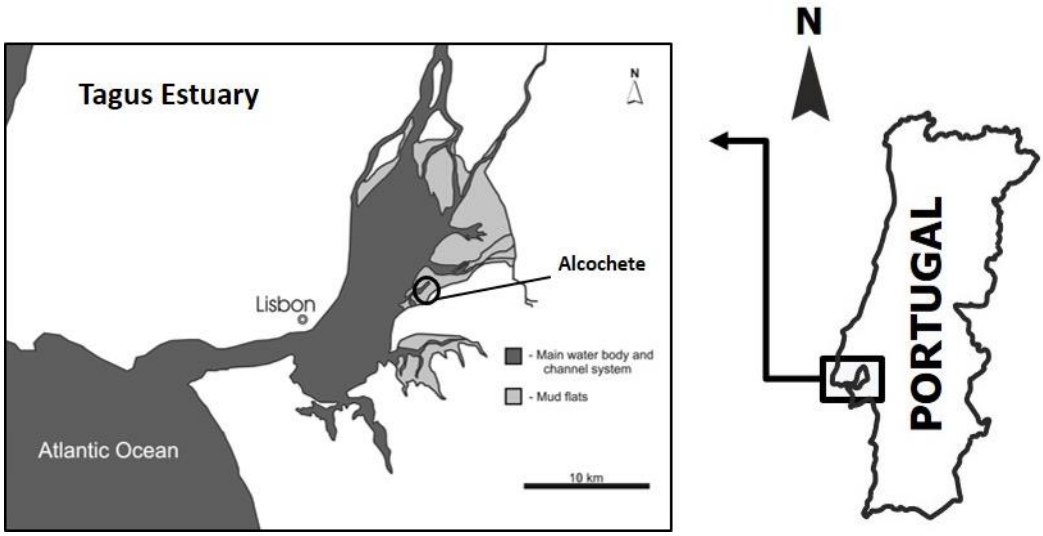

Figure 4.3.1. Tagus Estuary map and Alcochete sampling site.

Spartina patens and *C. longus* individuals were collected along with their sediment and brought back to the laboratory, where they were gently washed and its sediment removed. Both species colonize the upper marsh in sandy sediments. Plants were placed in five replicate pots per treatment containing perlite and

irrigated with ¼ Hoagland solution and placed in a Fitoscope chamber (Photon System Instruments, Czech Republic). The chamber was programmed to replicate the average field air temperatures (25 ± 2 °C), relative humidity (50 ± 2 %) and the PAR evolution along the day (16 h light/8h dark sine function with a maximum PAR of 500 μmol photons m^{-2} s^{-1}. Plants were kept for two weeks in order to acclimate to the new environment. After this period the Hoagland solution was removed and replaced by ¼ Hoagland solution supplemented with NaCl in order to attain the desired salinities (0, 171, 342.2, 513.3 604.4 and 855.5 mM). At the end of 10 days plants were harvested and for all analyses. All samples for biochemical measurements were immediately flash-frozen in liquid-N_2.

Elemental analysis

Leaves or photosynthetic steams for Na, K and Ca content were washed with ultra-pure water to eliminate salts in the surface of the leaf. Subsequently samples were treated and analysed by FAAS as described in Chapter 2, Section 2 (Duarte *et al*., 2014).

PAM fluorometry

Fluorometric analysis were preformed according to the described in Chapter II, Section 3 as described in Duarte *et al*. (2014). All derived variables were computed as described in Table 2.3.1.

Gauss Peak Spectra Pigment Analysis

Samples for pigment analysis were extracted using pure acetone after freeze-drying and analysed by UV-Vis spectrophotometry as described in Chapter III, Section 2 (Kupper *et al*., 2007).

Osmocompatible solutes

The amount of glycine betain was estimated according to the method of Grieve and Grattan (1983). Briefly, the plant tissue was finely ground, mechanically shaken with 20 mL deionized water for 24 h at 25 °C. The samples were then filtered and the filtrates were diluted to 1:1 with 2 N H_2SO_4 and kept in ice water for 1 hour.

Cold KI-I_2 reagent was then added and the reactants were gently stirred. The tubes were stored at 4 °C during 16 h and then centrifuged at 11 180 x g for 15 min at 0 °C. The supernatant was carefully discarded and the pellet composed by periodide crystals was dissolved in 9 mL of 1,2-dichloroethane. After 2 h, the absorbance was measured at 365 nm and compared with a standard curve of glycine betain and expressed in μmol g^{-1} FW.

Proline content was estimated according to Bates *et al*. (1973). The plant material was homogenized in 3% aqueous sulfosalicylic acid and the homogenate centrifuged a 11 180 x g for 15 min at 0 °C. The supernatant was used for proline determination. The reaction consisted of 2 mL of extract combined with 2 mL of glacial acetic acid and 2 mL of acid ninhydrin. The reaction occurred during 1 h at 100 °C, after which the reaction was stopped in an ice bath. The reaction mixture was extracted with 4 mL of toluene and its absorbance read at 520 nm and compared with a standard curve of proline and expressed in μmol g^{-1} FW.

Statistical Analysis

Due to the lack of normality and homogeneity, the statistical analysis of the data was based in non-parametric tests. In order to compare the effects of the NaCl concentrations within each group of individuals from the same species, the Krustal-Wallis test was performed using Statistica Software (Statasoft).

Results

Na^+, K^+ and Ca^{2+} accumulation in above and belowground tissues

On the basis of salt stress tolerance and resistance is the differential allocation of diferent ions within the plant above and belowground organs (Figure 4.3.2). In the present study, the first and most evident ion accumulation pattern arises from *S. patens* subjected to different levels of NaCl. This species showed no significant differences among Na and Ca accumulation upon application of different salt regimes, presenting only some differences regarding K accumulation in the bellowground organs. On the other hand, *C. longus* showed a very marked and distintic ionic profiles among salt treatments, specially between individuals cultured without NaCl and with different salt treatments. Significant increases in Na uptake

and translocation were also verified along the salinity gradient. Nevertheless, also some differences could be detected in root K concentrations, specially when compared with root tissues from individuals exposed to highest NaCl levels.

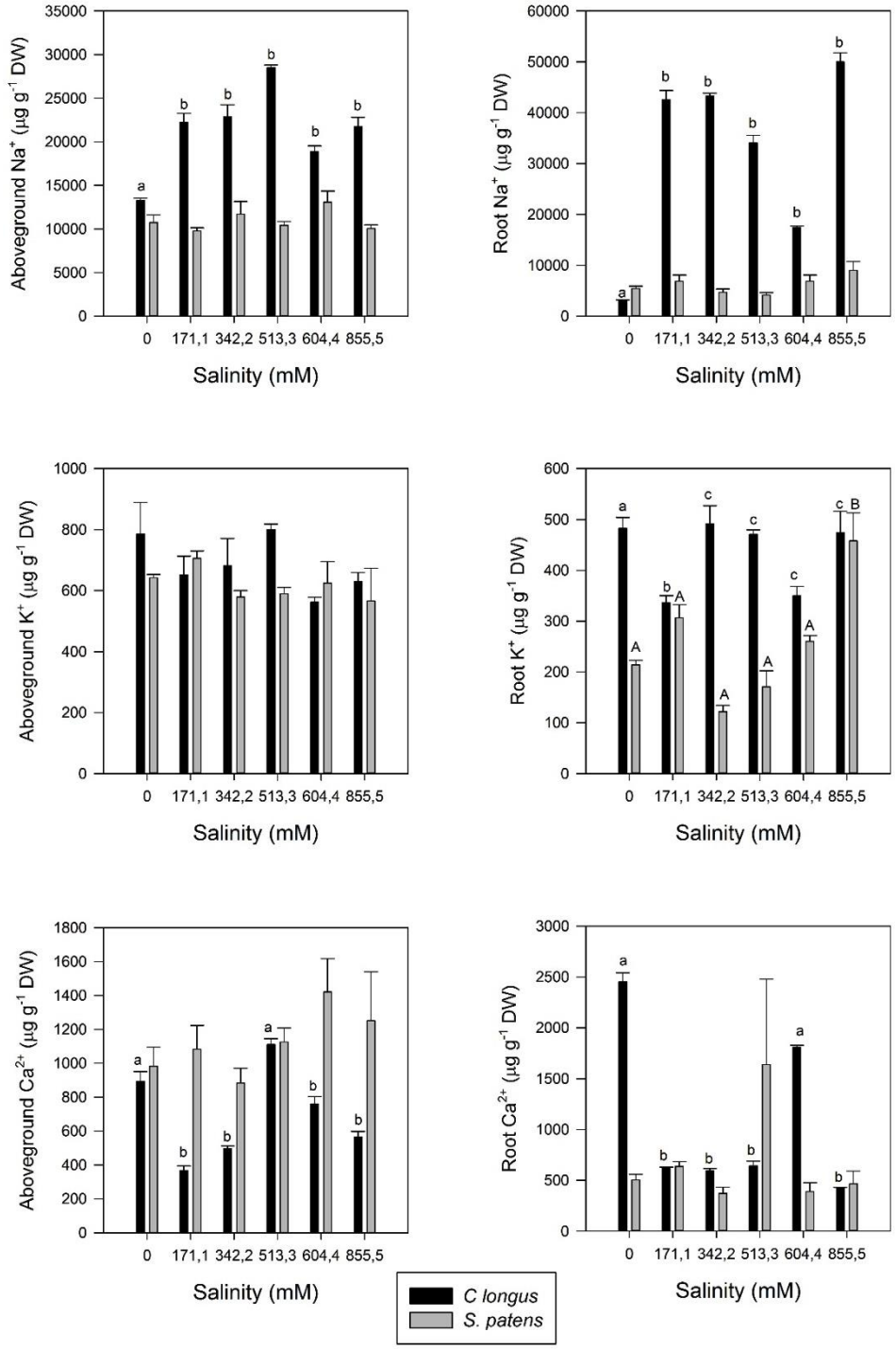

Figure 4.3.2. Na, K and Ca accumulation (average ± standard error, n = 5) in *S. patens* and *C. longus* above and belowground tissues along the tested NaCl concentrations. Lowercase (*C. longus*) and capital (*S. patens*) letters indicate significant differences among treatments at $p < 0.05$).

PS II Quantum Yields

PS II quantum efficiency and related parameters were also evaluated as a proxy of the overall photosynthetic light harvesting mechanisms (Figure 4.3.3).

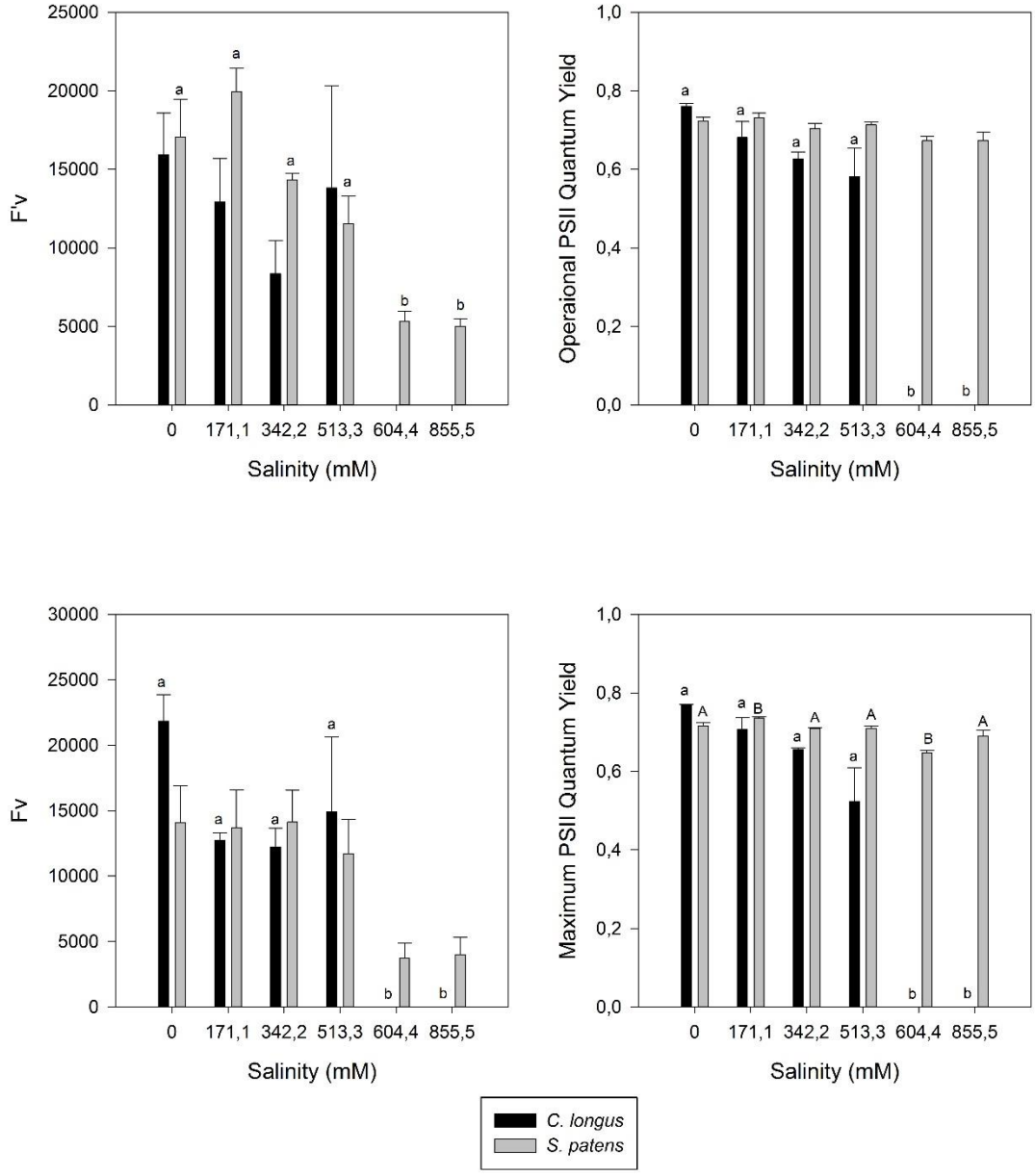

Figure 4.3.3. Variable fluorescence and PS II quantum yields (average ± standard error, n=5) in *C. longus* and *S. patens* light and dark-adapted leaves along the tested NaCl concentrations. Lowercase (*C. longus*) and capital (*S. patens*) letters indicate significant differences among treatments at $p < 0.05$.

Regarding the light adapted variable fluorescence (F'_v) in *S. patens*, it was found a maximum value at 171.1 mM NaCl (although without statistical significance), contrasting with the values observed at highests NaCl concentrations. While in *S. patens* some differences could be found, in *C. longus*, these differences only became evident while observing the variable fluorescence in darked adapted leaves (F_v). The individuals from this species exposed to highest salinity levels didn't survived the imposed stress and died after a week exposure to 604.4 and 855.5 mM NaCl. Thus, the PS II activity in these individuals was null. Nevertheless, a high F_v value could be observed in individuals not exposed to NaCl, decreasing greatly in the presence of NaCl. The same could be found in both operational (light-adapted) and maximum (dak-adapted) PS II quantum yields of *C. longus* leaves. On the other hand, *S. patens* proved again to be insensitive to the aplied salt concentrations even at high concentrations, with no significant changes in its leaves PS II quantum yields.

Electron Transport Rates (ETRs) at different light levels

Considering a light intensity gradient and its correspondent electron transport rates (Figure 4.3.4) some new insights arise. Independently of the NaCl exposure levels*, S. patens* showed very ETR similar patterns at photosynthetic (until 200 μmol photons m^{-2} s^{-1}) and photo-inhibitory (> 200 μmol photons m^{-2} s^{-1}) PAR levels. As for *C. longus* it showed the typical dose-dependent inhibition pattern, in response to NaCl. With increasing salt levels the ETR decreased under all PAR levels, until a complete absence of electron transport at highest salinity concentrations.

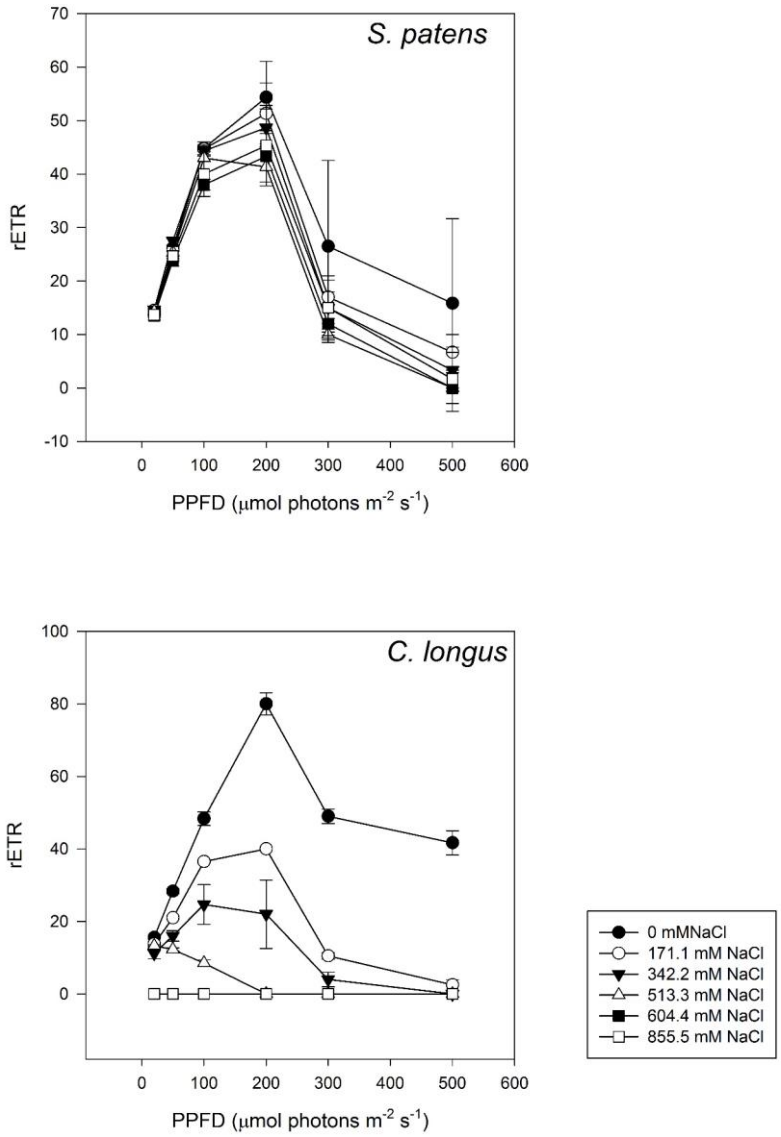

Figure 4.3.4. rETR at different PAR intensities (average ± standard error, n=5) in *C. longus* and *S. patens* dark adapted leaves along the tested NaCl concentrations.

From the light curves, some important parameters can be extracted (Figure 4.4.5). Considering the derived parameters, photosynthetic efficiency (α), maximum ETR (ETR_{max}) and onset of light saturation (E_k), *S. patens* exhibited very similar values of all parameters, independently from the applied exogenous NaCl dose. As for *C. longus* there was a marked decrase on its α and ETR_{max} along the tested salinity gradient. Although these similarities, both parameters decreased in different extents leading to an increase in the ETR_{max}/α ratio, here translated into an higher onset for light saturation, observed at 171.1 and 342.2 mM NaCl.

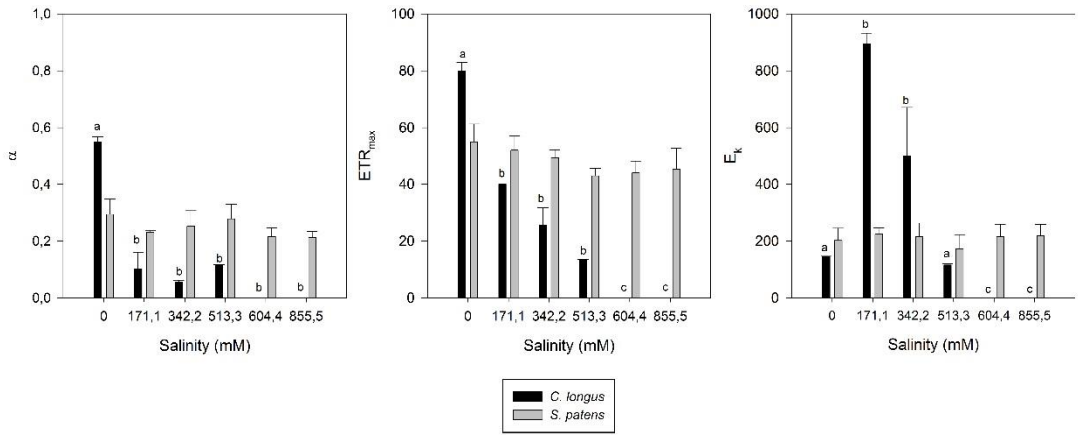

Figure 4.3.5. Photosynthetic efficiency, maximum ETR and light saturation constant (average ± standard error, n = 5) in *C. longus* and *S. patens* dark-adapted leaves along the tested NaCl concentrations. Lowercase (*C. longus*) and capital (*S. patens*) letters indicate significant differences among treatments at $p < 0.05$.

Chlorophyll OJIP transient analysis

If the processes underlying the whole photochemical energetic fluxes are observed, new insights are revealed supporting the above-mentioned differences. The Kautsky curves provide a very general view of the photochemical process from light harvesting to its dissipation (Figure 4.3.6). Although in previous analysis there were no differences in most of the evaluated treatments among *S. patens* individuals exposed to different tested NaCl, with this deeper analysis some differences are possible to identify. Although low salinity treatments (0 to 513.3 mM) produced very similar Kautsky curves, the highest NaCl concentrations decreased the overall fluorescence of the OJIP curve. *Cyperus longus* leaves also showed differences among treatments, with the individuals exposed to low salinities showing typical OJIP curves while all other treatments produced curves with lower fluorescence values and areas above the curves.

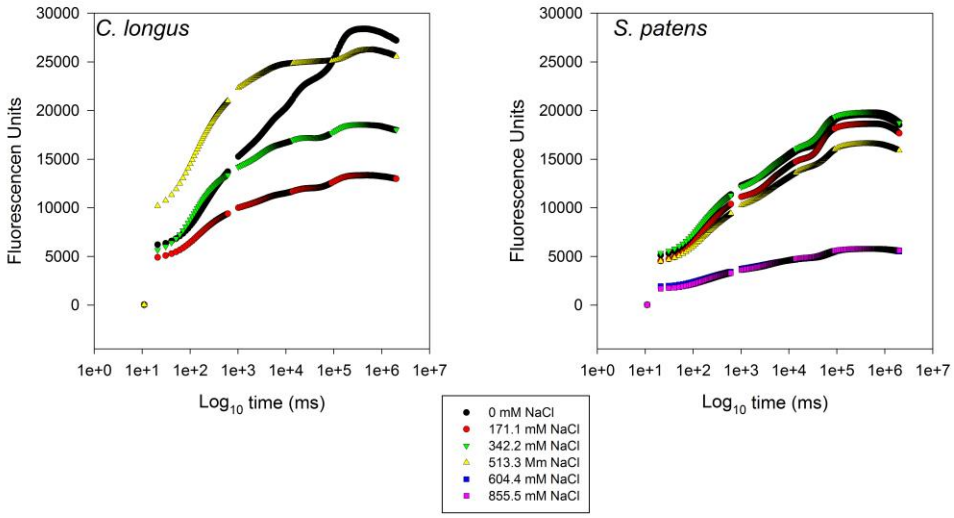

Figure 4.3.6. Kautsky curves (average, n=5) in *C. longus* and *S. patens* dark-adapted leaves along the tested NaCl concentrations.

These shape variations can be translated into the different driving forces that comprise the driving force for photosynthesis (DF_{ABS}). Observing its differences in relation to the non-saline treatment, a driving force variation plot was attained (Figure 4.4.7). In *C. longus* was possible to observe that, with the exception of the driving force for light energy absorption (DF_{RC}), all the other processes decreased its values (thus, presenting positive variations towards the control). The DF_{ABS} decrease was mainly due to a decrease in both the trapping (DF_{ψ}) of excitation energy and in the conversion of this energy into electron transport (DF_{φ}). Regarding *S. patens* only very slight fluctuations could be observed. Although the Kautsky curves showed a decrease in the fluorescence of *S. patens* leaves exposed to highest salinities, this was not evident in the driving force diagram.

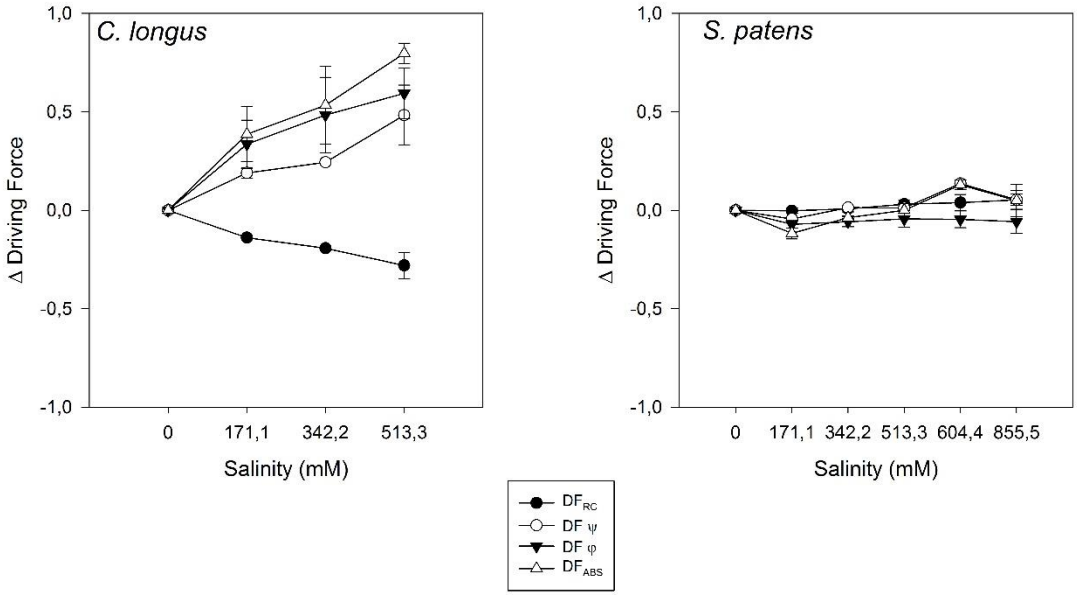

Figure 4.3.7. Driving force variation (driving force for photosynthesis (DF_{ABS}), driving force for light energy absorption (DF_{RC}), driving force for trapping of excitation energy (DFψ) and in the conversion of this energy into electron transport (DFφ), in *C. longus* and *S. patens* dark-adapted leaves along the tested NaCl concentrations (average ± standard error, n=5).

Using the Kautsky curves as basis, the energy fluxes within a leaf cross-section, were also calculated (Figure 4.4.8). Throughout this analysis it was possible to observe that, in both highest NaCl concentrations, the number of reaction centres available for photon harvesting (RC/CS) decreased significantly, whereas their number remained stable along the lower NaCl treatments. Concomitantly also the absorbed, trapped, transported and dissipated energy flux also decreased significantly under 604.4 and 855.5 mM NaCl. Due to this proportional decreases and integrating all energy fluxes into a performance index, it was found that this parameter remained undisturbed along treatments. As for *C. longus*, it showed an increased in the absorbed and trapped energy flux, although the transported energy flux showed an inverse pattern. Thus, this lead to an increase in the dissipated energy flux, that reached its maximum at estuarine salinities (513.3 mM), similarly to the verified for the absorbed and trapped energy fluxes. Overlooking the performance index for this species, it was found also a significant decrease in the energy fluxes processing efficiency.

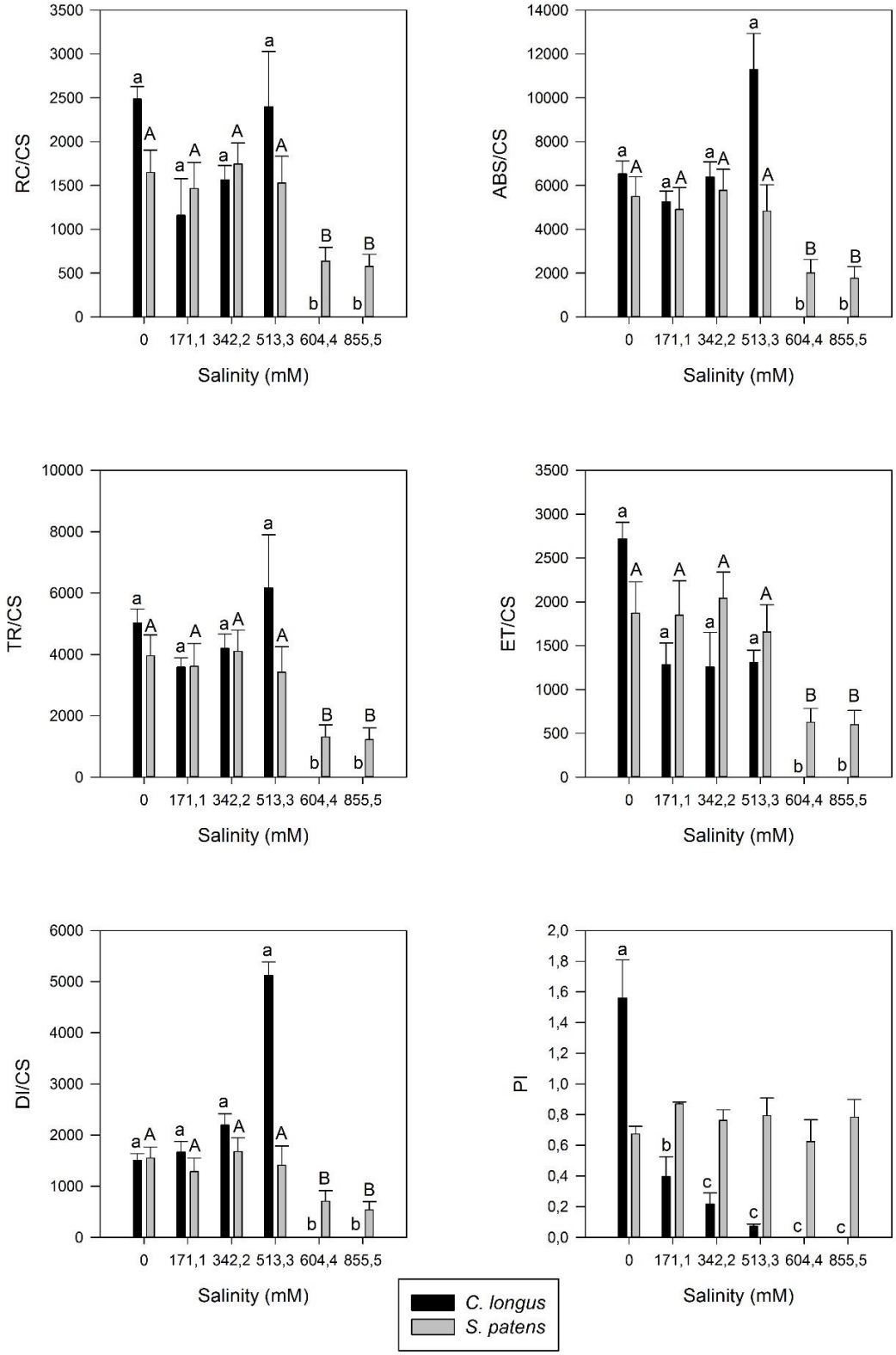

Figure 4.3.8. Energy fluxes per leaf cross section (average ± standard error, n = 5) in *C. longus* and *S. patens* dark-adapted leaves along the tested NaCl concentrations. Lowercase (*C. longus*) and capital (*S. patens*) letters indicate significant differences among treatments at $p < 0.05$.

Chlorophylls and Carotenoid concentrations

Following the same trend previously verified for the above-mentioned parameters, also chlorophyll and carotenoid contents were found to be rather stable along salinity treatments, especially in *S. patens* (Table 4.3.2). The only exceptions were found in chlorophyll a and b in *C. longus* exposed to 604.4 mM NaCl with a significant increase while comparing with plants irrigated with freshwater.

Table 4.3.2. Pigment ratios (average ± standard error, n = 5) in *C. longus* and *S. patens* leaves along the tested NaCl concentrations (letters indicate significant differences among treatments at $p < 0.05$).

	Salinity (mM)	Chl a/b	CDI	DES
C. longus	0	1.96 ± 0.21	1.00 ± 00	0.87 ± 0.00[b]
	171,1	2.91 ± 0.34	0.98 ± 0.01	0.80 ± 0.02[a]
	342,2	2.29 ± 0.49	0.87 ± 0.10	0.86 ± 0.05[b]
	513,3	2.27 ± 0.42	0.92 ± 0.05	0.94 ± 0.01[a]
	604,4	2.56 ± 0.18	0.96 ± 0.01	0.87 ± 0.03[b]
	855,5	2.82 ± 0.10	0.96 ± 0.01	0.86 ± 0.01[b]
S. patens	0	2.23 ± 0.17	0.80 ± 0.04	0.79 ± 0.09
	171,1	1.95 ± 0.20	0.83 ± 0.04	0.75 ± 0.02
	342,2	2.63 ± 0.23	0.93 ± 0.03	0.78 ± 0.01
	513,3	2.81 ± 0.28	0.95 ± 0.03	0.81 ± 0.03
	604,4	2.64 ± 0.06	0.95 ± 0.01	0.77 ± 0.03
	855,5	2.91 ± 0.19	0.96 ± 0.02	0.74 ± 0.05

The same could be observed for Lutein and Zeaxanthin (Table 4.3.2.). In *S. patens* this last carotenoid showed a significant reduction in the individuals exposed to the highest NaCl dose while compared with individuals irrigated with estuarine salinities (342.2 mM). As for the DES, only *C. longus* showed some differences among treatments, with the plants exposed to estuarine salinities presenting significantly higher DES values while compared with the group subjected to lower salinity (171.1 mM). Auroxanthin content in *C. longus* also showed differences, with a maximum accumulation at 604.4 mM NaCl treatment. In *S. patens* this pigment appeared in its basal levels along all treatments with the exception with the higher salinity treatment were there was a drastic increase in its leaf content.

Table 4.3.3. Pigment concentrations (μg g^{-1} FW, average ± standard error, n = 5) in *C. longus* and *S. patens* leaves along the tested NaCl concentrations (letters indicate significant differences among treatments at $p < 0.05$).

	Salinity (mM)	Chl a	Chl b	b-carotene	Auroxanthin	Antheraxanthin	Violaxanthin	Lutein	Zeaxathin
C. longus	0	31.65 ± 7.73^{a}	16.04 ± 0.80	7.47 ± 1.12	13.50 ± 1.29^{a}	5.98 ± 0.52	2.98 ± 0.16^{b}	13.15 ± 3.79^{a}	13.80 ± 0.46^{a}
	171,1	238.81 ± 100.72^{ab}	91.09 ± 20.04	35.95 ± 15.87	34.29 ± 8.33^{a}	21.78 ± 8.38	32.78 ± 2.96^{a}	48.92 ± 3.08^{ab}	106.98 ± 1.89^{ab}
	342,2	241.64 ± 114.41^{ab}	95.11 ± 24.47	35.69 ± 8.40	57.97 ± 15.73^{a}	25.90 ± 9.07	9.62 ± 0.39^{b}	35.98 ± 11.71^{ab}	55.47 ± 22.15^{ab}
	513,3	299.09 ± 130.84^{ab}	119.68 ± 33.35	32.69 ± 13.52	43.45 ± 14.50^{a}	17.04 ± 4.05	6.11 ± 0.75^{b}	55.81 ± 1.67^{ab}	83.86 ± 3.84^{ab}
	604,4	546.93 ± 95.27^{b}	211.36 ± 29.46	72.28 ± 15.24	60.77 ± 6.05^{b}	35.60 ± 8.16	33.38 ± 8.58^{a}	73.58 ± 2.48^{b}	180.47 ± 10.73^{b}
	855,5	313.62 ± 77.72^{ab}	109.82 ± 25.49	37.70 ± 5.85	25.14 ± 2.64^{a}	17.88 ± 3.22	13.93 ± 4.39^{b}	23.95 ± 6.22^{ab}	66.12 ± 15.76^{ab}
S. patens	0	238.22 ± 23.95^{a}	106.67 ± 7.30	35.35 ± 4.98	1.29 ± 0.80^{a}	11.24 ± 4.54	24.10 ± 9.19	23.96 ± 1.81	79.95 ± 8.22^{AB}
	171,1	475.85 ± 62.83^{ab}	243.70 ± 14.32	31.69 ± 2.89	1.00 ± 0.53^{a}	24.14 ± 3.91	36.59 ± 3.51	34.15 ± 2.50	88.25 ± 4.34^{AB}
	342,2	529.19 ± 71.06^{ab}	199.55 ± 8.93	35.55 ± 6.53	0.35 ± 0.18^{a}	23.60 ± 2.38	28.61 ± 2.72	32.83 ± 3.94	79.91 ± 1.03^{AB}
	513,3	623.39 ± 154.97^{ab}	227.46 ± 56.63	39.56 ± 6.93	0.00 ± 0.00^{a}	26.74 ± 5.07	34.19 ± 8.02	38.64 ± 7.65	117.87 ± 5.87^{A}
	604,4	519.13 ± 29.77^{b}	197.54 ± 15.62	34.65 ± 0.53	0.57 ± 0.24^{a}	19.92 ± 4.02	27.76 ± 4.40	32.68 ± 3.17	75.41 ± 14.40^{AB}
	855,5	534.75 ± 120.96^{ab}	179.95 ± 31.84	48.82 ± 3.23	13.17 ± 4.69^{b}	27.55 ± 0.31	34.53 ± 10.59	41.73 ± 6.94	64.68 ± 2.23^{B}

Proline and Betain accumulation

Comparing leaf proline content in both species (Figure 4.4.9), again the differences are evident between a halophyte and a glycophyte. *Cyperus longus* showed a decrease in proline content while *S. patens* showed a significant increase in this amino acid concentration, concomitant with increasing salinity treatments. As for betain concentration, both species exhibited stable concentrations among the salinity treatments with only minor and non-significant fluctuations.

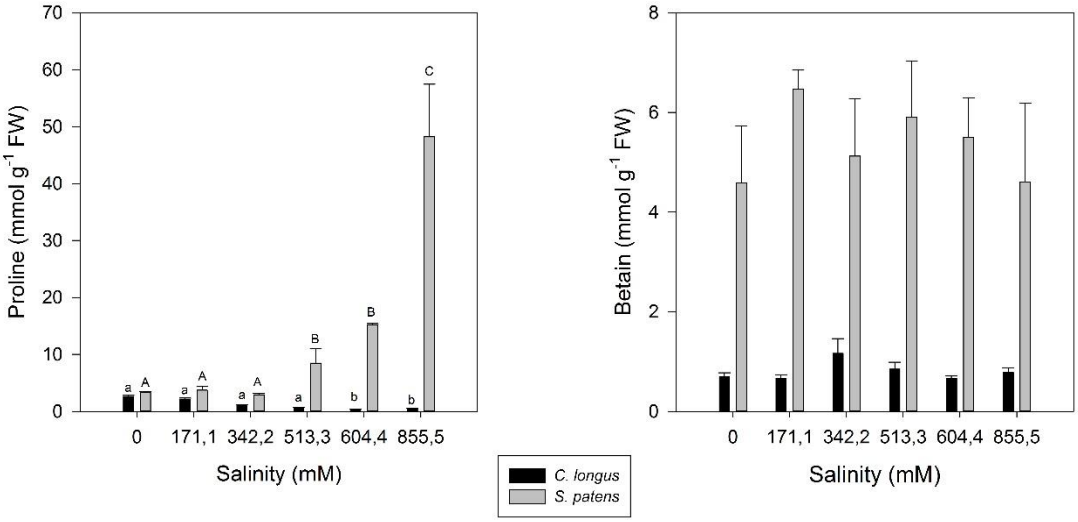

Figure 4.3.9. Proline and Betain contents in (average ± standard error, n = 5) leaves of *C. longus* and *S. patens* along the tested NaCl concentrations. Lowercase (*C. longus*) and capital (*S. patens*) letters indicate significant differences among treatments at $p < 0.05$.

Discussion

The success of plant colonization in salt marshes results from the compromise between the abiotic factors that shape the colonizing environment and plant tolerance towards these constrains (Duarte *et al*., 2013). Most of halophytes use basic mechanisms of controlled accumulation and sequestration of inorganic ions to adjust their internal osmotic balance to external salinity (Flowers and Yeo, 1986). However, halophytes greatly differ in their ionic allocation strategies as well as their overall degree of salt tolerance (Glenn *et al*. 1996). For example, in *Halosarcia pergranulata* and *Suaeda fruticosa* high NaCl concentrations lead to a reduction of K^+ absorption (Sleimi *et al*. 1999; Uddin *et al*. 2011). These differences

are even more evident if comparing a glycophyte (like *C. longus*) with a halophyte (like *S. patens*).

Both species ionic profiles indicate a very different ion uptake along a salinity gradient. *Spartina patens* is a salt excluding grass (Duarte *et al*., 2014b), keeping root Na concentrations very low, even at high external NaCl concentrations. Salt excluders avoid salt toxicity at the roots mostly due to blocking of Na and Cl at root epidermis through the cell membrane. Roots also have an endodermis containing waxy strips surrounding each cell, to obstruct the entry of Na and Cl ions. Although this mechanism is less common, selective permeability of the cell membrane into the halophyte roots is possible. In some plants, root cells are capable of actively pumping excess Na and Cl ions to the surrounding medium (Harrouni *et al*., 2003). Although the mechanisms of Na^+ toxicity are largely due to an obvious coupling between Na^+ uptake and K^+ efflux and replacement of K^+ by Na^+ in metabolically active compartments, traditionally, Na^+ exclusion mechanisms are considered more important for salt tolerance than intracellular K^+ retention (Tester and Davenport 2003; Munns 2005).

Alongside with this possible root block, *S. patens* also presented an elevated proline concentration in its leaves, increasing leaf water potential and thus counteracting the differential osmotic pressures between soil and leaves (Briens and Larher, 1982; Koyro *et al*., 2008; Aziz *et al*., 2011). On the other hand, in this species, glycine-betain concentrations did not vary along the salinity gradient, pointing out this species as a salt excluder and proline accumulator. Comparatively, *C. longus*, responded positively to the salinity gradient, uptaking and translocating significant amounts of Na and K and decreasing root Ca concentration. Sodium excess can lead to the displacement of membrane-bound Ca, essential for cell signalling (Cramer *et al*., 1985). Sodium can also affect K metabolism, by interfering with several K-cofactor enzymes (Khan *et al*., 2000). Concomitantly, observing the osmocompatible solute concentrations, the incapacity of this plant to counteract the high external osmotic potential is reinforced. The proline content in leaf showed a decrease with the increasing Na external dose applied. Glycine-betain did not show any significant variation along the salinity treatments, pointing out to an inefficiency of both these osmosolutes as counteractive measures to excessive Na. The high shoot Na

concentration and negative correlation with the leaf water content (data not shown), indicated a very limited capacity of this species in preventing Na^+ from reaching aerial tissues. This incapacity to maintain leaf water status in *C. longus*, is concomitant with the facts previously reported by Yang and Yen (2002) for *A. thaliana*, the widely used model glycophyte. This lack of ion compartmentalization and counteractive biochemical measures, make *C. longus* a typical glycophyte, and thus defenceless to salt stress. Similarly, also Vera-Estrella *et al*. (2005) showed a very high root Na^+ accumulation in *Thellungiella halophila*. Zid and Grignon (1986) reported that species, which are unable to compartmentalize Na^+ in their leaves, are significantly more sensitive to salinity, mostly due to high cytoplasmic Na^+ concentration. However, tolerant plants are able to protect their cytoplasm against the toxic accumulation of Na^+ throughout vacuolar sequestration (Zid and Grignon, 1991).

These differential ionic uptake and osmotic regulation mechanisms have deep and severe impacts on the plant metabolism, especially at the photosynthetic level. In fact, *C. longus* individuals subjected to the two highest salinity levels did not resist until the end of the trials. Nevertheless, PS II quantum efficiencies were already very low (almost null) in these individuals and coherent with the decreasing trend verified alongside increasing salt concentrations. One of the consequences of salinity-induced limitation of photosynthetic capacity is the exposure of plants to excessive light energy. In stress-conditions the energy dissipation mechanisms are not as efficient as required, having this way severe negative consequences on the photosystem II (Demming-Adams and Adams, 1992; Qiu *et al*., 2003; Megdiche *et al*., 2008). Observing the overall PS II light harvest mechanism, *S. patens* contrarily to *C. longus*, is apparently salt insensitive without differences on both maximum and operational PS II efficiency among treatments. This is concomitant with the abovementioned data regarding the maintenance of the ionic levels in the leaves of this species. In *S. patens* the maximum ETR, photosynthetic efficiency and onset of light saturation are very similar among healthy and stressed individuals, only with small non-significant differences also regarding the rETR at high light exposures. On the other hand, *C. longus* individuals exhibited very distinct photosynthetic parameters depending on the exogenous NaCl dose applied. At high NaCl

concentrations these parameters were reduced to values near zero, culminating in null ETRs. Observing the different test groups of *S. patens* individuals, there were no major differences neither between the ETRs nor in the onsets of light saturation, indicating a normal functioning of the ETC. As for *C. longus*, the reduction in all parameters relative to the ETC, indicate an incapacity to use the absorbed photons in primary photochemistry. This leads inevitably to an accumulation of large amounts of energy that, as stated before, can destroy the D1 protein, impairing all photochemical machinery (Demming-Adams and Adams, 1992; Qiu *et al*., 2003; Duarte *et al*., 2013). This excessive energy accumulation needs to be dissipated, in order to prevent oxidative damage inside the chloroplasts. One of the most efficient and frequent energy dissipation systems is throughout the xanthophyll cycle (Demming-Adams and Adams, 1992). In *C. longus* individuals exposed to the highest tolerated salinity there was an increase in the DES, reflection of a higher activity of the xanthophyll cycle attempting to dissipate the excessive redox power accumulated inside the stroma. Non-photochemical quenching and DES variations can be attributed to treatment effects on electron transport capabilities and on the redox state of the photosynthetic membranes (Föster *et al*., 2001). Excess of light energy leads inevitably to a decrease in the lumen pH, attributed to NPQ activation by protonation of the LHC proteins associated with the PS II (Cousins *et al*., 2002). Consequently, this induces the xanthophyll cycle activation, dissipating excessive energy and reducing the PS II and associated proteins excessive protonation. This was accompanied by an increase in Lutein and β-carotene concentrations, two typical anti-oxidant carotenoids produced as a possible counteractive measure against ROS (Duarte *et al*., 2013). Also auroxanthin leaf content showed an increase in both species stressed individuals. This pigment is a violaxanthin analogue (Wentworth *et al*., 2000). Auroxanthin is a C5,8 epoxy carotenoid that has previously been shown to enhance aggregation-associated quenching in isolated LHC IIb (Ruban *et al*., 1998). The effectiveness of auroxanthin has been suggested to come from the fact that its S1 energy level is higher than that of violaxanthin (Wentworth *et al*., 2000). This effect is explained by its structure where the end groups of auroxanthin lie in the plane of the conjugated carbon double bond chain, as in zeaxanthin, whereas they are expected to be out-of-plane in violaxanthin. In fact, the C5,8

epoxide would hold the end group rigidly in-plane, explaining why it is even more effective than zeaxanthin and thus be an efficient energy quencher under stress conditions (Horton *et al*., 1999; Ruban *et al*., 1998).

With the analysis of the Kautsky curves, a deeper look into the photochemical mechanisms provides new insights about the biophysical impacts of excessive salinity. The shape of the OJIP transient curve is very sensitive to environmental stresses (Zhang and Gao, 1999; Calatayud and Barreno, 2001; Strasser and Tsimilli-Michael, 2001; Sayed, 2003; van Heerden *et al*., 2003; Govindachary *et al*., 2004). The rapid O-J rise is a phase controlled by photochemical processes, while the J-I phase is strictly a thermal phase (Schreiber and Neubaeuer, 1987). The release of fluorescence from this last phase is controlled by the reactions occurring in the donor side of the PS II. Any abiotic stress that disturbs the structure and function of the OECs, affects the rate of oxygen evolution and thus increases the release of fluorescence quenching in the J-I phase (Panda *et al*., 2006). On the other hand, the rise in the O-J phase is due to the PS II quinone pool reduction net photochemical (Prakash *et al*., 2008). Comparing the donor (J-I) with the acceptor (O-J) PS II sides in *C. longus,* in individuals subjected to different salinity treatments, the donor side was more severely affected by NaCl application, probably due to the inactivation of the OECs and consequent impairment of the ETC (Panda *et al*., 2006). A reduction in the area above the transient curve could also be verified, directly related to the size of the quinone pool in the PS II acceptor side (Strasser *et al*., 1995; Joliot and Joliot, 2002). Alongside there was also a reduction in the quinone pool size available for reduction. Both the electron flow from the ETC to the quinone pool as well as the quinone reduction availability was rather decreased, leading to an excessive energy accumulation at this level (Kalaji *et al*., 2011). This approach also showed that in fact *S. patens* individuals subjected to the highest salinity levels also showed a depressed Kautsky curves with lower fluorescence values with a homogenous profile and undistinguishable peaks, characteristic of stress individuals. As evidenced by the driving forces diagram, in *C. longus*, the probability that an incident photon can move an electron throughout the ETC decreased simultaneously with a reduction in the efficiency of a trapped electron to move further than the oxidized quinone pool, and consequently reducing the maximum yield for primary photochemistry (Kalaji *et*

al., 2011). This reduction is in agreement with the overall deleterious effect of excessive ions on the PS II, as already was described for other plant species (Panda *et al*., 2006; Mateos-Naranjo *et al*., 2007). Inevitably, this F_M decrease in the transient OJIP affects the Fv/F_M relationship and thus the PS II quantum yields, as could also be verified along the different salt treatments. This reinforces the previous findings, pointing out to a reduction in the PS II capacity to reduce the primary acceptor, Q_A (Duarte *et al*., 2014a). Comparing the driving forces variation, all presented a decrease along the salinity treatments, with the exception of the driving force for energy absorption, resulting in an overall progressive decrease in the driving force for photosynthesis. As for *S. patens,* there was no apparent change in the driving forces per reaction centre. If this process is evaluated on a leaf cross-section basis, the reasons behind this homogeneity in the driving forces are unveiled. The number of reaction centres available for reduction in the individuals of this species maintained constant up to 513.3 mM NaCl. This was exactly the same trend observed for all the remaining energy fluxes, and thus when expressed by reaction centre these driving forces appear constant. The number of reaction centres available for reduction substantially decreases upon high salinity treatments, decreasing this way the capacity to trap the received energy. On the other hand, at the highest salinity treatment *C. longus,* showed an increased number of available reaction centres per leaf cross section, increasing this way the absorbed and trapped energy fluxes. Under high salinities, this species, showed reduced PS II photosynthetic efficiencies (α) and ETR, with a simultaneous increase in energy dissipation. In sum, the changes observed at the photosynthetic level were not due to alterations in electronic fluxes, but to changes in redox-regulated non-photochemical quenching mechanisms.

Conclusions

Salinity imposes one of the major constrains to the species colonization and distribution along salt marshes (Duarte *et al*., 2014b). The species ability to withstand, growth and complete its life cycle in salt environments, are determinant for the species ecological success in such environments. Salinity is not only a shaping factor of the marsh plant zonation can also act as a barrier to invasions by terrestrial

species. The two well-known invasive species here studied (*S. patens* and *C. longus*) appear to have completely different physiological finesses for salt marsh colonization. *Cyperus longus* appears as a glycophyte, with very low salt tolerance mostly due to its inability to counteract excessive ion uptake and therefore imposing severe damage to the photosynthetic apparatus mostly at the electron transport mechanisms. This species appears as an opportunistic species taking advantage of the low salinity periods, which are often observed in the rainy seasons in the Mediterranean marshes. On the other hand, *S. patens* appear as highly fit species, with efficient mechanisms to block salt uptake and well-adapted photosynthetic mechanisms, even in environments with twice the ocean salinity. This subject acquires a particular importance considering the aggressiveness of this invader and its potential effects on the marsh community potentiated by a highly tolerant metabolism allowing it to colonize and compete with other halophytes for the same ecological habitats, with consequent negative impacts on the marsh biodiversity.

References

Ainouche, M.L., Baumel, A., Salmon, A. and Yannic, G., 2004. Hybridization, polyploidy and speciation in *Spartina* Schreb. (Poaceae). *New Phytologist* 161, 165–172.

Ainouche, M.L., Fortune, P.M., Salmon, A., Parisod, C., Grandbastien, M.A., Fukunaga, K., Ricou, M. and Misset, M.T., 2009. Hybridization, polyploidy and invasion: lessons from *Spartina* (Poaceae). *Biological Invasions* 11, 1159-1173.

Asla, R., Bostan, N., Amen, N., Maria, M. and Safdar, W., 2011. A critical review on halophytes: Salt tolerant plants. *Journal of Medicinal Plants Research* 5, 7108-7118.

Aziz, I., Gul, B., Gulzar, S. and Khan, M.A., 2011. Seasonal variations in plant water status of four desert halophytes from semi-arid region of Karachi. *Pakistan Journal of Botany* 43, 587-594.

Bates, L.S., Waldren, R.P. and Teare, I.D., 1973. Rapid determination of free proline for water stress studies. *Plant and Soil* 39, 205-207.

Briens, M. and Larher, F. 1982 Osmoregulation in halophytic higher plants: a comparative study of soluble carbohydrates, polyols, betaines and free proline. *Plant, Cell and Environment* 5, 287-292.

Caçador, I., Tibério, S. and Cabral, H., (2007. Species zonation in Corroios salt marsh in the Tagus estuary (Portugal) and its dynamics in the past fifty years. *Hydrobiologia* 587, 205-211.

Calatayud, A. and Barreno, E., 2001. Chlorophyll a fluorescence, antioxidant enzymes and lipid peroxidation in tomato in response to ozone and benomyl. *Environmental Pollution* 115, 283-289.

Cramer, G.R., Lauchli, A. and Polito, V.S., 1985. Displacement of Ca^{2+} by Na^{+} from the plasmalemma or root cells: a primary response to stress. *Plant Physiology* 79, 207-211.

Demmig-Adams, B. and Adams, WW II., 1992. Photoprotection and other responses of plants to light stress. An*nual Review of Plant Physiology and Plant Molecular Biology* 43, 599-626.

Duarte, B., Santos, D., Marques, J. C. and Caçador, I., 2013. Ecophysiological adaptations of two halophytes to salt stress: photosynthesis, PS II photochemistry and anti-oxidant feedback - Implications for resilience in climate change. *Plant Physiology and Biochemistry* 67, 178-188.

Duarte, B., Santos, D., Marques, J.C. and Caçador, I., 2014a. Biophysical probing of *Spartina maritima* Photo-system II changes during increased submersion periods: possible adaptation to sea level rise. *Plant Physiology ad Biochemistry* 77, 122-132.

Duarte, B., Sleimi, N. and Caçador, I., 2014b. Biophysical and biochemical constrains imposed by salt stress: Learning from halophytes. *Frontiers in Plant Science* 5, 746.

Fan, Y., Li, P.F., Hou, Z.A., Ren, T.S., Xiong, C.L. and Zhang, B., 2012. Water adaptive traits of deep-rooted C3 halophyte (*Karelinia caspica* (Pall.) Less.) and shallow-rooted C4 halophyte (*Atriplex tatarica* L.) in an arid region Northwest China. *Journal of Arid Landscapes* 4, 469–478.

Flowers, T. J., 2004. Improving crop salt tolerance. *Journal of Experimental Botany* 55, 307-319.

Flowers, T.J. and Colmer, T.D., 2008. Salinity tolerance in halophytes. *New Phytologist* 179, 945-963.

Flowers, T.J. and Yeo, A.R., 1986. Ion relations of plants under drought and salinity. *Australian Journal of Plant Physiology* 13, 75-91.

Glenn, E.P., Poster, R., Brown, J.J., Thompson, T.L. and O'Leary, J.W., 1996. Na and K accumulation and salt tolerance of *Atriplex canescens* (Chenopodiaceae) genotypes. *American Journal of Botany* 83, 997-1005.

Govindachary, S., Bukhov, N.G., Joly, D. and Carpentier, R., 2004. Photosystem II inhibition by moderate light under low temperature in intact leaves of chilling-sensitive and –tolerant plants. *Physiologia Plantarum* 121, 322-333.

Grieve, C.M. and Grattan, S.R., 1983. Rapid assay for the determination of water soluble quaternary ammonium compounds. *Plant and Soil* 70, 303-307.

Harrouni, M.C., Daoud, S. and Koyro, H-W. 2003. Effects of seawater irrigation on biomass production and ion composition of seven halophytic species in Morocco. In: Lieth H, Mochtchenko M, eds.*Tasks for vegetation science 38 cash crop halophyte*. Dordrecht, the Netherlands: Kluwer, 59–70.

Hassine, A. B., Ghanem, M. E., Bouzid, S. and Lutts, S., 2008. An inland and a coastal population of the Mediterranean xero-halophyte species *Atriplex halimus* L. differ in their ability to accumulate proline and glycinebetaine in response to salinity and water stress. *Journal of Experimental Botany* 59, 1315-1326.

Horton, P., Ruban, A.V. and Young, A.J., 1999. Regulation of the structure and function of the light-harvesting complexes of photosystem II by the xanthophyll cycle. In: Frank HA, Young AJ, Cogdell JC, eds. *The photochemistry of carotenoids: applications in biology.* Kluwer Academic Publishers, 271–291.

James, R.A., Blake, C., Byrt, C.S. and Munns, R., 2011. Major genes for Na^+ exclusion, Nax1 and Nax2 (wheat HKT1;4 and HKT1;5), decrease Na^+ accumulation in bread wheat leaves under saline and waterlogged conditions. *Journal of Experimental Botany* 62, 2939-2947.

Joliot, P. and Joliot, A., 2002. Cyclic electron transport in plant leaf. *PNAS* 99, 10209-10214.

Kalaji, H., Govindjee, Bosa, K., Koscielniak, J., and Zuk-Golaszewska, K. 2011. Effects of salt stress on photosystem II efficiency and CO_2 assimilation of two Syrian barley landraces. *Environmental and Experimental Botany* 73, 64-72.

Koyro, H.-W., Geibler, N., Hussin, S. and Huchzermeyer, B., 2008. Survival at extreme locations: Life strategies of halophytes – The long way from system ecology, whole plant physiology, cell biochemistry and molecular aspects back to sustainable utilization at field sites. In: Abdelly C, Ashraf M, Oztürk M, Grignon C (ed.) *Biosaline Agriculture and Salinity Tolerance in Plants*. Birkhaäser Verlag AG, pp. 241-246.

Liphschitz, N. and Waisel, Y., 1982. Adaption of the plants to saline environments: salt excretion and glandular structure. In D.N. Sen and Rajpurohit (ed.). *Contribution to the ecology of halophytes*. Dr. W. Junker Publishers. The Hague.

Mahajan, S. and Tuteja, N., 2005. Cold, salinity and drought stresses: an overview. *Archives of Biochemistry and Biophysics* 444, 139-158.

Mateos-Naranjo, E., Castellanos, E.M. and Perez-Martin, A., 2014. Zinc tolerance and accumulation in the halophytic species *Juncus acutus*. *Environmental and Experimental Botany* 100, 114-121.

Megdiche, W., Hessini, K., Gharbi, F., Jaleel, C., Ksouri, R. and Abdelly, C., 2008. Photosynthesis and photosystem II efficiency of two salt-adapted halophytic seashore *Cakile maritima* ecotypes. *Photosynthetica* 46, 410-419.

Munns, R., 2005. Genes and salt tolerance: bringing them together. *New Phytologist* 167, 645–63.

Panda, D., Rao, D.N., Sharma, S.G., Strasser, R.J. and Sarkar, R.K., 2006. Submergence effects on rice genotypes during seedling stage: Probing of submergence driven changes of photosystem 2 by chlorophyll a fluorescence induction O-J-I-P transients. *Photosynthetica* 44, 69-75.

Panda, D., Sharma, S.G. and Sarkar, R.K., 2008. Chlorophyll fluorescence parameters, CO_2 photosynthetic rate and regeneration capacity as a result of complete submergence and subsequent re-emergence in rice (*Oryza sativa* L.). *Aquatic Botany* 88, 127-133.

Qiu, N., Lu, Q. and Lu, C., 2003. Photosynthesis, photosystem II efficiency and the xanthophyll cycle in the salt-adapted halophyte *Atriplex centralasiatica*. *New Phytologist* 159, 479-486.

Rahnama, A., James, R.A., Poutini, K. and Munns, R., 2011. Stomatal conductance as a screen for osmotic stress tolerance in durum wheat growing in saline soil. *Functional Plant Biology* 37, 255-263.

Ruban, A.V., Phillip, D., Young, A.J. and Horton, P., 1998. Excited state energy level does not determine the differential effect of violaxanthin and zeaxanthin on chlorophyll fluorescence quenching in the isolated light-harvesting complex of Photosystem II. *Photochemistry and Photobiology* 68, 829–834.

Sayed, O.H., 2003. Chlorophyll fluorescence as a tool in cereal crop research. *Photosynthetica* 41, 321-330.

Schreiber, U. and Neubauer, C., 1987. The polyphasic rise of chlorophyll fluorescence upon onset of strong continuous illumination: Partial control by the photosystem II donor side and possible ways of interpretation. *Zeitschrift für Naturforschung* 42c, 1255-1264.

Sleimi, N., Abdelly, C., Soltani, A. and Hajji, M., 1999. Biomass production and mineral nutrition of *Suaeda fruticosa* grown on high salinity medium in connection with nutrient availability. Halophyte uses in different climates I. *Progress in Biometeorology* 13, 19–31.

Sleimi, N., Bankaji, I., Dallai, M. and Kefi, O., 2014. Accumulation des éléments traces et tolérance au stress métallique chez les halophytes colonisant les bordures de la lagune de Bizerte. *Revue d'Ecologie (Terre Vie)* 69, 49-59.

Strasser, R.J. and Tsimilli-Michael, M., 2001. Stress in plants, from daily rhythm to global changes, detected and quantified by the JIP test. *Chimie nouvelle* (SRC) 75, 3321-3326.

Strasser, R.J., Srivastava, A. and Govindjee, 1995. Polyphasic chlorophyll a fluorescence transient in plants and cyanobacteria. *Photochemistry and Photobiology* 61, 32-42.

Tester, M. and Davenport, R., 2003. Na^+ tolerance and Na^+ transport in higher plants. *Annals of Botany* 91, 503–527.

Uddin, M.K., Juraimi, A.S., Ismail, M.R., Hossain, M.A., Othman, R. and Rahim, A.A., 2011. Effect of salinity stress on nutrient uptake and chlorophyll content of tropical turfgrass species. *Australian Journal of Crop Science* 5, 620–629.

van Heerden, P.D.R., Tsimilli-Michael, M., Krüger, G.H. and Strasser, R.J., 2003. Dark chilling effects on soybean genotypes during vegetative development; parallel studies of CO_2 assimilation, chlorophyll a fluorescence kinetics O-J-I-P and nitrogen fixation. *Physiologia Plantarum* 117, 476-491.

Vera-Estrella, R., Barkla, B.J., Garcia-Ramiry, L. and Pantoja, O., 2005. Salt stress in *Thellungiella halophila* activities Na^+ transport Mechanisms required for Salinity Tolerance. *Plant Physiology* 139, 1507–1517.

Wentworth, M., Ruban, A.V. and Horton, P., 2000. Chlorophyll fluorescence quenching in isolated light-harvesting complexes induced by zeaxanthin. *FEBS Letters* 471, 71–74.

Yang, J. and Yen, H.E., 2002. Early salt stress effects on the changes in chemical composition in leaves of ice plant and *Arabidopsis*. A Fourier transform infrared spectroscopy study. *Plant Physiology* 130, 1032–1042.

Zhang, J.-L. and Shi, H., 2014. Physiological and molecular mechanisms of plant salt tolerance. *Photosynthesis Research* 115, 1-22.

Zhang, S. and Gao, R., 1999. Diurnal changes of gas exchange, chlorophyll fluorescence, and stomatal aperture of hybrid poplar clones subjected to midday light stress. *Photosynthetica* 37, 559-571.

Zid, E. and Grignon, C., 1986. Effects composes de NaCl, KCl et Na2SO4 sur la croissance et la nutrition minérale de jeunes *Citrus auranthium* L. *Oceologia Plantarum* 7, 407–416.

Zid, E. and Grignon, C., 1991. Les tests de sélection précoce pour la résistance des plantes au stress. Cas des stress salin et hydrique. Dans l'Amélioration des Plantes pour l'Adaptation aux Milieux Arides. Eds AUPELEF-UREF, john libbey Eurotext, Paris. pp 91–108.

4.3. GENERAL INSIGHTS ON THE BIOPHYSICAL AND BIOCHEMICAL CONSTRAINTS IMPOSED BY SALT STRESS

As all other excessive ionic accumulation, excessive salinity has also redox implications at the cellular level, unbalancing the cellular electron fluxes. A decrease in the photosynthetic capacity is very common in salt stressed plants (Munns and Termaat, 1986; Munns, 1993; Jaleel *et al*., 2007; Qiu *et al*., 2003), mostly due to a low osmotic potential of the soil solution (osmotic stress), specific ion effects (salt stress), nutritional imbalances or more usually, a combination of all these factors (Zhu, 2003). One of the consequences of salinity-induced photosynthetic impairment is the exposure of plants to excess of light energy and its inevitable consequences for the photosystem II (PS II). Plants under salt stress use less light energy for photosynthesis (Megdiche *et al*., 2008). Therefore, the presence of efficient energy dissipation mechanisms is essential in order to prevent the accumulation of excessive energy within the cells in the form of excessive reducing potential (Demming-Adams and Adams, 1992; Qiu *et al*., 2003). Salinity constraints for photosynthesis are not restricted to the light harvesting processes. Also the photosynthetic carbon fixation reactions are affected under salt stress, mostly due to disturbances of leaf osmotic potential, of the chloroplast membrane systems and of pigment composition (Munns, 2002; Zhao *et al*., 2007). To avoid damage in the PS II, plants have developed several strategies to dissipate excessive energy. Comparing the PS II activity of glycophytes with halophytes in a salt medium, the differences are evident. In glycophyte species, both real (operational) and maximum PS II activities suffer drastic decreases under salt stress. On the other hand, halophytic species, well adapted to salt environments, show almost no differences along salinity gradients even under oceanic salt concentrations. PS II quantum yield provides rapid and valuable insights on the overall PS II energetic processes. Nevertheless, in order to understand the causes behind these changes, as well as the mechanisms that allow halophytes to overcome salt stress, we need to take a closer look into the biophysics

and energetics of the chloroplast. PS II efficiency relies essentially on two major processes: 1) photon harvesting, entrapment and energy transfer throughout the transport chain and 2) dissipation of excessive reducing power. The delicate balance between both these processes is important for the entire electron transduction pathway and evidently for energy production. Overlooking the first one, and focusing especially in the electron transport processes, two strategies can be observed depending on the plant tolerance and mechanisms of the salt tolerance. Observing *H. portulacoides* (excretion strategy) and *S. fruticosa* (exclusion strategy), the differences are evident. Although the exclusion strategy of *S. fruticosa* takes place in the roots, this will condition the Na^+ translocation for the aboveground organs. Nevertheless, excessive Na^+ translocation can still happen and in this case the swelled photosynthetic steams will act as sinks, storing Na^+ in their vacuoles (Flowers and Colmer, 2008). Two tolerance mechanisms are evidenced between these two *Amaranthaceae* species. *Sarcocornia fruticosa* presents a salinity tolerance mechanism that allows the photosystems to absorb light even under high Na^+ concentrations. On the other hand, in *H. portulacoides* these mechanisms appear to be absent or inactivated, leading to lower light harvesting and carbon fixation efficiencies. In fact, *S. fruticosa* exhibits a common feature among halophytes with an improvement of some energy conversion mechanisms under elevated salt concentrations (Rabbhi *et al*., 2012; Mateos-Naranjo *et al*., 2010).

A special group of fluorescence parameters derived from high-resolution measurements analysis of the chlorophyll *a* fluorescence kinetics, can offer detailed information on the structure and function of plant photosynthetic apparatus, mainly photosystem II. In most cases, excessive salt produces negative effects at different levels in both species. Nevertheless, all these effects can be well summarized in the reduced Performance Index (PI) observed in stressed individuals. This PI reduction outcome from its dependence on the primary photochemical and energetic yields. This type of analysis is very quick and allows a rapid interpretation of the overall energetic fluxes underlying the PS II activity. In this assessment two phases can be distinguished: O-J step or photochemical phase and the J-I-P step or thermal phase. The first one is considered to be a good proxy of the photochemical energy production realised inside the chloroplasts, while the second one reflects the ability

to dissipate excessive amounts of energy throughout thermal dissipation. Considering a desert halophyte, like *Tamarix gallica*, individuals have similar photochemical activity both with and without salt, but the individuals supplemented with 200 mM NaCl have a higher ability to dissipate excessive energy (Sghaier *et al*., 2015). This is one of the most common mechanisms by which halophytes overcome the accumulation of excessive reducing power, the primary source of reactive oxygen species, avoiding this way the photo-destruction of the photosynthetic apparatus (Duarte *et al*., 2013a). Another interesting phenomenon observable while analysing the Kautsky curves is the appearance of a new phase, called K-step at 300 μs. The appearance of this K-step with salt stress is associated with damage in the PS II donor side mostly at the level of the oxygen-evolving complexes (Chen and Cheng, 2009; Strasser *et al.*, 2001, 2004; Srivastava *et al*. 1997). This is evident in *Aster tripolium* exposed to different salt concentration and is normally indicative of a low stability of the oxygen evolving complexes (OECs) under excessive salt concentration, similarly to what was previously observed in plants subjected to thermal stresses (Duarte *et al*., 2014).

Beyond the biophysical processes, halophytes also have a battery of biochemical adjustments to counteract, at the molecular level, the cellular stress imposed by excessive ionic concentrations, namely Na^+. Still discussing the photosynthetic light harvesting mechanisms: the pigment profiles are frequently affected by elevated salt concentrations. On the other hand, under favourable conditions, the increased photosystem efficiency, driven by optimal salt concentrations is accompanied by a decrease of the PS II antenna size. Due to the lower requirements for light harvesting at optimum conditions, there is a reduction in the plant needs for larger light harvesting complexes (LHC) oppositely to the observed under stress conditions (Rabhi *et al*., 2012). This can be evaluated using the chlorophyll a/b ratio as proxy. An increase in the chlorophyll a/b ratio is directly related to higher number of active light harvesting reaction centres, being commonly used as indicator of an enhancement in the plant photochemical capacity. On the other hand, when the halophyte is out of its saline comfort concentrations, the excessive energy reaching the photo-systems must be dissipated (Duarte *et al*., 2013a). Nevertheless, this increase in LHC is sometimes not sufficient to sustain all

the incoming solar radiation. At this moment, the plant needs to dissipate the energy in excess, either by fluorescence quenching or throughout a pigment metabolic pathway involving a class of carotenoids called xanthophylls (Demming-Adams and Adams, 1992). As abovementioned, the salt stressed plants cannot withstand a usual dose of light as in a normal situation, and thus even at low solar radiances it undergoes photo-inhibition increasing the energy dissipation needs. An evident signal of environmental stress is enhanced activation of the xanthophyll cycle, revealed by an increase in the De-Epoxidation State (DES) index. When the absorbed light exceeds the plant photochemical capacity (as revealed above by the decrease in the chlorophyll a/b ratio), this excessive energy may be transferred to the ever-present oxygen, generating reactive oxygen species (ROS). These molecules affect many cellular functions by damaging nucleic acids, oxidizing proteins, and causing lipid peroxidation (Gill and Tuteja, 2010). Under steady state conditions, the ROS molecules are scavenged by various antioxidant enzymatic and non-enzymatic defence mechanisms (Foyer and Noctor, 2005). In this context, the conversion of violaxanthin to zeaxanthin throughout the xanthophyll cycle is considered to be one of the most effective energy dissipation mechanisms (Demmig-Adams and Adams, 1992). Zeaxanthin may be an important antioxidant in the thylakoid membrane bilayer itself, where it could scavenge reactive oxygen species and/or terminate lipid peroxidation chain reactions (Muller *et al*., 2001).

Sometimes an interesting phenomenon can be observed in large halophytic extensions, especially during summer. During warm seasons, sediment water evaporates increasing greatly the sediment salinity, to values sometimes twice the observed in seawater. Under these conditions, *Amaranthaceae* salt marshes frequently exhibit large areas of red-coloured plants. This coloration is due to the presence of water-soluble pigments from the betacyanin family, normally produced as response to salinity, anoxia or thermal stresses (Chang-Quan *et al*., 2006). Betacyanins play an important role in scavenging reactive oxygen species (ROS), generated under environmental stress conditions (Stintzing and Carle, 2004). Chang-Quan *et al*. (2006) found similar results for other *Amaranthaceae* species (*Suaeda salsa*), suggesting that this betacyanin production is part of a common defence mechanism against environmental stresses, namely salinity. Commonly, these

pigments are also related to a high betain production, a quaternary ammonium compound, mainly accumulated in the chloroplast in order to counteract high Na^+ concentrations in this compartment (Rhodes and Hanson, 1993; McNeil *et al*., 1999). Halophytes are highly adapted to salinity, with an enormous production of betain in order to balance and regulate the osmotic potential inside its photosynthetic compartments. In glycophytes, these pathways are not well developed and thus the osmoregulation mechanisms are only adapted to small salinity fluctuations within an extremely low salinity range. Regarding the cytosol, the plant tends to accumulate proline, an amino acid with also a quaternary ammonium-based structure. In this cellular compartment, proline acts as an effective osmoregulator of the ionic pressure exerted by excessive salt concentrations. The use of this compatible solute can also reflect the salt tolerance strategy of a species. Comparing e.g. an obligatory halophyte (*Arthrocnemum indicum*) with a salt-excreting facultative one (*Tamarix gallica*) the differences are evident (Duarte *et al*., 2014). While for *A. indicum* the absence of salt is an osmotic stress factor, in *T. gallica* the presence of salt, even at reduced concentration triggers the cytosolic accumulation of proline to counteract the osmotic imbalance. Allied with this compatible solute accumulation, *T. gallica* excretes the excessive salt from its leaves. In this case, the function of proline accumulation has a counteractive measure against the external medium osmotic pressure.

Halophytes are often classified as extremophile species, inhabiting extremely salinized and arid environments under extreme abiotic adverse conditions for life development. Another interesting adaptation developed by this group of plants was the acquisition and development of highly efficient battery of anti-oxidant enzymes. The interaction of high Na^+ concentrations, as well as any other excessive cation concentrations, with the cell organelles lead to generated ROS resulting to reactions with proteins and the cellular biological compounds in membranes (Duarte *et al*., 2013b). Halophytes developed a highly efficient enzymatic rapid response system towards salinity changes, quickly activated when the medium conditions shift aside from the saline comfort zone of a halophyte.

This battery has its higher expression at the first line of defence, superoxide dismutase (SOD). This enzyme catalysis the conversion of the highly toxic superoxide

anions to hydrogen peroxide. In the second line of defence, peroxidase-class enzymes, such as catalase (CAT), ascorbate peroxidase (APx) and guaiacol peroxidase (GPx) play key functions in the hydrogen peroxide detoxification, and thus in the reduction of ROS to non-damaging concentrations. While for glycophytes it would be expectable that these defence mechanisms are activated with the increasing salinity doses, in halophytes the lack of salt can also be a stress factor, especially if we are dealing with obligate halophytes. Some authors suggest that obligate halophytes not only exhibit optimum growing in salt mediums, but in fact they require salt as part of their nutrition in order to activate or de-activate several salt sensitive enzymes (Wang *et al*., 2011). These species frequently exhibit an activation of these enzymes at both very low Na^+ concentrations (below the physiological optimum) and at seawater Na^+ concentrations (considered excessive), pointing out to a physiological Na^+ dependence of certain halophytes, such as *H. portulacoides*.

Halophytes are extremely plastic species with a high degree of adaptation to saline habitats, being therefore excellent models to study salt resistance and tolerance mechanisms. Alongside, some halophytes have recently been pointed out as potential alternative cash crops for replacing usual crops in soils with excessive salt concentrations. Their tolerance to salt goes from simple morphological adjustments, like increasing turgescence or specific salt glands, to efficient energy dissipation mechanisms based on electron fluxes adjustment inside the chloroplast or to the production of specific molecules with the main objective to counteract the osmotic unbalance driven by excessive salt. Nowadays, the metabolic biophysical and biochemical mechanisms underlying these processes are relatively well described for several halophytes. This opens a new door where physiology can be allied to biotechnology, identifying the key genes underlying these processes and introducing them into non-tolerant crops. This will allow glycophyte species to be cultured in arid and saline lands maintaining the food supply in some of the poorest regions of the planet.

References

Chang-Quan, W., Zhao, J.-Q., Chen, M., and Wang, B.-S., 2006. Identification of betacyanin and effects of environmental factos on its accumulation in halophyte *Suaeda salsa*. *Journal of Plant Physiology and Molecular Biology* 32, 195-201.

Chen, L.S. and Cheng, L., 2009. Photosystem 2 is more tolerant to high temperature in apple (*Malus domestica* Borkh.) leaves than in fruit peel. *Photosynthetica* 47, 112-120.

Demmig-Adams, B. and Adams II, W. W., 1992. Photoprotection and other responses of plants to light stress. *Annual Review of Plant Physiology and Plant Molecular Biology* 43, 599-626.

Duarte, B., Santos, D. and Caçador, I., 2013b. Halophyte anti-oxidant feedback seasonality in two salt marshes with different degrees of metal contamination: search for an efficient biomarker. *Functional Plant Biology* 40, 922-930.

Duarte, B., Santos, D., Marques, J. C. and Caçador, I., 2013a. Ecophysiological adaptations of two halophytes to salt stress: photosynthesis, PS II photochemistry and anti-oxidant feedback - Implications for resilience in climate change. *Plant Physiology and Biochemistry* 67, 178-188.

Duarte, B., Sleimi, N. and Caçador, I., 2014. Biophysical and biochemical constrains imposed by salt stress: Learning from halophytes. *Frontiers in Plant Science* 5, 746.

Flowers, T. J. and Colmer, T. D., 2008. Salinity tolerance in halophytes. *New Phytologist* 179, 945-963.

Foyer, C.H. and Noctor, G., 2005. Redox homeostasis and antioxidant signalling: a metabolic interface between stress perception and physiological responses. *Plant Cell* 17, 1866-1875.

Gill, S.S. and Tuteja, N., 2010. Reactive oxygen species and antioxidant machinery in abiotic stress tolerance in crop plants. *Plant Physiology and Biochemistry* 48, 909-930.

Jaleel, C. A., Gopi, R., Manivannan, P. and Panneerselvam, R., 2007 Antioxidative potentials as a protective mechanism in *Catharanthus roseus* (L.) G. Don. plants under salinity stress. *Turkish Journal of Botany* 31, 245-251.

Mateos-Naranjo, E., Gómez-Redondo, S., Cambrollé, J. and Figueroa, M.E., 2010. Growth and photosynthetic responses of the cordgrass *Spartina maritima* to CO_2 enrichment and salinity. *Chemosphere* 81, 725-731.

McNeil, S. D., Nuccio, M. L. and Hanson, A. D., 1999. Betaines and Related Osmoprotectants. Targets for Metabolic Engineering of Stress Resistance. *Plant Physiology* 120, 945-949.

Megdiche, W., Hessini, K., Gharbi, F., Jaleel, C., Ksouri, R. and Abdelly, C., 2008. Photosynthesis and photosystem II efficiency of two salt-adapted halophytic seashore *Cakile maritima* ecotypes. *Photosynthetica* 46, 410-419.

Muller, P., Li, X.-P. and Niyogi, K.K., 2001. Non-Photochemical Quenching. A Response to Excess Light Energy. *Plant Physiology* 125, 1558-1566.

Munns, R. and Termaat, A., 1986. Whole-plant responses to salinity. *Australian Journal of Plant Physiology* 13, 143-160.

Munns, R., 1993. Physiological processes limiting plant growth in saline soil. Some dogmas and hypothesis. *Plant Cell and Environment* 16, 15-24.

Qiu, N., Lu, Q. and Lu, C., 2003. Photosynthesis, photosystem II efficiency and the xanthophyll cycle in the salt-adapted halophyte *Atriplex centralasiatica*. *New Phytologist* 159, 479-486.

Rabhi, M., Castagna, A., Remorini, D., Scattino, C., Smaoui, A., Ranieri, A. and Abdelly, C., 2012. Photosynthetic responses to salinity in two obligate halophytes: *Sesuvium portulacastrum* and *Tecticornia indica*. *South African Journal of Botany* 79, 39-47.

Rhodes, D. and Hanson, A. D., 1993. Quaternary ammonium and tertiary sulfonium compounds in higher plants. *Annual Review in Plant Physiology and Plant Molecular Biology* 44, 357–384.

Sghaier, D., Duarte, B., Bankaji, I., Caçador, I. and Sleimi, N. Growth, chlorophyll fluorescence and mineral nutrition in the halophyte *Tamarix gallica* cultivated in combined stress conditions: Arsenic and NaCl. *Journal of Photochemistry and Photobiology B: Biology* 149, 204-214

Srivastava, A., Guisse, B., Greppin, H. and Strasser, R.J., 1997. Regulation of antenna structure and electron transport in PS II of *Pisum sativum* under elevated temperature probed by the fast polyphasic chlorophyll a fluorescence transient: OKJIP. *Biochimica et Biophysica Acta* 1320, 95–106.

Stintzing, F. C. and Carle, R., 2004. Functional properties of anthocyanins and betalains in plants, food, and in human nutrition. *Trends in Food Science and Technology* 15, 19-38.

Strasser, R.J. and Stirbet, A.D., 2001. Estimation of the energetic connectivity of PS II centres in plants using the fluorescence rise O–J–I–P. Fitting of experimental data to three different PS II models. *Mathematics and Computers in Simulation* 56, 451-461.

Strasser, R.J., Tsimilli-Michael, M. and Srisvastava, A., 2004. Analysis of the chlorophyll-a fluorescence transient. In: Papageorgiou, G.C. and Govindjee (eds.) *Advances in photosynthesis and respiration*. Pp 321-362. Berlin, Springer.

Wang, W., Yan, Z., You, S., Zhang, Y., Chen, L. and Lin, G., 2011. Mangroves: obligate or facultative halophytes? A review. *Trees* 25, 953-963.

Zhao, G.Q., Ma, B.L. and Ren, C.Z., 2007. Growth, gas exchange, chlorophyll fluorescence, and ion content of naked oat in response to salinity. *Crop Science* 47, 123-131.

Zhu, J.-K., 2003. Regulation of ion homeostasis under salt stress. *Current Opinion in Plant Biology* 6, 441-445.

CHAPTER V

IMPACTS OF ALTERED THERMAL ENVIRONMENTS ON ESTUARINE SALT MARSHES

CHAPTER V

5.1. IMPACTS OF ALTERED THERMAL ENVIRONMENTS ON ESTUARINE SALT MARSHES

The IPCC Special Report on Extreme Events (SREX; IPCC, 2012) concludes that it is very likely that there has been an overall decrease in the number of cold days and nights, and an overall increase in the number of warm days and nights, at the global scale. If there has been an increase in daily maximum temperatures, then it follows, in our view that the number of heat-related deaths is likely to have also increased. For example, Christidis *et al*. (2012) concluded that it is "extremely likely" that anthropogenic climate change at least quadrupled the risk of extreme summer heat events in Europe in the decade 1999–2008. The 2003 heat wave was one such record event. The climate change scenarios modelled by the 5th Assessment Report Working Group 1 (WGI AR5 in IPCC, 2013) rising temperatures and an increase in frequency and intensity of heat waves in the near-term future.

As the climate continues to warm, changes in several types of temperature extremes have been observed (Donat *et al*., 2013), and are expected to continue in the future in concert with global warming (Seneviratne *et al*., 2012). Extremes occur on multiple time scales, from a single day or a few consecutive days (a heat wave) to monthly and seasonal events. Extreme temperature events are often defined by indices, for example, percentage of days in a year when maximum temperature is above the 90th percentile of a present day distribution or by long period return values. Although changes in temperature extremes are a very robust signature of anthropogenic climate change (Seneviratne *et al*., 2012), the magnitude of change and consensus among models varies with the characteristics of the event being considered (e.g., time scale, magnitude, duration and spatial extent) as well as the definition used to describe the extreme. A strong increase in warm temperature extremes and decrease in cold temperature extremes is found at the end of the 21st century, with the magnitude of the changes increasing with increased anthropogenic forcing. The coldest night of the year undergoes larger increases than the hottest day in the globally averaged time series. Similarly, increases in the frequency of

warm nights are greater than increases in the frequency of warm days (Sillmann *et al*., 2013). Impacts from recent climate-related extremes, such as heat waves, droughts, floods, cyclones and wildfires, reveal significant vulnerability and exposure of some ecosystems and many human systems to current climate variability.

Warming is leading to range shifts in vegetated coastal habitats. The poleward limit of mangrove forests is generally set by the 20 °C mean winter isotherm (Duke *et al*., 1998). Accordingly, migration of the isotherm with climate change (Burrows *et al*., 2011) should lead to a poleward expansion of mangrove forests, as observed in the Gulf of Mexico (Perry and Mendelssohn, 2009; Comeaux *et al*., 2011; Raabe *et al*. 2012), and New Zealand (Stokes *et al*., 2010), leading to increased sediment accretion. Seagrass meadows are already under stress due to climate change, particularly where maximum temperatures already approach their physiological limit. Heat waves lead to widespread seagrass mortality, as documented for *Zostera* species in the Atlantic (Reusch *et al*., 2005), and *Posidonia* meadows in the Mediterranean Sea (Marbà and Duarte, 2010) and Australia (Rasheed and Unsworth, 2011). Warming also favours flowering of *Posidonia* oceanica (Diaz-Almela *et al*., 2007), but the increased recruitment rate is insufficient to compensate for the losses resulting from elevated temperatures (Diaz-Almela *et al*., 2009).

While the impacts of thermal extremes is rather well-known for seagrasses and mangroves, their impacts on salt marshes are yet to be described. Not only the physiology and primary production of the marshes is likely to be affected, similarly to what happens in other terrestrial ecosystems, but also its biogeochemistry will certainly suffer shifts, namely in terms of carbon retention.

References

Burrows, M.T., Schoeman, D.S., Buckley, L.B., Moore, P., Poloczanska, E.S., Brander, K.M., Brown, C., Bruno, J.F., Duarte, C.M., Halpern, B.S., Holding, J., Kappel, C.V., Kiessling, W., O'Connor, M.I., Pandolfi, J.M., Parmesan, C., Schwing, F.B., Sydeman, W.J. and Richardson, A.J., 2011. The pace of shifting climate in marine and terrestrial ecosystems. *Science* 334, 652-655.

Christidis, A., Koch, C., Pottel, L. and Tsatsaronis, G., 2012. The contribution of heat storage to the profitable operation of combined heat and power plants in liberalized electricity markets. *Energy* 41, 75–82.

Comeaux, R.S., Allison, M.A. and Bianchi, T.S., 2011. Mangrove expansion in the Gulf of Mexico with climate change: implications for wetland health and resistance to rising sea levels. *Estuarine, Coastal and Shelf Science* 96, 81-95.

Díaz-Almela, E., Marbà, N. and Duarte, C.M., 2007. Consequences of Mediterranean warming events in seagrass (*Posidonia oceanica*) flowering records. *Global Change Biology* 13, 224-235.

Díaz-Almela, E., Marbà, N., Martínez, R., Santiago, R. and Duarte, C.M., 2009. Seasonal dynamics of *Posidonia oceanica* in Magalluf Bay (Mallorca, Spain): temperature effects on seagrass mortality. *Limnology and Oceanography* 54, 2170-2182.

Donat, M.G., Alexander, L.V., Yang, H., Durre, I., Vose, R., Dunn, R.J.H., Willett, K.M., Aguilar, E., Brunet, M., Caesar, J., Hewitson, B. Jack, C., Klein Tank, A.M.G., Kruger, A.C., Marengo, J.A., Peterson, T.C., Renom, M., Oria Rojas, C., Rusticucci, M., Salinger, J., Sanhouri Elrayah, A., Sekele, S.S., Srivastava, A.K., Trewin, B., Villarroel, C., Vincent, L.A., Zhai, P., Zhang, X. and Kitching, S. 2013. Updated analyses of temperature and precipitation extreme indices since the beginning of the twentieth century: the HadEX2 dataset. *Journal of Geophysical Research: Atmospheres* 118, 2098-2118.

Duke, N.C., Ball, M.C. and Ellison, J.C., 1998. Factors influencing biodiversity and distributional gradients in mangroves. *Global Ecology and Biogeography Letters* 7, 27-47.

IPCC, 2012. *Managing the Risks of Extreme Events and Disasters to Advance Climate Change Adaptation. A Special Report of Working Groups I and II of the Intergovernmental Panel on Climate Change* [Field, C.B., Barros, V., Stocker, T.F., Qin, D., Dokken, D.J., Ebi, K.L., Mastrandrea, M.D., Mach, K.J., Plattner, G.-K., Allen, S.K., Tignor, M. and Midgley, P.M. (eds.)]. Cambridge University Press, Cambridge, UK, and New York, NY, USA, 582 pp.

IPCC, 2013. *Climate Change 2013: The Physical Science Basis. Contribution of Working Group I to the Fifth Assessment Report of the Intergovernmental Panel on Climate Change* [Stocker, T.F., Qin, D., Plattner, G.-K., Tignor, M., Allen, S.K., Boschung, J., Nauels, A., Xia, Y., Bex, V. and Midgley, P.M. (eds.)]. Cambridge University Press, Cambridge, United Kingdom and New York, NY, USA, 1535 pp.

Marbà, N. and Duarte, C.M., 2010. Mediterranean warming triggers seagrass (*Posidonia oceanica*) shoot mortality. *Global Change Biology* 16, 2366-2375.

Perry, C.L. and Mendelssohn, I.A., 2009. Ecosystem effects of expanding populations of *Avicennia germinans* in a Louisiana salt marsh. *Wetlands* 29, 396-406.

Raabe, E.A., Roy, L.C. and McIvor, C.C., 2012. Tampa Bay coastal wetlands: nineteenth to twentieth century tidal marsh-to-mangrove conversion. *Estuaries and Coasts* 35, 1145-1162.

Rasheed, M.A. and Unsworth, R.K.F., 2011. Long-term climate-associated dynamics of a tropical seagrass meadow: implications for the future. *Marine Ecology Progress Series* 422, 93-103.

Reusch, T.B.H., Ehlers, A., Hämmerli, A. and Worm, B., 2005. Ecosystem recovery after climatic extremes enhanced by genotypic diversity. *Proceedings of the National Academy of Sciences of the United States of America* 102, 2826-2831.

Seneviratne, S.I., Nicholls, N., Easterling, D., Goodess, C.M., Kanae, S., Kossin, J., Luo, Y., Marengo, J., McInnes, K., Rahimi, M., Reichstein, M., Sorteberg, A., Vera, C. and Zhang, X., 2012. Changes in climate extremes and their impacts on the natural physical environment. In: *Managing the Risks of Extreme Events and Disasters to Advance Climate Change Adaptation. A Special Report of Working Groups I and II of the Intergovernmental Panel on Climate Change* [Field, C.B., Barros, V., Stocker, T.F., Qin, D., Dokken, D.J., Ebi, K.L., Mastrandrea, M.D., Mach, K.J., Plattner, G.-K., Allen, S.K., Tignor, M. and Midgley, P.M. (eds.)]. Cambridge University Press, Cambridge, UK and New York, NY, USA, pp. 109-230.

Sillmann, J., Kharin, V.V., Zwiers, F.W., Zhang, X. and Bronaugh, D., 2013. Climate extremes indices in the CMIP5 multimodel ensemble: Part 2. Future climate projections. *Journal of Geophysical Research: Atmospheres* 118, 2473-2493.

Stokes, D.J., Healy, T.R. and Cooke, P.J., 2010. Expansion dynamics of monospecific, temperate mangroves and sedimentation in two embayments of a barrier-enclosed lagoon, Tauranga Harbour, New Zealand. *Journal of Coastal Research* 26, 113-122.

5.2. ABIOTIC CONTROL MODELLING OF SALT MARSH SEDIMENTS RESPIRATORY CO_2 FLUXES: APPLICATION TO INCREASING TEMPERATURE SCENARIONS[1]

Abstract

Sediment microbial communities are responsible for several ecosystem key-processes such as decomposition. However, these communities depend on aerobic respiration making them a source of CO_2 to the atmosphere. Since sediments are a known important carbon sink, it becomes important to address the factors that modulate sediment respiration and therefore CO_2 efflux to the atmosphere. Therefore, the present work aimed to assess the main factors controlling sediment respiratory activity in salt marshes. Sediment respiration and several sediment abiotic characteristics were assessed in two salt marshes from Ria de Aveiro coastal lagoon with contrasting environmental conditions. Sediment respiration had significant differences across seasons and salt marshes, with different patterns of activity were found for each salt marsh. Statistical analysis and modelling by Generalized Linear Model (GLM) revealed that sediment respiration is mostly influenced by organic matter quality (C:N ratio), sediment temperature and sediment pH. Nevertheless, as temperature appeared to be one of the most important factors influencing CO_2 effluxes from the sediments, its influence during possible global warming scenarios was focused. The simulations produced by the GLM using the IPCC scenarios projections, indicated that salt marshes will tend to decrease their CO_2 emissions with the increasing temperatures, reinforcing their role as important carbon sinks. This can be interpreted as an ecosystem counteractive measure towards the reduction of the increasing temperature, by reducing the amounts of greenhouse gas emissions, namely CO_2.

[1] This section was published in: **Duarte, B.**, Freitas, J., Valentim, J., Medeiros, J.P., Costa, J.L., Silva, H., Dias, J.M., Marques, J.C. and Caçador, I., 2014. Modelling abiotic control of salt marsh sediments respiratory CO_2 fluxes: new insights for climate change scenarios. *Ecological Indicators* 46, 110-118.

Introduction

Although salt marshes were previously regarded as wastelands, their important ecological features and functions are now widely recognized. They present high rates of primary production and thus are a key source of nutrients and organic material for several marine communities (e.g. Boorman, 1999). They also serve as habitat and nursery grounds for different species, being crucial ecosystems for wildlife conservation (e.g. Vernberg, 1993). Moreover, salt marshes have been shown to have the capacity to act as a sink of nutrients and pollutants that would potentially damage the environment (Vernberg, 1993; Boorman, 1999). Therefore, they provide several ecosystem services such as disposal of wastes and dead organic matter, renewal of sediment fertility and regulation of major element cycles, processes that depend on the activity of sediment microbial community (Daily *et al*., 1997; Duarte *et al*., 2008; Gardi *et al*., 2009).

Sediment microbial community includes several groups of organisms, namely bacteria, fungi and algae. Fungi are generally the more representative group in terms of biomass, whereas the most active are the bacteria. Decomposition processes are mainly driven by both of these groups of organisms, mostly through the action of extracellular enzymes (Nannipieri and Badalucco, 2003). These enzymes are responsible for several organic matter breakdown processes, having a major role in nutrient mineralization and cycling as well as in organic matter re-mineralization (Acosta-Martinez *et al*., 2007; Duarte *et al*., 2009). Consequently, lower enzymatic activities are usually associated with lower decomposition rates (Kang *et al*., 2005).

Carbon dioxide is the most important greenhouse gas originated by anthropogenic activities (IPCC, 2007). According to this document, the atmospheric CO_2 concentration in 2005 was approximately 379 ppm, much higher than pre-industrial values (≈280 ppm) or values estimated from ice cores from the 650 000 years, which ranged from 180 to 300 ppm. Looking to a more recent time window, it is clear that the growth rate for atmospheric carbon dioxide concentration was higher between 1995 and 2005 than in the period from 1960 to 2005 (IPCC, 2007). Although these data point out to a direct intervention of the anthropogenic activity increasing emission due to fossil fuel usage, some side effects of this activity (e.g.

climate change) are also important to be regarded as possible drivers of changes in the non-anthropogenic emissions (e.g. ecosystem respiration) (Richey *et al*., 2002).

Salt marshes store carbon belowground (Caçador *et al*., 2004) allocated by plants throughout photosynthetic harvest and root exudation into the sediment (Allen *et al*., 2000; Bais *et al*., 2006), but also from root decomposition (Crow *et al*., 2009; Norby and Zak, 2011). The role of photosynthesis as sediment respiration modulator is well known, having not only a seasonal effect, but also important role at the diurnal scale (Han *et al*., 2014). One of the observed side effects of atmospheric CO_2 increase resides in the enhancement of some photosynthetic pathways and therefore plant productivity (Strain, 1987; Gunderson and Wullschleger, 1994; Duarte *et al*., 2014) and thus to increase the C inputs into sediments. However, Ineson *et al*. (1998) found that higher atmospheric CO_2 concentrations caused a decrease of CO_2 efflux from sediments, indicating other factors controlling sediment respiration. These authors hypothesized that a decreased root decomposition rate or a change in soil physical conditions could counteract the effect of increased C inputs from root biomass into the sediments, and thus bringing the question of what are the main factors driving respiration in the sediments.

In these ecosystems, carbon balance depends on the equilibrium between photosynthesis and respiration (Valentini *et al*., 2000; Lovelock, 2008). As such, sediment microflora plays an important role in carbon cycling, working as a sink or source of carbon. From this point of view, the study of sediment respiration is crucial and recently became a matter of significant importance in politics due to the need to counteract climate change (Luo and Zhou, 2006). Janssens *et al*. (2001) found that forest soil respiration has a significant contribution to the total ecosystem respiration and that gross primary productivity was related to respiration. Due to salt marshes high productivity and their central role in organic matter decomposition, it becomes important to draw attention to sediment respiration in these ecosystems. Therefore, the present work aims to assess the main factors controlling sediment respiratory activity in salt marsh sediments, through well-established field measurement protocols (Cardoso *et al*., 2013; Doering *et al*., 2011; Fromin *et al*., 2010; Leopold *et al*., 2013; Sasaki *et al*., 2009) and subsequent modelling, in order to

produce an explicative and predictive model of the abiotic factors controlling sediment respiratory CO_2 fluxes, under different plausible increasing temperature scenarios

Material and Methods

Site description and sample collection

The Ria de Aveiro (Figure 5.2.1) is a mesotidal lagoon located in the North-western Portuguese coast. It has a very complex geometry and is characterized by large areas of intertidal flats and a web of narrow channels (Dias and Picado, 2011). The lagoon covers an area ranging between 83 km^2 at high spring tide and 66 km^2 at low neap tide. It has 45 km long and 10 km wide, and is connected to the sea by a 350 m wide inlet, fixed by two jetties (Dias and Lopes, 2006). Four main branches radiate from this sea entrance: Mira, S. Jacinto, Ílhavo and Espinheiro channels (Picado *et al*., 2010). This system is also characterized by a large number of other smaller channels between which lie significant intertidal areas, essentially mudflats, salt marshes and old salt pans (Picado *et al*., 2010). The average depth of the lagoon relative to mean sea level is about 3 m (Picado *et al*., 2010).

Sampling was carried out in two salt marshes of Ria de Aveiro located in contrasting environments: Barra and Verdemilho. Barra salt marsh is mostly colonized by *Halimione portulacoides*, *Sarcocornia perennis*, *Juncus maritimus* and *Spartina maritima* being frequently (twice per day) tidal inundated. On the other hand, Verdemilho salt marsh is mostly colonized by *H. portulacoides*, *S. perennis*, and *Puccinellia maritima*, being sufficiently elevated to be away from the tidal range, and thus only receives water inputs by sediment diffusion. Although this topological differences, both marshes present similar species coverage. The two sampling sites were chosen in order to divert the results from possible salt marsh within-effects. Sampling occurred during two periods: warm (April-June) and cold (December) seasons. Sediment cores (n=14 during the warm season and n=15 during the cold season, considering the total samples in the two sites) were randomly collected in pure stands of the most abundant species, using PVC tubular cores (9 cm diameter, 50 cm long) and transported to the laboratory in refrigerated bags.

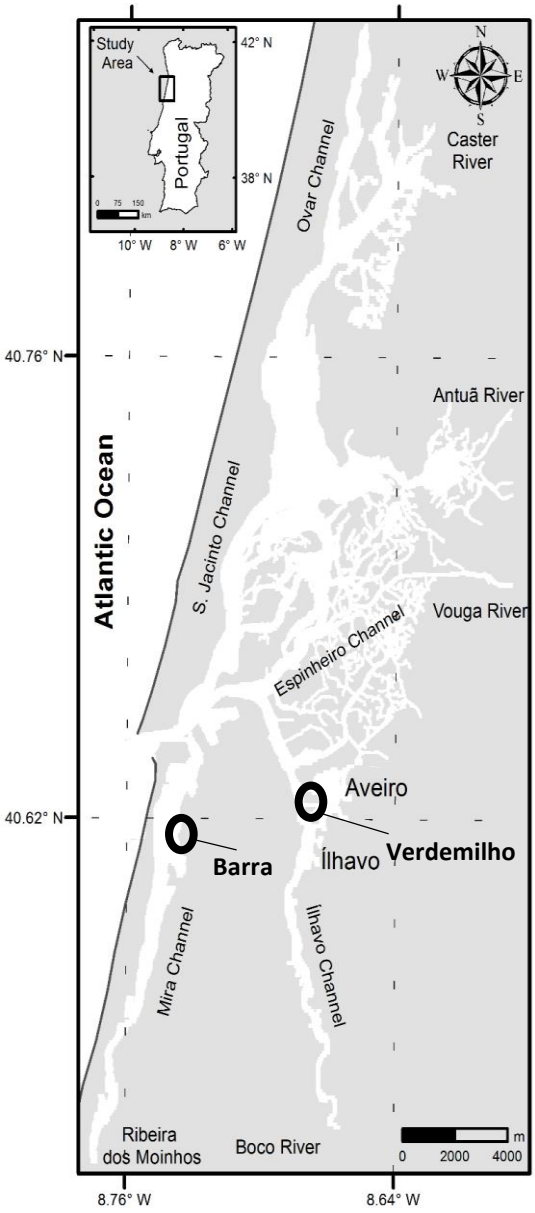

Figure 5.2.1. Ria de Aveiro with the location and sampling sites.

Sediment physicochemical characteristics

Sediment physicochemistry was measured according to the methods described in Chapter 3, Section 4 (*Duarte et al*., 2014).

Sediment CO_2 respiratory fluxes

For sediment CO_2 respiratory fluxes measurement intact cores were collected using dark PVC corers hermetically closed using gas tight lids connected to a QuBit Biosystems (Canada) infrared gas analyser (IrGA) CO750-FCM Field CO_2 Analysis

Package coupled with a sediment temperature probe. Measurements were made in the dark (to avoid photosynthetic fluxes) within 1 hour after core collection with minimum disturbance to the sediment using closed circuit system under controlled temperature. This procedure already proved to produce CO_2 fluxes not significantly different from the obtained in the field (Kristensen *et al*., 2011). Measurements were performed during 3 minutes in each core. Sediment respiratory CO_2 fluxes were expressed by sediment unit area taking in consideration the air volume within each core.

Data processing and Statistical analysis

Statistical analysis was primary performed using Statistica Software version 10 from Statsoft Inc. The lack of normality and homogeneity of the data package lead to the application of Kruskal-Wallis non-parametrical tests for significance analysis, in order to compare the different parameters analysed between season and marshes. Linear and polynomial correlations considering physicochemical parameters of all the analysed samples were made using SigmaPlot 12.0 regression packages.

After transformation, normality and homogeneity of variances was attained for both response (i.e. respiration rate, δCO_2, mmol h^{-1} m^{-2}) and predictor variables [i.e. organic content (loss on ignition, LOI) (%); pH; salinity; temperature (°C); Total Carbon (C); Total Nitrogen (N); C:N ratio; dehydrogenase activity (DH) (μg TPF g^{-1} FW h^{-1}); pyruvate oxidase (POX) (μg L-DOPA g^{-1} FW h^{-1}); relative water content (RWC) (%), a regression tree was performed in order to determine which predictor variables with the smallest deviation and thus the most important predictor variables for the patterns obtained regarding respiration rates. A cost-complexity measure was used to assess the compromise between explanatory power and complexity and identify how the tree could be pruned. A graphical tree was constructed to illustrate the hierarchy of the most important predictor variables. Complementarily, an Additive Multiple Linear Model (GLM) was conducted. The response variable showed non-normality and square root transformation was performed; non-homogeneity of variance and non-linearity were also not evident. These analyses, used to assess the

main factors controlling respiratory activity, were performed in RStudio Software version v0.97.551 from RStudio, Inc.

Based on the scenarios proposed by the IPCC report (IPCC, 2007) for the temperature increase in the atmosphere for 2100, several simulations were then performed by adding the expected temperature increases to the observed values producing an estimation of the respiratory CO_2 fluxes predicted according to the developed GLM. Five possible scenarios of rising temperature were considered: the B1 scenario (increase in 1.8°C), the B2 scenario (increase in 2.4°C), the A1B scenario (increase in 2.6°C), the A2 scenario (increase in 3.2°C) and the worst case scenario, A1F1 (increase in 4.0°C).

Results

Sediment characterization

No significant differences were observed in physicochemical characteristics of both salt marshes during the cold season (Table 5.2.1). Nevertheless, Barra salt marsh sediments showed a tendency for higher organic matter and water content, salinity and temperature and lower sediment pH. During the warm season Barra salt marsh evidenced sediments with higher temperature and water content. Barra sediments presented lower organic matter and pH than Verdemilho sediments, while salinity showed the opposite trend (Table 5.2.1). As for pH, organic matter and water content it was significantly lower in Barra sediments during the cold season. On the other hand, both salinity and temperature were significantly higher during the warm season (Table 5.2.1). Sediments collected from Verdemilho salt marsh did not present any significant differences in physicochemical characteristics between seasons, except for sediment temperature, which was significantly higher during the warm season.

Regarding sediment elemental composition (Table 5.2.1), samples collected from Barra were not significantly different from Verdemilho salt marsh, either during warm and cold seasons. Nevertheless, it could be noticed that Barra salt marsh had slightly lower nitrogen and carbon contents than Verdemilho salt marsh during the warm season. During the warm season, sediments from Barra salt marsh had significantly lower nitrogen and carbon contents than sediments collected during the

cold season. Verdemilho sediments presented the opposite trend, although in this case variations were not significant. As for the C:N ratios the values were very similar in both salt marshes.

Table 5.2.1. Seasonal elemental composition of the sediments in the two analysed salt marshes (average ± standard error; different letters indicate significant differences at $p < 0.05$).

	Barra		Verdemilho	
	Warm	**Cold**	**Warm**	**Cold**
Organic Matter (%)	10.62 ± 2.35^{a}	19.76 ± 1.84^{b}	19.90 ± 6.01^{b}	16.67 ± 4.07^{b}
pH	6.24 ± 0.18^{a}	6.78 ± 0.09^{b}	6.77 ± 0.34^{a}	6.90 ± 0.24^{a}
Water Content (%)	35.02 ± 0.50^{a}	29.67 ± 0.65^{b}	27.75 ± 4.64^{b}	27.33 ± 1.20^{b}
Salinity (PSU)	34.70 ± 0.50^{a}	29.67 ± 0.65^{b}	27.75 ± 4.64^{b}	27.33 ± 1.20^{b}
Temperature (°C)	22.68 ± 0.24^{a}	14.69 ± 0.17^{b}	18.38 ± 0.19^{c}	14.62 ± 0.07^{b}
Total N (%)	0.30 ± 0.06^{a}	0.66 ± 0.07^{b}	0.59 ± 0.19^{ab}	0.35 ± 0.13^{ab}
Total C (%)	3.43 ± 0.75^{a}	6.07 ± 0.73^{b}	4.37 ± 1.51^{ab}	3.90 ± 1.37^{ab}
C/N ratio	11.45 ± 0.34^{a}	9.13 ± 0.18^{a}	7.93 ± 1.02^{a}	11.74 ± 0.50^{a}

Sediment Microbial Community Respiration

Respiratory activity (Figure 5.2.2) was significantly higher during the cold season in Barra salt marsh ($p < 0.05$). On the contrary, Verdemilho salt marsh showed higher respiration rates during the warm season than sediments from Barra salt marsh ($p < 0.05$). In the cold season this trend showed changes, with respiration rates in Verdemilho sediments decreasing significantly ($p < 0.05$) while compared to the rates measured in Barra sediments.

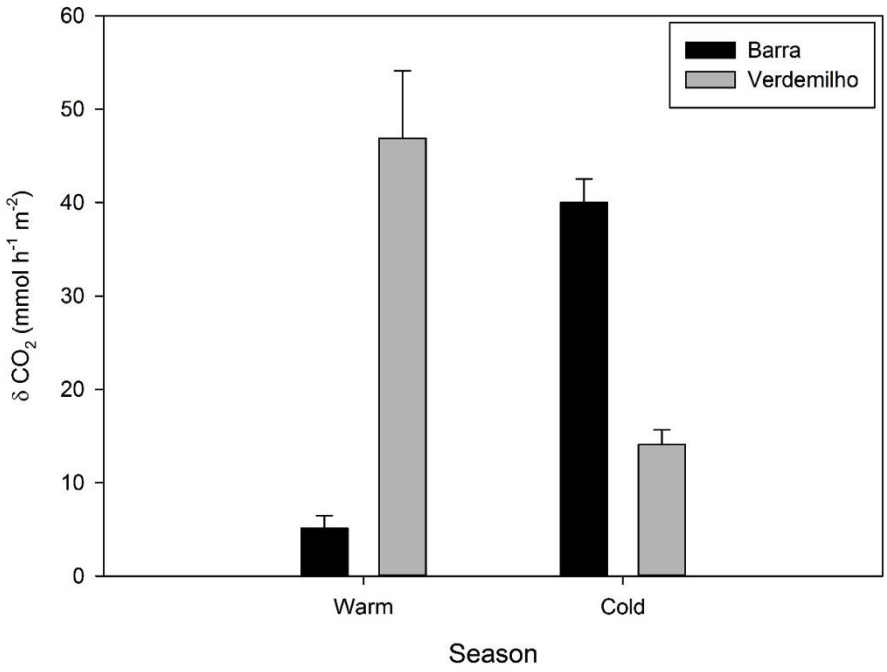

Figure 5.2.2. Sediment respiration rates (δCO_2) in both surveyed marshes during warm and cold seasons (average ± standard deviation).

Abiotic factors controlling microbial activity

Considering the similarities observed among salt marsh physicochemical characteristics and aiming to evaluate the possible abiotic factors underlying respiratory CO_2 fluxes, samples were pooled independently from the collection site (Figure 5.2.3). C:N ratio (proxy of the organic matter quality) and temperature showed the most evident relationships with the respiration rate. Considering the temperature influence on sediment CO_2 effluxes, the typical Gaussian curve can be observed with an optimum around 18 °C, and decreases in this rate at both lower and higher temperatures. As for the organic matter quality, it could be observed that higher carbon-contents and lower nitrogen-contents promote respiratory activity. Regarding the organic matter content, a potential Gaussian curve can also be observed, although its correlation is very low, indicative of a respiratory activity independent of the organic matter quantity. Relative water content showed a higher correlation with the respiratory mechanisms, however with a small correlation coefficient. Salinity and pH showed the lower correlation coefficients with the respiratory rates.

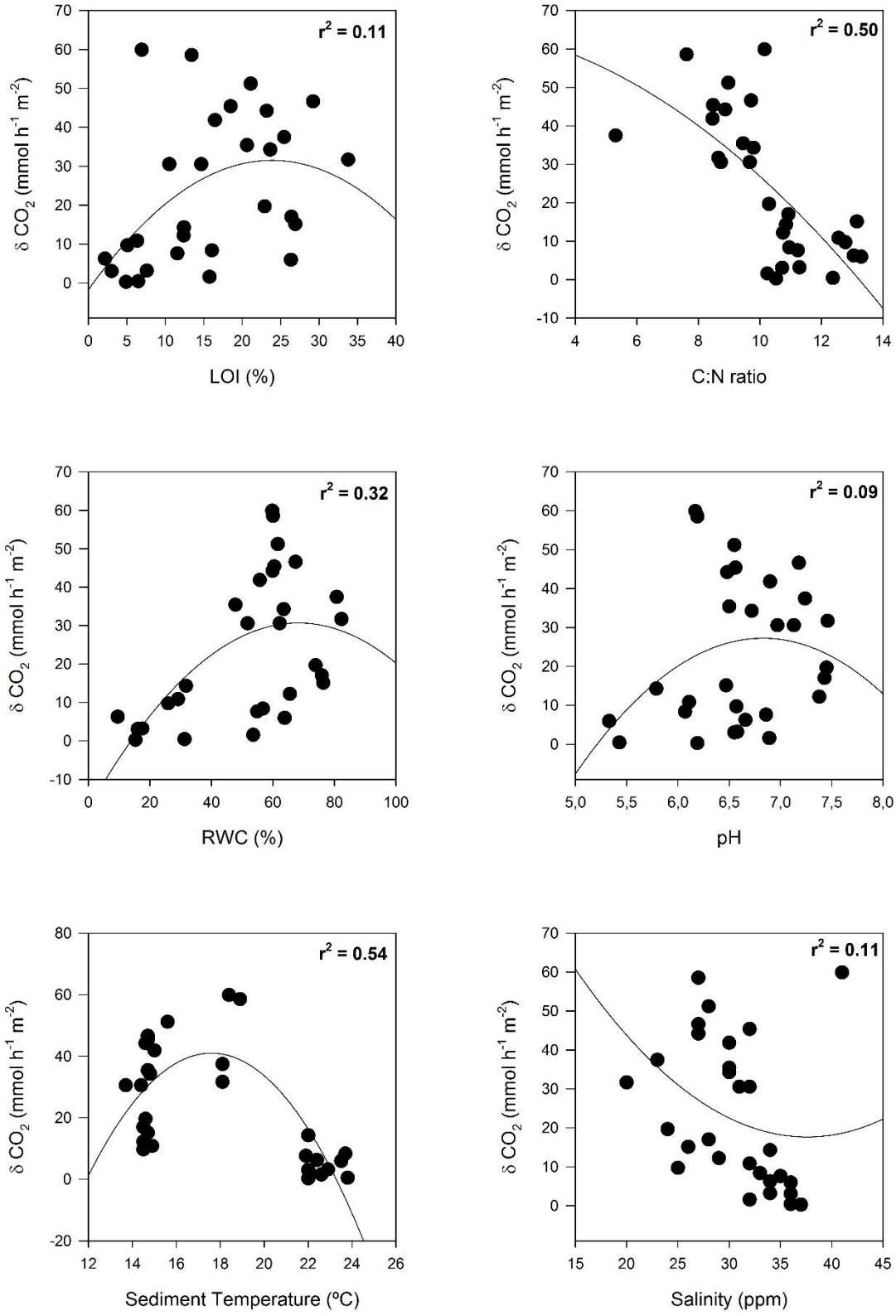

Figure 5.2.3. Polynomial regression plots between sediment respiration rates (δCO_2) and sediment organic matter content (LOI), organic matter quality (C:N ratio), relative water content (RWC), pH, temperature and pore water salinity considering all the analysed samples (n=29).

The examination of the cost-complexity measure showed that the additional deviance (fit) achieved by adding more nodes beyond 4 was very marginal, once cost-complexity curve began to asymptote at this point (Fig 5.2.4A).

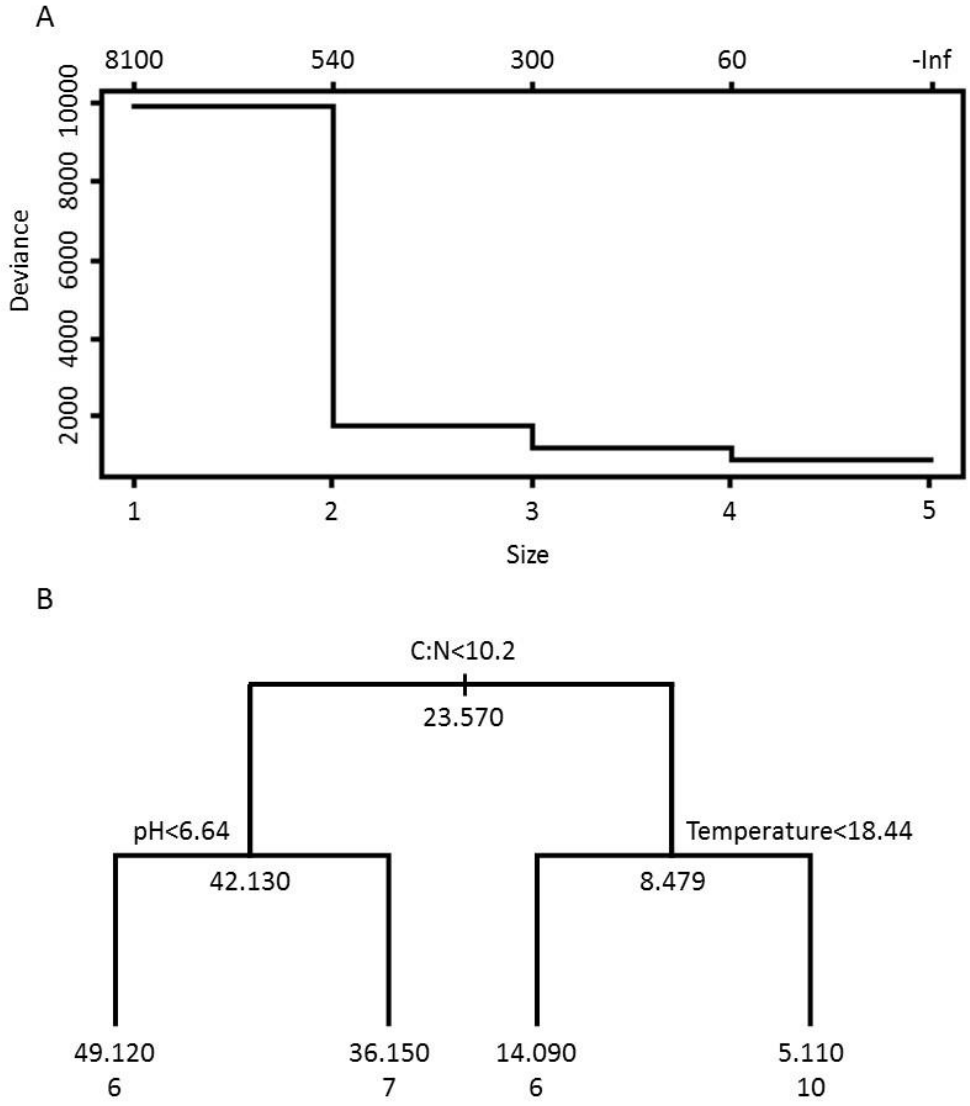

Figure 5.2.4. (A) Cost-complexity measure. It is clear that the additional deviance (fit) achieved by adding more nodes beyond 4 is very marginal (cost-complexity curve begins to asymptote at this point). This suggests that the tree could potentially be pruned to just three terminal branches without great loss of predictive power to achieve a more genuine predictive model. (B) Regression tree suggesting the most important predictor variables that better explain the respiration rates (C:N, pH and temperature).

So, the pruned regression tree suggested a predictive model with three variables (C:N ratio, pH and temperature). Finally, the additive multiple linear model was fitted to the data and the CO_2 production was explained and can be predicted according to the following expression:

$$\delta\ CO_2\ (\mu mol\ h^{-1}.m^{-2}) = (26.36 - 1.12\ pH - 0.34\ Temperature - 0.82\ C{:}N)^{\ 2}$$

The values produced by the GLM analysis (predicted) showed a very good correlation with the field measurements (observed), indicating that the variables selected throughout the GLM method are efficient in explaining the abiotic control of the respiratory fluxes for salt marsh sediments (Figure 5.2.5). Looking in more detail to the differences between the predicted and observed values (Figure 5.2.5), it can be observed that for low values of respiration the model produces very good estimates of the respiratory CO_2 fluxes, while high measured values are underestimated by the model.

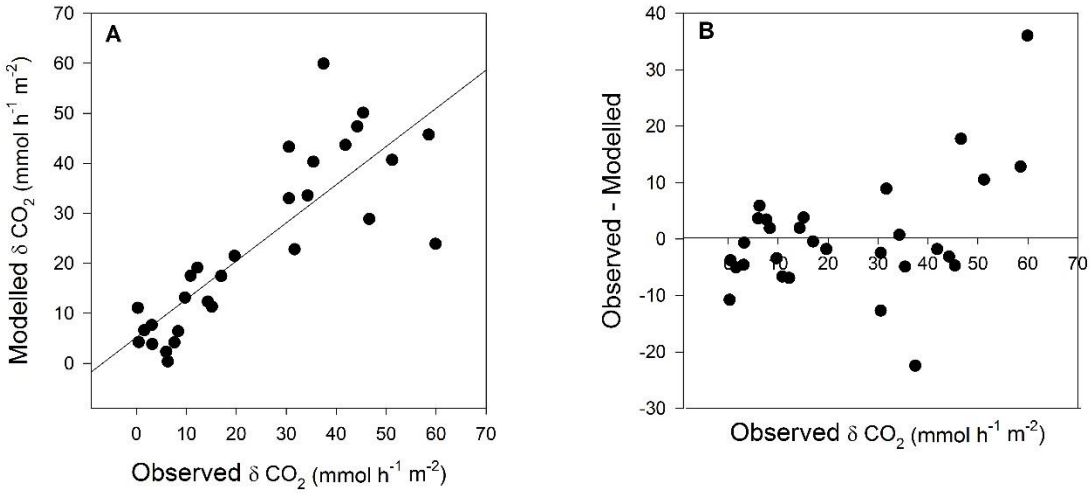

Figure 5.2.5. (A) Linear regression between observed and GLM modelled respiration values. (B) Dispersion plot of the differences among observed and modelled respiration rates.

CO_2 fluxes estimates under increasing temperature scenarios

According to the 4th Assessment IPCC report (IPCC, 2007), five possible scenarios of rising temperature were tested in the generated GLM: the B1 scenario (+1.8°C), the B2 scenario (+2.4°C), the A1B scenario (+2.6°C), the A2 scenario (+3.2°C) and the worst scenario, A1F1 (+4.0°C). All these temperature increases

were added to the verified temperatures keeping the remaining variables at field values and the respective CO_2 fluxes computed. GLM projections indicate that an increase in the air temperature will result in a proportional decrease in respiratory CO_2 emissions, especially during the cold season (Figure 5.2.6).

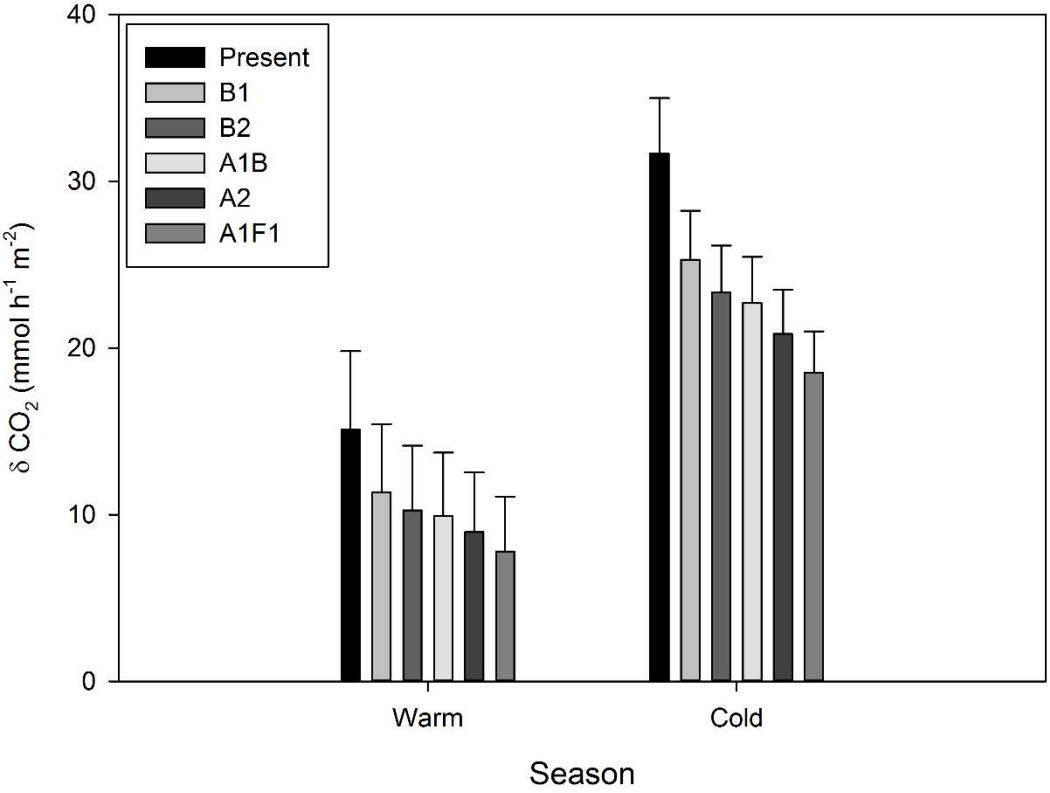

Figure 5.2.6. Modelled respiration rates considering the IPCC increased temperature scenarios (B1. B2, A1B, A2 and A1F1) during both warm and cold seasons (average ± standard deviation).

Discussion

According to the results of the present work, Barra and Verdemilho salt marshes have evident dissimilarities in terms of sediment respiration, mainly concerning the intensity of the fluxes generated and seasonality. Observing sediment characteristics as a whole these differences become clearer, as well as the factors behind them. GLM analysis showed that the variations in sediment respiration can be explained by an interaction of three factors: organic matter quality (C:N ratio), pH and temperature. Observing the temperature versus respiration plots it is easily observable the typical normal curve of an enzymatic

mechanism, showing a peak of activity around 18°C, decreasing towards extreme temperature values. This temperature optimum is coincident with the temperatures verified during 2/3 of the year in this ecosystem (Duarte *et al*., 2013). In mangrove forest sediments, respiration seems to have a similar feedback pattern to temperature, with this latter affecting respiration in a nonlinear way, having also two contrasting phases with a peak in respiration rates around 25-27°C (Lovelock, 2008). Degerman *et al*. (2013) showed that different microbial assemblages have different responses to temperature. This way, the different optimal temperature found in Lovelock (2008) and in the present study, is most likely due to the higher adaptation of mangrove microbial communities to higher (tropical) temperatures. Chen *et al*. (2000) found that decomposing woody roots respiration had its maximum respiration rates between 30 to 40°C and stated that the different respiration feedbacks to temperature in different ranges of temperature was mainly due to the characteristics of an enzymatic reaction. These reactions are enhanced with temperature until an optimal point and after which the activity decreases.

Although not evidenced by the GLM analysis, there is also an indirect effect of temperature on other highly correlated parameters, like the sediment water content. Orchard and Cook (1983) found that respiration increases with soil moisture and that rewetting soils caused a rapid increase in soil respiration. Other authors (Jia *et al*., 2007) described that soil moisture had a positive effect on the respiration of dry soils, and a negative effect when soils are excessively wet due to oxygen deficiencies. In water saturated soils (50% to 80% water content), moisture had little or no effect on respiration (Jia *et al*., 2007). In the present work, analysed samples showed water contents up to 80% describing again a weak, but visible, Gaussian distribution with a peak of sediment respiration around 70%. Therefore, oxygen seems to be a limiting factor in moister contents above this optimum value. Salt marsh vegetation also has some influence on sediment O_2 dynamics. Although salt marsh sediments are periodically flooded, plants are able to colonize these sediments, partly due to their ability to diffuse oxygen through their roots into the sediment (Lüdemann *et al*., 2000; Lillebo *et al*., 2006; Caetano *et al*., 2011) and thus promoting microbial activity in this environment (Duarte *et al*., 2008). This way, if

oxygen is not a limiting factor, increases in sediment water content may be beneficial for sediment respiration.

GLM analysis evidenced other factors as key-drivers for sediment respiration, namely the pH of the environment. This relationship with pH is in accordance to known factors controlling not only enzymatic activities but also microbial growth (Madigan *et al*., 2009). Recently, evidences were found pointing out the role of sediment pH shaping the activity of different extracellular phosphatase isoforms and thus, the decomposing efficiency of phosphorous-based respiratory substrates (Freitas *et al*., 2014). Other studies, focusing mainly forest and agriculture soils pointed out to a shift in the soil pH driven by litter and necromass introduction (Priha and Smolander, 1999; Smolander and Kitunen, 2002). Given the relatively high soil respiration rate at slightly acidic sediment pH, it is likely that a range in sediment pH exists where microbial activity and respiration is higher (Lee and Jose, 2003).

This leads us to another important factor that revealed a high influence in modulating sediment respiration: organic matter quality. The GLM analysis revealed a very interesting aspect in what concerns the organic substrates necessary for respiration. Organic matter content was not selected by the GLM nor showed an evident correlation with sediment respiration. Instead, the organic matter quality, had a very evident correlation with sediment CO_2 fluxes. This indicate that for salt marsh sediments, large amounts of organic matter are not required for respiration, but even at low amounts the carbon composition of the organic substrates is of extreme importance for the respiratory activity. Comparing these data with the obtained for Tagus estuary (Costa *et al*., 2007) an explanation could be found. Costa *et al*. (2007) found that the microbial communities inhabiting the sediments have preference for the degradation of carboxylic acids, carbohydrates and phenolic compounds, and only a small part of the microbial community showed any relation with nitrogen based organic molecules (amino acids and amines). Furthermore, other studies found that N addition to soils, and thus a decrease in the C:N ratio, leads to an enhancement of the soil respiration. Gallardo and Schlesinger (1994) found an increase in soil respiration when nitrogen was added experimentally to forest soils in central North Carolina. Similar results were reported in a temperate forest in Germany (Brume and Besse, 1992). This is in accordance to our results and

points out to a N-limited sediment system, where N-rich organic matter favours the decomposition processes and thus increases sediment respiration.

Seasonal differences in respiration in different salt marshes are easily understandable by the above-mentioned reasons. In Barra salt marsh, the sediments collected in warm seasons had lower respiration rates due to the negative effects of warm temperatures (above the optimum temperature) and lower water contents. In Verdemilho salt marsh, the sediments collected at the warm season had not only higher water contents and temperatures than the samples collected during the cold season, but also higher respiratory activities. At these conditions, the effect of temperature on respiration seems to be positive. This can be attributed to the fact that, during the warm season in Verdemilho, sediment temperature was around 18°C, and thus close to optimal conditions. In sum, sediment respiratory CO_2 fluxes depend not only on the effect of each of these abiotic factors, but also on their interactions, as revealed by the GLM.

Nowadays and with an increasing concern on the climatic changes undergoing on our planet, several studies aroused focusing the effects of global warming in respiration in several ecosystems (e.g. Florides and Christodoulides, 2009; Shakun *et al*., 2012). These studies point out to an important role of increasing temperatures while major contributors to enhance respiration and therefore the CO_2 fluxes to the atmosphere (Kirschbaum, 1995; Cox *et al*., 2000; Bond-Lamberty and Thomson, 2010). Concerning the GLM and the simulations produced according to the IPCC predictions (IPCC, 2007), temperature seems to have an opposite effect decreasing CO_2 effluxes due to respiration. This points out to a differential effect of the temperature in each ecosystem, as suggested before by Singh *et al*. (2010). It is interesting to note that in other types of ecosystem such as semiarid grasslands, or even regions with arid seasons, the effect of water content becomes dominant over temperature, while regulating soil respiration (Liu *et al*., 2009; Inglima *et al*., 2009). The effect of temperature may also vary seasonally, since below the optimum point, the effect of increasing temperature is opposite to its effect over optimum values. Nevertheless, and in which concerns the simulations produced according to the predicted IPCC scenarios, salt marshes will tend to decrease their CO_2 emissions with the increasing temperatures, reinforcing their role as important carbon sinks

(Caçador *et al*., 2004; Sousa *et al*., 2010; Couto *et al*., 2013). This can be interpreted as an ecosystem counteractive measure toward a reduction of the increasing temperature by reducing the amounts of greenhouse gas emissions, namely CO_2.

Conclusion

Temperature, alongside with pH and organic matter quality, is one of the main factor driving sediment respiration in salt marshes. It is therefore important to consider the different impacts of global warming in CO_2 effluxes in different ecosystems. In fact, the accuracy of the existent CO_2 efflux models may be improved by the inclusion of the above-described factors. Besides seasonality, the ecosystem type and climate are also factors that influence carbon fluxes. Nevertheless, it is important to notice that these ecosystems have an intrinsic ability to adaptation, counteracting the greenhouse effect and temperature rising by becoming more efficient carbon sinks, reducing the CO_2 emissions and therefore contributing for the mitigation of climate change impacts in coastal areas.

References

Acosta-Martinez, V., Cruz, L., Sotomayor-Ramírez, D. and Pérez-Alegría, L., 2007. Enzyme activities as affected by soil properties and land use in a tropical watershed. *Applied Soil Ecology* 35, 35-45.

Allen, A.S., Andrews, J.A., Finzi, A.C., Matamala, R., Richter, D.D. and Schlesinger, W.H., 2000. Effects of free-air CO_2 enrichment (FACE) on belowground processes in a *Pinus taeda* forest. *Ecological Applications* 10, 437-448.

Bais H.P., Weir, T.L., Perry, L.G., Gilroy, S. and Vivanco, J.M., 2006. The Role of Root Exudates in Rhizosphere Interactions with Plants and Other Organisms. *Annual Reviews of Plant Biology* 57, 233-266.

Bond-Lamberty, B. and Thomson, A., 2010. Temperature-associated increases in the global soil respiration record. *Nature* 464, 579-583.

Boorman, L.A., 1999. Salt marshes – present functioning and future change. *Mangroves and Salt Marshes* 3, 227-241.

Brumme, R. and Beese, F., 1992. Effects of liming and nitrogen fertilization on emissions of CO_2 and N_2O from a temperate forest. *Journal of Geophysical Research* 97, 12851–12858.

Caçador, I., Costa, A.L. and Vale, C., 2004. Carbon storage in Tagus saltmarsh sediments. *Water, Air, and Soil Pollution: Focus* 4, 701-714.

Caetano, M., Bernárdez, P., Santos-Echeandia J., Prego, R. and Vale C., 2011. Tidally driven N, P, Fe and Mn exchanges in salt marsh sediments of Tagus estuary (SW Europe). *Environmental Monitoring Assessment* 184, 6541-52.

Cardoso, S.J., Vidal, L.O., Mendonça, R.F., Tranvik, L.I., Sobek, S. and Roland, F., 2013. Spatial variation of sediment mineralization supports differential CO_2 emissions from a tropical hydroelectric reservoir. *Frontiers in Microbiology* 4, 1-8.

Chen, H., Harmon, M. E., Griffiths, R.P. and Hicks, W., 2000. Effects of temperature and moisture on carbon respired from decomposing woody roots. *Forest Ecology and Management* 138, 51-64.

Costa, A. L., Paixão, S.M., Caçador, I. and Carolino, M., 2007. CLPP and EEA Profiles of Microbial Communities in Salt Marsh Sediments. Jo*urnal of Soils and Sediments* 7, 418-425.

Couto, T., Duarte, B., Caçador, I., Baeta, A. and Marques, J.C., 2013. Salt marsh plants carbon storage in a temperate Atlantic estuary illustrated by a stable isotopic analysis based approach. *Ecological Indicators* 32, 305-311.

Cox, P.M., Betts, R.A., Jones, C.D., Spall, S.A. and Totterdell, I.J., 2000. Acceleration of global warming due to carbon-cycle feedbacks in a coupled climate model. *Nature* 408, 184-187.

Crow S., Lajtha, K., Filley, T. R., Swanston, C.W., Bowden, R.D. and Caldwell, B.A., 2009. Sources of plant-derived carbon and stability of organic matter in soil: implications for global change. *Global Change Biology* 15, 2003-2019.

Daily, G.C., Matson, P.A., Vitousek, P.M., 1997. Ecosystem services supplied by soil. In: Daily, G. C. (Ed.), Nature's Services: Societal Dependence on Natural Ecosystems. Island Press, Washington, DC, pp. 113-132.

Degerman, R., Dinasquet, J., Riemann, L., Sjostedt de Luna, S. and Andersson, A., 2013. Effect of resource availability on bacterial community responses to increased temperature. *Aquatic Microbial Ecology* 68, 131-142.

Dias, J.M. and Lopes, J.F., 2006. Implementation and assessment of hydrodynamic, salt and heat transport models: the case of Ria de Aveiro Lagoon (Portugal). *Environmental Modelling and Software* 21, 1-15.

Dias, J.M. and Picado, A., 2011. Impact of morphologic anthropogenic and natural changes in estuarine tidal dynamics. *Journal of Coastal Research* 64, 1490-1494.

Doering, M., Uehlinger, U., Ackermann, T., Woodtli, M. and Tockner, K., 2011. Spatiotemporal heterogeneity of soil and sediment respiration in a river-floodplain mosaic (Tagliamento, NE Italy). *Freshwater Biology* 56, 1297-1311.

Duarte, B., Almeida, P.R. and Caçador, I., 2009. *Spartina maritima* (cordgrass) rhizosediment extracellular enzymatic activity and its role in organic matter decomposition processes and metal speciation. *Marine Ecology* 30, 65-73.

Duarte, B., Reboreda, R., Caçador, I., 2008. Seasonal variation of Extracellular Enzymatic Activity (EEA) and its influence on metal speciation in a polluted salt marsh. *Chemosphere* 73, 1056-1063.

Duarte, B., Couto, T., Freitas, J., Valentim, J., Silva, H., Marques, J. C., Dias, J.M. and Caçador, I., 2013. Abiotic modulation of *Spartina maritima* photosynthetic ecotypic variations in different latitudinal populations. *Estuarine, Coastal and Shelf Science* 130, 127-137.

Duarte, B., Santos, D., Silva, H., Marques, J.C. and Caçador, I., 2014. Photochemical and Biophysical feedbacks of C_3 and C_4 Mediterranean halophytes to atmospheric CO_2 enrichment confirmed by their stable isotope signatures. *Plant Physiology ad Biochemistry* 80, 10-22.

Florides, G.A. and Christodoulides, P., 2009. Global warming and carbon dioxide through sciences. *Environmental International* 35, 390-401.

Freitas, J., Duarte, B. and Caçador, I., 2014. Biogeochemical drivers of phosphatase activity in salt marsh sediments. *Journal of Sea Research* 93, 57-62.

Fromin, N., Pinay, G., Montuelle, B., Landais, D., Ourcival, J. M., Joffre, R. and Lensi, R., 2010. Impact of seasonal sediment desiccation and rewetting on microbial processes involved in greenhouse gas emissions. *Ecohydrology* 3, 339-348.

Gallardo, A. and Schlesinger, W.H., 1994. Factors limiting microbial biomass in the mineral soil and forest floor of a warm-temperate forest. *Soil Biology and Biochemistry* 26, 1409–1415.

Gardi, C., Montanarella, L., Arrouays, D., Bispo, A., Lemanceau, P., Jolivet, C., Mulder, C., Ranjard, L., Römbke, J., Rutgers, M. and Menta, C., 2009. Soil biodiversity monitoring in Europe: ongoing activities and challenges. *European Journal of Soil Science* 60, 807–819.

Gunderson, C.A. and Wullschleger, S.D., 1994. Photosynthetic acclimation in trees to rising atmospheric CO_2: A broader perspective. *Photosynthesis Research* 39, 369-388.

Han, G., Luo, Y., Li, D., Xia, J., Xing, Q. and Yu, J., 2014. Ecosystem photosynthesis regulates soil respiration on a diurnal scale with a short-ter time lag in a coastal wetland. *Soil Biology aned Biochemistry* 68, 85-94.

Ineson, P., Coward, P.A. and Hartwig, U.A., 1998. Soil gas fluxes of N_2O, CH_4 and CO_2 beneath *Lolium perenne* under elevated CO_2: The Swiss free air carbon dioxide enrichment experiment. *Plant and Soil* 198, 89-95.

Inglima, I., Alberti, G., Bertolini, T., Vaccari, F. P., Gioli, B., Miglietta, F., Cotrufo, M.F. and Peressotti, A., 2009. Precipitation pulses enhance respiration of Mediterranean ecosystems: the balance between organic and inorganic components of increased soil CO_2 efflux. *Global Change Biology* 15, 1289-1301.

IPCC. Intergovernmental panel on climate change, WMO, UNEP. Climate change 2007. The physical science basis, Summary for policymakers. I*PCC WGI Fourth Assessment Report*. SPM2feb07; 2007.

Janssens, I.A ., Lankreijer, H., Matteucci, G., Kowalski, A.S., Buchmann, N., Epron, D., Pilegaard, K., Kutsch, W., Longdoz, B., Grünwald, T., Montagnani, L., Dore, S., Rebmann, C., Moors, E. J., Grelle, A., Rannik, Ü., Morgenstern, K., Oltchev, S., Clement, R., Guđmundsson, J., Minerbi, S., Berbigier, P., Ibrom, A., Moncrieff, J., Aubinet, M., Bernhofer, C., Jensen, N.O., Vesala, T., Granier, A., Schulze, E.-D., Lindroth, A., Dolman, A. J., Jarvis, P.G., Ceulemans, R. and Valentini, R., 2001. Productivity overshadows temperature in determining soil and ecosystem respiration across European forests. *Global Change Biology* 7, 269-278.

Jia, B., Zhou, B. and Yuan, W., 2007. Modelling and coupling of soil respiration and soil water content in fenced *Leymus chinensis* steppe, Inner Mongolia. *Ecological Modelling* 201, 157-162.

Kang, H., Freeman, C., Park, S. S. and Chun, J., 2005. N-Acetylglucosaminidase activities in wetlands: a global survey. *Hydrobiologia* 532, 103-110.

Kirschbaum, M.U.F., 1995. The temperature dependence of soil organic matter decomposition, and the effect of global warming on soil organic C storage. *Soil Biology and Biochemistry* 27, 753-760.

Kristensen, E., Mangion, P., Tang, M., Flindt, M.R., Holmer, M. and Ulomi, S., 2011. Microbial carbon oxidation rates and pathways in sediments of two Tanzanian mangrove forests. *Biogeochemistry* 103, 143-158.

Lee, K.-H. and Jose, S., 2003. Soil respiration, fine root production, and microbial biomass in cottonwood and loblolly pine plantations along a nitrogen fertilization gradient. *Forest Ecology and Management* 185, 263-273.

Leopold, A., Marchand, C., Deborde, J., Chaduteau, C. and Allenbach, M., 2013. Influence of mangrove zonation on CO_2 fluxes at the sediment–air interface (New Caledonia). *Geoderma* 202-203, 62-70.

Lillebø, A. I., Flindt, M. R., Pardal, M. A. and Marques, J. C., 2006. The effect of *Zostera noltii*, *Spartina maritima* and *Scirpus maritimus* on sediment pore-water profiles in a temperate intertidal estuary. *Hydrobiologia* 555, 175–183.

Liu, W., Zhang, Z. and Wan, S., 2009. Predominant role of water in regulating soil and microbial respiration and their responses to climate change in a semiarid grassland. *Global Change Biology* 15, 184-195.

Lovelock, C. E., 2008. Soil Respiration and Belowground Carbon Allocation in Mangrove Forests. *Ecosystems* 11, 342-354.

Lüdemann, H., Arth, I. and Wiesack, W., 2000. Spatial changes in the bacterial community structure along a vertical oxygen gradient in flooded paddy sediment cores. *Applied Environmental Microbiology* 66, 754–762.

Luo,Y. and Zhou, X., 2006. Soil Respiration and the Environment. Academic Press, U.S.A.

Madigan, M. T., Martinko, J. M., Dunlap, P. V. and Clark, D.P., 2009. *Brock Biology of Microorganisms*. Pearson Benjamin Cummings, U.S.A.

Nannipieri, P. and Badalucco, L., 2003. Biological processes. In: Handbook of Processes in the Soil–Plant System: Modelling Concepts and Applications (eds D.K. Bembi and R. Nieder). The Haworth Press, Binghamton, NY, in press.

Norby, R.J. and Zak, D.R., 2011. Ecological Lessons from Free-Air CO2 Enrichment (FACE) Experiments. *Annual Reviews of Ecology, Evolution and Systematics* 42, 181-203.

Orchard, V.A. and Cook, F.J., 1983. Relationship between soil respiration and soil moisture. *Soil Biology and Biochemistry* 15, 447-453.

Picado, A., Dias, J. M., Fortunato, A., 2010. Tidal changes in estuarine systems induced by local geomorphologic modifications. *Continental Shelf Research* 30, 1854-1864.

Prilha, O. and Smolander, A., 1999. Nitrogen transformations in soil under *Pinus sylvestris*, *Picea abies* and *Betula pendula* at two forest sites. *Soil Biology and Biochemistry* 31, 965-977.

Richey, J.E., Melack, J.M., Aufdenkampe, A.K., Ballester, V.M. and Hess, L.L., 2002. Outgassing from Amazonian rivers and wetlands as a large tropical source of atmospheric CO_2. *Nature* 416, 617-620.

Sasaki, A., Agimori, Y., Nakatsubo, T. and Hoshika, A., 2009. Tidal effects on the organic carbon mineralization rate under aerobic conditions in sediments of an intertidal estuary. *Ecological Research* 24, 723-729.

Shakun, J.D., Clark, P.U., He, F., Marcott, S.A., Mix, A.C., Liu, Z., Otto-Bliesner, B., Schmittner, A. and Bard, E., 2012. Global warming preceded by increasing carbon dioxide concentrations during the last deglaciation. *Nature* 484, 49-55.

Singh, B.K., Bardgett, R.D., Smith, P., and Reay, D.S., 2010. Microorganisms and climate change: terrestrial feedbacks and mitigation options. *Nature Reviews* 8, 779-790.

Smolander, A. and Kitunen, V., 2002. Soil microbial activities and characteristics of dissolved organic C and N in relation to tree species. *Soil Biology and Biochemistry* 34, 651-660.

Sousa, A.I., Lillebo, A.I., Pardal, M.A. and Caçador, I., 2010. The influence of *Spartina maritima* on carbon retention capacity in salt marshes from warm-temperate estuaries. *Marine Pollution Bulletin* 61, 215-223.

Strain, B.R., 1987. Direct Effects of Increasing Atmospheric CO_2 on Plants and Ecosystem. *Tree* 2, 18-21.

Valentini, R., Matteucci, G., Dolman, A. J., Schulze, E.-D., Rebmann, C., Moors, E. J., Granier, A., Gross, P., Jensen, N. O., Pilegaard, K., Lindroth, A., Grelle, A., Bernhofer, C., Grünwald, T., Aubinet, M., Ceulemans, R., Kowalski, A.S., Vesala, T., Rannik, Ü., Berbigier, P., Loustau, D., Gudmundsson, J., Thorgeirsson, H., Ibrom, A., Morgenstern, K., Clement, R., Moncrieff, J., Montagnani, L., Minerbi S. and Jarvis P. G., 2000. Respiration as the main determinant of carbon balance in European forests. *Nature* 404, 861-865.

Vernberg, F.J,. 1993. Salt-Marsh Processes: A Review. *Environmental Toxicology and Chemistry* 12, 2167-2195.

White, P.A., Kalff, J., Rasmussen, J.B. and Gasol, J.M., 1991. The effect of temperature and algal biomass on bacterial production and specific growth rate in freshwater and marine habitats. *Microbial Ecology* 21, 99-118.

5.3. ECOPHYSIOLOGICAL FEEDBACKS OF C_3 AND C_4 HALOPHYTES UNDER EXTREME THERMAL EVENTS [1]

Abstract

According to the newest predictions, it is expected that the Mediterranean systems experience more frequent and longer heat and cold treatments events. Salt marshes will be no exception. The recent IPCC WG2 5th Assessment Report (IPCC, 2014), notes an increase in the frequency and duration of extreme climatic events, especially for the Mediterranean region. Together with climate change, the invasion of natural communities by non-indigenous species (NIS) constitutes a serious threat to biodiversity. A predicted increase of heat and cold treatment events has a negative impact on the physiology and the photobiology of *H. portulacoides* and *A. tripolium* (C_3 plants). Intrinsic biophysical stress response mechanisms such as the activation of a dissipative energy pathway are ineffective under these circumstances, resulting in significant photosynthesis activity inhibition. Considering the cellular electronic processes, some ecological outcomes arise. The lower damage induced by cold exposure along with the higher levels of cellular defence point out to a higher tolerance of C_3 plants to cold periods. Considering the invasion ecology of the North American *S. patens* while compared with the Mediterranean native *S. maritima* some implications can also be withdrawn. *Spartina maritima* and *S. patens* appear to have different thermal tolerances conditioned by their adaptation to two different

[1] This section was published in: **Duarte, B.**, Marques, J.C. and Caçador, I., 2015. Impact of extreme heat and cold events on the energetic metabolism of the C_3 halophyte *Halimione portulacoides*. *Estuarine Coastal and Shelf Science* 167, 166-177. **Duarte, B.**, Marques, J.C. and Caçador, I. (*in press*) Ecophysiological responses of native and invasive *Spartina* species to extreme temperature events in Mediterranean marshes. *Biological Invasions* (doi: 10.1007/s10530-015-0958-4). **Duarte, B.**, Goessling, J., Marques, J.C. and Caçador, I., 2015. Ecophysiological constrains of *Aster tripolium* under extreme thermal events impacts: merging biophysical, biochemical and genetic insights. *Plant Physiology and Biochemistry* 97, 217-228.

climatic habitats of origin. *Spartina patens* appears to have a higher fitness for the incoming climatic scenarios, being more tolerant to heat stress, while *S. maritima* will have its photobiological fitness decreased according to these predictions. The physiological reactions of introduced /exotic species can predispose them to become invasive when climate change favours them over the native species.

Introduction

Wetlands are of the most importance as providers of a wide range of ecosystem services and for that reason are included among the most relevant ecosystems worldwide (Constanza *et al*., 1997; Teal and Howes, 2000). Within the services provided by these ecosystems at a global scale are included nutrient cycling, primary production, habitat for wildlife, and shoreline stabilization. Salt marsh vegetation has a major impact on sea defence, filtration of pollutants, and the provision of rare and unique habitats, functioning as a nursery-ground for fish and breeding/feeding grounds for birds. Halophytes are typically adapted to stressful environments, subjected to high levels of abiotic stress like flooding (Duarte *et al*., 2014a), high salinity (Duarte *et al*., 2013a) and pollution (Duarte *et al*., 2013b), showing morphological and physiological adaptations that allows them to survive in these adverse environments. Thus, sustainable use of halophytes in adverse environments has acquired an increasing interest from the scientific community (Pasternak, 1990; Koyro, 2006). These plants, also called cash crop halophytes (about 2500 halophyte known worldwide) have a high potential for utilization (Lieth *et al*., 1999 and Koyro, 2006), with application in various economic and ecologic purposes, e.g. food, fodder, source of timber, fibers, reed or chemicals, as ornamental plants, for coastal protection, land reclamation or desert revegetation (Lieth and Mochtchenko, 2002). *Halimione portulacoides* (L.) Allen is one of the most abundant halophytic species in the Mediterranean marshes, occupying approximately 24 % of all Portuguese salt marshes in both estuaries and coastal lagoons (Caçador *et al*., 2013). This halophyte has been recognized as key species for nutrient recycling (Sousa *et al*., 2010), contaminant remediation (Duarte *et al*., 2007) and as a possible source of important biomolecules (Grossi and Raphel, 2003). Another important C_3 halophyte is *Aster tripolium*, a promising potential cash crop halophyte, which can be used for human alimentation (the leaves have a high nutritional value and can be eaten as salad or vegetable), as forage or an ornamental plant (Larcher, 2003; Plieth *et al*., 1999), even with a possible application as nutraceutical. It has already been cultivated in pilot schemes in the Netherlands, in Belgium, Portugal and Pakistan. The members of the *Spartina* genus have C_4 photosynthesis using phosphoenolpyruvate carboxylase (PEPC) involved in primarily CO_2 assimilation, in a

more efficient way than it would be observed in a C_3 organism (Hatch, 1992; Álvarez *et al*., 2010). PEPC is regulated by light-dependent phosphorylation (Vidal *et al*., 1996), making it very dependent on the surrounding climatic environment. Interspecific differences among different *Spartina* species are likely to be found since leaves have high sensitivity to environmental pressures, such as climatic variations, contaminants and grazing (Heide, 2005; Stephenson *et al*. 2006). In addition, the activation of PEPC by its specific kinase is low in reduced light intensities (Bailey *et al*. 2007) and at low temperatures (Lara *et al*. 2001), both of which are abiotic factors that change with latitude and during climate extremes.

Besides climate change, the invasion of natural communities by non-indigenous species (NIS) poses a serious threat to biodiversity (Heywood, 1989). One of these NIS is the American *Spartina patens* (Ait.) Muhl. (Poaceae) native from these coasts (Fabre, 1849; Tutin, 1980; Van der Maarel and Van der Maarel-Versluys, 1996). Recently it has been widely found in Galicia and nowadays in several estuaries and costal lagoons from the west coast of Portugal (SanLeon *et al*., 1999). A dominant Portuguese salt marsh plant, *S. maritima* is present in the same marshes and locations as *S. patens*. *Spartina maritima* (Curtis) Fernald, has a very wide distribution in the northern hemisphere native to the coasts of western and northern Europe and western Africa, with also a disjunct population on the Atlantic coasts of Namibia and South Africa (Marchant and Goodman, 1969).

The recent IPCC WG2 5th Assessment Report (IPCC, 2014), points out to an increase in global air temperature along with a higher frequency and duration of extreme climatic events. Climate changes are very likely to increase the frequency and intensity of heat treatments, with mostly adverse implications for health, agriculture, forestry, energy production and use, transport, tourism, labour productivity, and the built environment. Oppositely, cold treatments seem to tend to decrease in frequency but not in intensity (IPCC, 2014). Recently the Mediterranean countries have been affected with higher frequency by heat and cold treatments (Niu *et al*., 2014). Extreme thermal events are defined by the World Meteorological Organization (WMO) as an extreme thermal event when the daily maximum (or minimum) temperature of more than five consecutive days increases (or decreases) the average maximum temperature by 5 °C, using the period comprised between

1961–1990 as reference. This was the case of the heat and a cold treatment occurred in 2003 and 2005 in southern Europe, respectively.

Different abiotic stressors trigger similar bottlenecks in the plant energetic metabolism, due to its impact on the same key metabolic pathways. Reduction of the photosynthesis activity during cold and heat treatments has been observed, although the effects of heat treatments on the growth parameters are also dependent on seasonal characteristics, such as water and nutrient availability, or priming events during earlier experienced stress (De Boeck *et al*. 2010; Larcher, 2003). Besides these similarities, cold and heat treatment events affect plant metabolism in different steps. For example, while heat stress causes degradation of proteins and membranes (Larcher, 2003), cold stress tend to induce decline in membrane fluidity. This last is considered to be a sensed factor in the plant response to temperature changes, affecting Ca^{2+} channels and triggering an increased Ca^{2+} influx (Monroy and Dhindsa, 1995). An altered cellular redox state - by imbalanced proportions of absorbed light energy and its metabolic consumption - might be sensed during stress (Emsminger *et al*., 2006). Reduced availability of oxidized electron acceptors in the electron transport chain triggers an uncontrolled formation of reactive oxygen species. Considering these effects as responses to different thermal stressors, several aspects of the plant metabolism must be addressed in thermal stress studies, namely its photochemical metabolism, anti-oxidant enzymatic defences and gene expression itself. Stress induced genes can be classified into the functional response (maintenance and protection of metabolic processes) and the regulatory response (signal transduction and transcription factors) (Ohno *et al*., 2003). Conversely, plant thermal resistance would be recognizable by a maintenance/improvement of the photochemical efficiencies, conservation of its pigment profile, anti-oxidant enzyme activity, all this associated to certain gene activation/deactivation.

In sum, the present chapter intents to evaluate the effects of heat and cold waves on C_3 and C_4 widely spread halophytic species in order to understand the biochemical and photochemical processes underlying the plant feedback to these extreme events and how the primary productivity of these halophytes will be affected during the first days of exposure to these conditions. Using a model

halophyte like *A. tripolium* also allows to explore the expression profile of some genes and its relationship with the abovementioned parameters. Considering the recent IPCC projections becomes of great importance to address these ecophysiological feedbacks as well as their consequences in terms of plant primary productivity and survival in a changing ecosystem.

Material and Methods

Plant Collection

Plants from both *Spartina* species were collected in a Tagus estuary salt marsh and brought back to the laboratory. Plants were placed in pots with a mixture of sand and perlite (1:1), irrigated with ¼ Hoagland solution and placed in a FitoScope 130 RGBIR chamber (Photon System Instruments, Czech Republic) for a 2-week period of acclimation. Although both species are considered halophytic grasses, they behave as salt excreting grasses, being tolerant to salinity. Previous works (Mateos-Naranjo *et al*., 2010; Duarte *et al*., 2015) show that both species present higher performance in the absence of salinity. This way in order to isolate the potential consequences of the tested thermal events, the growth medium was maintained without the addition of salt. *Halimione portulacoides* was sampled in the northern margin of the Tagus estuary, near the Expo 98 exhibition site (38°47'0.87"N, 9°5'29.05" W) during Spring. Samples were stored in plastic bags and quickly transported to the laboratory, where plants were washed with Mili-Q water to remove the dust and sediment. In order to make the grafts, the roots and a small part of the stems were cut, leaving at least two nods in the stem below the lowest branch, in order to develop grafts. The grafts were placed inside a FitoScope 130 RGBIR for a 4-week period of acclimation and for root development, irrigated with ¼ Hoagland solution. *Aster tripolium* seeds were collected during November 2013 at Tagus estuary salt marshes (Alcochete, 38°45'38.78"N, 8°56'7.37"W) and dried in a desiccator for a week in order to remove any humidity. Seeds were germinated in petri dishes with moistened filter paper inside a FitoScope 130 RGBIR in dim light (< 20 μmol photons m^{-2} s^{-1}, 16 h light/8 h dark; day temperature 20 ± 0.5 °C, night temperature 18 ± 0.5 °C). After two months, the plants were transferred to pots

with acid-washed sand and perlite (1:1) and replaced inside the chamber for another 2 months in order to increase the biomass, irrigated with ¼ Hoagland solution.

Experimental Setup

During growth and acclimation period, the chamber was programmed with a sinusoidal function simulating sunrise and sunset and with a maximum temperature and light intensity at noon to simulate a natural light environment (Maximum PAR 1000 μmol photons m^{-2} s^{-1}, 16/8 h day/night rhythm; day temperature 20 ± 0.5 °C, night temperature 18 ± 0.5 °C). After this period plants were separated into 3 groups per specie (n=5) and subjected to different thermal treatments (day/night): control (20/18 °C), cold-wave treatment (9/5 °C) and heat-wave treatment (42/38 °C). Temperature rises and falls with dawn and sunset was also performed gradually according to a sinusoidal function. Heat and cold treatments simulation were performed according to the records of air temperature for the Tagus estuary from the 2003 heat treatment and the 2005 cold treatment (www.snirh.pt). In order to detect early stress signs due to thermal shifts, all experiments lasted for 3 days after which plants were harvested.

Pulse Amplitude Modulated (PAM) Fluorometry

All measurements were made according to the manufacturer instructions and as described in Duarte *et al*. (2014a) and in Chapter 2, Section 3, allowing to attain the variables described in the table 2.3.1.

Pigment Profiling

Pigment quantifications were made using UV-Vis spectrophotometry and a mathematical algorithm designed for the effect, according to Kupper *et al*. (2007) and as described in Chapter 2, Section 3.

Oxidative biomarkers assays

Anti-oxidant enzymatic activities, oxidation products and protein content quantifications were made using UV-Vis spectrophotometry according to standard methods and as described in Chapter 2, Section 3.

***Aster tripolium* RNA extraction, reverse transcription, and quantitative PCR**

RNA was extracted from leaves with the TRIzol protocol (Chomczynski, 1993). RNA purity and concentration was estimated with a NanoDrop (NanoDrop Technologies, Wilmington, DE). One unit of DNAse (Thermo Scientific) per µg RNA was incubated in a final concentration of 2 mM MgCl for 30 minutes at 37°C, which was then denaturated for 15 minutes at 70°C. Approximately one µg of RNA was incubated with 50 pmol random nonamer primer for 5 minutes at 70°C, and rapidly cooled down on ice to induce primer annealing. 200 Units of moloney murine leukemia virus reverse transcriptase, and 1mM dNTPs were added to the buffer (provided by the manufacturer). Linearity of the cDNA synthesis was controlled with dilutions on the RNA level. cDNA synthesis in the absence of reverse transcriptase was used to estimate DNA contamination. Quantitative PCR was performed with SYBR green fluorescence (Platinum SYBR Green qPCR Mix, Invitrogen) detection using an ABI PRISM 7000 cycler (Applied Biosystems). The oligo-nucleotide (Thermo Scientific) concentration was 200 mM, and MgCl concentration was 3 mM. The final reaction volume was 20 µl. Details about the used primer are indicated in Table 5.3.2. A dilution series of *A. tripolium* cDNA pool was used to quantify the transcript abundance in the samples. Amplification fragments were verified by melting temperature, and on a 1.5% Agarose gel (not shown). Transcript abundance was standardized on the relative gene expression of ribulose-1,5-bisphosphate carboxylase/oxygenase large subunit (rbcL).

Table 5.3.1. Details of the selected genes in *A. tripolium.*

Accession	***Gene name***	***Forward primer***	***Reverse primer***	***Fragment size [bp]***	***Fragment melting temp. [°C]***
JN894915	maturase K	GCC AAT CAT TCC CTT GAC TTT CTG	GGA ACA AGA GTA TCA AAC TTC TTA ATA GC	131	77.2
JN891980	rbcL	CTG ATA TCT TGG CAG CAT TTC GAG	CAT CGG TCC ACA CAG TTG TC	98	81.3
AB161375	cysteine protease	CTT GAT CCA ACT GCC AAA CAC G	GCT TTA TTA GCA TCA GCT GGA AGC	119	75.3
AB090885	dehydrin	GAG GAC ATG GCA TCG GAA GTA C	CAT CCT CCG AAG AGC TGG AAC	135	81.2
AB090884	C4 steryl methyl oxidase	GAGATTGCATCTCAATTGCTGGTCTAC	CGG TTG GTG CTG TGT ATT C	133	77.2

Statistical Analysis

Due to the lack of normality and homogeneity, the statistical analysis of the data was based in non-parametric tests. In order to compare the effects of the tested temperature regimes, a Kruskal-Wallis analysis of variance was performed using Statistica Software (Statasoft). Significance was assumed when $p < 0.05$.

Results

PAM fluorometry

Halimione portulacoides exposure to heat and cold spells lead to very similar reductions in both maximum and operational quantum yields (Figure 5.3.1B and D). The same could be observed with the variable fluorescence in both light and dark-adapted leaves (Figure 5.3.1A and C). As for *A. tripolium*, both light and dark-adapted PS II quantum yields were significantly decreased in plants subjected to heat wave treatment (Figure 5.3.1B and D). Nevertheless, a slight decrease could also be observed in individuals under cold wave-treatment. Regarding the variable fluorescence (light adapted), the effect of both treatments is more evident, with significant decreases observable in the individuals exposed to both extreme thermal treatments. As for the dark-adapted F_v the only the individuals exposed to heat wave-treatments showed significant decreases. PS II quantum yields and variable fluorescence showed that both *Spartina* species were insensitive to the cold wave treatment, without any significant changes for both the dark (Figure 5.3.1C and D) and light (Figure 5.3.1A and B) adapted states. However, the heat wave treatment for *S. maritima* led to significant decreases in all the above-mentioned variables. The PS II operational quantum yield (Figure 5.3.1B) in *S. patens* showed a significant increase in the plants subjected to the heat wave treatment. Similar increases were observed for variable fluorescence in both light and dark-adapted states (Figure 5.3.1A and C).

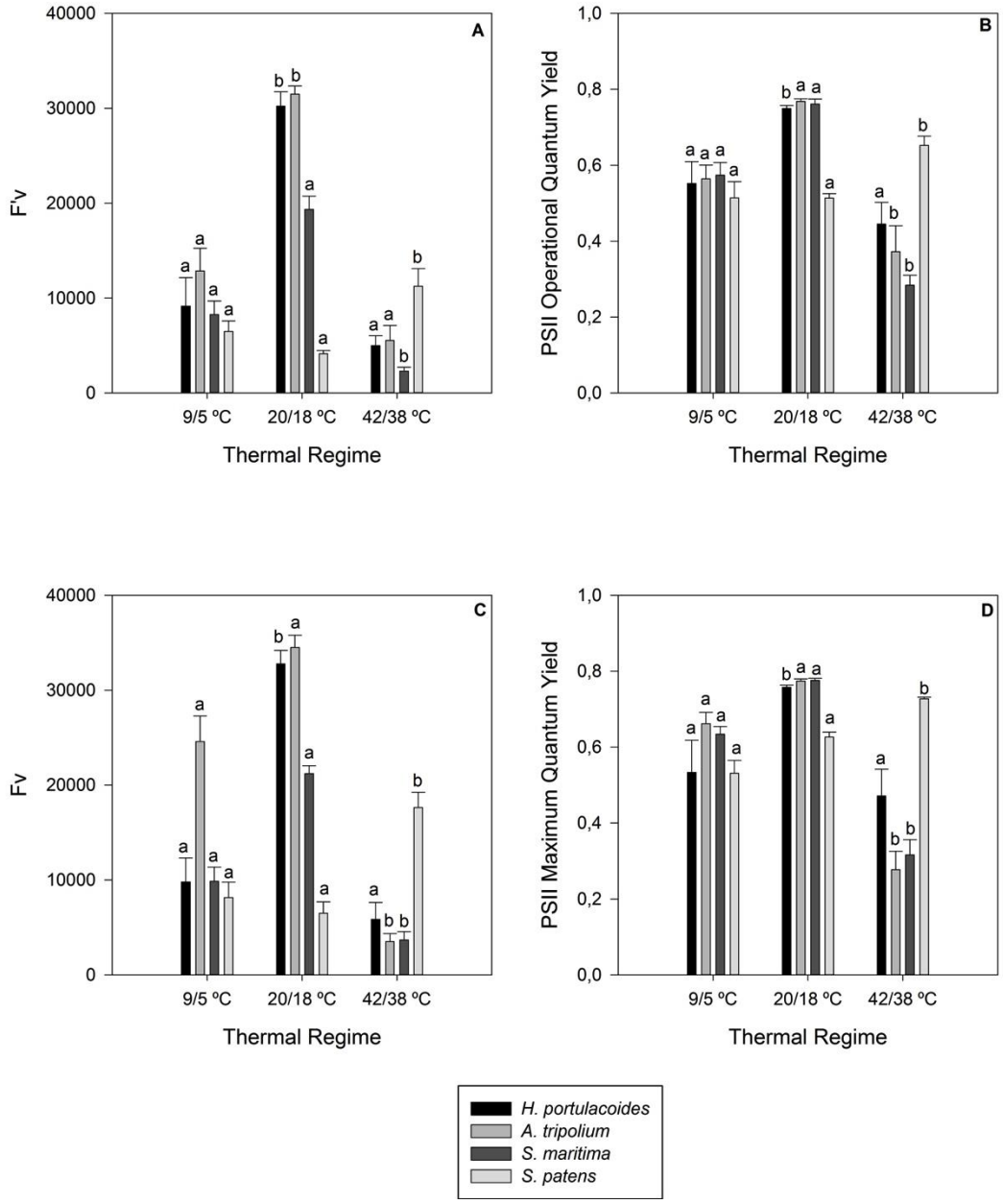

Figure 5.3.1. PS II quantum efficiency and variable fluorescence in light and dark adapted leaves of the four tested halophyte species under normal thermal regimes and after exposure to heat and cold waves (average ± standard error, n=5. Letters indicate significant differences among thermal treatments at $p < 0.05$).

Heat stress led to a marked decrease in *H. portulacoides* electron transport rates (ETR) under different light intensities (Figure 5.3.2), with an expected depletion in the maximum ETR (Figure 5.3.3). Alongside, and similarly to what could be observe in cold stressed individuals, there was also a significant increase ($p < 0.05$) in the onset for light saturation, E_k (Figure 5.3.3). Nevertheless, the photosynthetic

efficiency (α) given by the initial slope of the ETR curves didn't suffer any changes independently of thermal regime applied (Figure 5.3.3). On the other hand, *A. tripolium* individuals upon cold wave and heat wave treatments, showed a very marked decrease in the ETR at all tested light levels (Figure 5.3.2). This is more evidently reflected if RLC-derived parameters are analysed. Both ETR_{max} and α showed significant decreases in individuals subjected to extreme temperature treatments, presenting a rather similar response to both heat wave and cold wave. Due to this similar decrease in α and ETR_{max}, the onset for light saturation was found to be affected in a very similar way among treatments and thus didn't show any significant differences upon the application of different thermal treatments. Comparing both C_4 grasses, the rETR vs PPFD measurements showed that both species have different thermal tolerances (Figure 5.3.2). This is even more obvious if the derived parameters are considered. The α of the plants exposed to cold wave treatment showed two different responses. *Spartina maritima* increased its α under extreme cold, while *S. patens* had low photosynthetic efficiency, similar to that observed for the heat wave treatment (Figure 5.3.3). As for *S. maritima*, the high temperatures lead to a significant decrease of the leaves α and ETR_{max}. In *S. patens* this last parameter was only reduced upon exposure to the heat wave treatment (Figure 5.3.3). The E_k also proved to be negatively affected by heat exposure, showing significant decreases in individuals from both species exposed to heat wave treatment (Figure 5.3.3).

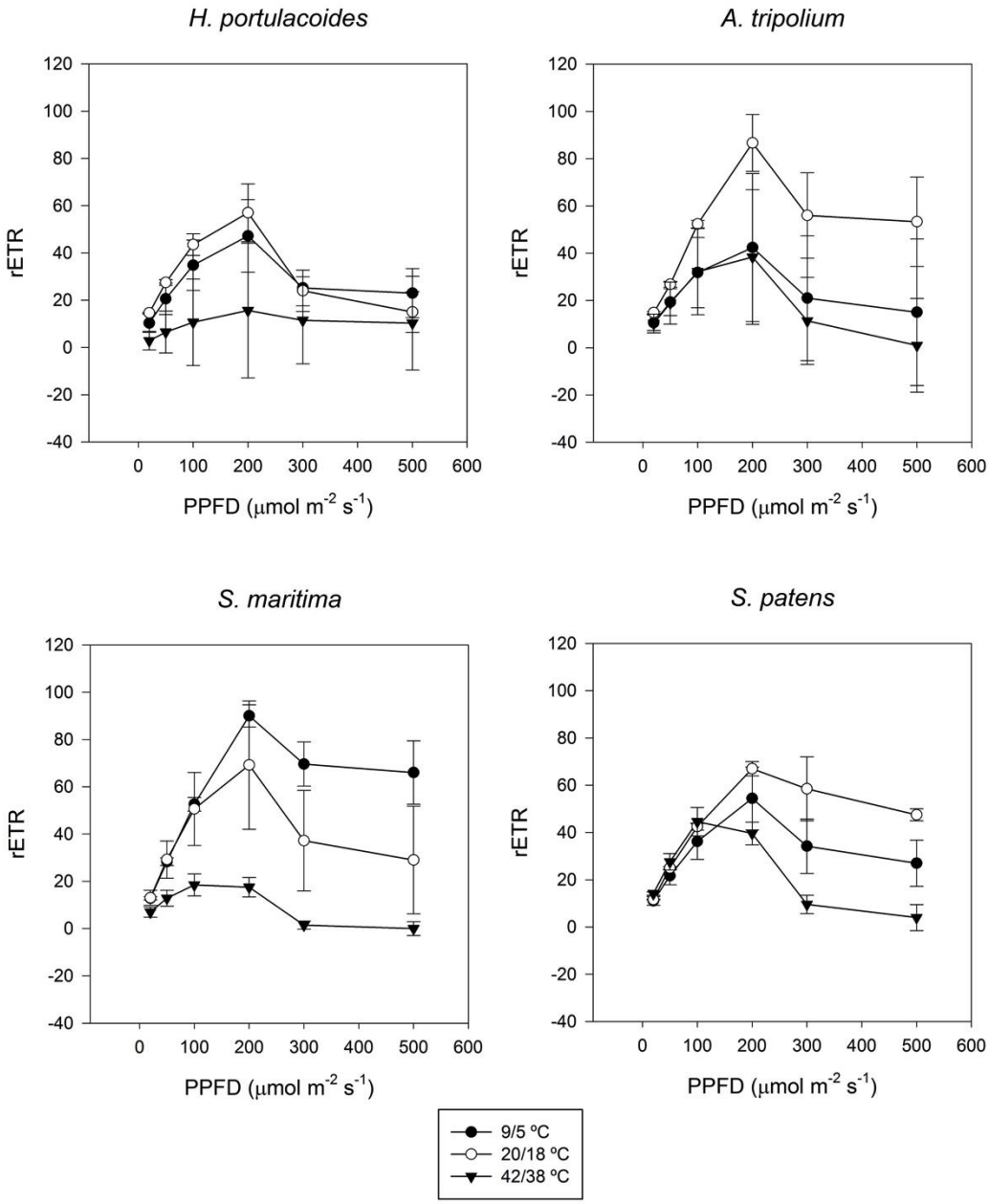

Figure 5.3.2. Relative electron transport rates (rETR) in the dark adapted leaves of the four tested halophyte species under normal thermal regimes and after exposure to heat and cold waves (average ± standard error, n=5).

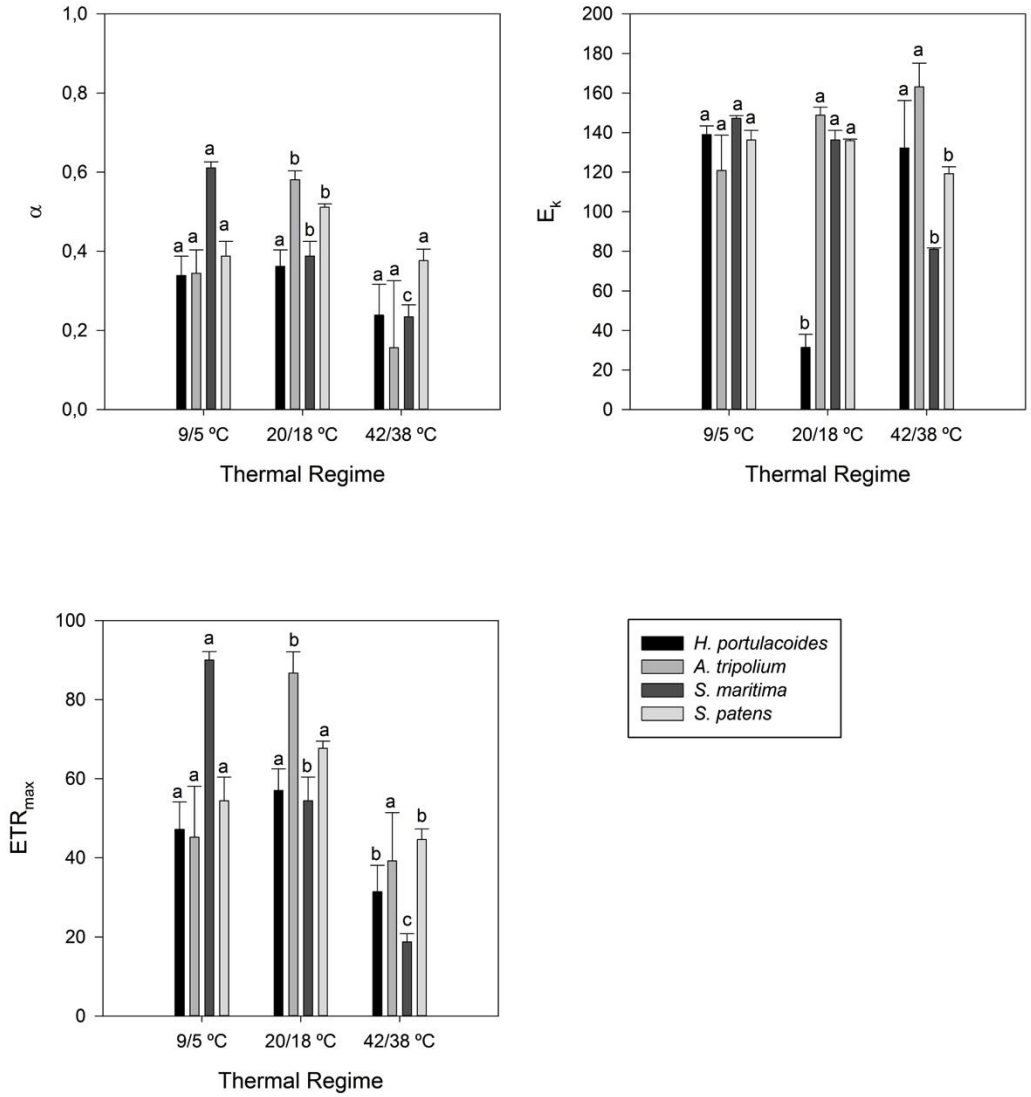

Figure 5.3.3. Photosynthetic efficiency (α), maximum electron transport rate (ETR_{max}) and onset of light saturation (E_k) in the dark-adapted leaves of the four tested halophyte species under normal thermal regimes and after exposure to heat and cold waves (average ± standard error, n=5. Letters indicate significant differences among thermal treatments at $p < 0.05$).

Observing the Kautsky plots from the individuals subjected to the two tested thermal treatments (Fig. 5.3.4), there is an evident decrease of the fluorescence values in both groups of *H. portulacoides* plants exposed to extreme conditions. Also to notice, in both extreme thermal treatments, there is a disappearance of the JIP steps. Similar effects could be observed in *A. tripolium* individuals exposed to extreme temperature treatments. Observing the Kautsky plots from the individuals

subjected to the two tested thermal treatments (Fig. 5.3.4), there is an evident decrease of the fluorescence values more drastic in the individuals exposed to heat wave. Also similar to the observed in *H. portulacoides*, in both extreme thermal treatments, there is a disappearance of the JIP steps being indistinguishable in the plants subjected to cold wave and heat wave. Comparing the Kautsky curves of both *Spartina* species (Fig. 5.3.4), the interspecific differences are evident even under normal temperature conditions. There was a decrease in the fluorescence intensity of the entire Kautsky curves for both species at low temperature. For extreme heat temperatures, *S. patens* showed an increased fluorescence signal, even when compared with the control group, while *S. maritima* showed a drastic decrease under the same experimental treatment.

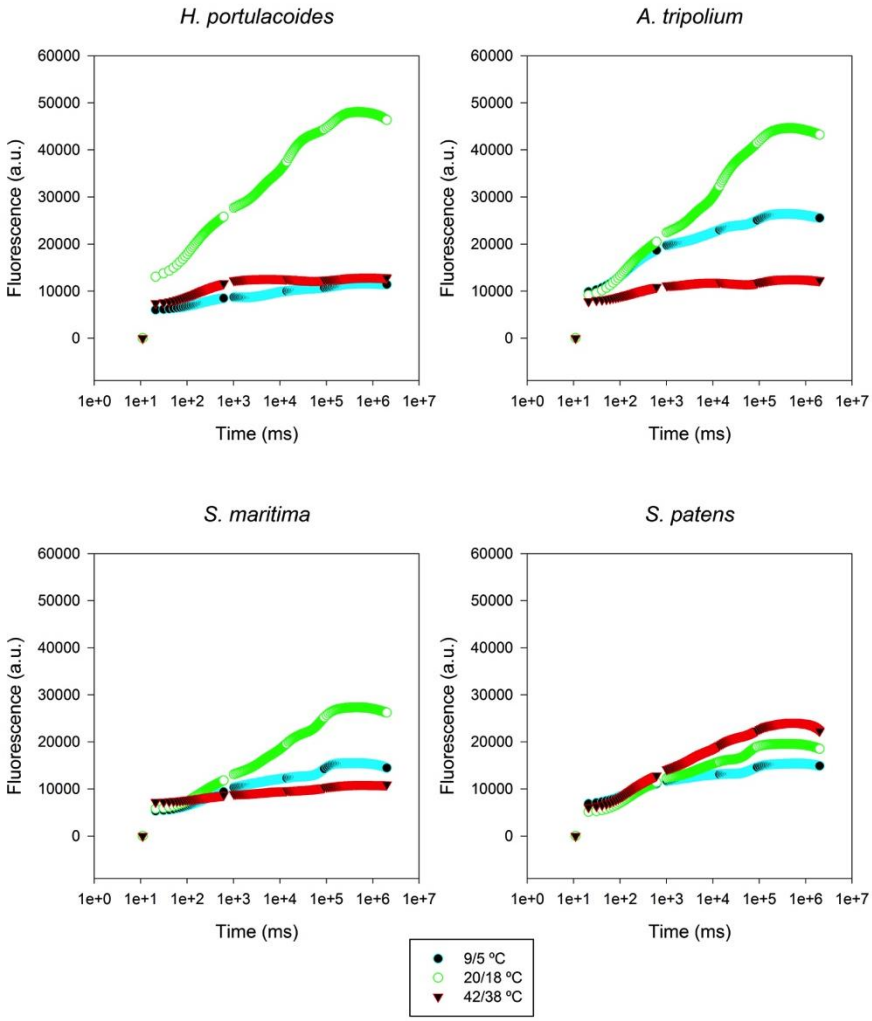

Figure 5.3.4. Kautsky curves in the dark-adapted leaves of the four tested halophyte species under normal thermal regimes and after exposure to heat and cold waves (average, n=5).

Considering the J-step normalized fluorescence in *H. portulacoides* and *A. tripolium* plants, some differences arise specially in the so-called K-step (300 ms), being more pronounced in the plants exposed to cold treatment (Fig. 5.3.5).

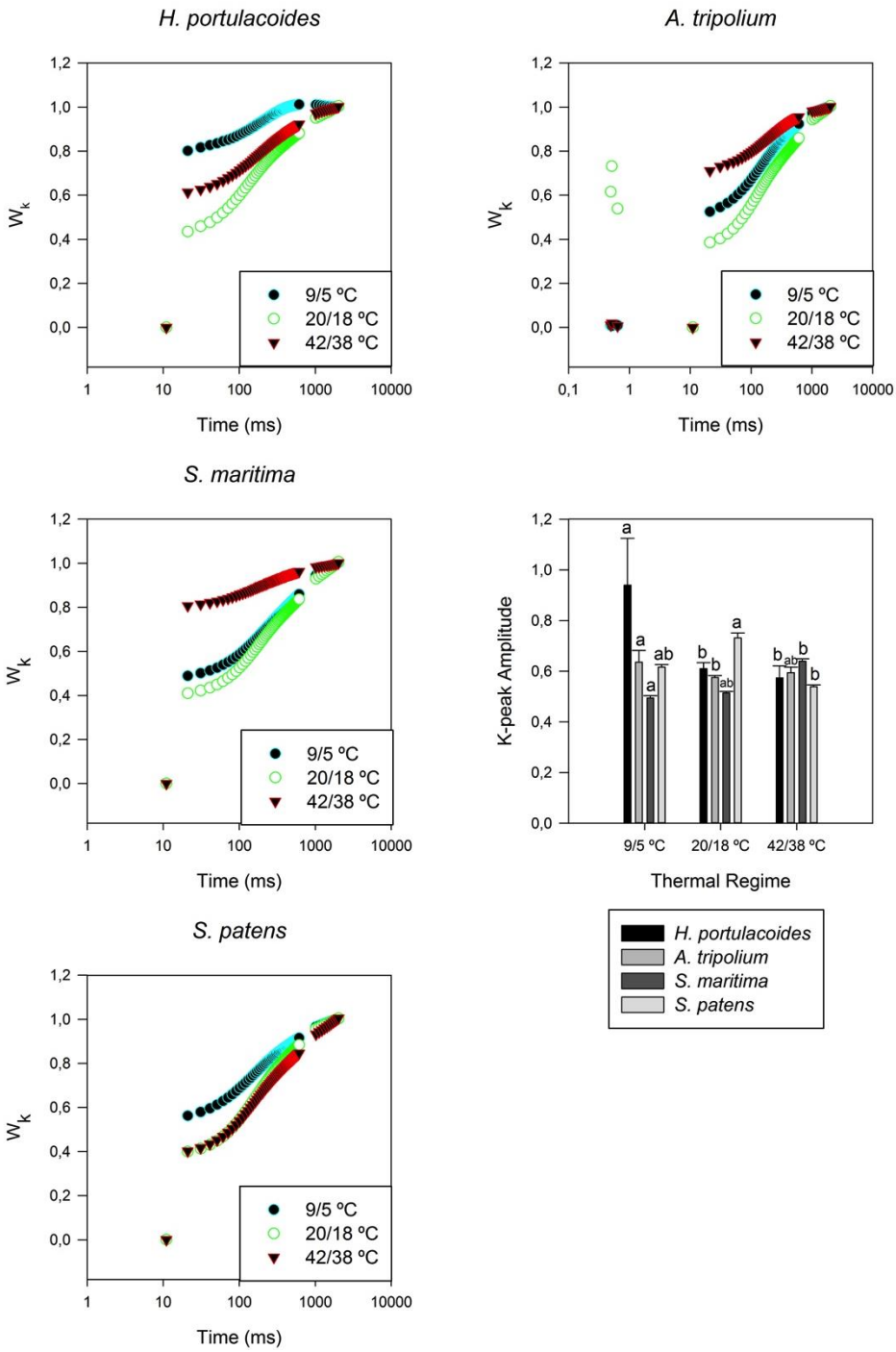

Figure 5.3.5. J-step normalized fluorescence and K-step amplitude in the dark-adapted leaves of the four tested halophyte species under normal thermal regimes and after exposure to heat and cold waves (average ± standard error, n=5. Letters indicate significant differences among thermal treatments at $p < 0.05$).

The amplitude of the K-phase (W_K) was severely increased ($p < 0.05$) in the plants exposed to cold treatment. In *S. maritima*, the exposure to heat wave treatment seems to induce an increase in the fluorescence in all phases when compared to the control (Fig. 5.3.5), especially if the normalized fluorescence values are analysed (Fig. 5.3.5). On the other hand, in *S. patens* under low and high temperature treatments presented antagonistic behaviours, with the cold wave treatment inducing fluorescence values above the verified in the control group (Fig. 5.3.5). In *S. maritima* the amplitude of the K-step, although not different from the control, was significantly increased during the heat treatment, if compared with the verified in plants exposed to the cold wave treatment. Oppositely, *S. patens* showed a reduction in the K-step amplitude upon exposure to heat wave treatment.

Interpreting these curves in terms of energetic balance, several differences could be observed (Fig. 5.3.6). Both C_3 plants exhibited the exact same trends in all the described parameters. This way, in *H. portulacoides* and *A. tripolium*, both the probability that an absorbed photon will move an electron into the ETC (Fig. 5.3.6, φ_{E0}) and the probability that a PS II trapped electron can be transported from Q_A to Q_B (Fig. 5.3.6, ψ_0) were severely reduced in both heat treatment and cold treatments. This was also accompanied by a decrease in the oxidized quinone pool size (Fig. 5.3.7), in both species test groups. Concomitantly, this resulted in a decrease in the maximum yield of primary photochemistry (Fig. 5.3.6, φ_{P0}). In heat treatment treated plants there was also a significant increase in the quantum yield of the non-photochemical reactions (Fig. 5.3.6, φ_{D0}). As for the connectivity between PS II antennae (inversely proportional to P_G), there was an evident decrease in the individuals exposed to cold treatment (Fig. 5.3.7). Regarding the M_o, there was also an enhancement effect driven by the exposure to heat treatment (Fig. 5.3.7). The same could be observed in which concerns the efficiency with which an electron can move from the reduced intersystem electron acceptors to the PS I end electron acceptors (Fig. 5.3.7). As for the C_4 grasses some differences could be found from the observed in *H. portulacoides* and *A. tripolium*. Both *Spartina* species showed a reduction in the quinone pool transport yield of a PS II trapped electron upon exposure to cold stress (Fig. 5.3.6). The same could be verified for the photon-

induced electron transport in *S. patens* (Fig. 5.3.6). As for *S. maritima*, this value was only reduced in the plants exposed to heat stress. Consistently, the overall maximum yield of the primary photochemistry in *S. maritima* also showed significant decreases in the plants exposed to heat wave treatment, while in *S. patens* this reduction was more markedly verified in plants exposed to cold wave (Fig. 5.3.6). This can be confirmed by the increase in the quantum yield of the non-photochemical reactions observed in *S. maritima* individuals exposed to heat stress (Fig. 5.3.6). Furthermore, in *S. patens*, the size of the oxidized quinone pool was also affected by the thermal treatments (Fig. 5.3.7). This parameter was severely reduced in both species upon exposure to both thermal stresses. In *S. maritima* the P_G value was considerably increased in individuals exposed to heat stress, indicative of a loss of connectivity between the PS II antennae. Once again, the behaviour exhibited by *S. patens* points out to a contrary feedback towards the thermal environment, presenting increased PS II antennae connectivity under cold exposure. Regarding the net rate of PS II reaction centre closure, both thermal treatments induced a M_0 increase in both C_4 species, although for *S. patens* individuals subjected to heat wave treatment, this increase was not significantly higher than the control (Fig. 5.3.7). Considering the electron movement efficiency from the reduced intersystem to the PS I electron acceptors, some changes could also be perceived (Fig. 5.3.7). In *S. maritima* this efficiency was increased in plants exposed to both extreme thermal environments. On the other hand, in *S. patens* there were no detectable changes under both experimental treatments, in comparison with the control group. Still, the exposure to heat wave led to a decrease in the δR_0 if compared with the values verified in the plants exposed to cold stress.

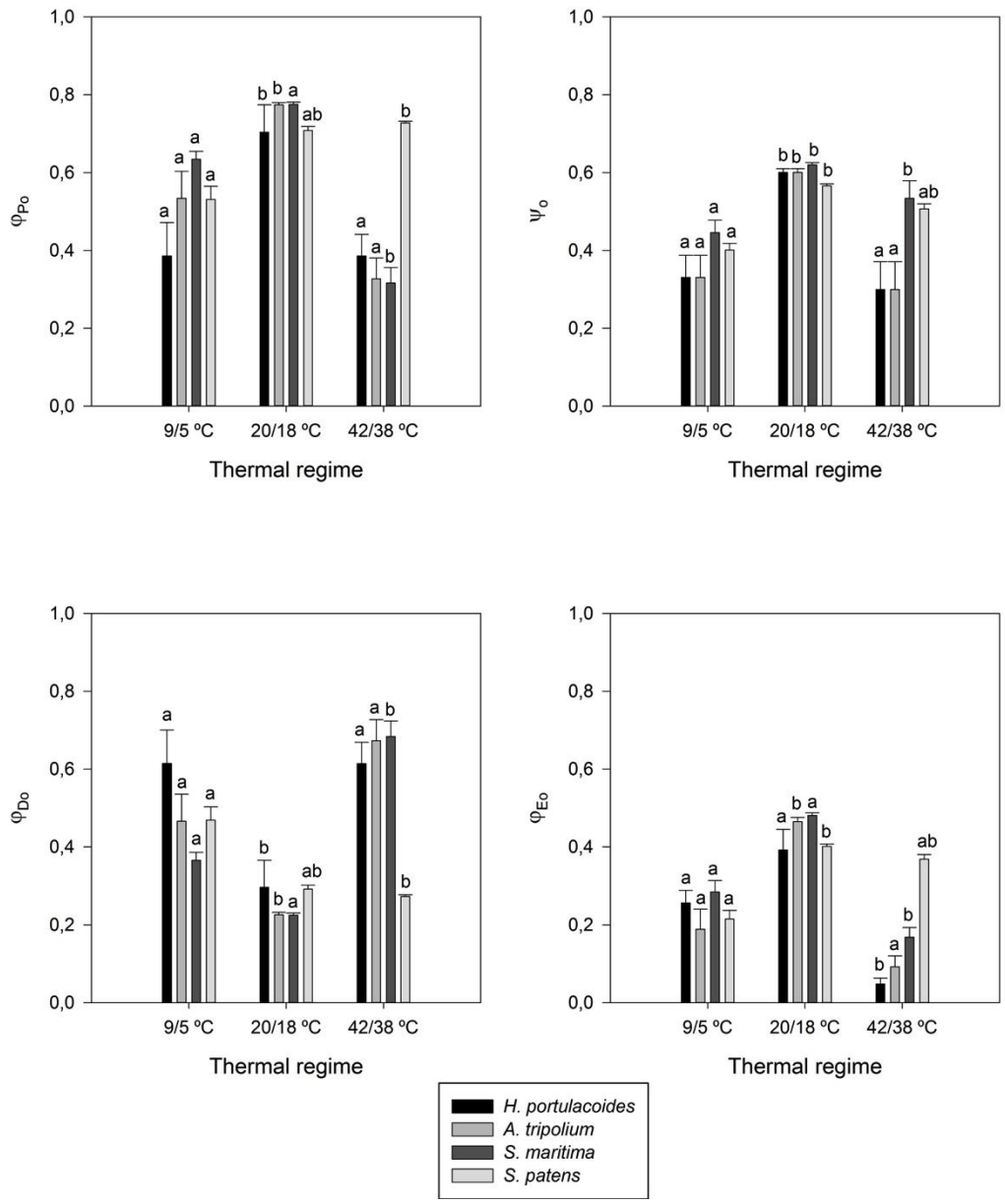

Figure 5.3.6. Probabilistic electron flows in the dark-adapted leaves of the four tested halophyte species under normal thermal regimes and after exposure to heat and cold waves (average ± standard error, n=5. Letters indicate significant differences among thermal treatments at $p < 0.05$).

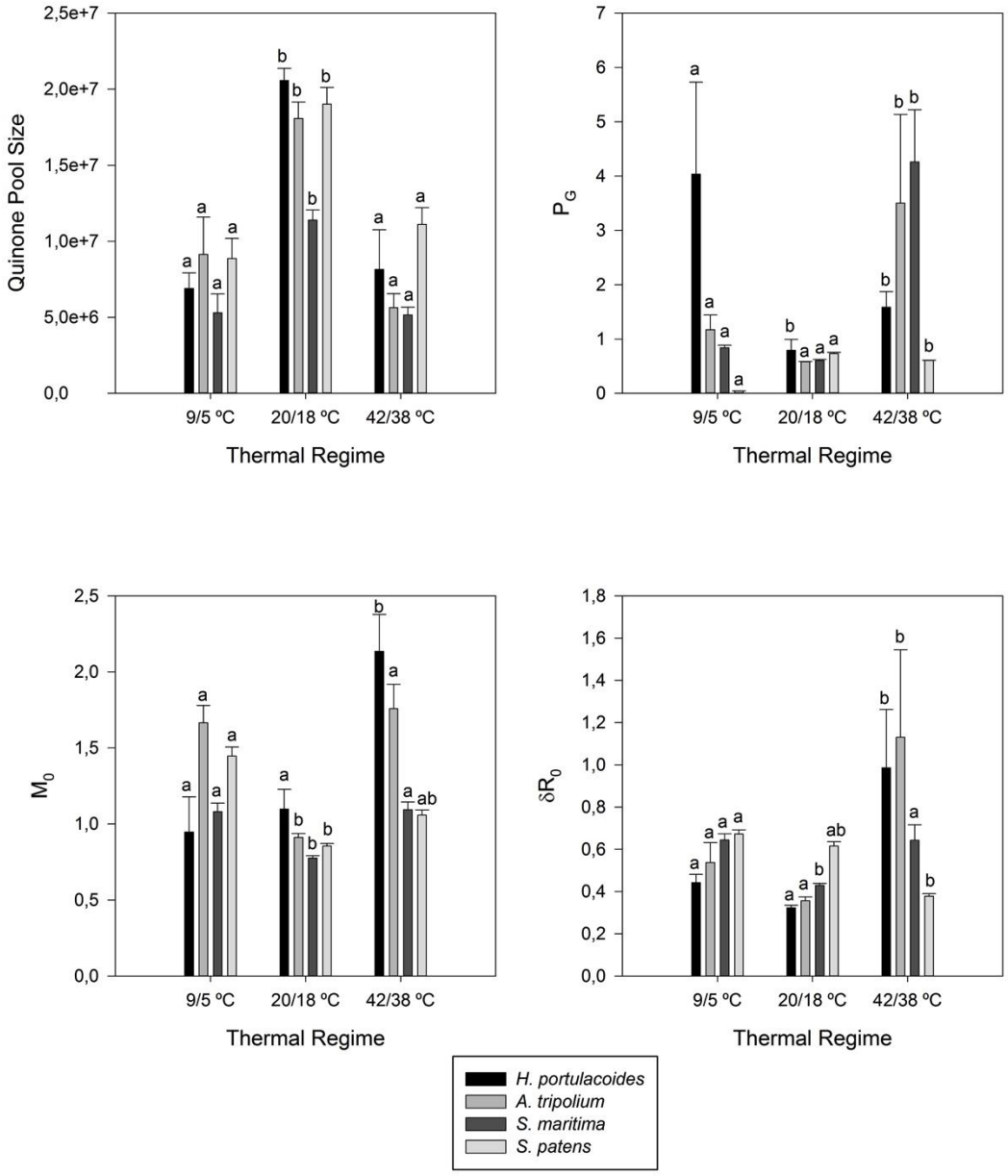

Figure 5.3.7. OJIP derived parameters in the dark-adapted leaves of the four tested halophyte species under normal thermal regimes and after exposure to heat and cold waves (average ± standard error, n=5. Letters indicate significant differences among thermal treatments at $p < 0.05$).

Regarding the energetic fluxes within the chloroplasts of *H. portulacoides* (Fig. 5.3.8), it was possible to observe a significant reduction of the absorbed energy flux in the plants exposed to heat and cold treatment, concomitant with a decrease in the number of reaction centres available for reduction, and thus in the amount of energy trapped per leaf cross section. On the other hand, the transported energy

flux was more severely reduced in the individuals exposed to extreme heat treatment. The amount of dissipated energy didn't show significant differences in both thermal stress treatments, while compared with the control group. In sum, all these fluxes can be translated into a significant reduction in the performance index (PI) of the individuals exposed to heat treatment. In *A. tripolium* some similar patterns could be observed. Analysing the energetic fluxes on a leaf cross-section basis there was also an evident decrease in the number of reaction centres available for light harvesting resulting from extreme temperature regimes. Although this fact, these individuals showed a maintenance of the absorbed light energy flux. Besides this difference *A. tripolium* individuals exposed to heat wave-treatment showed a similar decrease in the ability to trap this energy. Consequently, this resulted in an also very low amount of energy transported along the electronic transport chain. Although the maintenance of the TR/CS in cold wave exposed individuals, there was also a significant decrease in their ET/CS energy flux. Both these decreases resulted in a significant increase in the dissipated energy flux in both groups of individuals exposed to extreme temperature treatments. As above-mentioned for *H. portulacoides*, these changes in the energetic fluxes also resulted in a significant decrease of the PI in both *A. tripolium* test groups. Applying the same integrative index of performance to both C_4 grasses different patterns were also attained. *Spartina maritima* exhibited a significant decrease in the PI of the plants exposed to both extreme thermal treatments. Oppositely, in *S. patens* this reduction was only evident in the plants subjected to cold wave treatment. Although no differences were observed in the absorbed energy flux, there was a significant decrease in the number of active reaction centres in *S. maritima* plants exposed to heat stress and in *S. patens* individuals subjected to cold stress. Alongside this depletion, *S. maritima* also showed a decrease in the trapped energy flux and consequent increase in the dissipated energy flux. On the other hand, the same thermal environments didn't affect *S. patens* trapping ability, although cold wave treatment affected negatively the transported energy flux with a consequent increase in the energy dissipation.

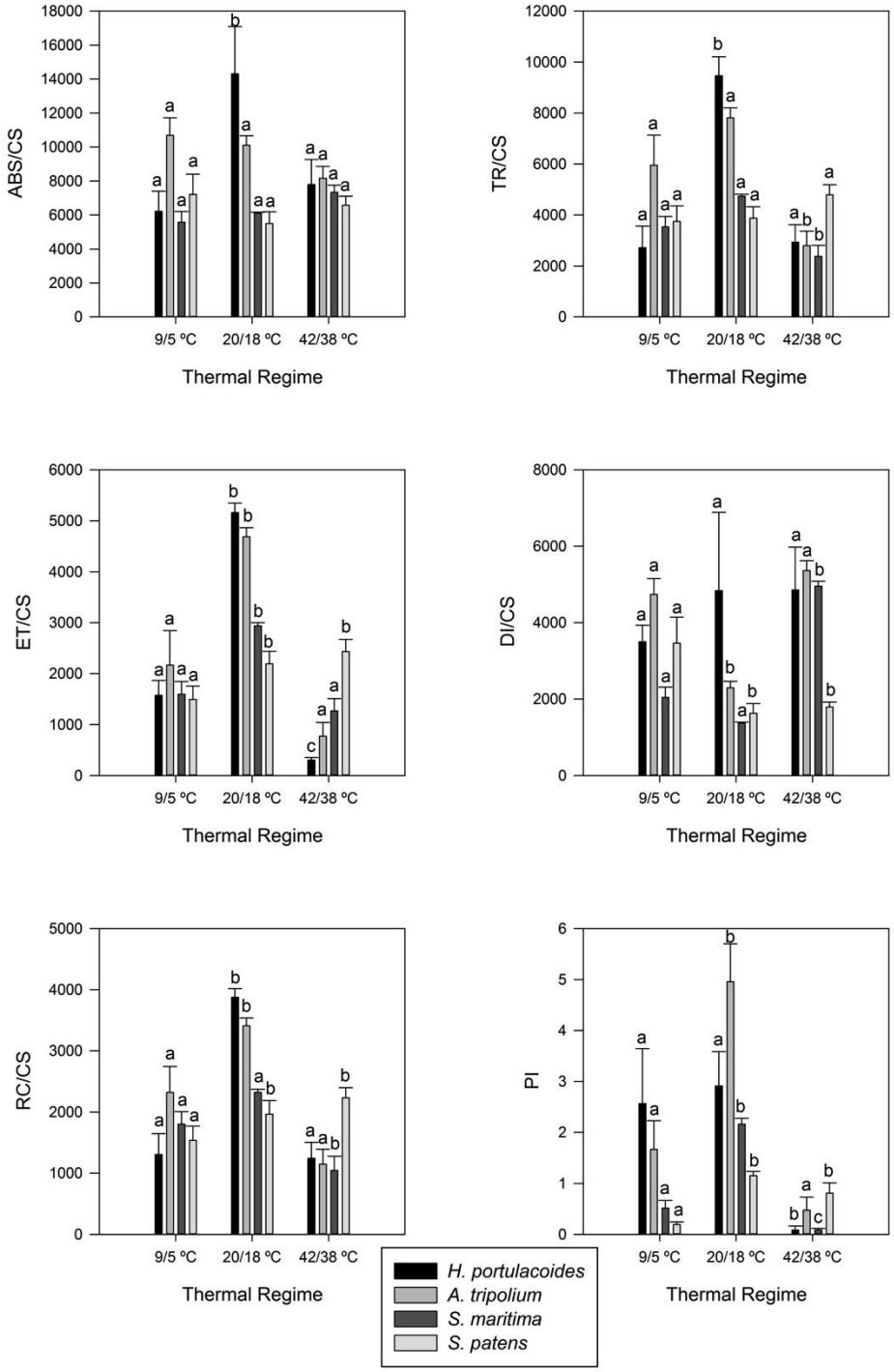

Figure 5.3.6. Phenomological energetic parameters in the dark-adapted leaves of the four tested halophyte species under normal thermal regimes and after exposure to heat and cold waves (average ± standard error, n=5. Letters indicate significant differences among thermal treatments at $p < 0.05$).

Pigment concentrations

Regarding the leaf pigment concentration in *H. portulacoides* some differences could be detected in the individuals exposed to different thermal treatments (Table 5.3.2). Plants exposed to cold treatment exhibited a significant increase in its leaf chlorophyll a and auroxanthin content. In contrast, zeaxanthin content in these individuals was found to be significantly lower than control and heat-treated plants. Heat treatment exposed individuals also exhibited an increase in their auroxanthin content alongside with a significant decrease in their violaxanthin content. All the remaining analysed pigments maintained its concentrations independently of the applied thermal treatment. Still, these small changes affect some pigment ratios with physiological meaning. Concerning the chlorophyll a/b ratio, there was also an increase in this parameter in the individuals exposed to cold treatment, while the plants exposed to heat stress had this ratio significantly reduced. As for the xanthophyll cycle, evaluated throughout the DES index, it was possible to observe a significant increase in this index in the leaves of the heat-treated plants. Regarding the pigment profile in *A. tripolium* exposed to cold wave treatment, there was a marked decrease in their chlorophyll a and b content. On the carotenoid side, the most abrupt decrease was detected in β-carotene, lutein, violaxanthin and zeaxanthin concentrations. As observed in *H. portulacoides* it is also to notice the high increase in auroxanthin concentrations in the individuals exposed to this cold treatment. All these changes lead to a decrease in the total chlorophyll and carotenoid content. On the other hand, the plants exposed to heat wave treatment presented a very distinct pigment profile. The leaves collected from these individuals presented only a decrease in the antheraxanthin concentration. Comparing both *Spartina* species some differences were also found, similar to what was above described for other photochemical parameters. There was a significant increase in the concentration of chlorophyll a in *S. maritima* plants exposed to extreme heat. On the other hand, in *S. patens* this was only observed in the plants exposed to the cold treatment. This treatment also leads to changes in the chlorophyll b concentrations, although in opposite directions in both species. Regarding the carotenoids, with the exception of β-carotene and lutein, all the considered photo-protective pigments showed significant changes in the individuals

exposed to thermal stresses. Auroxanthin content was higher in *S. patens* leaves exposed to the cold wave treatment. On the other hand, *S. maritima* individuals subjected to heat wave treatment showed a significant decrease in the content of this pigment. These same trends were observed in both species for antheraxanthin leaf content. Violaxanthin content in *S. maritima* was insensitive to the applied thermal treatments but for *S. patens* the pigment increased in concentration in the plants subjected to cold stress. Finally, the last of the xanthophyll cycle pigments, zeaxanthin, also showed specific changes. In *S. maritima* the exposure to extreme thermal stresses lead to a decrease in the leaf zeaxanthin content, while in *S. patens* only the exposure to extreme cold lead to an increase in this pigment content. The de-epoxidation state and the chlorophyll a/b ratio, in *S. patens* didn't show any variation under any of the tested treatments. As for the DES, all *S. maritima* individuals exposed to thermal stress showed a decrease in this index. Concerning the chlorophyll a/b ratio both thermal treatments induced a significant increase in this ratio.

Table 5.3.2. Leaves pigment concentration (μg g^{-1} FW) and ratios in the leaves of the four tested halophytes under normal thermal regimes and exposed to heat and cold waves (average ± standard error, n=5. Letters indicate significant differences among thermal treatments at $p < 0.05$).

	Chl a	Chl b	Auroxanthin	Antheraxanthin	β-carotene	Lutein	Violaxanthin	Zeaxanthin	DES	Chl a/b
H. portulacoides										
9 / 5 °C	378.98 ± 13.15^{a}	117.15 ± 4.18^{a}	5.58 ± 0.90^{a}	12.37 ± 3.16^{a}	19.84 ± 6.94^{a}	20.78 ± 6.03^{a}	15.53 ± 5.35^{a}	34.72 ± 11.68^{a}	0.76 ± 0.01^{a}	3.24 ± 0.00^{a}
20 / 18 °C	277.74 ± 63.28^{b}	93.82 ± 17.51^{a}	2.06 ± 1.00^{b}	12.49 ± 2.97^{a}	20.02 ± 5.77^{a}	20.63 ± 3.87^{a}	15.07 ± 1.73^{a}	165.20 ± 7.06^{b}	0.71 ± 0.06^{a}	2.92 ± 0.16^{b}
42 / 38 °C	237.39 ± 82.15^{b}	101.50 ± 34.84^{a}	9.95 ± 5.06^{a}	11.48 ± 2.83^{a}	28.40 ± 8.97^{a}	19.95 ± 8.61^{a}	6.09 ± 2.48^{b}	123.74 ± 28.72^{b}	0.91 ± 0.03^{b}	2.32 ± 0.10^{c}
A. tripolium										
9 / 5 °C	120.42 ± 16.11^{a}	40.77 ± 4.66^{a}	5.44 ± 0.47^{a}	8.42 ± 1.01^{a}	3.46 ± 1.02^{a}	5.51 ± 1.17^{a}	1.34 ± 0.06^{a}	14.51 ± 2.61^{a}	0.94 ± 0.01^{a}	2.96 ± 0.19^{a}
20 / 18 °C	296.22 ± 39.33^{b}	104.57 ± 11.01^{b}	0.00 ± 0.00^{b}	9.67 ± 0.19^{a}	15.36 ± 1.76^{b}	14.69 ± 1.64^{b}	14.37 ± 2.57^{b}	33.46 ± 3.23^{b}	0.75 ± 0.02^{a}	2.82 ± 0.09^{a}
42 / 38 °C	290.86 ± 46.56^{b}	100.79 ± 16.90^{b}	0.45 ± 0.23^{b}	0.45 ± 0.23^{b}	23.01 ± 0.74^{b}	21.84 ± 1.41^{b}	17.41 ± 3.00^{b}	42.91 ± 5.33^{b}	0.77 ± 0.02^{a}	2.89 ± 0.10^{a}
S. maritima										
9 / 5 °C	397.3 ± 24.0^{a}	132.2. ± 6.1^{a}	10.8 ± 4.4^{a}	36.7 ± 1.9^{a}	45.2 ± 0.2^{a}	50.4 ± 1.2^{a}	51.3 ± 1.4^{a}	107.3 ± 10.3^{a}	0.72 ± 0.05^{a}	3.00 ± 0.05^{a}
20 / 18 °C	394.9 ± 30.0^{a}	226.4 ± 13.4^{b}	19.6 ± 1.2^{a}	35.0 ± 2.1^{a}	62.9 ± 0.1^{a}	55.4 ± 1.7^{a}	37.1 ± 3.5^{a}	185.9 ± 2.9^{b}	0.86 ± 0.01^{b}	1.74 ± 0.04^{b}
42 / 38 °C	595.7 ± 10.7^{b}	227.9 ± 9.6^{b}	0.0 ± 0.0^{b}	14.7 ± 3.1^{b}	47.0 ± 0.9^{a}	43.7 ± 0.8^{a}	41.6 ± 2.9^{a}	103.9 ± 2.1^{a}	0.74 ± 0.01^{a}	2.63 ± 0.16^{a}
S. patens										
9 / 5 °C	742. 1 ± 82.6^{q}	270.5 ± 12.5^{a}	57.2 ± 6.2^{a}	47.3 ± 2.0^{a}	26.8 ± 8.0^{a}	26.2 ± 1.1^{a}	45.4 ± 3.7^{s}	139.9 ± 5.5^{s}	0.80 ± 0.01^{a}	2.73 ± 0.18^{a}
20 / 18 °C	238.2 ± 23.9^{B}	106.7 ± 7.3^{b}	1.3 ± 0.8^{b}	11.2 ± 4.5^{b}	35.4 ± 5.0^{a}	24.0 ± 1.8^{a}	24.1 ± 9.2^{b}	79.9 ± 8.2^{b}	0.79 ± 0.09^{a}	2.23 ± 0.17^{a}
42 / 38 °C	309.4 ± 55.4^{B}	112.5 ± 16.7^{B}	2.2 ± 1.9^{b}	13.1 ± 4.2^{b}	37.2 ± 6.1^{a}	31.2 ± 4.0^{a}	18.3 ± 4.3^{b}	70.8 ± 12.5^{b}	0.82 ± 0.04^{a}	2.73 ± 0.14^{a}

Oxidative stress biomarkers

Heat and cold treated plants exhibited differential anti-oxidant enzyme patterns of activity (Fig. 5.3.9). At this level the response was not similar among C_3 plants like it was observed for the majority of the photochemical parameters. In *H. portulacoides*, while cold treatment enhanced the leaf CAT, APx and SOD activities, in heat-treated plants only APx and SOD showed a significant increase. Guaiacol peroxidase activity was found to be insensitive to the tested thermal treatments. Considering the leaf protein content in the different test groups, a significant reduction could be observed in the plants exposed to cold treatment. As for the membrane damage, here evaluated by the leaf MDA concentration, there were no significant changes among the tested groups. On the other hand, in *A. tripolium*, cold wave-treatment enhanced significantly CAT and GPx activity while inhibiting APx and SOD. Heat wave didn't affect the enzymatic activity profile. Both these mechanisms were accompanied by a reduction of the protein content in both the individuals exposed to both thermal treatments. As for membrane damage, there was an evident increase in the accumulation of lipid peroxidation products, namely MDA, in the individuals exposed to high temperatures. As for the C_4 grasses another pattern of anti-oxidant activity was detected. While comparing with the control group, CAT showed an enhanced activity in *S. maritima* plants exposed to both extreme thermal treatments. Still in *S. maritima*, cold and heat wave treatments both lead to a decrease in the APx activity. As for GPx, this enzyme had its activity decreased only in the native specie exposed to cold stress. SOD showed a decrease in its activity in *S. maritima* individuals exposed to heat stress. No changes in the protein content could be detected in these individuals. Regarding *S. patens*, there was no effects of the tested treatments in CAT activity, although both APx and SOD had its activity greatly increased during cold stress. As for GPx in *S. patens*, both thermal treatments lead to a decrease in its activity. The total protein content in *S. patens* individuals was also reduced in the plants exposed to cold wave treatment.

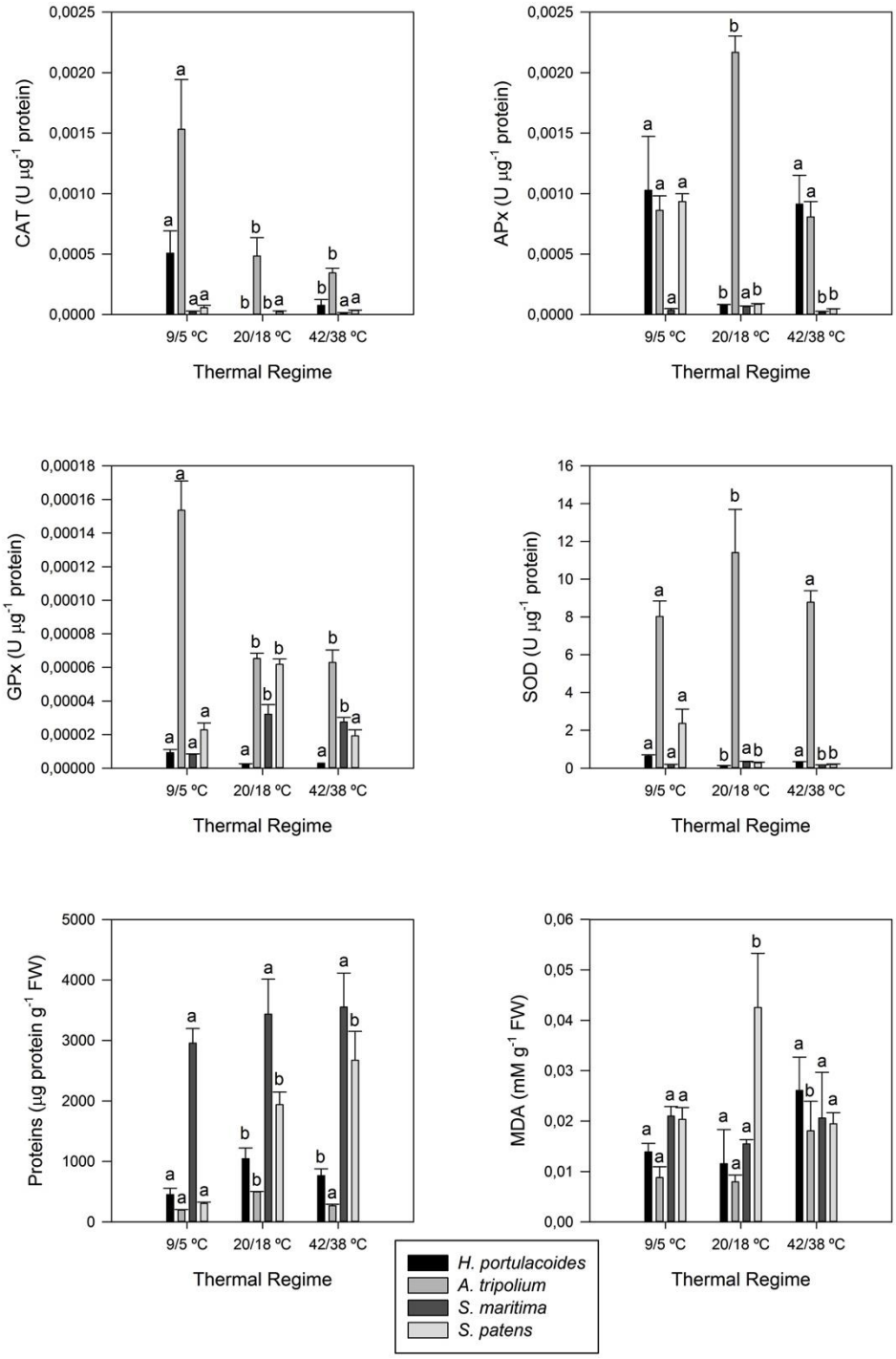

Figure 5.3.9. Oxidative stress biomarkers and protein content in the leaves of the four tested halophyte species under normal thermal regimes and after exposure to heat and cold waves (average ± standard error, n=5. Letters indicate significant differences among thermal treatments at $p < 0.05$).

Gene Expression in the model halophyte A. tripolium

Gene expression values were standardized on the Rubisco (RbLC) gene expression (Fig. 5.3.10).

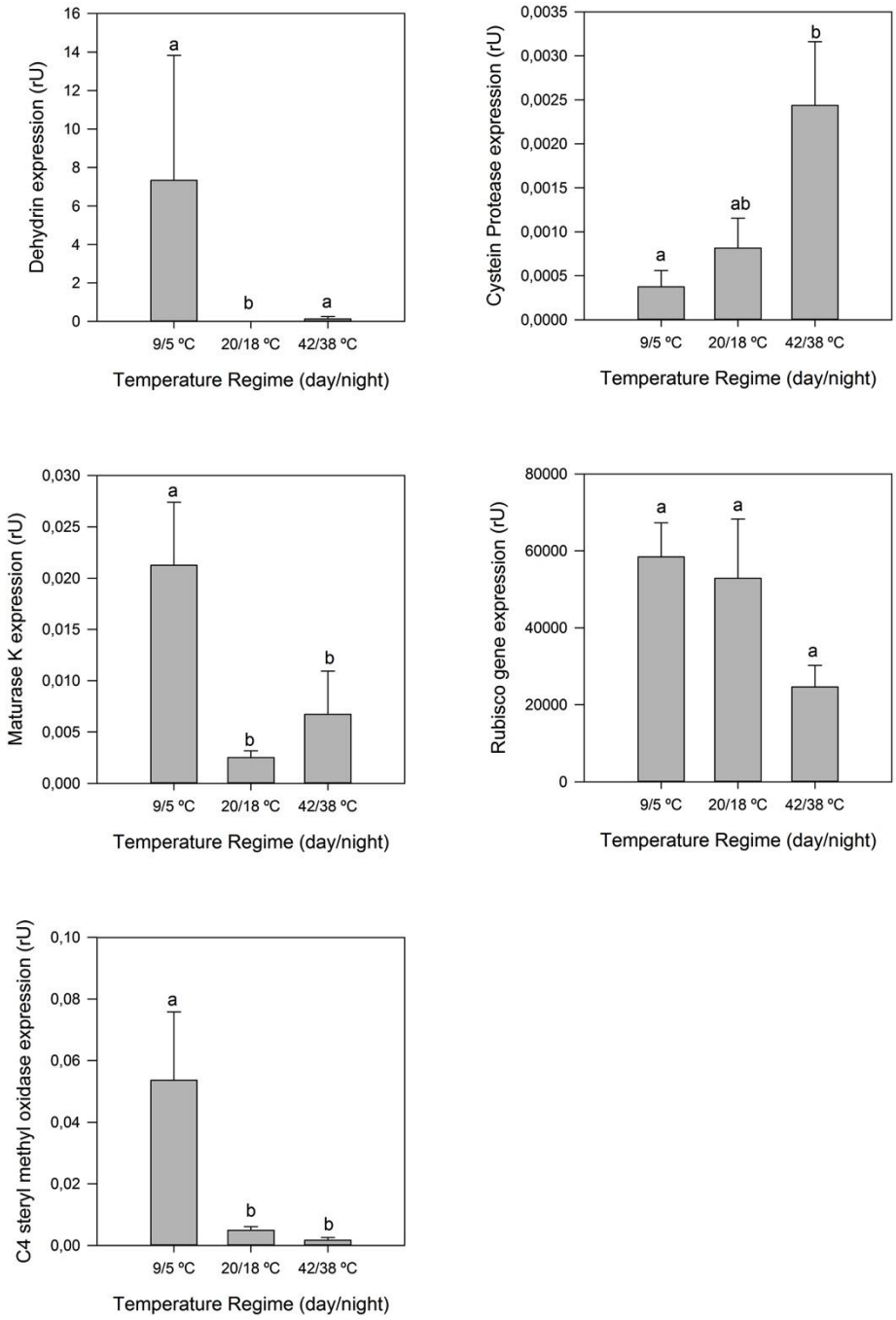

Figure 5.3.10. Normalized gene expression in leaves of *A. tripolium* under normal thermal regimes and when exposed to heat and cold waves (average ± standard error, n=5. Letters indicate significant differences among thermal treatments at $p < 0.05$).

The repression of RbLC gene expression in heat wave samples by an average fold change of 0.47 compared to the control was not significant. Dehydrin, ITS-1 ribosomal DNA, Maturase K and C4 steryl methyl oxidase gene expressions were significantly induced during the cold wave treatment. Dehydrin expression in heat wave samples was significantly higher compared to the control, but in average on a lower level compared to the cold wave samples. Cystein protease gene expression was induced during the heat wave treatment, but only significantly compared to a slightly repression in the cold wave treatment.

Discussion

The latest IPCC report on climatic changes (IPCC, 2014) points out extreme thermal events as major stressors to the Mediterranean environments, imposing critical changes to the ecosystems. Under these circumstances it is fair to assume that the plants best adapted to harsh environments such as salt marshes, where they are constantly subjected to abiotic stresses, will be more fit to this new climatic reality (Duarte *et al*., 2012, 2013a, 2014a and 2014b). Still, these recent on-going environmental changes tend to modify the climatic habitats available for colonization within ecosystems. Salt marshes are no exception to this. In these environments species distribution is mostly modulated by marsh elevation, which is a key factor affecting the sediment flooding, redox potential, pH and salinity. However, air temperature affects all the marsh indiscriminately. In recent years, extremely high and low temperature events have become more frequent and intense in the Mediterranean area. Although these events only last for 2-4 days, the species resistance and resilience during these periods shape their ability to maintain their biomass and therefore their colonization capacity. Considering this becomes important to address the photobiological traits that underlie the species primary production. Beyond these common responses, the exposure of the individuals to extreme thermal environments, have also serious implications on its photobiology, and thus on its primary production. C_3 plants are known to be highly affected by the surrounding thermal environment (Sage and Kubien, 2007). These plants electron transport capacity is highly affected by shifts from its thermal optimum, where a

strong decline in the electron transport capacity can cause the RuBP regeneration capacity to fall below the Rubisco capacity (Sage and Kubien, 2007).

During heat stress, both C_3 halophytes and the native C_4 grass *S. maritima* showed a highly significant decrease in both maximum and operational quantum yield. Although these differences are different between thermal treatments on a global scale, some similarities arise when the processes underlying light harvesting are investigated. Compared to the control group, both heat and cold treated individuals had their photosynthetic efficiency decreased, as indicated by a decrease in the maximum electron transport rates. This was mainly affected by decrease connectivity between PS II and its antennae, as shown by P_G (Strasser and Stirbet, 2001; Panda *et al*., 2006). Reduction of the connectivity between the antennae of the PS II units causes impairment and disruption of the energetic transport. Decrease in fluorescence at the J, I, and P level of the Kautsky curves point on either donor or acceptor site limitation at PS II (Zushi *et al*., 2012). In fact, the damage to the PS II donor side has a characteristic appearance of a K-peak in the OJIP curves at about 300 ms (Strasser and Stirbet, 2001; Chen and Cheng, 2009; Strasser *et al*., 2004). The K-step under heat stress is related to damages at the oxygen-evolving complex of PS II (Srivastava *et al*., 1997). Increased amplitudes of the K-step were pronounced in plants exposed to cold wave treatment, indicating a low thermo-stability of the oxygen evolving complexes (OECs) (Wen *et al*., 2005). On the other hand, *S. patens* OECs appear to be temperature insensitive. In both thermal treatments, all species showed a significant increase in the rate of RC closure, as indicated by an increase in M_0. Similar observations were made in pea leaves after exposure to 40 °C and 44 °C (Stefanov *et al*., 2011) and in apple peel after exposure to 44 °C (Chen and Cheng, 2009). Crossing this information with the light absorption energy flux and number of reaction centres available for reduction per leaf cross section, it is possible to conclude that the maintenance in the light absorption energy flux is due mainly to an increased net rate of RC centre closure. This mechanism appears as a counteractive measure to compensate the reduced number of RC, rather than to an increase in the Q_A to Q_A^- reduction rates as observed in similar studies (Zushi *et al*., 2012). Although the similarity in the counteractive measures among species, in *S. patens* the number of reaction centres available for reduction per leaf cross section, was more

negatively affected in plants subjected to cold stress. This was recently confirmed by increasing the probability of electrons being trapped at PS II. In addition, the quinone pool size - indicated by the reduction of the area above the Kautsky curve – was reduced in all species. All these data indicate that both cold and heat stress reduced the maximum yield of the primary photochemistry. Consequently, the conversion of physical to chemical energy decreased, while the proportion of non-photochemical energy quenching increased. Similar observations have been made in several halophytes subjected to abiotic stresses [Duarte *et al*,, 2014a; Duarte *et al*., 2014b; Duarte *et al*., 2013a). Under normal and extreme heat conditions, *S. patens* had a comparatively higher photosynthetic efficiency (α). In contrast, during cold wave events the native *S. maritima* is far more efficient. These responses are related to the ecology of both species. *Spartina maritima* is found in Mediterranean and North Atlantic habitats, prone to prolonged cold during the winter (Duarte *et al*., 2013c), providing this species with an ecological adaptation to this condition. On the other hand *S. patens*, is native from warmer climates (SanLeón *et al*., 1999) and thus is highly adapted to high temperatures. This study showed that *S. patens* was well adapted to heat stress, improving in some cases its PS II quantum efficiency, while *S. maritima* was insensitive to cold stress. If both PS I and PS II energy fluxes are observed, there are evident differences in the thermal tolerance of both photosystems. Compared with the remaining tested species, *S. patens* showed a reduction in the probability of an absorbed photon to move an electron through the ETC in the plants exposed to cold stress, although without a simultaneous increase in the dissipated energy fluxes. This indicates the presence of compensatory measures to counteract this excess of energy, avoiding losses of energy.

Our results indicate that heat stress-induced changes in energy flux were different between PS I and PS II. Compared to the control group, in both C_3 plants, the energy flux rates φE0 , ψ0, and φP0 of PS II were lower at both, heat and cold stress treatment, whereas δR0 of PS I were higher under both extreme thermal stress treatments than in the control. This increase of δR_0 was observed in bean plants immediately after heat treatment (Zushi *et al*., 2012; Stefanov *et al*., 2011). In general, PS II is the most thermally labile component of the photosynthetic apparatus (Apostolova *et al*., 2011), whereas PS I is comparatively heat resistant

(Havaux, 1996). Previous studies with apple leaves, showed that heat-treated leaves exhibited increased δR_0 indicative of lower damage at PS I (Chen and Cheng, 2009). Similar to these reports, our results suggest that in *A. tripolium* and *S. maritima* PS I activity is more heat-resistant than PS II. Although all these similarities between both C_3 studied species, some differences arise in the OJIP profile between *A. tripolium* heat wave and cold wave treated individuals that can explain the lack of differences in the PS II quantum yields between cold wave subjected individuals and the control group. The first and more evident one arises from the maintenance of the connectivity between PS II antennae allowing these individuals to trap higher energy amounts (TR/CS energy flux) feeding a higher energy flux to the ETC (higher ET/CS than in heat wave treated individuals) to reach PS I electron acceptors, as shown by an unaffected δR_0. Nevertheless, excessive energy is being accumulated in these stressed photosystems. Effects on PS I activity in cold wave treated individuals were more pronounced. When the ratio between absorbed light energy and electron acceptors in the photosynthetic electron transport chain is too high, photo-protective mechanisms are activated.

When the ratio between absorbed light energy and electron acceptors in the photosynthetic electron transport chain is too high, photoprotective mechanisms are activated. A crucial drop down in the luminal pH induces the xanthophyll cycle – a pronounced protection mechanism in halophytes (Duarte *et al*,, 2014a; Duarte *et al*., 2014b; Duarte *et al*., 2013a). Increased de-epoxidation of the luminal violaxanthin pool towards zeaxanthin decreases an overload of the photosynthetic light harvesting apparatus, by dissipating the elevated reducing power accumulated within the stroma (Demmig-Adams, 1990). With the exception of *H. portulacoides* exposed to heat stress, none of the species exposed to either thermal treatments showed signs of conversion of violaxanthin to zeaxanthin. In cold wave-treated individuals, all species, showed a decrease in all carotenoids with the exception of auroxanthin, a violaxanthin analogue (Wentworth *et al*., 2000) that evidently increased in concentration. Auroxanthin is a C5,8 epoxy carotenoid that has previously been shown to enhance aggregation-associated quenching in isolated LHC IIb (Ruban *et al*., 1998). The effectiveness of auroxanthin has been suggested to come from the fact that its S1 energy level is higher than that of violaxanthin

(Wentworth *et al*., 2000). This effect is explained by its structure where the end groups of auroxanthin lie in the plane of the conjugated carbon double bond chain, as in zeaxanthin, whereas they are expected to be out-of-plane in violaxanthin. In fact, the C5,8 epoxide would hold the end group rigidly in-plane, explaining why it is even more effective than zeaxanthin and thus be an efficient energy quencher under stress conditions (Horton *et al*., 1999; Ruban *et al*., 1998). In heat wave-treated plants carotenoid driven mechanisms were not activated, with the exception of *H. portulacoides* that exhibited both energy dissipation mechanisms. The coupled activation of the xanthophyll cycle along with a higher auroxanthin synthesis suggests that the heat-treated *H. portulacoides* individuals had higher needs to dissipate excessive energy than the cells exposed to cold treatment.

Allied to this quenching mechanism driven by pigment conversions, the stress individuals also showed a very active line of defence for reactive oxygen species (ROS) scavenging, promoted by increased activities in three of the four analysed anti-oxidant enzymes. At this level there was observed a higher degree of dissimilarity, indicative a specie-specific feedback to the oxidative burst. Nevertheless, and also important to consider, the levels of excessive energy between the four analysed species under different thermal stress were also very different, and thus can have implications on the activation of different oxidative mechanisms. Conversely, *H. portulacoides* heat-treated individuals only presented an increased APx and SOD activity coupled to the auroxanthin and xanthophyll cycle mechanisms. In both cases it appears to exist an efficient scavenging mechanism of these ROS species. This is confirmed by the maintenance of the lipid peroxidation levels within normal basal levels, in both treatment groups. In *A. tripolium*, cold wave-treated individuals showed increased enzyme activity to scavenge reactive oxygen species (ROS) scavenging, while in heat wave treated individuals only some antioxidant response mechanisms were activated. Individuals subjected to cold wave treatment showed a highly significant increase in the peroxidase activity, which contributed to higher CAT and GPx. In both C_3 species this anti-oxidant activity profiles allowed the maintenance of the lipid peroxidation in normal basal levels under cold-wave treatment. Nevertheless, in *A. tripolium* the reduced anti-oxidant enzymatic activity was not sufficiently to eliminate ROS. Comparing both C_4 grasses some differences

also arise with interesting ecological implications. *S. patens* cold wave-treated individuals displayed an active line of enzymatic defences for ROS scavenging. In fact, only cold treated individuals of this species presented higher activities of anti-oxidant enzymes, revealing some degree of adaptation to this new host environment. In contrast in *S. maritima* the exposure to extreme heat periods led, in most cases, to a decrease in the enzymatic defences, leaving a high amount of ROS free inside the cell, injuring the cellular machinery including the membranes essential for energy transduction (Duarte *et al*., 2013b).

Using *A. tripolium* as a model C_3 halophyte the current study suggests that cold and heat wave events reduce the ecophysiological fitness of this species, at the gene expression level. While cold waves seem to induce stress by desiccation - leading to losses of the membrane stability - heat waves seem to trigger protein instability. Gene expression pattern (tested on representative genes) suggest that cold waves crucially affect the leaf water availability (increased dehydrin) and the membrane integrity (increased C4 steryl methyl oxidase), and trigger regulatory responses on the RNA maturation level (increased Maturase K), while heat waves affect the protein integrity (increased cysteine protease). Dehydrin gene expression showed a crucial increase during cold stress. Dehydrins are among several ubiquitous water-stress-responsive proteins in plants (Close, 1996) that are increased during heat and cold stress (Sakai and Larcher, 1987). Cryoprotective activities for freeze-sensitive enzymes were detected in dehydrins from several plants including citrus, peach and spinach (Hara *et al*., 2001). Hara *et al*. (2001) suggested that these dehydrins are associated with a peroxidase activity that targets cold-generated ROS. It has also been shown that dehydrins decrease electrolyte leakage even at sub-zero temperatures (Kaye *et al*., 1998), by interactions with plant membranes and inhibition of freezing-induced lamellar-to-hexagonal II phase transitions (Thomashow, 1999). In *A. tripolium* individuals that were exposed to cold waves there was a correlation of the catalase activity and the guaiacol peroxidase activity simultaneously with a reduction of lipid peroxidation and with increased dehydrin gene expression. This might point out the importance of anti-oxidative response to and membrane stabilization to cold waves. In addition, C4 sterol methyl oxidase gene expression increased in response to cold, as observed previously

(Uemura and Steponkus, 1994), most likely to increase the membrane fluidity. Concomitantly the individuals exposed to cold wave treatment also showed a decreased lipid peroxidation products concentration, that together with the high C4 sterol methyl oxidase gene expression points out to maintenance and protection of membrane stability in cold wave exposed individuals. Maturase K gene was significantly stronger expressed in cold wave treated individuals. The protein encoded has as primary splicing function, participating in RNA maturation (Zoschke *et al*., 2007). The changes in Maturase K expression imply that RNA modification and transport are altered for further regulation of the gene expression (Tan *et al*., 2013). Changes in the gene expression pattern can point on stimulation of repair mechanisms in order to protect cellular and photosynthetic components, and on activation of stress defensive processes (Forster *et al*., 2006). During heat stress only one of the analysed genes – the cysteine protease -showed an altered expression pattern. Cysteine protease mRNAs accumulate under environmental stress conditions or during specific stages of plant development. Previous studies showed that the gene expression of the cysteine protease was up-regulated in response to both, low and high temperature treatment, to drought, to salinity, and to ABA treatment (Schaffer and Fisher, 1990). Cysteine proteases degrade misfolded proteins, which has been shown to can fuel *denovo* synthesis of enzymes that are associated with temporary stress-adaptations including compatible-solute biosynthesis, ion sequestration, water uptake, and long-term adaptations such as CAM (Forsthoefel *et al*., 1998). Regulatory functions in signal transduction and on growth surveillance have been attributed to cysteine proteases. Comparing cysteine protease gene expression with the protein content of the leaves subjected to heat wave treatment, the results are concomitant to each other. Alongside with this gene expression enhancement it was also verified a significant decrease in the protein content from the individuals exposed to heat waves.

Conclusions

Our data suggests that a predicted increase of heat and cold treatment events has a negative impact on the physiology and the photobiology of both C_3 plants. Intrinsic biophysical stress response mechanisms, as described in several

studies on long-term stresses (Duarte *et al*., 2013a) - such as the activation of a dissipative energy pathway - seem not to respond, resulting in significant photosynthesis activity inhibition. The results support the findings of Saidi *et al*. (2010), who observed a correlation between the intensity of the stress response and the change in temperature relative to the growth temperature. Furthermore, this author suggested that rapid thermal changes are more effective on the plant metabolism than the ambient temperature level (Plieth *et al*. 1999). Considering all these cellular electronic processes, some ecological outcomes arise, as outcomes from these early stress signs. The lower damage induced by cold exposure along with the higher levels of cellular defence point out to a higher tolerance of this plant to cold periods. Having in mind the IPCC predicted reduction in cold spell frequency and intensity, along with a serious aggravation of heat wave events, it becomes likely that the survival of this species will be at stake. On the other and considering the invasion ecology of the North American *S. patens* while compared with the Mediterranean native *S. maritima* some implications can also be withdrawn. Considering all the photobiological processes underlying the light harvesting mechanisms, *S. maritima* and *S. patens* appear to have different thermal tolerances conditioned by their adaptation to two different climatic habitats of origin. Endemic and exotic species are good case studies for understanding the adaptation capacity of a species to climatic environments different from their original climate. According to the IPCC projections, the frequency and intensity of extreme heat events will increase in the near future, while cold waves will decrease in intensity. Results from this study have shown that *S. patens* appears to have a higher fitness for the incoming climatic scenarios, being more tolerant to heat stress, while *S. maritima* will have its photobiological fitness decreased according to these predictions. The physiological reactions of introduced/exotic species can predispose them to become invasive when climate change favours them over the native species.

References

Álvarez, R., Castillo, J.M., Mateos-Naranjo, E., Gandullo, J., Rubio-Casal, A.E., Moreno, F.J. and Figueroa, M.E., 2010. Ecotypic variations in phosphoenolpyruvate carboxylase activity of the cordgrass *Spartina densiflora* throughout its latitudinal distribution range. *Plant Biology* 12, 154-160.

Apostolova, E.L. and Dobrikova, A.G., 2011. Effect of high temperature and UV-A radiation on photosystem II. M. Passarakli (Ed.), *Handbook of Plant and Crop Stress*, CRC press, Boca Raton, London, New York, pp. 577–591.

Bailey, K., Gray, J., Walker, R. and Leegood R., 2007. Coordinate regulation of phosphoenolpyruvate carboxylase and phosphoenolpyruvate carboxykinase by light and CO_2 during C_4 photosynthesis. *Plant Physiology* 144, 479–486.

Browse, J. and Xin, Z., 2001. Temperature sensing and cold acclimation. *Current Opinion in Plant Biology* 4, 241–246.

Caçador, I., Neto, J.M., Duarte, B., Barroso, D.V., Pinto, M. and Marques, J.C., 2013. Development of an Angiosperm Quality Assessment Index (AQuA – Index) for ecological quality evaluation of Portuguese water bodies – A multi-metric approach. *Ecological Indicators* 25, 141-148.

Chen, L.S. and Cheng, L., 2009. Photosystem 2 is more tolerant to high temperature in apple (*Malus domestica* Borkh.) leaves than in fruit peel. *Photosynthetica* 47, 112-120.

Close, T.J., 1996. Dehydrins: emergence of a biochemical role of a family of plant dehydration proteins. *Physiologia Plantarum* 97, 95–803.

Costanza, R., d'Arge, R., de Groot, R.S., Farber, S., Grasso, M., Hannon, B., Limburg, K., Naeem, S., O'Neill, R.V., Paruelo, J., Raskin, R.G., Sutton, P. and van den Belt, M., 1997. The value of the world's ecosystem services and natural capital. *Nature* 387, 253–260.

De Boeck, H.J., Dreesen, F.E., Janssens, I.A. and Nijs, I., 2010. Climatic characteristics of heat treatments and their simulation in plant experiments. *Global Change Biology* 16, 1992–2000.

Demmig-Adams, B., 1990. Carotenoids and photoprotection in plants: a role for the xanthophyll zeaxanthin. *Biochimica et Biophysica Acta* 1020, 1–24.

Duarte, B., Couto, T., Freitas, J., Valentim, J., Silva, H., Marques, J. C. and Caçador, I., 2013c. Abiotic modulation of *Spartina maritima* photosynthetic ecotypic variations in different latitudinal populations. *Estuarine, Coastal and Shelf Science* 130, 127-137.

Duarte, B., Delgado, M., and Caçador, I., 2007. The role of citric acid in cadmium and nickel uptake and translocation, in *Halimione portulacoides*. *Chemosphere* 69, 836-840.

Duarte, B., Santos, D. and Caçador, I., 2013b. Halophyte anti-oxidant feedback seasonality in two salt marshes with different degrees of metal contamination: search for an efficient biomarker. *Functional Plant Biology* 40, 922-930.

Duarte, B., Santos, D., Marques, J. C. and Caçador, I., 2013a. Ecophysiological adaptations of two halophytes to salt stress: photosynthesis, PS II photochemistry and anti-oxidant feedback - Implications for resilience in climate change. *Plant Physiology and Biochemistry* 67, 178-188.

Duarte, B., Santos, D., Marques, J.C. and Caçador, I., 2014a. Biophysical probing of *Spartina* maritima Photo-system II changes during increased submersion periods: possible adaptation to sea level rise. *Plant Physiology ad Biochemistry* 77, 122-132.

Duarte, B., Santos, D., Marques, J.C. and Caçador, I., 2015. Ecophysiological constraints of two invasive plant species under a saline gradient: halophytes versus glycophytes *Estuarine Coastal and Shelf Science* 167, 154-165.

Duarte, B., Santos, D., Silva, H., Marques, J.C. and Caçador, I., 2014b. Photochemical and Biophysical feedbacks of C_3 and C_4 Mediterranean halophytes to atmospheric CO_2 enrichment confirmed by their stable isotope signatures. *Plant Physiology and Biochemistry* 80, 10-22.

Duarte, B., Silva, V. and Caçador, I., 2012. Hexavalent chromium reduction, uptake and oxidative biomarkers in *Halimione portulacoides*. *Ecotoxicology and Environmental Safety* 83, 1-7.

Emsminger, I., Busch, F. and Huner, N.P.A., 2006. Photostasis and cold acclimation: sensing low temperature through photosynthesis. *Physiologia Plantarum* 126, 28–44.

Fabre, M.E., 1849. Description d'une nouvelle espèce de Spartina, abondante sur une portion du littoral méditerranéen. *Annales des Sciencies Naturelles. Botanique*. Paris, 3, 122–125.

Forster, R., Weiss, M., Zimmermann, T., Reynaud, E. G., Verissimo, F., Stephens, D. J. and Pepperkok, R., 2006. Secretory cargo regulates the turnover of COPII subunits at single ER exit sites. *Current Biology* 16, 173-179.

Forsthoefel, N.R., Cushman, M.A.F., Ostrem, J.A and Cushman, J.C., 1998. Induction of a cysteine protease cDNA from *Mesembryanthemum crystallinum* leaves by environmental stress and plant growth regulators. *Plant Science* 136, 195-206.

Grossi, V. and Raphel, D., 2003. Long-chain (C19–C29) 1-chloro-n-alkanes in leaf waxes of halophytes of the *Chenopodiaceae*. *Phytochemistry* 63, 693-698.

Hara, M., Terashima, S. and Kuboi, T., 2001. Characterization and cryoprotective activity of cold-responsive dehydrin from *Citrus unshiu*. *Journal of Plant Physiology* 158, 1333–1339.

Hatch M., 1992. C_4 photosynthesis: an unlikely process full of surprise. *Plant Cell Physiology* 33, 333–342.

Havaux, M., 1996. Temporary responses of photosystem I to heat stress. *Photosynthesis Research* 47, 85-97.

Heide O., 2005. Ecotypic variation among European arctic and alpine populations of *Oxyda digyna*. *Arctic, Antarctic and Alpine Research* 37, 233–238.

Heywood, V. H., 1989. Patterns, extends, and modes of invasions by terrestrial plants. In *Biological invasions: A global perspective*, edited by J. A. Drake, H. A. Mooney, F. DiCastri, R. H. Groves, F. J. Kruger, M. Rejmanek, and M. Williams, 31–60. New York: John Wiley.

Horton, P., Ruban, A.V. and Young, A.J., 1999. Regulation of the structure and function of the light-harvesting complexes of photosystem II by the xanthophyll cycle. In: Frank HA, Young AJ, Cogdell JC, eds. *The photochemistry of carotenoids: applications in biology.* Kluwer Academic Publishers, 271–291.

Intergovernmental Panel on Climate Change (IPCC) (2014) Climate change 2014: Impacts, Adaptation and Vulnerability. Contribution of working group II to the fifth assessment report of the IPCC.

Kaye, C., Neven, L., Hofig, A., Li, Q.B., Haskell, D. and Guy, C., 1998. Characterization of a gene for spinach CAP160 and expression of two spinach cold-acclimation proteins in tobacco. *Plant Physiology* 116, 1367-1377.

Koyro, H.W., 2006. Effect of salinity on growth, photosynthesis, water elations and solute composition of the potential cash crop halophyte *Plantago coronopus* (L.). *Environmental and Experimental Botany* 56, 136-146.

Lara, M., Casati, P. and Andreo, C., 2001. In vivo phosphorylation of phosphoenolpyruvate carboxylase in *Egeria densa*, a submersed aquatic species. *Plant Cell Physiology* 42, 441–445.

Larcher, W., 2003. Physiological Plant Ecology. Springer Verlag, Berlin, Germany.

Lieth, H., Mochtchenko, M. (Eds.), 2002). Halophyte Uses in Different Climates. IV. Cash crop Halophytes for Future Halophyte Growers. *Progress in Biometeorology* 18. Backhuys Publishers, Leiden.

Lieth, H., Moschenko, M., Lohmann, M., Koyro, H.-W., and Hamdy, A., 1999. Halophyte uses in different climates. I. *Ecophysiological studies*. Backhuys Publishers, Leiden, 258 pp.

Marchant, C. and Goodman, P., 1969. *Spartina maritima* (Curtis) Fernald. *Journal of Ecology* 57, 287-291.

Marshall, H.J., Geider, R.J. and Flynn, K.J., 2000. A mechanistic model of photoinhibition. *New Phytologist* 145, 347–359.

Mateos-Naranjo, E., Redondo-Gómez, S., Andrades-Moreno, L. and Davy, A.J., 2010. Growth and photosynthetic responses of the cordgrass *Spartina maritima* to CO_2 enrichment and salinity. *Chemosphere* 81, 725-731.

Monroy, A.F. and Dhindsa, R.F., 1995. Low Temperature Signal Transduction: lnduction of Cold Acclimation-Specific Genes of Alfalfa by Calcium at 25°C. *The Plant Cell* 7, 321-331.

Niu, S., Luo, Y., Li, D., Cao, S., Xia., J., Li, J. and Smith, M.D., 2014. Plant growth and mortality under climatic extremes: An overview. *Environmental and Experimental Botany* 98, 13-19.

Panda, D., Rao, D.N., Sharma, S.G., Strasser, R.J. and Sarkar, R.K., 2006. Submergence effects on rice genotypes during seedling stage: Probing of submergence driven changes of photosystem 2 by chlorophyll a fluorescence induction O-J-I-P transients. *Photosynthetica* 44, 69-75.

Pasternak, D., 1990. Fodder Production with Saline Water, Project Report, January 1982-December 1989. Report No. BGUN-ARI-35-90. The Institutes for applied Research, Ben-Gurion University of the Negev, Beer-Sheva, pp. 113-173.

Plieth, C., Hansen, U.-P., Knight, H. and Knight, M.R., 1999. Temperature sensing by plants I: The primary mechanisms of signal perception. *Plant Journal* 18, 491–497.

Ruban, A.V., Phillip, D., Young, A.J. and Horton, P., 1998. Excited state energy level does not determine the differential effect of violaxanthin and zeaxanthin on chlorophyll fluorescence quenching in the isolated light-harvesting complex of Photosystem II. *Photochemistry and Photobiology* 68, 829–834.

Sage, R.F. and Kubien, D.S., 2007. The temperature response of C3 and C4 photosynthesis. *Plant, Cell and Environment* 30, 1086-1106.

Saidi, Y., Finka, A. and Goloubinoff, P., 2010. Heat perception and signalling in plants: a tortuous path to thermotolerance. *New Phytologist* 190, 556–565.

Sakai, A. and Larcher, W., 1987. *Frost survival of plants: responses and adaptation to freezing stress*. Berlin: Springer-Verlag. 321pp.

SanLeon, D.G., Izco, J. and Sanchez, J.M., 1999. *Spartina patens*: a weed in Galician saltmarshes (NW Iberian Peninsula). *Hydrobiologia* 15, 213–222.

Schaffer, M.A. and Fisher, R.L., 1990. Transcriptional activation by heat and cold of a thiol protease gene in tomato. *Plant Physiology* 93, 1486–1491.

Sousa, A.I., Lillebo, A.I., Pardal, M.A. and Caçador, I., 2010. Productivity and nutrient cycling in salt marshes: Contribution to ecosystem health. *Estuarine Coastal and Shelf Science* 87, 640-646.

Srivastava, A., Guisse, B., Greppin, H. and Strasser, R.J., 1997. Regulation of antenna structure and electron transport in PS II of *Pisum sativum* under elevated temperature probed by the fast polyphasic chlorophyll a fluorescence transient: OKJIP. *Biochimica et Biophysica Acta* 1320, 95–106.

Stefanov, D., Petkova, V. and Denev, I.D., 2011. Screening for heat tolerance in common bean (*Phaseolus vulgaris* L.) lines and cultivars using JIP-test. *Scientia Horticulturae* 128, 1–6.

Stephenson D., Oliver, L., Burgos, N. and Gbur E., 2006. Identification and characterization of pitted morning glory (*Ipomoea lacunose*) ecotypes. *Weed Science* 54, 78–86.

Strasser, R.J. and Stirbet, A.D., 2001. Estimation of the energetic connectivity of PS II centres in plants using the fluorescence rise O–J–I–P. Fitting of experimental data to three different PS II models. *Mathematics and Computers in Simulation* 56, 451-461.

Strasser, R.J., Tsimilli-Michael, M. and Srisvastava, A., 2004. Analysis of the chlorophyll-a fluorescence transients. In: Papageorgiou, G.C. and Govindjee, ed. *Advances in photosynthesis and respiration.* Berlin: Springer p. 321-362.

Tan, J., Wang, C., Xiang, B., Han, R., and Guo, Z., 2013. Hydrogen peroxide and nitric oxide mediated cold-and dehydration-induced myo-inositol phosphate synthase that confers multiple resistances to abiotic stresses. *Plant, Cell and Environment* 36, 288-299.

Teal, J., and Howes, B., 2000. Salt marsh values: Retrospection from the end of the century. In: Weinstein, M.P. and Kreeger, D.A. (eds.). *Concepts and Controversies in Tidal Marsh Ecology*, Springer, Netherlands, pp. 9–19.

Thomashow, M.F., 1999. Plant Cold Acclimation: Freezing tolerance genes and regulatory mechanisms. *Annual Reviews in Plant Physiology and Plant Molecular Biology* 50, 571–599.

Tutin, T.G., 1980. Spartina Schreber. In: Tutin, T.G., Heywood, V.H., Burges, N.A., Moore, D.M., Valentine, D.H., Walters, S.M., Webb, D.A. (eds.) *Flora Europaea*, Vol. 5. Cambridge, UK: Cambridge University Press, 259–260.

Uemura, M. and Steponkus, P.L., 1994. A contrast of the plasma membrane lipid composition of oat and rye leaves in relation to freezing tolerance. *Plant Physiology* 104, 479-496.

Van der Maarel, E. and Van der Maarel-Versluys, M., 1996. Distribution and conservation status of littoral vascular plant species along the European coasts. *Journal of Coastal Conservation* 2, 73–92.

Vidal J., Pierre J. and Echevarría C., 1996. The regulatory phosphorylation of C4 phosphoenolpyruvate carboxylase, a cardinal event in C_4 photosynthesis. In: Dennis T.S., Hohn B., King P.G., Schell G., Verma D.P.S. (Eds), *Plant Gene Research. Signal Transduction in Plant Growth and Development*. Springer-Verlag, New York: 141–160.

Wen, X.G., Qiu, N.W., Lu, Q.T. and Lu, C.M. (2005) Enhanced thermotolerance of photosystem II in salt-adapted plants of the halophyte *Artemisia anethifolia*. *Planta* 220, 486–497.

Wentworth, M., Ruban, A.V. and Horton, P., 2000. Chlorophyll fluorescence quenching in isolated light-harvesting complexes induced by zeaxanthin. *FEBS Letters* 471, 71–74.

Zoschke, R., Liere, K. and Börner, T., 2007. From seedling to mature plant: *Arabidopsis* plastidial genome copy number, RNA accumulation and transcription are differentially regulated during leaf development. *Plant Journal* 50, 710–722.

Zushi, K., Kajiwara, S. and Matsuzoe, N., 2012. Chlorophyll a fluorescence OJIP transient as a tool to characterize and evaluate response to heat and chilling stress in tomato leaf and fruit. *Scientia Horticulturae* 148, 39-46.

5.4. CONCLUSIONS ON THE IMPACTS OF ALTERED THERMAL ENVIRONMENTS ON ESTUARINE SALT MARSHES

Warming of the climate system is unequivocal, and since the 1950s, many of the observed changes are unprecedented over decades to millennia. The atmosphere and ocean have warmed, the amounts of snow and ice have diminished, sea level has risen, and the concentrations of greenhouse gases have increased (IPCC, 2013). Additionally, the frequency and intensity of extreme thermal events is expected to increase (IPCC, 2012). The same working group developed five possible scenarios of rising temperature of increasing thermal severity: the B1 scenario (+1.8°C), the B2 scenario (+2.4°C), the A1B scenario (+2.6°C), the A2 scenario (+3.2°C) and the worst scenario, A1F1 (+4.0°C). One of the salt marsh ecosystem services most dependent on the thermal environment, is its carbon retention and emissions throughout sediment heterotrophic respiration. With a snowball effect, if the carbon emissions increase, the greenhouse effect follows the same pattern leading to an increased atmospheric temperature. Nevertheless, salt marshes once again act as a buffer, counteracting global warming. In all projected scenarios, salt marshes tend to decrease their carbon emissions with the temperature increase, leading to higher carbon stocks and counteracting the greenhouse effect (Duarte *et al*., 2014). This will certainly be an important service preformed by wetlands in a future altered thermal environment. Additionally, to this projected global warming, some episodic extreme events will also affect inevitably all communities. Halophytes will be no exception. Another metabolic process highly dependent on temperature is photosynthesis. Namely, C_3 photosynthesis is expected to be more negatively affected by the occurrence of heat waves. This will have impacts not only on the marsh foundations, due to a decreased productivity of *A. tripolium*, but also on the sediment stabilization and marsh build-up, due to its negative effects on *H. portulacoides* productivity (Duarte *et al*., 2015a; Duarte *et al*., 2015b). Cold spells will also have its negative impacts on these species, although at a smaller scale.

Additionally, these punctual events will also have its impacts on the invasion ecology of some non-indigenous species, altering inevitably the marsh structure and function. The invasor *S. patens* is more fit during heat spells and along with its C_4 metabolism, will be able to replace the less adapted C_3 species from the upper marsh. The native C_4 *S. maritima*, will also suffer dramatically from the increase of frequency and intensity of heat wave events. Again, the foundations and spreading of new marshes will be threatened, with another pioneer specie having its primary productivity reduced (Duarte *et al*., 2015c). In contrast to the native *S. maritima*, under the present climate reality, the NIS *S. patens* proved to have a lower photosynthetic fitness under the Mediterranean climate, which seems to be slowing down its spread but not arresting it. Also, this NIS N-nutrition appears to be on of the factors impairing it spreading at higher rates (Duarte *et al*., 2015d). Thus, as the on-going climatic changes can be favouring drivers for a faster expansion of this species, taking part of less productive Mediterranean species in a climate change scenario, the need arises to monitor this NIS and consider its spreading as a potential threat to the ecosystem biodiversity.

Overall, although being punctual events, extreme thermal conditions will leave their signature on the marsh structure. Although with more organic and cohesive sediments due to higher organic carbon accumulations, marshes will tend to reduce its area as their spreading and accretion abilities will be decreased due to a progressive reduction of pioneer species abundance. Alongside, NIS will pose an increased threat substituting the native halophytes in the already mature marshes, changing completely its functions and services provided to the estuarine system.

References

Duarte, B., Baeta, A., Rousseau-Gueutin, M., Ainouche, M., Marques, J.C. and Caçador, I., 2015. A tale of two *Spartinas*: climatic, photobiological and isotopic insights on the fitness of invasive versus native species. *Estuarine Coastal and Shelf Science* 167, 178-190.

Duarte, B., Freitas, J., Valentim, J., Medeiros, J.P., Costa, J.L., Silva, H., Dias, J.M., Marques, J.C. and Caçador, I., 2014. Modelling abiotic control of salt marsh sediments respiratory CO_2 fluxes: new insights for climate change scenarios. *Ecological Indicators* 46, 110-118.

Duarte, B., Goessling, J.W., Marques, J.C. and Caçador, I., 2015. Ecophysiological constrains of *Aster tripolium* under extreme thermal events impacts: merging biophysical, biochemical and genetic insights. *Plant Physiology and Biochemistry* 97, 217-228

Duarte, B., Marques, J.C. and Caçador, I., 2015c. Ecophysiological responses of native and invasive *Spartina* species to extreme temperature events in Mediterranean marshes. *Biological Invasions* (10.1007/s10530-015-0958-4).

Duarte, B., Santos, D., Marques, J.C. and Caçador, I., 2015a. Impact of extreme heat and cold events on the energetic metabolism of the C_3 halophyte *Halimione portulacoides*. *Estuarine Coastal and Shelf Science* 167, 166-177.

IPCC, 2012. *Managing the Risks of Extreme Events and Disasters to Advance Climate Change Adaptation. A Special Report of Working Groups I and II of the Intergovernmental Panel on Climate Change* [Field, C.B., Barros, V., Stocker, T.F., Qin, D., Dokken, D.J., Ebi, K.L., Mastrandrea, M.D., Mach, K.J., Plattner, G.-K., Allen, S.K., Tignor, M. and Midgley, P.M. (eds.)]. Cambridge University Press, Cambridge, UK, and New York, NY, USA, 582 pp.

IPCC, 2013. *Climate Change 2013: The Physical Science Basis. Contribution of Working Group I to the Fifth Assessment Report of the Intergovernmental Panel on Climate Change* [Stocker, T.F., Qin, D., Plattner, G.-K., Tignor, M., Allen, S.K., Boschung, J., Nauels, A., Xia, Y., Bex V. and Midgley, P.M. (eds.)]. Cambridge University Press, Cambridge, United Kingdom and New York, NY, USA, 1535 pp.

CHAPTER VI

GENERAL DISCUSSION AND CONCLUSIONS

CHAPTER VI

GENERAL DISCUSSION AND CONCLUSIONS

Back in 1977, the resilience of salt marshes to human activities was already recognized (Niering, 1977). These are in fact resilient ecosystems, but as all resilience mechanisms it implies that the adaptation and recovery of the ecosystems keep up to pace with the applied stressor. The climatic conditions nowadays impose here a shift in the resilience capacity of our marshes. The speed at which changes are likely to occur in the future outpaces by far the ability of the marshes to adapt and thus the resilience of these ecosystems may be at stake. Niering (1977) unveiled the human signatures on New England salt marshes, and pioneered the study of human impacts on coastal wetlands. Over the past several decades, however, eutrophication, overfishing, and climate change have become global drivers of catastrophic impacts in coastal ecosystems (Jackson *et al*., 2001; Lotze *et al*., 2006), beyond Niering's predictions.

Human impacts are concentrated in coastal ecosystems due to a synergism of nearshore human activities, spillover from terrestrial impacts, and the concentration of human settlement along shorelines (UNEP, 2006). Although this anthropogenic degradation of the world coastal areas, human populations continue to rely heavily on coastal ecosystem services. Estuaries and salt marshes provide more services than any other ecosystem (UNEP, 2006). As stated several times before, these are important sources of storm protection (Costanza *et al*., 2008), nutrient regeneration (Valiela and Cole, 2002), nurseries for commercially important fish and shellfish (Boesch and Turner, 1984) and shelter for migratory birds (Teixeira *et al*., 2014). To preserve these functions and ecosystem services along with aesthetic and recreational value, salt marshes have become important conservation priorities in several countries under the shelter of the Ramsar Convention and other important directives (for e.g. EU Water Framework Directive, EU Habitats Directive, South Africa Water Act and the USA Clean Water Act).

Ecologists soon developed founding studies of plant succession (Clements 1916), assemblages (Chapman, 1940), salt marsh development (Redfield, 1965), and advances in community (Bertness, 1991) and ecosystem ecology (Valiela and Teal, 1979). The concern with the Portuguese marshes vegetation goes back to Esteves-de-Sousa (1950), who provided one of the first systematic surveys of the Tagus estuary marsh vegetation. A systematic understanding of these systems should provide tools to understand marsh dynamics and predict how these ecosystems will respond to human impacts associated with ongoing global changes. In fact, these are already impacted ecosystems, like it could be observed from the data presented in Chapter II (section 2.4), with an intense contamination record from industrial sources back to the 1960s (Duarte *et al*., 2013). A similar record can be found in which concerns the eutrophication of some marshes (Caçador and Duarte, 2014; Caçador and Duarte, 2012). Going back to the resilience subject, it is admissible that in already disturbed ecosystems, any increasing stressor can overcome the resilience of its species. Nevertheless, to understand this, one must understand the physiological and biogeochemical mechanisms underlying the plasticity and resistance mechanisms of the marsh and its community.

Like other marshes around the world the sediment supply in the Tagus estuary between 1961 and 2000 still allowed the marshes to keep up to pace with sea level rise, accreting vertically more than this rise in the water level. Nevertheless, the most recent predictions impose an increased problem. If in the last decades sea level rise was mainly due to the melting of the polar ice caps, nowadays this was added by a decrease in the radiative energy dissipation of our planet, leading to increasing temperatures and inevitable expansion of the water bodies (IPCC, 2013). This is likely to increase the rate of sea level rise by 2100 to values that can outpace the accretion rates of some slow growing marshes, like the ones located in the south side of the Tagus estuary, where in fact most of the marsh extensions are located. This will inevitably affect the tidal-regulated circadian rhythms of the plants, with prolonged flooding times and higher submersion heights, especially in the lower marsh. Although the low marsh isn't the most productive area of these systems (Caçador *et al*., 2009), the typical species found in the lowest part of the marsh, have an extremely important role as "founding fathers" of the marshes, with an occupation that can go from 20-90%

of the marsh (Caçador *et al*., 2013). The productivity of these species, (for e.g. *S. maritima*) will be inevitably affected, although in a smaller extent than it could be expected. *Spartina maritima* exhibited a great plasticity and adaptation capacity, allowing it to suffer only minor decreases in its primary productivity when exposed to prolonged submersion periods (Duarte *et al*., 2014a). Nevertheless, a reduction is evident, which in a longer term can have significant effects on the population of these pioneer species. The initiation and expansion of ponds in waterlogged marshes is considered to be an additional mechanism of marsh loss attributed to SLR in mid-Atlantic salt marshes (Hurting *et al*. 2002). Although there are few quantitative estimates of the expected extent of marsh loss as sea levels rises, most scientists agree that loss will be severe. Using current IPCC SLR scenarios and a salt marsh accretion model, Craft *et al*. (2009) predicted that 20-45% of salt marsh area in a Georgia estuary will be converted to low salinity marsh, tidal flat or open water by the year 2100. All these predictions are intrinsically connected with the physiological tolerance ranges exhibited by the different species, as observed by for the pioneer *S. maritima*. Coupling these physiological evidences with robust hydrodynamic models (Valentin *et al*., 2013) the insights gathered from the physiological evidences are reinforced. Sea level rise scenario will inevitably lead to changes in nutrients and sediments patterns around the salt marshes and thus vegetation coverage percentage would be affected. Additionally, as a consequence of flood duration increase, sediment moisture will increase imposing a stress condition to plants. Hence, the ratio below/aboveground biomass might increase, becoming critical to plants survival under conditions of accelerated SLR (Valentim *et al*., 2013). In the lower marsh the main constrains impairing primary productivity and pioneer species establishment is the prolonged submersion time that plants will be exposed under increased sea level. On the other hand, in the upper marsh this feature will have an additional stressor associated: increased salt-water intrusion. Combined with increased temperature and evapotranspiration, this will increase the salinity in the upper and middle marsh affecting the species hyaline habitat. This has consequences at the primary productivity level of namely the succulent shrubs, reducing it beyond its physiological optimum (Duarte *et al*., 2013a; Duarte *et al*., 2014b). Again this will decrease the survival of species like *H. portulacoides* and *S. fruticosa*. Additionally, this opens space to the spreading of other

species, namely invasive ones, like *S. patens*. This specie is highly resistant to salinity changes tolerating very high salinity values (Duarte *et al*., 2015a). Nowadays the expansion of this specie is constrained by a physiological misfit to the present climatic conditions observed in the Mediterranean marshes (Duarte *et al*., 2015b), preventing its fastest expansion. Thus, the on-going climatic changes can be favouring drivers for a faster expansion of this species, taking part of less productive Mediterranean species in a climate change scenario, by direct competition. In the areas where salt marsh is converted to vegetated mudflat or open water, the provision of ecosystem services is expected to decrease (Craft *et al*. 2009). This was also evident in one of the most important ecosystem services provided by Mediterranean marshes. These systems are often pointed out as sinks of contaminants and excessive nutrients. If this is true on the present conditions, under SLR scenarios this will be seriously affected. On the present conditions the marsh detritus exports return to the marsh area after some tidal cycles or are maintained within the vicinity of their point of origin (Duarte *et al*., 2014c; Duarte *et al*., 2015c), maintaining the remediative service provide by these areas. In the future a large part of these exports will reach the outer estuary and even the adjacent ocean shelf, transporting contaminants and organic nutrients trapped within these detritus (Duarte *et al*., 2014b; Duarte *et al*., 2015c). This is one of the more intrinsic evidences of the effects of climate change on the halophyte physiology and on the ecosystem services provided, with impacts beyond the estuarine system. These increased reach of the marsh generated detritus has inevitable consequences on the coastal contamination levels, but can also produce shifts in the coastal communities by enhancing the fuelling of secondary production in the coastal shelf or due to possible eutrophication processes promoted by excessive N exports (Duarte *et al*., 2014b; Duarte *et al*., 2015c).

As referred before the main driver of all climatic changes is the increasing greenhouse effect promoted by the increasing atmospheric concentrations of GHGs, namely CO_2. While SLR apparently affects the marsh vegetation by similar mechanisms (prolonged submersion, drowning and increased salinity), the increase in atmospheric CO_2 concentrations has a differential impact on the species depending on their own inherent characteristics. While an atmospheric increase of CO_2 concentration will favour C_3 primary production, C_4 photosynthesis apparently suffers no enhancement,

even showing some signs of distress (Duarte *et al.*, 2014d). Once again this will have its more negative effects on the marsh foundation and establishment, since as abovementioned, the most abundant pioneer specie, *S. maritima*, has a C_4 photosynthesis profile. In fact, the expansion of C_3 plants can also be at risk, if the C_4 pioneer species do not provide the conditions (for e.g. marsh elevation, sediment oxidation, hydrodynamical protection) for this increased productivity. This way all the marsh will have its area reduced by this negative impact of the increased CO_2 on the sensitive and essential pioneer species. On the other hand, a photosynthetic enhancement due to increased dissolved CO_2 was found for C_3 and C_4 halophytes, probably due to an alleviation of the stressful conditions imposed by submersion (as abovementioned) by an increased CO_2 availability (Duarte *et al.*, 2014e). Transposing these findings to the ecosystem, and assuming increased dissolved CO_2 concentration scenarios, the halophyte community displays a new ecosystem function, in terms of water column oxygenation and as buffers of its acidification by withdrawing excess CO_2. As it will be further discussed for temperature rise, this appears to be a counteractive measure of the ecosystem towards the changes in the water chemistry. This buffer function allows reducing the excessive CO_2 levels in the water column and thus increasing its potential to again reabsorb higher amounts of atmospheric CO_2 while providing increased O_2 concentrations for the heterotrophic life forms inhabiting nearby. At a biogeochemical level a similar buffer effect could be observed. Most of the carbon-related enzymes will be impaired during under CO_2 increase (Caçador *et al.*, 2015). If by one side this will impose serious constrains on the essential recycling processes provided by the marsh sediments, on the other hand apparently also counteracts the excessive CO_2 concentrations, by reducing the mineralization of organic carbon sources to CO_2. Nevertheless, this will impose in the future a significant unbalance of the marsh biogeochemical cycles, shifting the ecosystem functions with inevitable changes at the ecosystem services provided, namely at the nutrient regeneration level.

As abovementioned, this self-buffering capacity of the ecosystem is not exclusive of its feedback towards an increased atmospheric CO_2. A similar counteractive measure can be found will examining the effects of increased temperature on the marsh CO_2 effluxes (Duarte *et al.*, 2014f). Going through the IPCC

storyline scenarios, it is evident that the sediments act as buffers of the temperature increase, by decreasing the CO_2 efflux, and thus minimizing the greenhouse gas effect. This has inevitable consequences at the ecosystem services level, increasing this way the sediment organic carbon pool and thus shifting the biogeochemical functions of these systems as abovementioned and observed under CO_2 increase scenarios (Caçador *et al*., 2015). While permanent and long-term thermal disruptions, like warming, can impose long-term medium scale effects on plant productivity, punctual but abrupt and extreme thermal events can induce severe damage on plant productivity on a shorter term (IPCC, 2012). At this level C_3 halophytes will be more severely damaged by heat waves (Duarte *et al*., 2015d; Duarte *et al*., 2015e), events which are expected to be more intense and more frequent in a near future (IPCC, 2012). Nevertheless, a significant damage will be again felt by the pioneer species, either C_3 (for e.g. *A. tripolium*) or C_4 (for e.g. *S. maritima*). As previously referred, this will have its more seriously effects on the marsh establishment and growing, becoming this way more prone for example to SLR, also inherent to this global warming increase. Moreover, the reduction of the primary productivity of the most abundant native species, will also open space for the colonization by NIS, changing completely the marsh landscape and, of course, its ecosystem services to the estuarine community (Duarte *et al*., 2015f).

It is from far evident that all these climatic changes are not only interconnected on a physical way, but also at an ecological level. Mediterranean marshes will be more severely affected on its foundations, putting the entire ecosystem at risk and prone to other climate change side effects or to synergistic events. Accelerating human impacts are overwhelming salt marsh development and recovery by altering inundation regimes and the presence, identity, and productivity of salt marsh foundation species. Humanity alongside with marshes face a new challenge until the end of the century. Management efforts must highlight desired marsh attributes and ecosystem services in the face of human activities that threaten salt marsh ecosystems. This requires abandoning old-fashioned restoration goals, aiming to achieve "pristine" or "reference" conditions, replacing them by objectives aiming for enduring ecosystem subsistence and preservation of essential ecosystem services – contaminant sink, nursery habitat, nutrient regulation, and shoreline protection.

References

Bertness, M.D., 1991. Interspecific interactions among high marsh perennials in a New England salt marsh. *Ecology* 72, 125-137.

Boesch, D.F., and Turner, R.E., 1984. Dependence of fishery species on salt marshes: The role of food and refuge. *Estuaries* 7, 460-468.

Caçador, I. and Duarte, B., 2012. Tagus Estuary Salt Marshes: a Historical Perspective. *Estuaries: Classification, Ecology and Human Impacts*. Jordan, J.J. (Ed.) Nova Science Publishers, Inc.

Caçador, I. and Duarte, B., 2014. Eutrophication impacts on salt marshes natural metal remediation. *Eutrophication: Causes, Consequences and Control.* Volume 2. Ansari, Abid A. and Gill, Sarvajeet Singh (Eds.) Springer.

Caçador, I., Caetano, M., Duarte, B., Vale, C., 2009. Stock and losses of trace metals from salt marsh plants. *Marine Environmental Research*, 67, 75-82.

Caçador, I., Duarte, B., Marques, J.C. and Sleimi, N., 2015. Carbon mitigation: a salt marsh ecosystem service in times of change. *Halophytes for Food Security in Dry Lands.* Muhammad Ajmal Khan, Munir Ozturk, Bliquees Gul and Muhammad Zaheer Ahmed (Eds.) Elsevier.

Caçador, I., Neto, J.M., Duarte, B., Barroso, D.V., Pinto, M. and Marques, J.C., 2013. Development of an Angiosperm Quality Assessment Index (AQuA – Index) for ecological quality evaluation of Portuguese water bodies – A multi-metric approach. *Ecological Indicators* 25, 141-148.

Chapman, V.J. 1940. Succession on the New England salt marshes. *Ecology* 21, 279-282.

Clements, F.E., 1916. Plant succession: an analysis of the development of vegetation. Carnegie Institution of Washington, Washington.

Costanza, R., Perez-Maqueo, O., Martinez, M.L., Sutton, P., Anderson, S.J., and Mulder, K., 2008. The value of coastal wetlands for hurricane protection. *Ambio* 37, 241-248.

Craft, C., Clough, J., Ehman, J., Joye, S., Park, R., Pennings, S., Guo, H. and Machmuller, M., 2009. Forecasting the effects of accelerated sea-level rise on tidal marsh ecosystem services. *Frontiers in Ecology and the Environment* 7, 73-78.

Duarte, B., Baeta, A., Rousseau-Gueutin, M., Ainouche, M., Marques, J.C. and Caçador, I. 2015b. A tale of two *Spartinas*: climatic, photobiological and isotopic insights on the fitness of invasive versus native species. *Estuarine Coastal and Shelf Science* 167, 178-190.

Duarte, B., Caçador, I., Marques, J.C. and Croudace, I., 2013. Tagus Estuary salt marshes feedback to sea level rise over a 40-year period: insights from the application of geochemical indices. *Ecological Indicators* 34, 268-276.

Duarte, B., Freitas, J., Valentim, J., Medeiros, J.P., Costa, J.L., Silva, H., Dias, J.M., Marques, J.C. and Caçador, I., 2014f. Modelling abiotic control of salt marsh sediments respiratory CO2 fluxes: new insights for climate change scenarios. *Ecological Indicators* 46, 110-118.

Duarte, B., Goessling, J., Marques, J.C. and Caçador, I., 2015e Ecophysiological constrains of *Aster tripolium* under extreme thermal events impacts: merging biophysical, biochemical and genetic insights. *Plant Physiology and Biochemistry* 97, 217-228.

Duarte, B., Marques, J.C. and Caçador, I., 2015d Impact of extreme heat and cold events on the energetic metabolism of the C_3 halophyte *Halimione portulacoides Estuarine Coastal and Shelf Science* 167, 166-177.

Duarte, B., Marques, J.C. and Caçador, I., 2015f. Ecophysiological responses of native and invasive *Spartina* species to extreme temperature events in Mediterranean marshes. *Biological Invasions* (10.1007/s10530-015-0958-4).

Duarte, B., Santos, D., Marques, J. C. and Caçador, I., 2013a. Ecophysiological adaptations of two halophytes to salt stress: photosynthesis, PS II photochemistry and anti-oxidant feedback - Implications for resilience in climate change. *Plant Physiology and Biochemistry* 67, 178-188.

Duarte, B., Santos, D., Marques, J.C. and Caçador, I., 2014a. Biophysical probing of *Spartina maritima* Photo-system II changes during increased submersion periods: possible adaptation to sea level rise. *Plant Physiology ad Biochemistry* 77, 122-132.

Duarte, B., Santos, D., Marques, J.C. and Caçador, I., 2015a. Ecophysiological constraints of two invasive plant species under a saline gradient: halophytes versus glycophytes. *Estuarine Coastal and Shelf Science* 167, 154-165.

Duarte, B., Santos, D., Silva, H., Marques, J.C. and Caçador, I., 2014d. Photochemical and Biophysical feedbacks of C_3 and C_4 Mediterranean halophytes to atmospheric CO_2 enrichment confirmed by their stable isotope signatures. *Plant Physiology ad Biochemistry* 80, 10-22

Duarte, B., Silva, H., Marques, J.C., Caçador, I. and Sleimi, N., 2014e. Light-dark O_2 dynamics in submerged leaves of C_3 and C_4 halophytes under increased dissolved CO_2: Clues for saltmarsh response to climate change. *Annals of Botany Plants* 6, plu067.

Duarte, B., Sleimi, N. and Caçador, I., 2014b. Biophysical and biochemical constrains imposed by salt stress: Learning from halophytes. *Frontiers in Plant Science* 5, 746

Duarte, B., Valentim, J.M., Dias, J.M., Silva, H., Marques, J.C. and Caçador, I., 2014c. Modelling Sea Level Rise (SLR) impacts on salt marsh detrital outwelling C and N exports from an estuarine coastal lagoon to the ocean (Ria de Aveiro, Portugal). *Ecological Modelling* 289, 36-44.

Duarte, B., Vaz, N., Valentim, J.M., Dias, J.M., Silva, H., Marques, J.C. and Caçador, I. Revisiting the Outwelling Hypothesis: Modelling Salt Marsh Detrital Metal Exports under Extreme Climatic Events. (under revision in *Marine Chemistry)*.

Esteves-de-Sousa, A., 1950. Acerca da sub-halosérie da região salgadiça litoral, entre Corroios e Talaminho. *Revista da Faculdade de Ciências (Lisboa), Revista de Ciências Naturais.*

Hartig, E.K., Gornitz, V., Kolker, A., Mushacke, F. and Fallon, D., 2002. Anthropogenic and climate-change impacts on salt marshes of Jamaica Bay, New York City. *Wetlands* 22, 71-89.

IPCC, 2012. Managing the Risks of Extreme Events and Disasters to Advance Climate Change Adaptation. *A Special Report of Working Groups I and II of the Intergovernmental Panel on Climate Change* [Field, C.B., Barros, V., Stocker, T.F., Qin, D., Dokken, D.J., Ebi, K.L., Mastrandrea, M.D., Mach, K.J., Plattner, G.-K., Allen, S.K., Tignor, M. and Midgley, P.M. (eds.)]. Cambridge University Press, Cambridge, UK, and New York, NY, USA, 582 pp.

IPCC, 2013. Climate Change 2013: The Physical Science Basis. *Contribution of Working Group I to the Fifth Assessment Report of the Intergovernmental Panel on Climate Change* [Stocker, T.F., D. Qin, G.-K. Plattner, M. Tignor, S.K. Allen, J. Boschung, A. Nauels, Y. Xia, V. Bex and P.M. Midgley (eds.)]. Cambridge University Press, Cambridge, United Kingdom and New York, NY, USA, 1535 pp.

Jackson, J.B., Kirby, M.X., Berger, W.H., Bjorndal, K.A., Botsford, L.W., Bourque, B.J., Bradbury, R.H., Cooke, R., Erlandson, J., Estes, J.A., Hughes, T.P., Kidwell, S., Lange, C.B., Lenihan, H.S., Pandolfi, J.M., Peterson, C.H., Steneck, R.S., Tegner, M.J. and Warner, R.R., 2001. Historical overfishing and the recent collapse of coastal ecosystems. *Science* 293, 629-638.

Lotze, H.K., Lenihan, H.S., Bourque, B.J., Bradbury, R.H., Cooke, R.G., Kay, M.C., Kidwell, S.M., Kirby, M.X., Peterson, C.H. and Jackson, J.B.C., 2006. Depletion, degradation, and recovery potential of estuaries and coastal seas. *Science* 312, 1806-1809.

Niering, W.A., 1977. Our dynamic tidal marshes: vegetation changes as revealed by peat analysis. *The Connecticut Arboretum Bulletin* 22, 2-12.

Redfield, A.C., 1965. Ontogeny of a salt marsh estuary. *Science* 147, 50-55.

Teixeira, A., Duarte, B. and Caçador, I., 2014. Salt marshes and Biodiversity. *Tasks for Vegetation Science Vol. 47. Sabkha Ecosystems: Volume IV: Cash Crop Halophytes and*

Biodiversity Conservation. Khan, M.A., Böer, B., Öztürk, M., Al Abdessalaam, T.Z., Clüsener-Godt, M. and Gul, B. (Eds.) Springer.

UNEP, 2006. Marine and coastal ecosystems and human well-being: A synthesis report based on the findings of the Millennium Ecosystem Assessment. UNEP.

Valentim, J.M., Vaz, N., Silva, H., Duarte, B., Caçador, I. and Dias, J.M., 2013. Tagus Estuary and Ria de Aveiro Salt Marsh Dynamics and the Impact of Sea Level Rise. *Estuarine, Coastal and Shelf Science* 130, 138-151.

Valiela, I., and Cole, M.L., 2002. Comparative evidence that salt marshes and mangroves may protect seagrass meadows from land-derived nitrogen loads. *Ecosystems* 5, 92-102.

Valiela, I., and Teal, J.M., 1979. The nitrogen budget of a salt marsh ecosystem. *Nature* 280, 652-656.